

MATHEMATICAL MODELS FOR INVESTIGATING THE  
LONG-TERM IMPACT OF *GYRODACTYLUS SALARIS*  
INFECTIONS ON ATLANTIC SALMON POPULATIONS

SCOTT JOHN DENHOLM



Doctor of Philosophy

Computing Science and Mathematics

University of Stirling

June 2013

## DECLARATION

---

I, Scott John Denholm, hereby certify that the work presented in this thesis is, to the best of my knowledge and belief, original, except as acknowledged in the text, and that it has not been submitted, either in whole or in part, in any previous application for a higher degree at this or any other university.

I was admitted as a research student in October 2009 and as a candidate for the degree of Doctor of Philosophy in June 2010; the higher study for which this is a record was carried out at the University of Stirling, Scotland, between 2009 and 2013 under the supervision of Prof Rachel A. Norman, Dr Andrew P. Shinn, Dr Andrew S. Hoyle and Dr Nicholas G. H. Taylor.

*Stirling, June 2013*

---

Scott John Denholm

## ABSTRACT

---

*Gyrodactylus salaris* Malmberg, 1957, is a notifiable freshwater ecto-parasite that infects both wild and farmed populations of Atlantic salmon (*Salmo salar*, L.). It has caused catastrophic damage to wild salmon stocks in Norway since its accidental introduction in 1975, reducing salmon density in some rivers by 98% over a period of five years. It is estimated that *G. salaris* has cost the Norwegian salmon industry more than €500 million. Currently the UK has *G. salaris* free status under EU law, however, it is believed that if *G. salaris* emerged in the UK the impact would be similar to that witnessed in Norway. The aim of this thesis is to develop mathematical models that describe the salmon-*G. salaris* system in order to gain a greater understanding of the possible long-term impact the parasite may have on wild populations of Atlantic salmon in *G. salaris*-free territories such as the UK.

Mathematical models, including deterministic, Leslie matrix and individual based models, were used to investigate the impact of *G. salaris* on Atlantic salmon at the individual and population level. It is known that the Atlantic strain of Atlantic salmon, examples of which occur naturally in Norway and the UK, does not have any resistance to *G. salaris* infections and the parasite population is able to quickly grow to epidemic levels. In contrast, the Baltic strain of Atlantic salmon, examples of which occur naturally in Sweden and Russia, exhibits some form of resistance and the parasite is unable to persist. Thus, baseline models were extended to include immunity to infection, a trade-off on salmon reproductive rate, and finally, to consider interactions between populations of *G. salaris* and multiple strains of salmon exhibiting varying levels of immunity from fully susceptible to resistant.

The models proposed predict that in the absence of host resistance or an immune response infections by *G. salaris* will result in an epidemic followed by the extinction of the salmon host population. Models also predict that if salmon are able to increase their resistance to *G. salaris* infections through mutations, salmon population recovery after the epidemic is indeed possible within 10-15 years post introduction with low level parasite coexistence. Finally, models also highlight areas where additional information is needed in order to improve predictions and enable the estimation of important parameter values. Model predictions will ultimately be used to assist in future contingency planning against *G. salaris* outbreaks in the UK and possibly as a basis for future models describing other fish/ecto-parasite systems.

This research was supported by the Department for Environment, Food and Rural Affairs (Defra, project no. FC1197) and the Centre for Environment, Fisheries and Aquaculture Science (Cefas).

## ACKNOWLEDGMENTS

---

It is a pleasure to thank all the people who supported me in the writing of this thesis. I would like to show my appreciation to Defra and Cefas for providing the funding for this research and the University of Stirling for giving me the opportunity to carry it out.

I owe my deepest gratitude to my supervisor Professor Rachel Norman for her support and expertise during my time at the University of Stirling. Without her guidance and encouragement this work would not have been possible. I am also very grateful to Dr Andy Shinn and Dr Nick Taylor for their expertise, help and guidance on all things fish and *G. salaris* related and to Dr Andy Hoyle for his expertise and input, especially on the evolution aspect of the study. I would also like to take this opportunity to thank all four of my supervisors for their friendship and for making me feel welcome from my initial interview through to the submission of this thesis.

A very special thanks goes to my fellow office mathematicians Nicky McPherson, Rachel Lintott, Jen McKeown and Gill Ogg. Their support, input and friendship was invaluable and I wish them all the best in their future endeavours. Additionally, I wish to thank Giuseppe Paladini for his friendship and the good times spent in Norway counting parasites and drinking Norwegian and Austrian home-brew!

My time at Stirling was a happy one thanks to the friendly staff in Computing Science & Maths, especially Kate Howie and Donald Smith, and all the PhD students both past and present that I befriended along the way. I also wish to thank the computing support staff, Sam Nelson and Graham Cochrane, for their technical expertise and keeping my computer running for the past three and a half years, the secretaries, Grace McArthur, Linda Bradley and Gemma Gardiner, and all family and friends who supported and encouraged me during this research, especially my grandmother, Ann, and Kev (thanks for keeping my car running so that I could make it through to Stirling on a regular basis).

My greatest thanks goes to my parents Les and Julie for always believing in me. Their continued encouragement, unwavering love and support have enabled me to get to this point. I thank them for this, not only in regards to the work contained in this thesis but in all aspects of my life. Finally, I wish to thank my brother, Steven (cheers for helping with the many programming dilemmas), and sister, Jillian, for putting up with the maths chat for the last 8 years.

*Do. Or do not. There is no try.*

— Yoda

This thesis is dedicated to my parents, Les and Julie, and grandparents, Robert, Jeannie,  
Anthony & Ann.

## PUBLICATIONS

Denholm SJ, Norman RA, Hoyle AS, Shinn AP, Taylor NGH (in prep) Temperature induced reproductive trade-offs may moderate the impact of *Gyrodactylus salaris* in warmer climates.

Denholm SJ, Norman RA, Hoyle AS, Shinn AP, Taylor NGH (in prep) Predicting salmon population recovery from *Gyrodactylus salaris* infections: A multiple-host-strain modelling approach.

## CONTENTS

---

<b>i</b>	<b>INTRODUCTION</b>	<b>1</b>
<b>1</b>	<b>AN INTRODUCTION TO THE <i>GYRODACTYLUS SALARIS</i> PROBLEM</b>	<b>2</b>
1.1	A brief history of the <i>Gyrodactylus salaris</i> epidemic in Norway . . . . .	3
1.2	Current status of <i>Gyrodactylus salaris</i> in the UK . . . . .	6
1.3	<i>Gyrodactylus salaris</i> . . . . .	9
1.3.1	Life-cycle and reproduction . . . . .	10
1.3.2	Transmission . . . . .	14
1.3.3	Host-parasite-environment interactions . . . . .	15
1.3.4	Treatment . . . . .	16
1.4	The Atlantic salmon ( <i>Salmo salar</i> L.) . . . . .	17
1.4.1	Life-cycle . . . . .	17
1.4.2	Territories . . . . .	21
1.5	Mathematical modelling . . . . .	23
1.5.1	A brief history of infectious disease modelling . . . . .	23
1.5.2	Modelling host-parasite interactions . . . . .	23
1.5.3	Modelling of <i>Gyrodactylus</i> infections . . . . .	26
1.6	Thesis aim and structure . . . . .	28
<b>ii</b>	<b>MY CONTRIBUTION</b>	<b>30</b>
<b>2</b>	<b>THE BASIC MODEL AND DENSITY DEPENDENT HOSTS</b>	<b>31</b>
2.1	Introduction . . . . .	31
2.2	Constructing the basic model . . . . .	31
2.2.1	The basic model . . . . .	32
2.2.2	Equilibria and stability . . . . .	36
2.3	Model A: Density dependent constraints on host population . . . . .	40
2.3.1	Equilibria and stability . . . . .	41
2.4	Estimating parameter values . . . . .	44
2.4.1	Atlantic salmon . . . . .	44
2.4.2	<i>Gyrodactylus salaris</i> . . . . .	45
2.5	Simulating the model for a UK river system . . . . .	45
2.6	Summary . . . . .	46
<b>3</b>	<b>DETACHED PARASITES IN THE EXTERNAL ENVIRONMENT</b>	<b>48</b>
3.1	Making the model more realistic . . . . .	49
3.1.1	Equilibria and stability . . . . .	50

3.2	Re-evaluating the model . . . . .	54
3.2.1	Equilibria and stability . . . . .	56
3.2.2	The second zero equilibrium - Parasite induced extinction . . . . .	57
3.3	Investigating the occurrence of parasite induced host extinction . . . . .	57
3.4	Model B: Detached parasites in the external environment . . . . .	61
3.5	Estimating parameter values . . . . .	65
3.6	Simulating the model for a UK river system . . . . .	66
3.7	Summary . . . . .	67
4	MECHANISMS FOR RESISTANCE IN <i>SALMO SALAR</i> L. . . . .	68
4.1	Introduction . . . . .	68
4.1.1	The biology of <i>Gyrodactylus</i> . . . . .	69
4.2	Data . . . . .	70
4.3	Modelling techniques . . . . .	70
4.3.1	Leslie matrix models . . . . .	71
4.3.2	Parameterising Leslie matrix models . . . . .	72
4.3.3	Individual based models . . . . .	74
4.3.4	Parameterising individual based models . . . . .	74
4.4	Mechanisms for resistance . . . . .	76
4.4.1	Baseline simulations . . . . .	76
4.4.2	Delayed parasite first birth . . . . .	77
4.4.3	Reduced number of parasite births . . . . .	79
4.4.4	Reduced parasite survival . . . . .	80
4.4.5	Combination of mechanisms . . . . .	82
4.5	Summary . . . . .	83
5	ADDING IMMUNITY AND TRADE-OFFS TO THE SYSTEM . . . . .	85
5.1	Extending Model B for two host strains . . . . .	85
5.2	Model C: Adding immunity to Model B . . . . .	86
5.2.1	Estimating parameter values . . . . .	90
5.2.2	Investigating the impact of immunity on salmon density . . . . .	93
5.3	Model D: Adding a trade-off . . . . .	93
5.3.1	Investigating the effect of trade-off shape . . . . .	96
5.4	Summary . . . . .	100
6	MODELS WITH MULTIPLE HOST STRAINS . . . . .	101
6.1	Return to the two-strain model . . . . .	101
6.2	Extending the model for n-salmon strains . . . . .	104
6.2.1	Baseline simulations in the absence of infection . . . . .	105
6.2.2	Adding <i>G. salaris</i> infection . . . . .	105
6.3	Model E: Multiple host strains . . . . .	108

6.3.1	Adding mutations . . . . .	108
6.3.2	Baseline simulations in the absence of infection . . . . .	109
6.3.3	Adding <i>G. salaris</i> infection . . . . .	110
6.4	Investigating time to salmon population recovery . . . . .	111
6.4.1	Mutation rate . . . . .	114
6.5	Simulating the model for a UK river system . . . . .	121
6.6	Summary . . . . .	122
<b>iii</b>	<b>RESULTS AND CONCLUSIONS</b>	<b>124</b>
<b>7</b>	<b>DISCUSSION</b>	<b>125</b>
7.1	Model development . . . . .	126
7.2	Model limitations . . . . .	128
7.3	Future work . . . . .	129
7.4	Conclusions . . . . .	131
<b>iv</b>	<b>BIBLIOGRAPHY</b>	<b>133</b>
<b>v</b>	<b>APPENDICES</b>	<b>143</b>
<b>A</b>	<b>DATA</b>	<b>144</b>
<b>B</b>	<b>THE MODELS</b>	<b>152</b>
<b>C</b>	<b>ALGEBRAIC ANALYSIS</b>	<b>158</b>
<b>D</b>	<b>SENSITIVITY ANALYSIS</b>	<b>166</b>
<b>E</b>	<b>SELECTED MATHEMATICA CODE</b>	<b>170</b>

## LIST OF FIGURES

---

Figure 1.1	SEM images of <i>G. salaris</i> . . . . .	3
Figure 1.2	Map of <i>G. salaris</i> status in Europe . . . . .	4
Figure 1.3	<i>Gyrodactylus salaris</i> opisthaptor . . . . .	10
Figure 1.4	SEM images of <i>G. salaris</i> infecting Atlantic salmon . . . . .	10
Figure 1.5	Atlantic salmon parr . . . . .	11
Figure 1.6	SEM images of damage caused by <i>G. salaris</i> infections . . . . .	11
Figure 1.7	<i>Gyrodactylus salaris</i> giving birth . . . . .	12
Figure 1.8	Simplified diagram of the <i>Gyrodactylus</i> sp. asexual reproductive cycle . . . . .	13
Figure 1.9	The Atlantic salmon ( <i>Salmo salar</i> L.) . . . . .	17
Figure 1.10	The Atlantic salmon life-cycle . . . . .	18
Figure 1.11	Schematic representation of a host-microparasite interaction . . . . .	24
Figure 1.12	Schematic representation of a simple host-macroparasite interaction . . . . .	25
Figure 2.1	Basic model schematic . . . . .	33
Figure 2.2	Basic Model: The zero equilibrium . . . . .	37
Figure 2.3	Basic Model: Other possible situations . . . . .	39
Figure 2.4	Model A: Density dependent hosts schematic . . . . .	40
Figure 2.5	Model A: The zero equilibrium . . . . .	42
Figure 2.6	Model A: The disease-free equilibrium . . . . .	43
Figure 2.7	Model A: Other situations . . . . .	43
Figure 2.8	Model A: River Dee example . . . . .	46
Figure 3.1	Model B: Detached parasites schematic . . . . .	49
Figure 3.2	Model B: The zero equilibrium . . . . .	52
Figure 3.3	Model B: The disease-free equilibrium . . . . .	52
Figure 3.4	Model B: The coexistence equilibrium - possible scenarios . . . . .	54
Figure 3.5	Model B: varying parasite birth rate . . . . .	55
Figure 3.6	Model B re-evaluated: Parasite induced extinction . . . . .	58
Figure 3.7	Model B re-evaluated using a negative binomial distribution . . . . .	60
Figure 3.8	Model B - increased realism: Zero equilibrium . . . . .	62
Figure 3.9	Model B - increased realism: Disease-free equilibrium . . . . .	63
Figure 3.10	Model B - increased realism: Coexistence equilibria . . . . .	64
Figure 3.11	Model B - increased realism: Parasite induced extinction . . . . .	65
Figure 3.12	Model B: River Dee example . . . . .	66
Figure 4.1	Schematic representation of the Leslie/individual based model . . . . .	71

Figure 4.2	Leslie matrix baseline simulation . . . . .	76
Figure 4.3	IBM baseline simulation . . . . .	77
Figure 4.4	Delayed parasite first birth (0.5 days, Leslie) . . . . .	78
Figure 4.5	Delayed parasite first birth (0.5 days, IBM) . . . . .	78
Figure 4.6	Delayed parasite first birth (1 day) . . . . .	79
Figure 4.7	Delayed parasite first birth (1 day, IBM) . . . . .	79
Figure 4.8	Reduced parasite births (Leslie) . . . . .	80
Figure 4.9	Reduced parasite births (IBM) . . . . .	81
Figure 4.10	Reduced parasite survival (Leslie) . . . . .	81
Figure 4.11	Reduced parasite survival (IBM) . . . . .	82
Figure 4.12	Combination of mechanisms for resistance to <i>G. salaris</i> infections . . . . .	83
Figure 5.1	Impact of a host immune response - single host simulation . . . . .	89
Figure 5.2	Data from Bakke <i>et al.</i> (1990) . . . . .	89
Figure 5.3	Impact of $\tilde{m}$ . . . . .	92
Figure 5.4	Salmon density against $\tilde{m}$ . . . . .	93
Figure 5.5	Position of Atlantic and Baltic salmon birth rates with respect to $\tilde{m}$ . . . . .	94
Figure 5.6	Salmon birth rate against $\tilde{m}$ . . . . .	95
Figure 5.7	Salmon density against immunity ( $\tilde{m}$ ), $\theta = 0$ . . . . .	96
Figure 5.8	Possible trade-off shapes . . . . .	97
Figure 5.9	$\tilde{m}vH$ with trade-off . . . . .	98
Figure 5.10	Salmon density against immunity ( $\tilde{m}$ ), $1 < \theta < 0$ . . . . .	98
Figure 5.11	The occurrence of asymptotes when $\theta > 0$ . . . . .	99
Figure 5.12	Salmon density against immunity ( $\tilde{m}$ ), $\theta > 0$ . . . . .	99
Figure 6.1	Two host strain model . . . . .	101
Figure 6.2	Two host strain model simulation . . . . .	103
Figure 6.3	Model E: multiple host strains . . . . .	104
Figure 6.4	Multiple host strain model simulations with zero infection . . . . .	106
Figure 6.5	Multiple host strain model simulations with infection added after 100 years . . . . .	106
Figure 6.6	Multiple host strain model simulations, 6 to 36 years after <i>G. salaris</i> introduction . . . . .	107
Figure 6.7	Adding mutations to the multiple host strain model . . . . .	108
Figure 6.8	Multiple host strain model simulations with mutant host births and zero infection . . . . .	110
Figure 6.9	Multiple host strain model simulations with mutant host births and infection . . . . .	111
Figure 6.10	Multiple host strain model simulations with mutant host births and infection (total salmon density) . . . . .	112

Figure 6.11	Simulating the n-strain model for $n = 5, 10, 15$ and 20 salmon strains in the absence of infection . . . . .	112
Figure 6.12	Simulating the n-strain model for $n = 5, 10, 15$ and 20 salmon strains, infection added after 25 years . . . . .	113
Figure 6.13	Mutation rate against time to recovery . . . . .	115
Figure 6.14	Total salmon density over time (10 host strains) . . . . .	119
Figure 6.15	Simulating 25 host strains in the absence of infection . . . . .	120
Figure 6.16	Total salmon density over time (25 host strains) . . . . .	120
Figure 6.17	Model E: River Dee example . . . . .	121
Figure E.1	Screenshot of plot generated with user alterable parameter values . . .	172

## LIST OF TABLES

---

Table 1.1	Risk estimation for routes of introduction of <i>G. salaris</i> to the UK . . . . .	8
Table 1.2	Salmon parr classifications . . . . .	20
Table 1.3	Definition of host classes . . . . .	24
Table 1.4	Description of parameters (Anderson & May, 1978) . . . . .	26
Table 2.1	Description of parameters . . . . .	33
Table 2.2	Routh-Hurwitz conditions for polynomials of degree $2 \leq n \leq 4$ . . . . .	35
Table 2.3	UK river systems . . . . .	44
Table 4.1	Leslie matrix and individual based model parameter values . . . . .	74
Table 5.1	<i>Gyrodactylus salaris</i> growth rate estimations . . . . .	91
Table 5.2	Values for salmon birth rate with trade-off, $\hat{a}(\tilde{m})$ . . . . .	94
Table 6.1	Values for $\tilde{m}$ in baseline simulations . . . . .	105
Table 6.2	Host strain coexistence after recovery from infection . . . . .	114
Table 6.3	Mutation rate versus time to initial recovery (60% of $K_{\min}$ ) . . . . .	116
Table 6.4	Mutation rate versus time to initial recovery (60% of $K_{\max}$ ) . . . . .	117
Table 6.5	Stable salmon population recovery . . . . .	117
Table 6.6	Level of salmon population recovery . . . . .	118
Table A.1	Parameter estimations . . . . .	144
Table A.2	Results from Cable <i>et al.</i> (2000) . . . . .	145
Table A.3	Results from Bakke <i>et al.</i> (1990) . . . . .	145
Table A.4	Results from Jansen & Bakke (1991) experiment 1 . . . . .	146
Table A.5	Results from Paladini <i>et al.</i> (in prep.) (control) . . . . .	147
Table A.6	Results from Paladini <i>et al.</i> (in prep.) . . . . .	148
Table A.7	Parameter estimations for <i>G. turnbulli</i> infecting <i>Poecilia reticulata</i> from Scott & Anderson (1984) . . . . .	149
Table A.8	Results from dead fish trial 1 - Paladini & Denholm (unpublished) . . .	150
Table A.9	Results from dead fish trial 2 - Paladini & Denholm (unpublished) . . .	150
Table A.10	Results from alive fish trial 1 - Paladini & Denholm (unpublished) . . .	151
Table A.11	Results from alive fish trial 2 - Paladini & Denholm (unpublished) . . .	151
Table D.1	Sensitivity analysis of parameters used in Leslie and individual based models . . . . .	167
Table D.2	Sensitivity of $\theta$ in time to initial 60% salmon recovery . . . . .	168
Table D.3	Sensitivity of $\theta$ in time to initial 60% salmon recovery . . . . .	168
Table D.4	Sensitivity analysis of Model E - Multiple host strains (with mutations)	169

Part I

INTRODUCTION

## An introduction to the *Gyrodactylus salaris* problem

The dictionary defines a mathematical model as “a simplified description of a system, process, etc., put forward as a basis for theoretical or empirical understanding” (New Shorter Oxford English Dictionary, 2007). Models are useful tools that are employed by mathematicians to solve problems in a variety of fields from traffic flow to wound healing. An increasingly popular field of study, mathematical biology, is bringing together mathematicians and biologists into a new partnership looking to study the mysteries of all aspects of biology and epidemiology. A large part of this field concerns the study of disease and host-parasite interactions. In these areas models are used to make predictions about what can happen under a variety of conditions and help gain a greater understanding of the course an epidemic might take. Models also give an insight into knowledge gaps and highlight areas where more research and data is required. Mathematical modelling can in some way help to explain and understand biological phenomena witnessed in nature, however, as noted above models give a simplified description of a system and hence care must be taken when interpreting results.

*Gyrodactylus salaris* Malmberg, 1957, (Figure 1.1) is a viviparous (*i.e.*, live-bearing) freshwater ecto-parasite that infects both wild and farmed populations of Atlantic salmon (*Salmo salar* L.), and can result in the death of the host. It is an important pathogen and was first described by Malmberg in 1957 from the fins and skin of its natural host, the Baltic strain of Atlantic salmon (Malmberg, 1957), from a hatchery in Sweden located near the Indalsälva river (Bakke *et al.*, 2007). *Gyrodactylus salaris* is believed to be native to the waters of northern Russia, western Sweden and northern Finland (Peeler & Thrush, 2004). Within the European area (Figure 1.2) the parasite is known to have been introduced to Norway (Johnsen & Jensen, 1991) and Denmark (Buchmann & Bresciani, 1997; Nielsen & Buchmann, 2001). Between 2003 and 2009 studies confirmed the presence of *G. salaris* in Germany (Cunningham *et al.*, 2003), Macedonia (Zištara *et al.*, 2007), Poland (Rokicka *et al.*, 2007), Romania (OIE, 2009) and on rainbow trout (*Oncorhynchus mykiss*) from fish farms in Italy (Paladini *et al.*, 2009). At present there are unconfirmed reports of infections in France, Portugal and Spain (Bakke *et al.*, 2007). Moreover, it is believed that *G. salaris* is in fact present in more countries than those currently known OIE (2003). A recent review of the parasites distribution across Europe by Paladini *et al.* (subm.) confirmed the presence of *G. salaris* in Bosnia-Herzegovina, Estonia, Georgia,

Latvia, Moldova and the Ukraine. Although *G. salaris* has been confirmed in Finland some watersheds have been declared free from the parasite (Lautraite *et al.*, 1999). Since its accidental introduction to Norway, the parasite has caused catastrophic damage to both farmed and wild populations of Atlantic salmon parr. Within 5 years of being introduced, the parasite reduced salmon stock by approximately 98% (Johnsen & Jensen, 1991) causing severe damage to the Norwegian economy and salmon industry. At present only the United Kingdom and Ireland are confirmed as free from *G. salaris* (see Shinn *et al.* (1995); OIE (2003, 2009)).

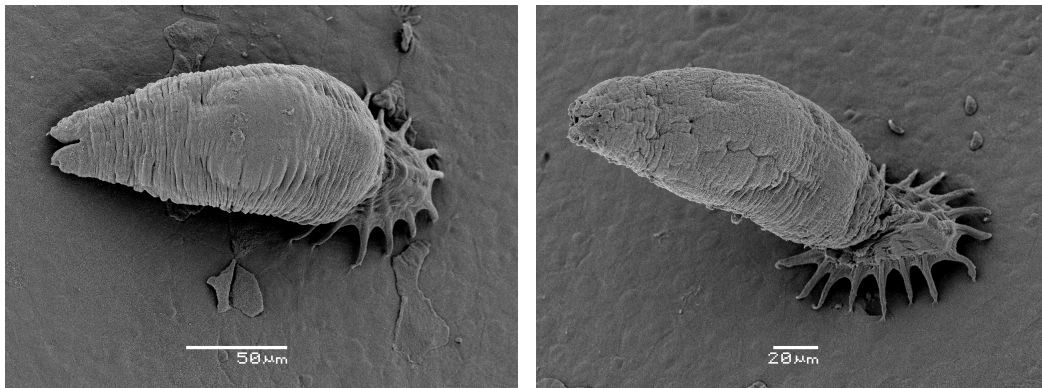


Figure 1.1: Images of *Gyrodactylus salaris* obtained through the use of a Scanning Electron Microscope (SEM). A single *G. salaris* parasite is approx 0.5 - 1mm in length. Photographs kindly taken and provided by Giuseppe Paladini.

### 1.1 A BRIEF HISTORY OF THE *GYRODACTYLUS SALARIS* EPIDEMIC IN NORWAY

*Gyrodactylus salaris* was first discovered in Norway after a dramatic increase in mortality rates of salmon at the Institute of Aquaculture Research hatchery at Sunndalsøra, Møre og Romsdal County, in July of 1975 (Tanum, 1983; Malmberg, 1988 as cited by Johnsen & Jensen, 1991 and Bakke & MacKenzie, 1993). It was originally thought that *G. salaris* was native to Norway and the salmon mortality epidemic witnessed was caused by environmental pollution (Johnsen, 1978), however, Johnsen & Jensen (1986) confirmed that the epidemic was not caused by environmental factors. Approximately one month later, in August 1975, *G. salaris* was found infecting wild Atlantic salmon parr in the river Lakselva, Misvær, Nordland County, in the northern region of Norway (Johnsen, 1978). Over the next three years a study of Atlantic salmon and brown trout presmolt (freshwater juveniles, *i.e.*, fingerlings and parr) was conducted in the Lakselva region. The results of this study showed a catastrophic decrease in Atlantic salmon densities but no change in brown trout densities (Johnsen, 1978; Johnsen & Jensen, 1991), allowing the conclusion to be drawn that unlike the Atlantic salmon, brown trout are not susceptible to *G. salaris* infections or disease. One year after the results of Johnsen's study (1978) in the autumn of 1979, *G. salaris* was found infecting Atlantic salmon

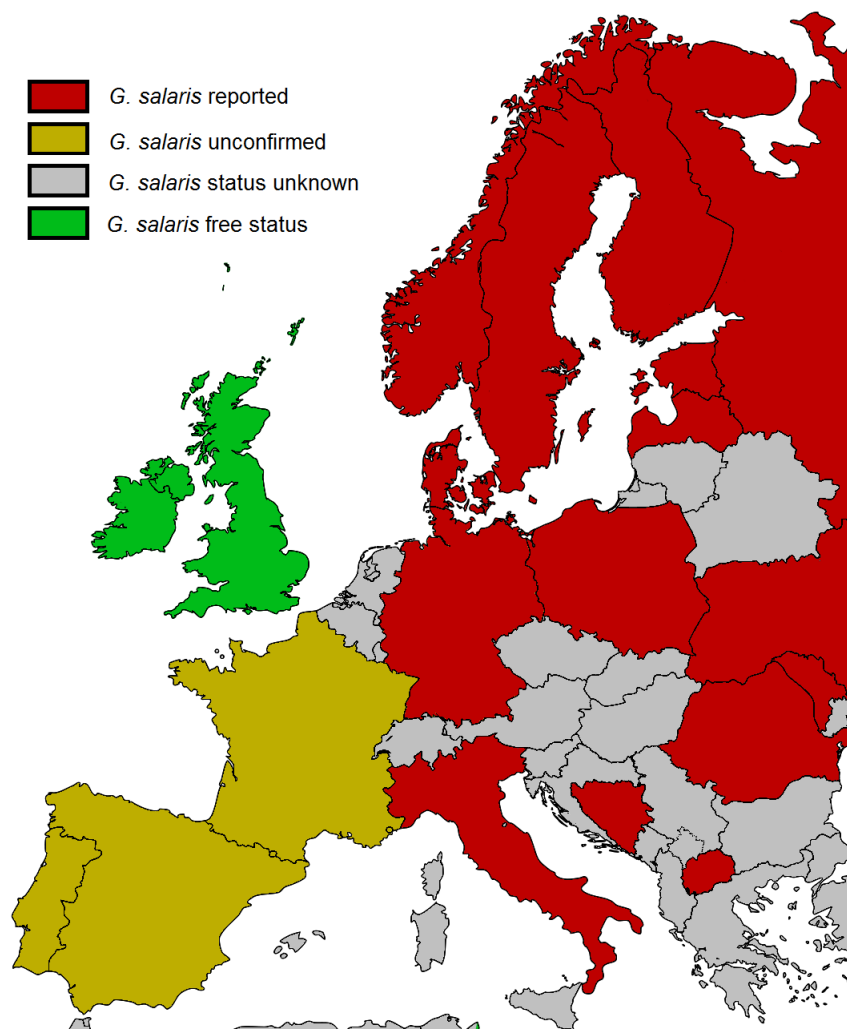


Figure 1.2: A map of Europe identifying territories that have reported *G. salaris* infections (red), territories that have unconfirmed reports (yellow), territories with unknown *G. salaris* status (grey) and finally territories that are free of the parasite (green). The United Kingdom and the Republic of Ireland are the only such territories with confirmed *G. salaris* -free status. Some watersheds in Finland have now been declared free from infection, however, the country is still considered *G. salaris* positive.

parr in two additional rivers, the Ranaelva and the Vefsna. This new information, together with the results obtained by Johnsen (1978) prompted the formation of a “*Gyrodactylus* committee” and surveillance program in 1980 (Johnsen & Jensen, 1991).

The committee and surveillance program were tasked with assessing the *G. salaris* problem and tracking its spread throughout Norway. The *Gyrodactylus* committee itself consisted of a council of representatives from different bodies concerned with aquatic health and included; the Fish Research Department at the Directorate for Nature Management, the Veterinarian Authorities, the fish farming industry and the Zoological Museum, University of Oslo (Johnsen & Jensen, 1991). After its formation, the committee began its study of the *G. salaris* epidemic. This research began in 1980, lasted two years and was completed in 1982. The committee studied juvenile Atlantic salmon, both farmed and wild, from hatcheries and over

200 rivers (Johnsen & Jensen, 1986). The results of the committee's research was published in three annual reports (*Gyrodactylus*prosjektet, 1981, 1982, 1983 as cited by Johnsen 1986) which confirmed that 26 rivers were infected with *G. salaris* (nine additional rivers were found to be infected with other *Gyrodactylus* species) and concluded that the parasite posed a major threat to Atlantic salmon populations in Norway (Johnsen & Jensen, 1986, 1991). The report warned that adult salmon production was severely threatened in infected rivers due to the fact that few or no young salmon parr survived long enough to reach the smolt stage of their life-cycle. The results of the study also confirmed that *G. salaris* was a new species to Norway and that it was most likely spread via hatcheries, restocking and fish migration. This meant the original theory that *G. salaris* was native to Norway was false (later investigations have provided evidence that *G. salaris* was most probably introduced to Norway via Swedish salmon hatcheries). Further evidence supporting this view was provided by Bakke *et al.* (1990) in their study of the effects of *G. salaris* from Norway on Atlantic salmon from the Baltic and east Atlantic Sea. In 1983, as a result of the *Gyrodactylus* committee's findings, *G. salaris* was declared a notifiable disease (Group B) in Norway and recognised as a "significant fish disease" by the Office International des Epizooties (OIE) (Johnsen & Jensen, 1991; Bakke *et al.*, 2007; Mo *et al.*, 2008).

Research into the *G. salaris* problem continued, to a lesser extent, in the period 1983-85. Between 1980 and 1985 a total of 212 rivers were tested for *G. salaris*. By the end of 1985 the infection was known to have spread to 26 rivers and 6 hatcheries (Johnsen & Jensen, 1986, 1991). Johnsen & Jensen (1986) were able to demonstrate that the distribution of *G. salaris* was closely connected to the stocking of fish from infected hatcheries by grouping the 26 rivers known to be infected into 14 regions, with neighbouring rivers being placed in the same geographical location. By the end of 1989, approximately 14 years after the infection was first discovered, 34 rivers and 35 hatcheries were recorded as being infected with the parasite (Johnsen & Jensen, 1991). A major cause of the spread of the parasite between rivers has been attributed to brackish water dispersal followed by the restocking of fish from hatcheries known to be infected (Bakke *et al.*, 2007).

The Norwegian authorities quickly began treating infected rivers with the biocide rotenone which kills all life including the host, parasite and plant life (see Section 1.3.4). After the success of rotenone treatment in the river Vikja, eight more rivers were treated between 1986 and 1989. However, treatment of infected rivers does not protect from future *G. salaris* infections and some rivers have become re-infected post treatment. Between 1975 and 2010 a total of 48 out of 379 rivers, 13 Atlantic salmon hatcheries/farms and 26 rainbow trout hatcheries/-farms have been recorded as infected with *G. salaris* (Bakke *et al.*, 2007; Sviland *et al.*, 2012). Arctic charr (*Salvelinus alpinus*) from many lakes across Norway have also tested positive for

a non-pathogenic strain of *G. salaris* (Sviland *et al.*, 2012). Extermination of the parasite has been successfully achieved in all hatcheries/farms and 20 rivers. A further 25 rivers are still known or suspected to be infected with *G. salaris* and eradication in an additional 3 rivers remains unconfirmed as at December 31 2011 (Sviland *et al.*, 2012).

## 1.2 CURRENT STATUS OF *GYRODACTYLUS SALARIS* IN THE UK

Like Norway the UK is recognised as being an important producer of salmon with the UK fishing industry providing over 12,000 direct jobs and generating between £800 - £1,200 million to the British economy (FAO, 2004-2013). Scotland alone is the second largest salmon producer in the European economic area (Norway being the largest) and generates approximately £300 million per annum. However, it is the UK's wild stocks that are more important due to the fact that they are already declining and threatened (WWF, 2001). As mentioned earlier the UK is currently recognized as being free from *G. salaris* (OIE, 2003, 2009). This was confirmed by Shinn *et al.* (1995) after a study of 227 British water bodies and samples from nine species of salmonid. Hence, the UK has *G. salaris* free status under EU law (Defra, 2008a) and is officially a *G. salaris*-free zone under EC Decision 2004/453/EC\* and its subsequent amendments provided under EC Decision 2006/272/EC†. Further screenings of freshwater salmon and trout farms and sampling of populations of wild salmon by fish health authorities on a routine basis have shown no subsequent signs of *G. salaris* infections. It is highly likely that UK salmon stocks are as susceptible to the parasite as the Norwegian stocks (Bakke & MacKenzie, 1993), this was confirmed by Paladini *et al.* (in prep.). Hence, *G. salaris* is regarded as a major exotic disease threat to the UK's valuable wild and farmed salmon populations (Defra, 2008a). It is also likely that *G. salaris*, if introduced, would spread within and between UK rivers before it is detected (Peeler & Thrush, 2004). Due to this contingency plans were drawn up to set out a set of actions to follow in the event of an outbreak (Defra, 2008a).

Peeler & Thrush (2004) and Peeler *et al.* (2004, 2006) used risk analysis techniques to estimate the probability of introduction of *G. salaris* to UK water systems and highlight the most significant routes of establishment. Peeler & Thrush (2004) identified three main categories that all pathways of introduction fall into (see Table 1.1 for overall risk estimations):

1. Importation of live fish and gametes, such as the importation of live salmonids, eels, non-salmonids and rainbow trout eggs;
2. Importation of eviscerated fish carcasses, such as the importation of fresh or chilled fish carcasses from countries that are not free from *G. salaris*;

\* <http://eurlex.europa.eu/LexUriServ/LexUriServ.do?uri=CONSLEG:2004D0453:20060407:EN:PDF>

† <http://eurlex.europa.eu/LexUriServ/LexUriServ.do?uri=OJ:L:2006:099:0031:0034:EN:PDF>

3. Mechanical transmission, such as the movement of inanimate materials that have come into contact with infected water or hosts.

They used qualitative risk analysis and divided their results into four categories: release assessment, exposure assessment, consequence assessment and risk estimation. Their research showed the risk of *G. salaris* being released via the importation of live salmonids or live non-salmonids is negligible. Live salmonids are currently not imported to the UK and there is no evidence to suggest that illegal imports are taking place. Salmonid egg imports are common and can even come from *G. salaris* infected farms as long as they are thoroughly disinfected. The exposure risk of live salmonid importation is considered very high and the exposure risk of salmonid eggs and eel importation is moderate. Overall, the risk from imported live salmonid fish is considered negligible with non-salmonid imports considered extremely low (Peeler & Thrush, 2004).

The risk of release via the importation of fresh or chilled Atlantic salmon is estimated as negligible, this is because Atlantic salmon carcasses come from the sea (*G. salaris* cannot survive full strength salinity). However, there is a high risk of release via the importation of rainbow trout from European freshwater sites. The majority of fresh rainbow trout carcasses come from freshwater sites in France and Denmark (*G. salaris* is known to be present in Denmark and is unconfirmed in France). It is also worth noting that transport conditions from Denmark to the UK are suitable for the survival of *G. salaris* and the transport time is short. The exposure risk of fresh or chilled rainbow trout being imported to processing plants on fish farms is considered moderate with the exposure risk of any other salmonid import being negligible. The overall risk from imports of salmonid carcasses is considered negligible. The most important risk from imported fresh salmonid carcasses is on farm processing of fresh rainbow trout from infected farms (Peeler & Thrush, 2004).

The risk of introduction to the UK via mechanical transmission can be split into four areas: Live fish transporters; canoes and angling equipment; leisure craft, well boats and ballast water; aquatic plants and lumber imports. The highest risk of parasite introduction via mechanical means come from live fish transporters that travel between Europe and the UK. If a vehicle has visited an infected farm and has not been properly disinfected, or if it contains infected water or hosts (living or dead), it could potentially introduce the parasite on return to the UK. Fortunately, the number of journeys of this nature is low and the risk of release is considered very low, however, the risk of exposure is estimated as moderate. The risk of release from canoes, angling equipment, leisure craft and ballast water is estimated as extremely low, with an exposure risk ranging from very low to negligible. This is due to short survival time of *G. salaris* off the host. Similarly, the risk from well boats (from Norwegian hatcheries) and aquatic plants and lumber imports (from infected countries) is considered

negligible as all Norwegian hatcheries have substantiated freedom from *G. salaris* and the probability of contact between infected fish and aquatic plants/lumber is extremely low. The exposure risk is considered extremely low to negligible. Overall, the risk of introduction via mechanical spread is negligible. The most important risk from this area is live fish transports (very low), followed by spread by canoes/angling equipment (extremely low) (Peeler & Thrush, 2004).

Table 1.1: Overall risk estimation for routes of introduction of *Gyrodactylus salaris* to the UK as determined by Peeler & Thrush (2004).

<b>Route of introduction</b>	<b>Overall risk estimation</b>
<b>Live fish and gametes</b>	
Importation of live salmonids	Negligible
Importation of eels	Negligible
Importation of non-salmonid fishes	Extremely low
Importation of rainbow trout eggs	Negligible
<b>Fish carcasses</b>	
Fresh/chilled Atlantic salmon from Norway/Finland/Sweden	Negligible
Fresh/chilled rainbow trout from European freshwater production	Negligible
Fresh/chilled rainbow trout from European freshwater production imported for on-farm processing in the UK	Negligible
<b>Mechanical transmission</b>	
Lorries moving live salmon fish travelling from mainland Europe to a UK fish farm	Very low
Ships' ballast water	Negligible
Well-boats travelling from Norway	Negligible
Freshwater tanks on leisure craft	Negligible
Canoes and angling equipment	Extremely low
Importation of lumber from Baltic countries	Negligible
Importation of aquatic plants from Baltic countries	Negligible

Due to the complexity of many British water systems it is most likely that authorities will focus on containing the infection to stop its spread to neighbouring rivers. As a step to ensure *G. salaris* does not establish in the UK, the importation of live salmonids from freshwater in territories that have not substantiated freedom from *G. salaris* has been restricted by authorities (Defra, 2008a,b). Other measures currently being taken to ensure *G. salaris* is not introduced include: disinfection of imported salmonid eggs; disinfection or disposal of live fish, eggs, containers and residual water that may have come into contact with the parasite; cleaning and disinfection of live fish transporters before entry to UK; disinfection of any angling equipment that may have come into contact with infected water/hosts; discharge of ballast water outside UK coastal waters of all boat traffic (Peeler & Thrush, 2004). The

only tried and tested method of treatment is the removal of all life in a river by the use of rotenone. However, rotenone treatment in the UK is highly unlikely due to environmental and legislative constraints (Peeler *et al.*, 2004; Peeler & Thrush, 2004).

As mentioned above, the UK is the second largest salmon producer in the European economic area and is currently free from the parasite. This chapter seeks to review published information regarding *G. salaris*, the Atlantic salmon and the mathematical modelling of infectious disease with the intention of using the information as a basis for building theoretical mathematical models. As it is unknown what effect a *G. salaris* outbreak would have on UK rivers and water systems the models will be used to gain a greater understanding of the long term consequences of infection. This will be achieved by studying the dynamics of both parasite and host as well as the evolution of single and multiple strains of host in order to answer the following questions - “*under what circumstances and in what time-frame would...*”

1. The parasite population become extinct?
2. The host population become extinct?
3. Low level host/parasite coexistence occur?
4. Host/parasite coexistence with host population recovery occur?

### 1.3 *GYRODACTYLUS SALARIS*

*Gyrodactylus salaris* (Figure 1.1) is a monogenean (flatworm) of the genus *Gyrodactylus* and a member of the family Gyrodactylidae, of which there are currently 409 described species (Harris *et al.*, 2004). An individual *G. salaris* parasite is approximately 0.5 - 1mm in length (Johnsen, 2006), making it one of the smallest monogeneans (Bakke *et al.*, 2007). *Gyrodactylus salaris* is worm-like in appearance and attaches to its host via the opisthaptor (Figure 1.3), a circular structure found at one end of the body armed with 16 marginal hooks and a pair of ventrally orientated hamuli (the two “Fish-hook” like structures located top-centre within the opisthaptor) (Bakke *et al.*, 2007). The mouth of the parasite is found at the opposite end to opisthaptor.

*Gyrodactylus salaris* is most commonly found on the fins and skin of juvenile Atlantic salmon (Figure 1.4), *i.e.*, those between fry and smolt stages (Figure 1.5) - see Section 1.4.1 for definitions, and less commonly on the gills (Johnsen & Jensen, 1992; Johnsen, 2006; OIE, 2009). The parasite is thought to feed on mucus and epidermal cells (Bakke *et al.*, 2007), as seen in Figure 1.6, causing gyrodactylosis (OIE, 2009), which is associated with high mortality caused by disruption of the osmotic permeability of the epidermis (Cusack & Cone, 1986), or via secondary infections by bacteria or viruses (FRS, 2004).

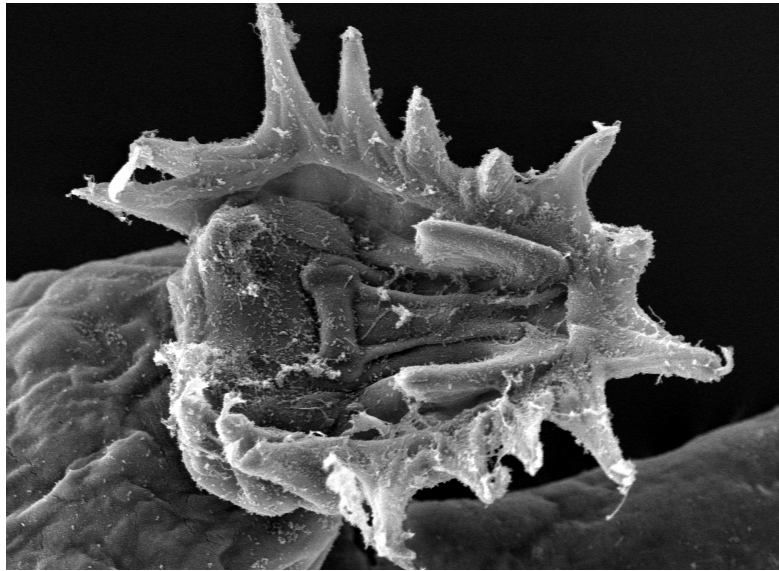


Figure 1.3: *Gyrodactylus salaris* attaches to its host via the opisthaptor, a circular structure found at one end of the body armed with 16 marginal hooks and a pair of ventrally orientated “fish-hook” shaped hamuli. SEM image courtesy of Dr Andy Shinn.

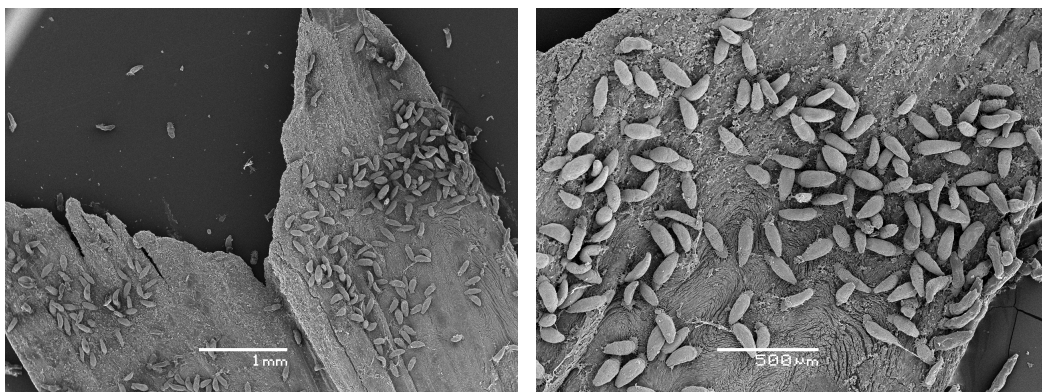


Figure 1.4: Images of *Gyrodactylus salaris* infecting the fins and skin of an Atlantic salmon obtained through the use of a Scanning Electron Microscope (SEM). Photographs kindly taken and provided by Giuseppe Paladini.

*Gyrodactylus salaris* can potentially reduce salmon populations by 98% within 5 years, as witnessed in Norway (Johnsen & Jensen, 1991). In Norwegian populations of Atlantic salmon prevalence of up to 100% has been observed, whereas for other salmonid species (e.g., rainbow trout) less than 10% prevalence has been observed (Peeler *et al.*, 2006; Johnsen, 2006; OIE, 2009).

### 1.3.1 Life-cycle and reproduction

The life-cycle of *G. salaris* is short and direct with no offspring being born off the host. In ideal conditions it is possible for the life-span of an individual parasite to reach approximately 58 days (Jansen & Bakke, 1991), however, this is not always the case in the field where conditions such as water temperature, salinity and pH can vary. *Gyrodactylus salaris* is considered a



Figure 1.5: Atlantic salmon parr. Atlantic strains of Atlantic salmon, examples of which occur naturally in Norway and the UK, are highly susceptible to *G. salaris* infections and on juvenile hosts (parr) the parasite population is able to increase in size rapidly and cause substantial mortality (Bakke *et al.*, (1990); Bakke & MacKenzie, (1993); Hansen *et al.*, (2003)), hence, killing salmon hosts before smoltification and run to sea. Image source: <http://www.public-domain-image.com>

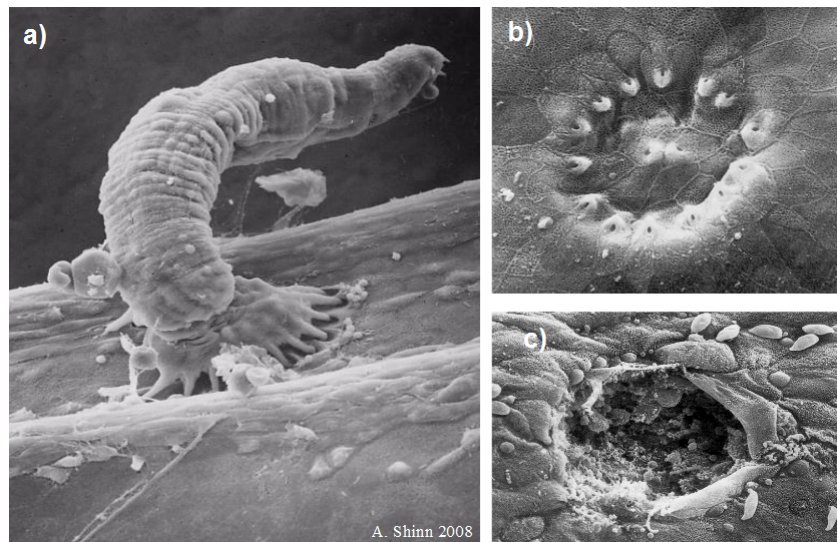


Figure 1.6: The current hypothesis of how gyrodactylids kill a host is through attachment, (a) - (b), and grazing activity, (c), leading to gyrodactylosis (OIE, 2009) and disruption of the osmotic permeability of the epidermis (Cusack & Cone, 1986). Secondary infections via bacteria or viruses has also been cited as a cause (FRS, 2004). SEM images courtesy of Dr Andy Shinn, (c) found in (Malmberg & Malmberg, 1993).

macroparasite but its life-cycle has similarities to that of a microparasite as it reproduces directly on the host instead of producing free-living stages. One of the most interesting aspects of gyrodactylid biology is their reproduction. Gyrodactylids are highly fecund and can reproduce both sexually and asexually. Individual parasites give birth to a single fully grown offspring (Figure 1.7) that is itself pregnant at birth with a pregnant offspring (Cable *et al.*, 2000). Gyrodactylid reproduction is commonly compared to that of a “Russian doll” (see Figure 1.8). This means that in theory a single parasite can cause an epidemic. The first birth occurs within a few days of infection (Jansen & Bakke, 1991; Cable *et al.*, 2000) and is

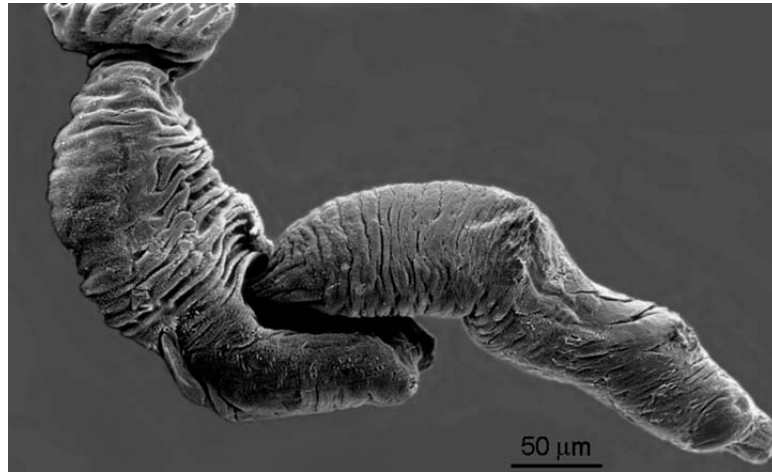


Figure 1.7: A *G. salaris* parasite giving birth to a fully grown offspring. The newly born offspring is already pregnant at time of birth. This polyembryonous state has led to this parasite being dubbed the 'Russian doll' when describing the parasite. Image by Dr T. A. Mo, National Veterinary Institute, Oslo. Source: Bakke TA *et al.* (2007) The biology of gyrodactylid monogeneans: The "Russian-doll killers" *Advances In Parasitology*, **64**, 161–460.

asexual (Harris *et al.*, 1994), subsequent births are either sexual or asexual (Bakke *et al.*, 2007). In general asexual reproduction will occur at low parasite densities with sexual reproduction occurring when the parasite population is high (Johnsen, 2006). After the offspring is born the mother is quiescent for a short period of time before moving to a different location (normally to the anterior) on the host, away from her daughter (Bakke *et al.*, 2007). In situations where the mother becomes detached from the host while giving birth, both mother and daughter will die. This is because the daughter cannot pull itself free from the mother (Bakke *et al.*, 2007).

#### 1.3.1.1 Survival

The survival time of *G. salaris* is dependent on a variety of conditions. Salinity (measured in parts per thousand, ‰, which is approximately grams of salt per kilogram of solution) and temperature of the water are very important in determining parasite survival with survival possible between 0.0 ‰ and 20.0 ‰ at 3°C - 20°C (Jansen & Bakke, 1991; Soleng *et al.*, 1998). Another important factor in *G. salaris* survival is whether parasites are on or off a host. Species and strain of host also impact survival times. The survival of *G. salaris* in low salinity waters is negatively correlated with water temperature and hence, it can survive longer, both on and off the host, in such waters at lower temperatures (Soleng *et al.*, 1998). As mentioned above *G. salaris* can tolerate, and hence transmit, in brackish water up to 20 ‰, however, parasites cannot survive in full strength salinity (Soleng *et al.*, 1998). Parasites can survive and reproduce indefinitely on Atlantic salmon and causes clinical disease which can result in host death. Similarly, *G. salaris* can survive and reproduce indefinitely on rainbow trout (Bakke *et al.*, 1991b). However, in rainbow trout clinical disease does not always occur with some fish being susceptible and others resistant. *Gyrodactylus salaris* can also survive on

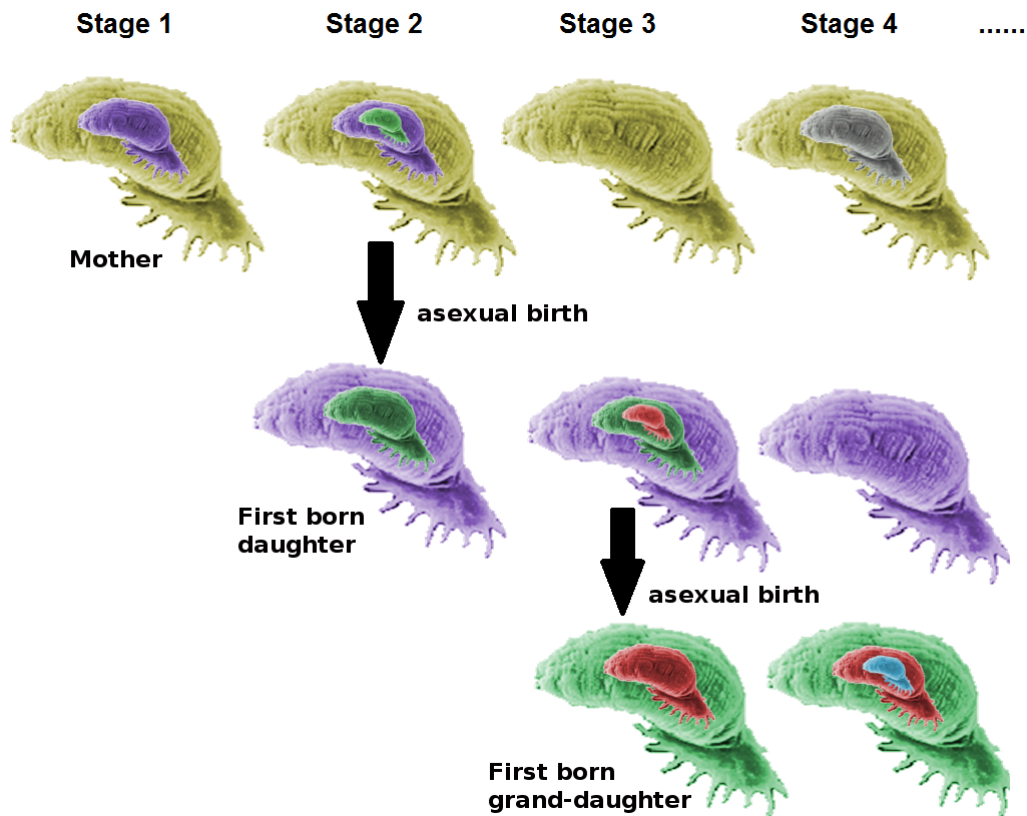


Figure 1.8: A simplified diagram showing the basis of the *Gyrodactylus* sp. asexual reproductive cycle. As can be seen, a progenic parasite gives birth to a pregnant offspring. First birth (Stage 2) is always asexual. After first birth is achieved there is a period of recovery when a parasite is not pregnant (Stage 3). Subsequent pregnancy is via sexual or asexual means (Stage 4 onwards). *Gyrodactylus* sp. image courtesy of Dr Andy Shinn.

other salmonid and non-salmonid fish species without causing clinical disease for anything between 7 and 150 days in ideal conditions (Bakke *et al.*, 1991b,a, 1992b,a; Jansen & Bakke, 1995; Bakke *et al.*, 1996, 1999; Soleng & Bakke, 2001). The parasite can survive for 50 days, on grayling (*Thymallus thymallus*) and brown trout (*Salmo trutta*) with limited reproduction (Jansen & Bakke, 1995; Soleng & Bakke, 2001). It is also capable of surviving (with reproduction) for 70 days on brook trout (*Salvelinus fontinalis*) (Bakke *et al.*, 1992a) and approximately 8 days on eels (*Anguilla anguilla*) with no reproduction (Bakke *et al.*, 1991a) (*G. salaris* is not believed to reproduce on non-salmonids, Peeler *et al.*, 2004). However, it survives longest, up to 150 days (280 in laboratory conditions), on Arctic charr (*Salvelinus alpinus*) (Bakke *et al.*, 1996). *Gyrodactylus salaris* cannot survive freezing, desiccation or elevated temperatures, and when detached from the host parasites can only survive for a maximum of 6-7 days in ideal conditions (Mo, 1987, as cited by Peeler *et al.*, 2006). Parasites can also be killed via the use of certain treatments, these treatments and the impact they have on parasites, hosts and the external environment are discussed in Section 1.3.4.

### 1.3.2 *Transmission*

*Gyrodactylus salaris* is highly efficient at locating and transferring to a susceptible host (Soleng *et al.*, 1999a). In general gyrodactylids have no specific free-living transmission stage, hence, *G. salaris* must rely on direct contact with a susceptible host in order to spread. However, when a suitable host is found rapid colonization can occur and the consequences of infection to an individual host, and hence entire host population, can be catastrophic.

#### 1.3.2.1 *Transmission in a river*

There are four main routes of transmission that an individual *G. salaris* parasite may take to infect a new uninfected host. Individual parasites can move from an infected fish to an uninfected fish via direct fish to fish contact; from a substrate (detached) to an uninfected fish via fish to parasite contact; from a dead infected fish to a live uninfected fish via fish to fish contact and from the water column (detached) to uninfected fish via fish to parasite contact. These four routes were identified by Bakke *et al.* (1992b). Parasites can also move from an infected fish to another less/more infected fish. The most common of these routes is direct contact between a susceptible and infected fish, for example when a susceptible fish contacts an infected fish. *Gyrodactylus salaris* lacks the ability to swim but is able to jump from one host to another that is in close proximity (Bakke *et al.*, 1992b; Soleng *et al.*, 1999a).

#### 1.3.2.2 *Transmission between rivers*

In addition to the four main routes a parasite might take to infect a susceptible host, Peeler *et al.* (2004) proposed that the movement of live infected fish and mechanical transmission of free-living parasites on fomites (objects capable of spreading the parasite) are the two main routes of transmission between rivers. They identified four categories that movement of live fish can be split into:

- Movement of live rainbow trout or Atlantic salmon;
- Movement of other live fish species that *G. salaris* can survive on for short periods of time but not reproduce;
- Migration of eels overland between river catchments;
- Movement of Atlantic salmon in low-salinity water between rivers entering an estuary in close proximity.

Movement of live rainbow trout or Atlantic salmon has been identified as the most important transmission route of *G. salaris* to the UK (Peeler *et al.*, 2004).

### 1.3.2.3 Mechanical transmission

As mentioned above, an important route of transmission between rivers is via mechanical means. Peeler *et al.* (2004) identified four potential routes of mechanical transmission by fomites:

- Movement of any farming equipment, vehicles, staff, *etc.* that has been in contact with infected water or hosts;
- Any angling equipment that has been in contact with infected fish (such as keep nets) if reused within a few days on a different location;
- Movement of boats, canoes and leisure craft that contain infected water between river catchments;
- Movement of eggs from an infected hatchery that have not been disinfected.

Any of the items mentioned above that have come into contact with infected water or hosts can potentially spread the parasite to a new location if they have not been thoroughly disinfected. Mechanical transmission has been identified as a potential route of entry for *G. salaris* to the UK (Peeler *et al.*, 2004; Peeler & Thrush, 2004).

There are other possible routes that could potentially spread the parasite. For example, piscivorous birds may eat an infected fish then regurgitate it by a river in a different location (Peeler *et al.*, 2004).

As mentioned above, *G. salaris* can survive and reproduce indefinitely on Atlantic salmon but cannot survive full strength salinity, hence, the parasite mainly infects juvenile salmon, *i.e.*, fry and parr, resulting in fewer smolts migrating to the sea.

### 1.3.3 Host-parasite-environment interactions

The way in which hosts, parasites and even the external environment interact with one another plays an important role in the spread of *G. salaris* infections. Within rivers, factors such as water flow, pH, salinity, quality and temperature as well as the composition of the gravel, climate and competition all have a direct effect on the salmon population (Mills, 1999). The composition of the gravel on the bed of a river and the temperature of the water are particularly important in the early part of the salmon life-cycle, mainly the spawning and intra-gravel stages, and determine hatching times (Crisp, 1981, 2000). It is worth noting that young salmon parr spend the majority of their time in close proximity to the gravel (during resting periods) and are continuously brushing over the substrate (Crisp, 1981), this may lead to infection by detached parasites. The external environment also has an impact on the parasite.

In situations where water velocity is high, detached parasites have the potential to drift further down a river and infect new populations of hosts. Infection may also have an impact on the way in which salmon interact with each other, for example, in populations of guppies, *Poecilia reticulata*, (where individuals are infected with *Gyrodactylus turnbulli*) females have been observed preferring, and selecting, males with low parasite burdens (Kennedy *et al.*, 1987), changes in feeding behaviour have also been witnessed (van Oosterhout *et al.*, 2003). It is also worth noting that juvenile Atlantic salmon are highly territorial (see Section 3.2) and hence have a high chance of becoming infected due to fish to fish contact when defending a territory against an infected individual.

#### 1.3.4 Treatment

*Gyrodactylus salaris* parasites are eliminated by most disinfectants (Peeler *et al.*, 2006), aqueous aluminium at 202µg Al/l (after a period of four days) (Soleng *et al.*, 1999b), acidic aluminium-poor water at a pH of 5 (after 9 days) (Soleng *et al.*, 1999b) and the poison rotenone (Johnsen & Jensen, 1991). However, the majority of these treatments also result in host mortality. In order to prevent the spread of *G. salaris* and remove it from all infected rivers and hatcheries the Norwegian salmon authorities quickly adopted the use of the ATPase inhibitor, rotenone. Rotenone is a biocide that exhibits insecticidal, piscicidal and acaricidal properties. It occurs naturally and is obtained from the roots of several tropical plants (IPCS-INCHEM, 1992). Rotenone is highly toxic to all living organisms, this is especially the case with fish as the chemical is absorbed more quickly through the gills. Rotenone acts at a cellular level making it impossible for fish to use oxygen, after which the synthesis of adenosine triphosphate (ATP) ceases and death quickly follows. When added to an infected river rotenone destroys all life, fish and plant alike, resulting in the eradication of the *G. salaris* infection due to lack of hosts (Holm *et al.*, 2003). The Vikja was the first river in Norway to be treated with rotenone and took place on November 1981, then again in May 1982 with subsequent monitoring of salmon and trout populations each year there after. As a result of the treatment *G. salaris* was eradicated from the river Vikja (Johnsen & Jensen, 1991). The use of rotenone in this way in other EU countries is unlikely as it would break the Water Framework Directive (WFD). As mentioned above aqueous aluminium and many disinfectants can also be used to treat infected rivers (Soleng *et al.*, 1999b; Peeler *et al.*, 2006). At present the use of acidified aluminium sulphate is under development by Norwegian authorities as a means of eradicating *G. salaris* from infected rivers without killing host species (Sviland *et al.*, 2012).



Figure 1.9: The Atlantic salmon (*Salmo salar* L.). A species of anadromous fish that is indigenous to both sides of the Atlantic Ocean as well as the rivers which flow into it. These fish spend the majority of their juvenile life in freshwater and adult life at sea, only returning to its natal river to spawn. Adult males are able to grow to 1.5 m in length and 36 kg in weight, whereas adult females can grow to a maximum of 1.2 m and 20 kg. Image source: <http://www.public-domain-image.com>

#### 1.4 THE ATLANTIC SALMON (*SALMO SALAR* L.)

The Atlantic salmon (Figure 1.9) is the primary host for the parasite *G. salaris*, it is a species of anadromous fish (fish that spawn in freshwater, migrate to the ocean to grow before returning to freshwater to spawn again). It is indigenous to both sides of the Atlantic Ocean as well as the rivers which flow into it. It is of the genus *Salmo* and is a member of the Salmoninae, a subfamily of the Salmonidae family. The Atlantic salmon was first given its binomial classification, *Salmo salar*, in 1758 by the Swedish botanist and zoologist Carolus Linnaeus (Verspoor *et al.*, 2007).

##### 1.4.1 *Life-cycle*

The Atlantic salmon spends the majority of its juvenile life in freshwater and the rest of its life at sea, where it matures into an adult, before returning to its natal river to spawn. It is worth noting that some salmon get lost on return from the sea and spawn in a different river to their natal one. Due to this anadromous process, and the fact that salmon go through many biological and physiological changes from egg to adult, they have a multi-stage life-cycle (Figure 1.10).

There are seven stages in the salmon life cycle:

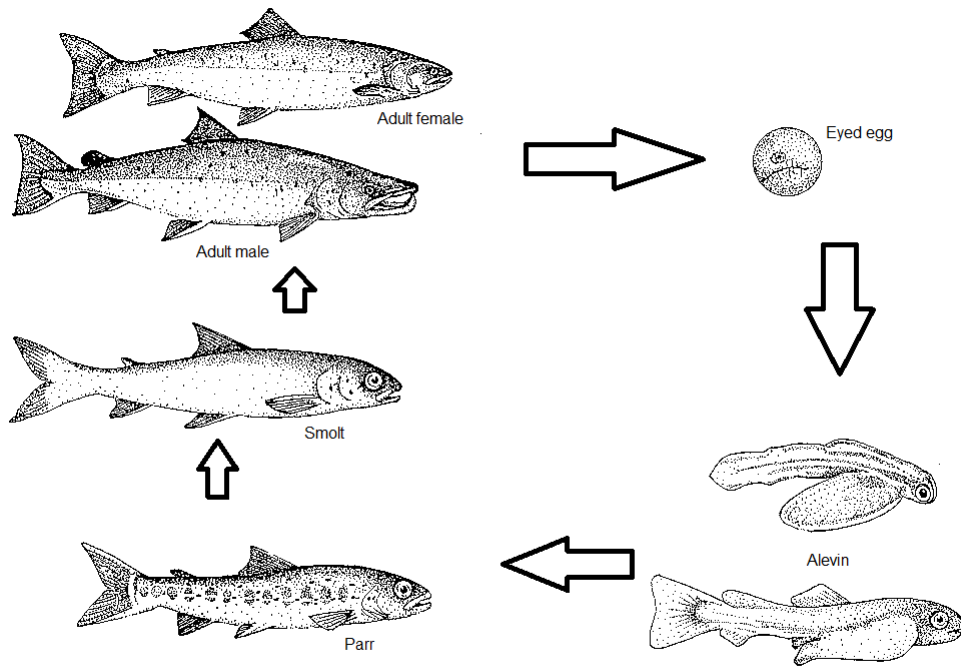


Figure 1.10: Diagram showing the Atlantic salmon life-cycle and its various stages. Salmon images source: <http://commons.wikimedia.org>

Alevin → Fry → Parr → Smolt → Post-smolt → Salmon → Kelt

The first three stages occur exclusively in fresh water and the last four occur in both fresh and salt water (Shearer, 1992). A salmon can spend up to 4 years in freshwater but on average spend around 2 years in a river before running to sea (Hendry & Cragg-Hine, 2003). An adult at the salmon stage is referred to as a grilse, after spending one winter at sea, or a multi-sea winter (MSW) salmon, after spending more than one winter at sea. Salmon can spend a maximum of 10 years at sea but most commonly spend anything from 1 to 6 years there (Hendry & Cragg-Hine, 2003). Salmon are referred to a kelt once they have spawned (Hendry & Cragg-Hine, 2003).

#### 1.4.1.1 Redd formation and spawning

The first stage in the salmon life-cycle takes place in a gravelly area of a freshwater river, usually between mid October and late February (Shearer, 1992), spawning is seasonal and hence a discrete process. The female salmon selects a site in which there is clean flowing water and gravel that is of an appropriate size and composition. Once a suitable site has been selected, the female begins to dig a pit in the river bed by repeatedly turning on her side and making exaggerated swimming motions. This process dislodges the gravel which is then carried slightly downstream by the flow of the river and results in the creation of a pit with a tail of gravel directly downstream of it. The female salmon then lowers her anal fin into the newly created pit to test the flow of water at the bottom (if for any reason the pit is deemed

unsatisfactory it is abandoned, creating a false redd, and a new site is selected and the pit creation process is repeated). If the pit location is satisfactory the female will deposit eggs which are fertilized by a male salmon. A female salmon will lay approximately 1,100 eggs per kilogram of her body weight (Hendry & Cragg-Hine, 2003). Hence, a small female grilse weighing 2.3 kg will lay approximately 2,500 eggs whereas a large multi seas winter female weighing 8 kg will lay in excess of 8,800 eggs (Hendry & Cragg-Hine, 2003). At this point a new pit is excavated immediately upstream and any dislodged gravel is carried downstream, concealing the eggs in the first pit. The entire process is repeated until one or more pits contain fertilized eggs, at this point the complete structure is referred to as a redd. A redd is usually guarded by a dominant male who will defend the redd site, as well as the female, from other males until spawning is complete (Crisp, 2000).

#### 1.4.1.2 *Intra-gravel and juvenile stages*

The early part of the salmon life-cycle takes place exclusively in the gravel (as opposed to the silt, rock, *etc.*) of the river bed. These stages are known as the intra-gravel stages and their duration in this state depends on the temperature of the water. The first stage occurs when the eyes of the embryo can be seen through the egg shell, at this point the eggs are known as “eyed eggs”. After a period of time (approximately 38 days at 12°C; Crisp, 1981) the eggs hatch into “alevin”, hatching times are directly dependent on water temperature. Crisp (1981) proposed a model to estimate the hatching times of salmonids at different temperatures developed using information on temperature (°C) and time from fertilization to 50% hatch (in days) for five species of salmonid fishes (brown trout, brook trout, rainbow trout, Chinook salmon and Atlantic salmon). He proposed that by incorporating a temperature correction factor (Equation 1.2) a better fit was obtained to that obtained by the basic model (Equation 1.1). The two models are as follows:

$$\log D = b \log T + \log a \quad (1.1)$$

$$\log D = b \log(T - \alpha) + \log a \quad (1.2)$$

where T is temperature (°C), D is time from fertilization to 50% hatch (days),  $\alpha$  is a temperature correction in °C and a and b are constants. Values of the constants  $\alpha$ , a and b are given in Table 2 found in Crisp (1981). Using these equations Crisp determined both models were able to produce a good fit to the data, accounting for 94% or more of the variance of D in its regression on T, for each of the five salmonid species. He also highlighted that the second model, Equation (1.2), gave the best fit, accounting for over 97% of the variance of D.

The alevin remain in the gravel for up to two months feeding on residual egg yolk which it carries in a yolk sac located on the underside of the body. The mass of the yolk sac decreases as the alevin grows due to the consumption of the yolk. When the yolk sac is almost empty the alevin makes its way through the gravel into the river. At this point the intra-gravel stages are over, the alevin now fills its swim bladder with air, for buoyancy, and begins to forage. From this point the alevin are renamed “fry”. Newly emerged fry quickly leave the redd and take on feeding stations. Salmon are highly territorial and the fry waste no time in establishing territories and defending them. At this point a change in appearance can be observed as the fry develop dark, vertical markings, known as “parr marks”, along its sides. When this happens the fry are renamed “parr” (Crisp, 2000).

#### 1.4.1.3 *The smolting process*

The juvenile salmon remain in the river as parr for one to four years (0+ parr, 1+ parr, 2+ parr and 3+ parr, Table 1.2) (Shearer, 1992) before going through the “smolting” process. This is the process in which salmon go through hormonal and physiological changes that allow them to migrate and live in salt water. The salmon lose their parr marks and take on a silvery appearance, the darkening of the edges of the pectoral and caudal fins also occurs. Smolting is thought to occur when parr reach a certain size, usually 12.5 to 17.0 cm in length (Crisp, 2000). At this point in the life-cycle the parr are renamed “smolts”. After smoltification is complete, new smolts begin their journey downstream to the sea. A small proportion of the male parr population become sexually mature in fresh water and may stay there to attempt to participate in the spawning of the mature salmon that return from the sea, these are called “precocious male parr” (Crisp, 2000).

Table 1.2: Salmon parr classifications. Description of salmon in the various parr classes as described by Shearer (1992).

<b>Term</b>	<b>Description</b>
0+ parr	Parr that are less than 1 year old (from previous years hatch)
1+ parr	Parr that are 1 year or over but less than 2 years
2+ parr	Parr that are 2 year or over but less than 3 years
3+ parr	Parr that are 3 year or over but less than 4 years
Precocious male parr	Male parr that become fully mature in fresh water
Partially silvered parr	Parr that become partially silvered and begin to migrate downstream prior to the normal smolt run

#### 1.4.1.4 *Life at sea*

When smolts enter the sea their growth rates rapidly increase and they embark on long distance journeys, sometimes reaching the Norwegian Sea or areas of Greenland (Shearer, 1992). Smolts may remain at sea for one or more winters before returning to their natal river to spawn. If they return to freshwater after one winter at sea they are referred to as grilse or

“one-sea-winter-fish”. If they return to freshwater after more than one winter at sea they are referred to as mature adult salmon or “multi-sea-winter-fish” (Crisp, 2000).

#### 1.4.1.5 *Return to natal river*

After spending between 1 and 4 winters at sea, salmon tend to return to their natal tributary in their natal river to spawn (Crisp, 2000). The homing ability of salmon is a well known and much studied topic. It is thought that imprinting with the smell of the natal stream during early life is an important factor in developing the homing mechanism (Crisp, 2000). Even though many salmon accurately navigate their way home a proportion of them do not make it back to their natal tributary, which results in them spawning in the wrong river. This can be due many factors such as obstructions and obstacles or as a result of a malfunction of their homing mechanism. Nevertheless, after spawning, the salmon are referred to as “kelt”. The majority of kelts die, this is in part due to starvation as returning salmon only feed at sea (Jones, 1959). Studies of salmon in the Scottish River Conon over a period of 6 years showed survival and return to sea of post-spawning kelts was between 20 and 36% (Hendry & Cragg-Hine, 2003). However, some do find their way back to sea and return to fresh water to spawn on one or more subsequent occasions (Crisp, 2000).

#### 1.4.2 *Territories*

An important aspect of Atlantic salmon behaviour is the establishment and defence of territories. Territorial behaviour is observed in juvenile salmon (fry and parr) but not in post-smolt salmon which are less aggressive and live in “schools” (Keenlyside & Yamamoto, 1962; Crisp, 2000). After establishing its territory the young salmon rests near the substrate, only moving to feed or chase away intruders, and in doing so ensures seclusion from others (Keenlyside & Yamamoto, 1962). Hence, juvenile Atlantic salmon tend not to live in groups. Territory-holding salmon spend the majority of their time in one position, called a station, within their territory. From here they remain still, sometimes in contact with the substrate if the current is particularly strong (Keenlyside & Yamamoto, 1962). From within a territory, its holder will exhibit threatening motions to deter any intruders that approach. If an intruding fish continues to approach the defending fish will move off its station and dash towards the intruder, chasing it back out the territory (Keenlyside & Yamamoto, 1962).

##### 1.4.2.1 *Agonistic behaviour*

When defending its territory a young salmon will demonstrate six elements of agonistic behaviour. Agonistic behaviour is any social behaviour related to fighting and is often witnessed in animal species when resources are limited (Scott & Fredericson, 1951). Keenlyside & Yamamoto (1962) classed these six elements as:

1. Charging - territory holder quickly swims towards the intruder;
2. Nipping - attacking fish biting another fish after a charge or during an approach in lateral display. Generally, the attacker will nip the the tail of the other fish;
3. Chasing - repeated charging, with nipping attempts on the retreating fish;
4. Frontal display - demonstrated by territory holder when approaching another fish (head pointed towards opponent);
5. Lateral display - demonstrated by two aggressive fish when fighting during defence of their territories (side shown to opponent);
6. Fleeing - demonstrated by non-aggressive fish being chased and attacked by territory holders.

There are generally two reasons for a territory-holding fish to leave its station (1) to defend the territory from an intruder and (2) to feed. In the second situation the territory-holder quickly moves away from the station in search of food before quickly swimming back to the exact position it came from (Keenlyside & Yamamoto, 1962). Territories are generally situated close to a valuable source of food (Kalleberg, 1958; Keenlyside & Yamamoto, 1962; Crisp, 2000). This suggests that the territories are primarily established as feeding territories (Kalleberg, 1958; Keenlyside & Yamamoto, 1962).

#### 1.4.2.2 *Territoriality in an aquarium*

In laboratory conditions Keenlyside & Yamamoto (1962) observed the following: one fish will emerge as the dominant fish with the largest territory. This fish will expand its territory over time and “win” fights with any other fish that have established a territory until it is the only territory holder. When this happens the other fish become submissive and group together in close proximity to a wall of the aquarium and rarely challenge the territory holder. The dominant fish will generally ignore the submissive fish as long as they do not venture into its territory. If a submissive fish does leave the group the dominant fish darts towards it and attacks until the submissive fish retreats back to the group. When food is added the submissive group dispatches and all fish, including the dominant territory holder, take part in feeding activities for a short period of time, after which the dominant fish chases all fish out of its territory and the *status quo* is restored.

## 1.5 MATHEMATICAL MODELLING

### 1.5.1 *A brief history of infectious disease modelling*

Mathematics, of some form, has been used to study disease for hundreds of years. In 1662 John Graunt used rudimentary numerical methods (in this case statistics) in his study of the *Bills of Mortality* for London parishes in order to determine the causes of death of 229,250 people whom had died over a period of 20 years, and thus, enabling him to compare the potential hazards of diseases present in the population at the time (Gani, 2009). The earliest evidence of a mathematical model being used to study disease and is attributed to Daniel Bernoulli (1700–1782) in his study of the effectiveness of variolation (vaccination) techniques against smallpox in 1760 (Anderson & May, 1991; Dietz & Heesterbeek, 2002). However, deterministic models did not appear until the early 20<sup>th</sup> Century. Hamer’s study of measles in 1906 resulted in the first statement of the so called “mass action principle”. Hamer (1906) noted that the rate at which susceptible hosts come into contact with infectious hosts has a direct effect on the course that an epidemic might take. Building on Hamer’s discrete model Ross formulated a continuous-time model in his studies of malaria (Anderson & May, 1991). Then in 1927, Kermack & McKendrick theorised that in a population an epidemic cannot occur if the population density is below a certain threshold value. The mass action principle combined with threshold theory make up a basis for the mathematical modelling of epidemics.

### 1.5.2 *Modelling host-parasite interactions*

The relationship between host and parasite populations can be thought of as an extension of the general predator-prey interaction. However, in order to model disease one must distinguish between microparasites and macroparasites. This is particularly the case for *G. salaris* in that it is a macroparasite that has micro-parasitic qualities, the reasons for which will be described in the following sections.

#### 1.5.2.1 *Microparasites*

Microparasites, for example bacteria, viruses, *etc.*, are those parasites that have direct reproduction within the host. Microparasites generally have a very high reproduction rate, short generations times and are very small in size. In order to study the effects of microparasites the host population can be split into several discrete categories (see Table 1.3).

This type of model is called a compartmental model (Anderson & May, 1991) and is commonly referred to as an SIR (susceptible-infected-recovered) model. A schematic repres-

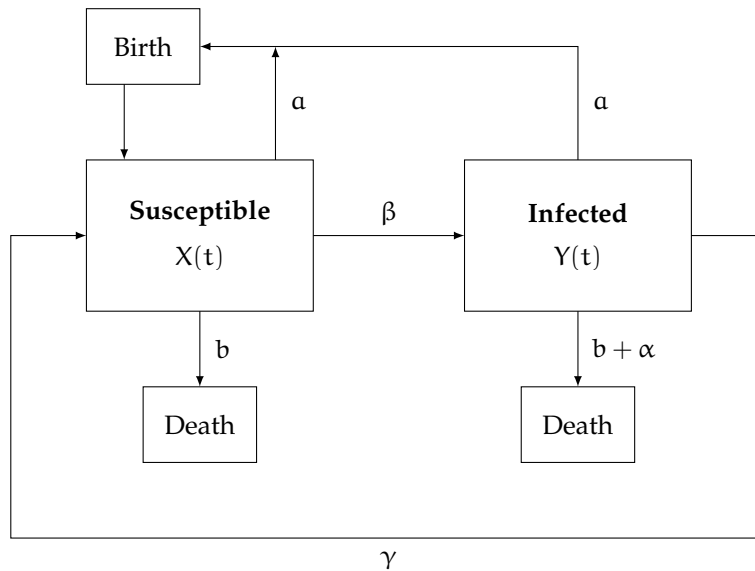


Figure 1.11: Schematic representation of a host-microparasite interaction

Table 1.3: Definition of host classes. Descriptions of host classes used in SIR type models.

Class	Description
Susceptible	Members of the population who are vulnerable to infection
Latent/Exposed	Members of the population who are infected but not yet infectious
Infected	Members of the population who are infectious
Recovered/Immune	Members of the population who are no longer infected

entation of such a model is given in Figure 1.11. In this situation susceptible hosts become infected and pass into the infected class where there is an additional “parasite induced” death rate. If the host survives then it may pass into the recovered class and become immune for a short period of time (indefinitely in some cases) or pass back into the susceptible class and become reinfected.

Anderson & May (1981) derived the basic fundamental microparasite model (SI model):

$$\frac{dX}{dt} = \alpha(X + Y) - bX - \beta XY + \gamma Y \quad (1.3)$$

$$\frac{dY}{dt} = \beta XY - (\alpha + b + \gamma)Y \quad (1.4)$$

Where  $\frac{dX}{dt}$  is the rate of change of the susceptible host population  $X(t)$  and  $\frac{dY}{dt}$  is the rate of change of the infected host population  $Y(t)$ . Here birth rate,  $\alpha$ , is independent of infection, giving a net birth rate of  $\alpha(X + Y)$ . Susceptibles become infected at a rate  $\beta$ , the transmission coefficient, and die at a rate  $b$ . Infected individuals die at a rate  $b + \alpha$ , where  $\alpha$  represents parasite induced host mortality. Finally, if an infected individual survives infection they pass back into the susceptible class at a rate  $\gamma$ . Anderson & May (1981) then modified

their basic model to deal with (a) parasite induced reduction of host reproduction; (b) vertical transmission; (c) latent periods of infection; (d) disease and stress; (e) density dependent constraints and (f) free-living infective stages.

### 1.5.2.2 Macroparasites

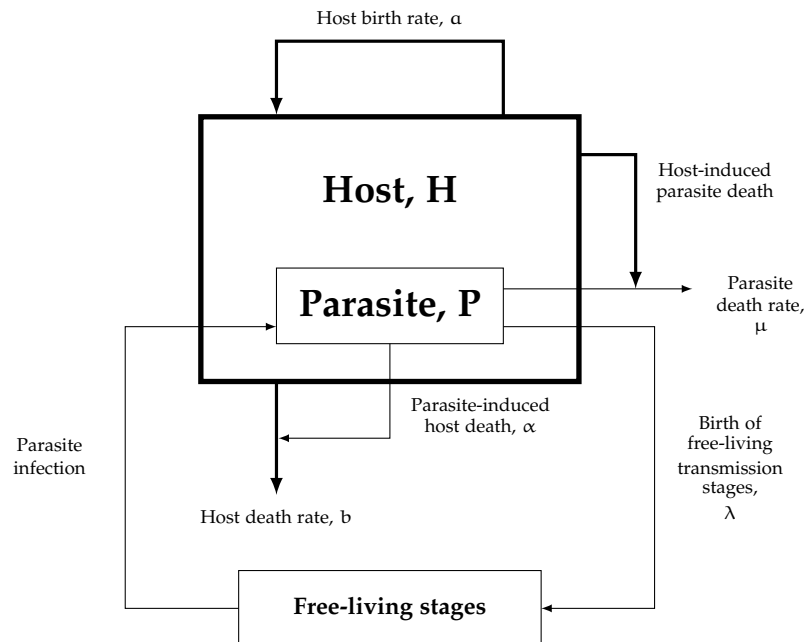


Figure 1.12: Schematic representation of a simple host-macroparasite interaction

Macroparasites, for example helminths, arthropods, *etc.*, are those parasites that have no direct reproduction within the host (Anderson & May, 1991). They are generally much larger than microparasites and have longer generations times. In general reproduction and infection is via transmission stages. Host-macroparasite interactions are represented by distributional models in contrast to the compartmental models used to study microparasites (Anderson & May, 1991). A schematic representation of such a model is given in Figure 1.12. These distributional models are more complicated than the compartmental ones in that they must take into account the distribution of the parasites among the hosts (Anderson & May, 1991).

Anderson & May (1978) and May & Anderson (1978) defined the fundamental macroparasite model on which modern models are based. This model assumes reproduction occurs off the host via transmission stages such as spores or eggs that pass out of the host:

$$\frac{dH}{dt} = (\alpha - b)H - \alpha P \quad (1.5)$$

$$\frac{dP}{dt} = \frac{\lambda PH}{H_0 + H} - (b + \mu)P - \alpha H E_t(i^2) \quad (1.6)$$

Here  $\frac{dH}{dt}$  is the rate of change of the total host population with  $\frac{dP}{dt}$  describing the rate of change of the total parasite population within the hosts.  $H(t)$  and  $P(t)$  are the magnitudes of the host and parasite populations at time  $t$ , hence, the average number of parasites per host is  $\frac{P(t)}{H(t)}$ . In this model hosts are born at rate  $a$  and die due to natural causes at rate  $b$ . Hosts also die due to infection at rate  $\alpha$ . In this model parasites give birth to free living transmission stages which pass out of the host, these stages are produced at rate  $\lambda$ . Since free-living infective stages have a short life-span this model assumes that such short-lived infective stages are adjusted to equilibrium almost immediately for any  $H$  and  $P$ . Transmission occurs at rate  $H/(H_0 + H)$ , where  $H_0$  is a constant which determines the efficiency of transmission (Anderson & May, 1978). Hence, the net rate of parasite gain within the host population is  $\lambda PH/(H_0 + H)$  with the assumption that transmission occurs almost instantaneously. Finally, parasites die due to natural causes at rate  $\mu$  and also die when the host dies. As mentioned above host mortality is split into two categories, natural mortalities and parasite induced mortalities, hence, parasites die due to natural host mortalities at rate  $b$  and parasite induced host mortalities at rate  $\alpha E_t(i^2)$ , where  $E_t(i^2)$  depends on the form of the probability distribution of parasite numbers per host (Anderson & May, 1978). A summary of the parameters is given in Table 1.4. Anderson & May (1978) and May & Anderson (1978) modified their basic model to include (a) non-random parasite distributions; (b) non-linear parasite induced host deaths; (c) density dependence in parasite population growth; (d) parasite induced reduction in host reproduction; (e) parasites that reproduce within their hosts and (f) the influence of time delays. Dobson & Hudson (1992) extended the Anderson & May (1978) and May & Anderson (1978) models to look at the dynamics of free-living and arrested larval stages of the parasite.

Table 1.4: Description of parameters (Anderson & May, 1978). Descriptions of the population parameters used by Anderson and May in their models (Anderson & May, 1978).

Parameter	Description
$a$	Host birth rate
$b$	Host death rate
$\alpha$	Host death due to parasite
$\lambda$	Birth rate of parasite transmission stages
$\mu$	Parasite death rate due to natural or host induced causes
$H_0$	Transmission efficiency constant

### 1.5.3 Modelling of *Gyrodactylus* infections

In 1984 Scott & Anderson published a study concerning *Gyrodactylus turnbulli* which explored SIR models with parameter values based on experimental data carried out on laboratory populations of guppies. Their aim was to determine which factors directly influence parasite

transmission dynamics. Then in 1993, des Clers developed age structured population models to study the effects of *G. salaris* on different stages of the salmon life-cycle.

Other techniques, such as Monte Carlo models, have also been employed to study *G. salaris* on salmon (Paisley *et al.*, 1999; Hogasen & Brun, 2003). Paisley *et al.* (1999) used this modelling technique to assess the risk of introduction of *G. salaris* to the Tana river in Norway, whereas Hogasen & Brun (2003) used the same technique to estimate the risk of inter-river transmission of *G. salaris* by migrating Atlantic salmon smolts.

The work by Peeler *et al.* (2004), Peeler & Thrush (2004) and Peeler *et al.* (2006) concerned the use of qualitative risk assessment and analysis techniques to highlight routes of transmission and risk of introduction of *G. salaris* into UK and the risk of the spread of *G. salaris* to uninfected areas of Europe and was discussed in depth in Section 1.2 above.

Jansen *et al.* (2007) used a dispersal model to study the risk of secondary infections by examining the hypothesis of inter-river dispersal of the parasites whereas van Oosterhout *et al.* (2008) used an individual-based computer model to forecast gyrodactylid infections on fish hosts.

Finally, more recent modelling work has been carried out by Ramírez *et al.* (2012). In their study they propose an individual agent-based model of *G. salaris* infection on a single salmon host in order to estimate the error in gyrodactylid population growth rates subject to stochastic variation in survivorship and reproduction. The model was simulated assuming two contrasting death functions; constant death of parasites throughout the simulation, and secondly, a parasite death that is positively correlated with parasite age (probability of death increases with parasite age) as in Cable *et al.* (2000). Their results highlighted the fact that estimates of the error structures of population growth rates follow a normal distribution, especially in populations greater than 20 parasites in size, and that this rate can be a useful parameter for comparing gyrodactylid populations that are in excess of 20 - 30 parasites. However, in cases where less than 20 parasites are present in a population the error is disproportionately large making comparison of gyrodactylid population growth on different hosts via the population growth parameter less useful (Ramírez *et al.*, 2012). The results obtained by Ramírez *et al.* (2012) showed that declining parasite population growth rates cannot be explained through stochastic error, and hence, must be rooted in biology. They conclude that the majority of gyrodactylid-host studies, that are of a similar nature to that found in their work, are not large enough to allow the successful detection of subtle differences in local adaptation of gyrodactylid monogeneans between fish stocks.

As can be seen, until now there has not been a great deal of modelling work concerning the dynamics of *G. salaris* infections on populations of Atlantic salmon, with the majority of work concerning *G. salaris* being centred on using statistical and computer models for assessing and estimating the risk of the parasite's spread to new rivers (Paisley *et al.*, 1999; Hogasen & Brun, 2003; Peeler *et al.*, 2004; Peeler & Thrush, 2004; Peeler *et al.*, 2006; Jansen *et al.*, 2007; van Oosterhout *et al.*, 2008). Some work has been carried out on other gyrodactylid species, for example, the host-parasite dynamics of *G. turnbulli* (known as *G. bullatarudis* at the time, Harris 1986) on guppies has been studied extensively by Scott & Anderson (1984); Scott (1985); Leberg & Vrijenhoek (1994); Richards & Chubb (1996). Hence, there is much scope, and requirement, for models of host-parasite interactions with respect to the *G. salaris* - salmon system. Also, in addition to understanding the short term dynamics there is a pressing need to understand the long term consequences of infections by the parasite.

## 1.6 THESIS AIM AND STRUCTURE

The aim of this thesis is to develop a model of the *G. salaris* - Atlantic salmon disease system to enable predictions to be drawn on the long-term consequences/impact of infections in territories that are free from *G. salaris*, with particular emphasis on the United Kingdom. Model results are also used to make recommendations, assist with contingency planning and strategies and highlight areas where more study is required. The models that are found in the chapters that follow use the differential equations of Anderson & May (1978) and May & Anderson (1978) as a foundation and extend them for the *G. salaris* - Atlantic salmon system. All models appear in the text and are collected in Appendix B. Where possible, algebraic analysis of equilibria is carried out to determine conditions for stability. Such analysis can be found collected in Appendix C for information. Appropriate mathematical computer software is employed in cases where systems contain a large number of complicated ODEs making algebraic analysis by hand difficult, if not impossible. Wolfram Mathematica<sup>TM</sup> version 8 (2008) is used to program all models and enable the running of simulations, giving predictions for both short-term and long-term dynamics of *G. salaris* and salmon populations. Selected Mathematica code is provided in Appendix D.

Chapter 1 gives an introduction to the witnessed impact of *G. salaris* infections in Norway and background information on the biology and behaviour of both *G. salaris* and its Atlantic salmon host as well as models of gyrodactylid infections. It also provides an insight into the current status of *G. salaris* in the U.K. and gives justification for this thesis.

Chapter 2 sets out the basic model and considers density dependence in the host population.

Chapter 3 considers the addition of a detached parasite population present in the external environment, investigates the occurrence of parasite induced extinction of the host population and determines the effect of parasite distribution. The final model put forward in this chapter serves as the basis for those that follow it.

Chapter 4 takes a contrasting approach, making use of Leslie and individual based models to investigate the behaviour of *G. salaris* on individual fish of different strains of Atlantic salmon and the possible mechanisms required for resistance to infection. Model predictions are used to determine which mechanism has the largest impact on the dynamics.

Chapter 5 explores the inclusion of host immunity to parasite infection. The effect of immunity on the model dynamics is investigated via the addition of a trade-off on host birth. Models presented include a baseline immunity model as well as trade-off model.

Chapter 6 considers a multiple strain model with  $n > 2$  salmon strains (*e.g.*, Atlantic, Baltic) and one *G. salaris* strain that displays differing behaviour on each host (as in Chapter 4). Model predictions are used to determine which salmon strains, if any, will win over time and how long host recovery from infection might take.

Chapter 7 provides a discussion of the model results and seeks to answer key policy questions regarding the long-term consequences of *G. salaris* infections. Knowledge gaps and possible future work is highlighted.

Appendix A collects the various data sources from the literature that have been used for parameter estimation throughout this thesis.

Appendix B collects all the models presented herein.

Appendix C contains algebraic analysis of the models in the thesis.

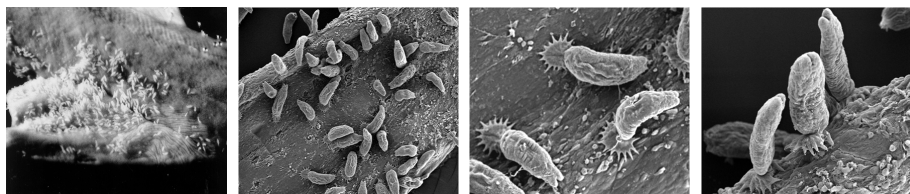
Appendix D contains model and sensitivity analyses.

Appendix E provides selected Mathematica code for model simulations.

Part II

MY CONTRIBUTION

## The basic model and density dependent hosts



Images of *G. salaris* infected salmon at different magnifications obtained via a Scanning Electron Microscope (SEM) courtesy of Dr Andy Shinn.

### 2.1 INTRODUCTION

In general *Gyrodactylus salaris* is a very interesting parasite, this is especially true from a mathematical modelling point of view. This is in part due to the fact that *G. salaris* is a macroparasite with a life-cycle that exhibits microparasitic qualities. As mentioned in Section 1.3.1 individual progenic parasites give birth to fully grown pregnant offspring. This occurs directly on the skin of the host removing the requirement for a free-living transmission stage or transmission via a vector. When thinking of the *G. salaris* life-cycle one must first decide whether to use compartmental models or distributional models. As mentioned in Chapter 1, SIR style compartmental models are traditionally used to model microparasite infections which would suit the birthing method and short generation times of *G. salaris* parasites, however, the parasite itself is an ectoparasite which is traditionally modelled using distributional models. Hence, due to this and our interest in how host and parasite densities change over time, it was decided that the latter would be best to model the dynamics of *G. salaris* infection.

### 2.2 CONSTRUCTING THE BASIC MODEL

In order to study the interaction between *G. salaris* and Atlantic salmon (*Salmo salar*, L.) we require equations for the the salmon host population and the on-host *G. salaris* population. We hence form these equations by assuming the following:

For salmon hosts

- New hosts are born at rate  $a$ ;
- Individual hosts die from natural causes at rate  $b$ ;
- Hosts can also die due to infection, this happens at rate  $\alpha$  and is assumed to be linearly proportional to the number of parasites infecting a host.

For *G. salaris* parasites

- New parasites are born at rate  $\mu$ ;
- Individual parasites die due to natural causes at rate  $\epsilon$ ;
- Parasites also die as a result of natural host death  $b$ , and parasite-induced host death  $\alpha H(t)E_t(i^2)$  where  $i$  is number of parasites and  $E_t(i^2)$  is the mean-squared number of parasites per host.

Figure 2.1 gives a schematic representation of a simple host-macroparasite system based on the macroparasite models by Anderson & May (1978) and May & Anderson (1978). In this case, and throughout this thesis, the term host refers to populations of Atlantic salmon and the term parasite refers to populations of *G. salaris* Malmberg, 1957. The host population (Atlantic salmon) has magnitude  $H(t)$  at time  $t$ , likewise, the parasite population (*G. salaris*) has magnitude  $P(t)$  at time  $t$ , hence, the average number of parasites per host is given by  $P(t)/H(t)$  (Anderson & May, 1978).

### 2.2.1 The basic model

As discussed earlier the models proposed and developed by Anderson & May (1978) and May & Anderson (1978) serve as the underlying models of our system and a more detailed description of the construction of the basic model (Equations 2.1 and 2.2) is given in Appendix B. The model, represented schematically in Figure 2.1, is described by the following set of differential equations:

$$\frac{dH}{dt} = (a - b)H - \alpha P \quad (2.1)$$

$$\frac{dP}{dt} = \mu P - (\epsilon + b)P - \alpha H E_t(i^2) \quad (2.2)$$

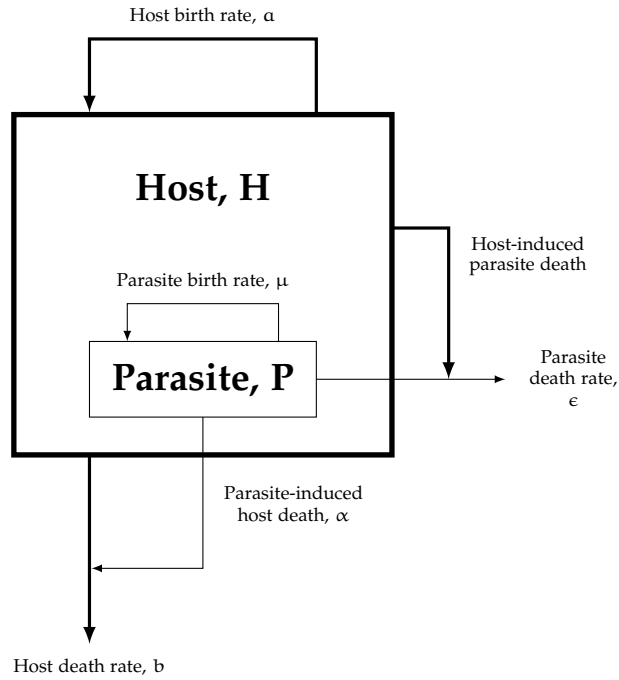


Figure 2.1: A schematic representation of a simplified Atlantic salmon-*G. salaris* system based on models proposed by Anderson & May (1978) and May & Anderson (1978).

$\frac{dH}{dt}$  and  $\frac{dP}{dt}$  represents the rate of change of the host population and the rate of change of the parasite population respectively. Table 2.1 gives a description of all parameters used by the models in this work.

Table 2.1: Description of parameters. Descriptions of the population parameters used in the models throughout this thesis.

Parameter	Description
$a$	Host birth rate
$b$	Host death rate due to natural causes
$s$	Density dependent constraint
$\mu$	Parasite birth rate
$\epsilon$	Parasite death rate (natural)
$\alpha$	Host death rate due to infection (depends on parasite)
$\lambda$	Rate that parasites leave hosts
$\sigma$	Detached parasite death rate (natural)
$\beta$	Transmission rate of detached parasites to new hosts
$\tilde{m}$	Immunity growth rate
$\zeta$	Immunity decay rate

Fish to fish transmission of the parasite is not explicitly modelled due to the fact that the model gives the total number of *G. salaris* parasites in the salmon population and not the number of *G. salaris* parasites on individual fish. Hence, if a parasite transfers from one salmon host to another the total size of the *G. salaris* population remains unchanged and the effect on the distribution of parasites is negligible.

As mentioned above the  $E(i^2)$  term represents mean-square number of parasites per host. This parameter depends on the probability distribution of parasites per host, and thus, on  $P(t)/H(t)$  (Anderson & May, 1978). Assuming parasites are independently randomly distributed among hosts we use the Poisson distribution to determine  $E_t(i^2)$ .

**Aside** (Anderson & May, 1978)

The probability generating function for the Poisson distribution is given as  $\Pi(Z) = \exp\{m(Z - 1)\}$ , where  $m$  is the average number of parasites per host. This has expectation and variance  $E(i) = m$  and  $\text{var}(i) = m$ . Hence, the expectation of  $i^2$  is  $E(i^2) = m^2 + m$ .

Adding the Poisson distribution into the system gives the following for the rate of change of the *G. salaris* population:

$$\frac{dP}{dt} = \mu P - (\epsilon + b)P - \alpha H \left( \frac{P^2}{H^2} + \frac{P}{H} \right) \quad (2.3)$$

$$= (\mu - \epsilon - b)P - \alpha \frac{P^2}{H} - \alpha P \quad (2.4)$$

$$= P \left( \mu - \epsilon - b - \alpha - \alpha \frac{P}{H} \right) \quad (2.5)$$

Hence, our expression for  $\frac{dP}{dt}$  is now given by:

$$\frac{dP}{dt} = P \left( \mu - \epsilon - b - \alpha - \alpha \frac{P}{H} \right) \quad (2.6)$$

Equation (2.1) together with equation (2.6) gives the basic model:

$$\begin{aligned} \frac{dH}{dt} &= (a - b)H - \alpha P \\ \frac{dP}{dt} &= P \left( \mu - \epsilon - b - \alpha - \alpha \frac{P}{H} \right) \end{aligned} \quad (2.7)$$

In order to study the dynamics of infection we perform an equilibria and stability analysis. The methods used to investigate equilibria and stability are outlined below and used throughout this thesis when such algebraic analyses are possible.

### *Equilibrium analysis*

To determine the existence of equilibria for a system of equations the standard methods of analysis are followed (Anderson & May, 1981; Murray, 2002, 2003) with equilibria found by setting the equations in the model to zero and solving for  $H$ ,  $P$ , etc.

### Stability of equilibria

The standard methods of analysis, as outlined by Anderson & May (1981), are employed to determine stability of equilibria. If small perturbations from equilibrium return to said equilibrium point (when certain conditions are met) then the system is locally stable. For each equilibrium point the resulting Jacobian matrix is calculated via

$$J(H, P) = \begin{pmatrix} \partial H_H & \partial H_P \\ \partial P_H & \partial P_P \end{pmatrix}$$

From the Jacobian, the characteristic equation and eigenvalues are obtained. If the eigenvalues of the Jacobian have negative real parts then the equilibrium point is locally stable.

#### Aside: Routh-Hurwitz Theorem

The Routh-Hurwitz Theorem tells us that all eigenvalues of a matrix, with characteristic polynomial of the form  $\lambda^n + a_1\lambda^{n-1} + \dots + a_{n-1}\lambda + a_n = 0$  (where  $a_i \in \forall\mathbb{R}$ ), are negative or will have negative real parts if and only if the determinants of all Hurwitz matrices are positive.

Hurwitz matrices are of the form:

$$H_n = \begin{pmatrix} a_1 & 1 & 0 & 0 & \dots & 0 \\ a_3 & a_2 & a_1 & 1 & \dots & 0 \\ a_5 & a_4 & a_3 & a_2 & \dots & 0 \\ \vdots & \vdots & \vdots & \vdots & \ddots & \vdots \\ 0 & 0 & 0 & 0 & \dots & a_n \end{pmatrix}, a_i = 0 \text{ if } i > n$$

For a polynomial of degree  $n = 2, 3, 4$ , conditions for  $\det(H_i) > 0$ ,  $i = 1, 2, \dots, n$ , are given in Table 2.2.

Table 2.2: Conditions for determinants of Hurwitz matrices to be positive for polynomials of degree  $2 \leq n \leq 4$ .

<b>n</b>	<b>Conditions</b>
2	$a_1 > 0$ and $a_2 > 0$
3	$a_1 > 0$ , $a_3 > 0$ and $a_1 a_2 > a_3$
4	$a_1 > 0$ , $a_3 > 0$ , $a_4 > 0$ and $a_1 a_2 a_3 > a_3^2 + a_1^2 a_4$

### 2.2.2 Equilibria and stability

#### Equilibrium analysis

As mentioned above, equilibria of the system are found by setting  $\frac{dH}{dt} = \frac{dP}{dt} = 0$  in the equations in (2.7) and solving for H and P.

$$(2.1) \Rightarrow 0 = (a - b)H - \alpha P \quad (2.8)$$

$$\Rightarrow \frac{P^*}{H^*} = \frac{a - b}{\alpha} \quad (2.9)$$

$$(2.6) \Rightarrow 0 = P \left( \mu - \epsilon - b - \alpha - \alpha \frac{P}{H} \right)$$

$$(2.9) \Rightarrow 0 = \mu - \epsilon - b - \alpha - \alpha \left( \frac{a - b}{\alpha} \right)$$

Hence, equation (2.6)  $\Rightarrow$  no  $(H^*, P^*)$  exist other than  $(0, 0)$ .

In this case the only equilibrium is the trivial (zero) equilibrium,  $(H, P) = (0, 0)$ , with no salmon hosts or *G. salaris* parasites. Hence, when disease is present ( $P > 0$ ), exponential growth occurs.

#### Stability analysis

The general form of the Jacobian for this model is as follows:

$$J(H^*, P^*) = \begin{pmatrix} a - b & -\alpha \\ \alpha \frac{P^{*2}}{H^{*2}} & \mu - \epsilon - b - \alpha - 2\alpha \frac{P^*}{H^*} \end{pmatrix} \quad (2.10)$$

The eigenvalues of Jacobian at  $(0, 0)$  are given by:

$$J(0, 0) = \begin{pmatrix} a - b & -\alpha \\ 0 & \mu - \epsilon - b - \alpha \end{pmatrix} \quad (2.11)$$

$$\lambda^2 + [\alpha + 2b + \epsilon - (a + \mu)]\lambda + (a - b)(\mu - \epsilon - b - \alpha) = 0 \quad (2.12)$$

The Routh-Hurwitz Theorem tells us that both eigenvalues of (2.11) will have negative real parts (which corresponds to a locally stable equilibrium point) if and only if both coefficients of (2.12) are positive. Hence (by the Routh-Hurwitz theorem),  $(0, 0)$  is locally stable if and

only if the conditions in (2.13) are satisfied. Biologically, this means we require birth rates to be lower than death rates in both salmon and *G. salaris* populations.

$$a < b, \quad \mu < \epsilon + b + \alpha \quad (2.13)$$

Here  $a < b$  is the condition on the salmon population and  $\mu < \epsilon + b + \alpha$  is the condition on the *G. salaris* population. The second condition is required so that there is no growth in the parasite population as the host population decays, there can be no parasites if there are no hosts.

As can be seen in Figure 2.2, when the inequalities in (2.13) are satisfied both the host and parasite populations quickly decay to zero. This is expected when host births are less than host deaths ( $a < b$ ) as *G. salaris* parasites require a host to survive. The inequalities in (2.13) also give two situations:  $\mu < \epsilon + a + \alpha < \epsilon + b + \alpha$  as seen in Figure 2.2a, and  $\epsilon + a + \alpha < \mu < \epsilon + b + \alpha$  as seen in Figure 2.2b. The rate of decay of the *G. salaris* population is dependent on that of the salmon population and whether  $\mu$  is greater or less than  $\epsilon + a + \alpha$  such that if  $\mu < \epsilon + a + \alpha$  the parasite population decays to zero faster than if  $\mu > \epsilon + a + \alpha$ .

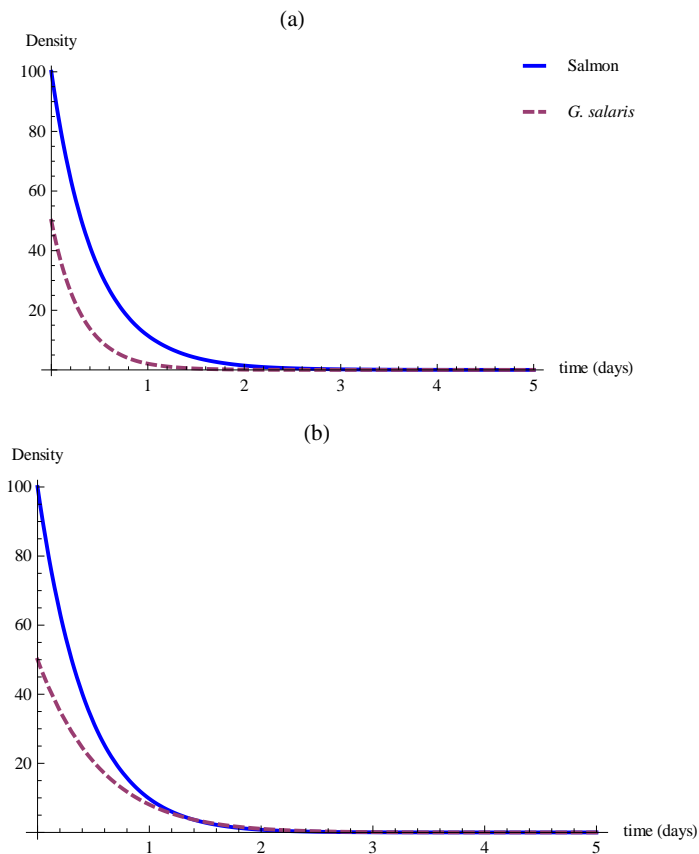


Figure 2.2: The zero equilibrium. Trajectories of host and parasite populations in time as predicted by the basic model. When host births are less than host deaths ( $a < b$ ) the host population, and hence the parasite population, decay to zero. (a)  $\mu < \epsilon + a + \alpha < \epsilon + b + \alpha$  (b)  $\epsilon + a + \alpha < \mu < \epsilon + b + \alpha$ . In both cases  $H(0) = 100$ ,  $P(0) = 50$ ,  $a = 3.0$ ,  $b = 5.0$ ,  $\epsilon = 0.5$  and  $\alpha = 0.5$ .  $\mu = 3.0$  and  $\mu = 4.5$  in (a) and (b) respectively. Hosts (—), parasites (---).

If the inequalities in (2.13) are not satisfied then four possible situations arise. These can be seen in Figure 2.3 and are as follows:

- $\mu < \epsilon + b + \alpha < \epsilon + a + \alpha$ , host growth with parasite death (Figure 2.3a);
- $\epsilon + b + \alpha < \mu < \epsilon + a + \alpha$ , host growth with small parasite growth (Figure 2.3b);
- $\epsilon + a + \alpha < \epsilon + b + \alpha < \mu$ , host death with initial parasite growth then decay (Figure 2.3c);
- $\epsilon + b + \alpha < \epsilon + a + \alpha < \mu$ , short epidemic ending in host and parasite death (Figure 2.3d).

As can be seen in Figure 2.3 (and as one would expect) when host births are greater than host deaths ( $a > b$ ) the host population is able to grow. This growth is exponential due to the fact that there is no density dependent constraint on the host population. Figure 2.3a ( $\mu < \epsilon + b + \alpha < \epsilon + a + \alpha$ ) shows that if  $\mu < \epsilon + b + \alpha$  then the parasite population is unable to grow and hence decays to zero. Increasing  $\mu$  such that  $\epsilon + b + \alpha < \mu < \epsilon + a + \alpha$  allows the parasite population to grow albeit at very low levels (Figure 2.3b). Figure 2.3c depicts a large parasite birth rate combined with a negative host growth rate resulting in extinction for both populations.

Finally, we turn our attention to the situation observed in Figure 2.3d. Here we have initial positive salmon growth combined with positive *G. salaris* growth. This results in the *G. salaris* population rapidly growing to epidemic levels, forcing the salmon population to extinction. Once the salmon hosts are extinct the *G. salaris* population quickly decays to zero. Hence, the scenario observed in 2.3d actually highlights a second zero equilibrium that was not discovered in the original equilibrium analysis. This second zero equilibrium represents parasite/disease induced host extinction and is more commonly witnessed in models dealing with micro-parasitic infections. Due to the simplistic nature of the basic model this equilibrium is investigated and discussed in depth for the more complex models in Chapter 3 (Sections 3.2 and 3.3) leading to more relevant results.

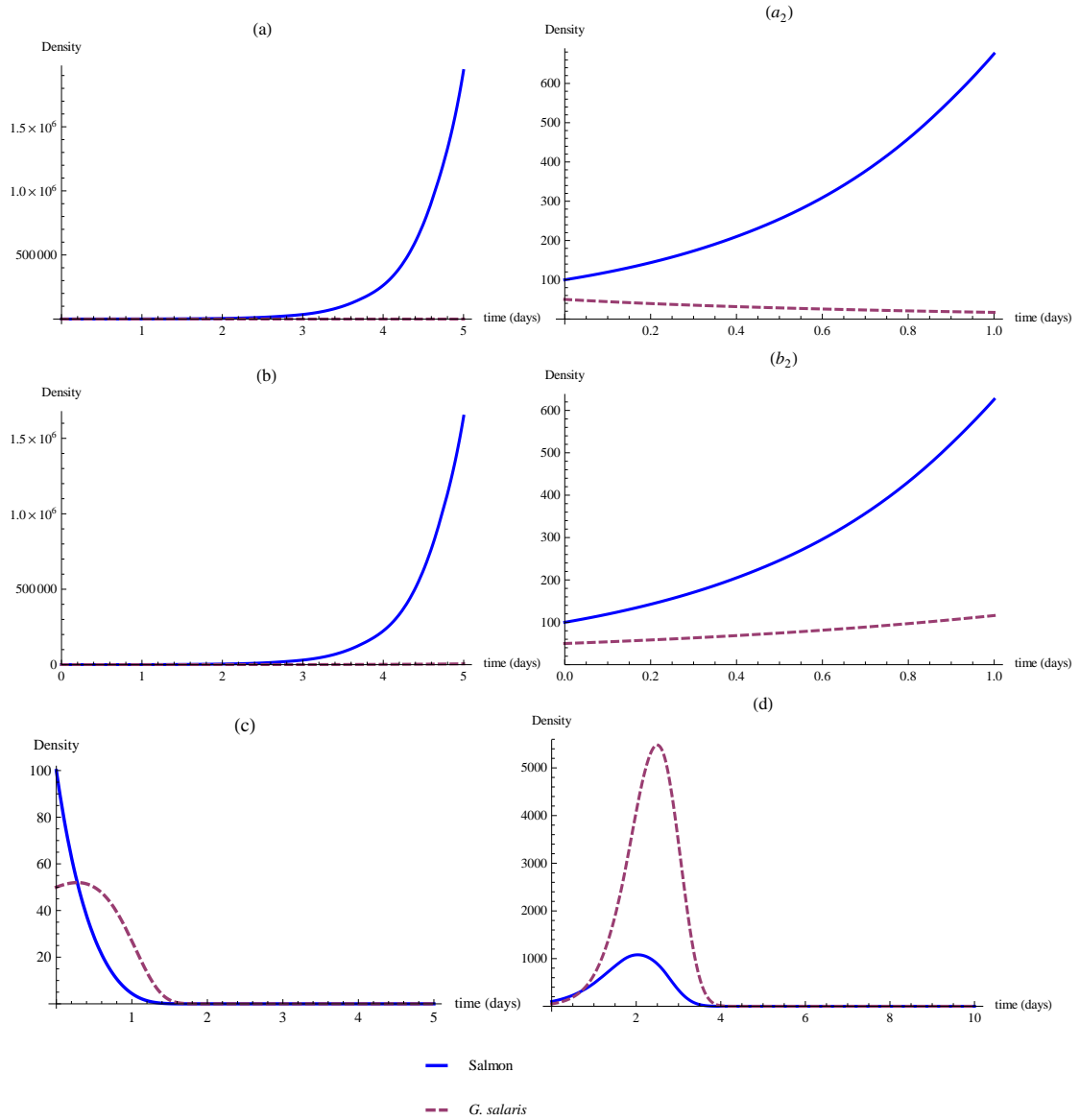


Figure 2.3: Trajectories of host and parasite populations in time as predicted by the basic model. The 4 possible situations when (2.13) is not satisfied. (a)  $\mu < \epsilon + b + \alpha < \epsilon + a + \alpha$ :  $a = 3.0$ ,  $b = 1.0$ ,  $\mu = 1.0$ ,  $\epsilon = 0.5$ ,  $\alpha = 0.5$ . (b)  $\epsilon + b + \alpha < \mu < \epsilon + a + \alpha$ :  $a = 3.0$ ,  $b = 1.0$ ,  $\mu = 3.0$ ,  $\epsilon = 0.5$ ,  $\alpha = 0.5$ . (c)  $\epsilon + a + \alpha < \epsilon + b + \alpha < \mu$ :  $a = 3.0$ ,  $b = 5.0$ ,  $\mu = 6.5$ ,  $\epsilon = 0.5$ ,  $\alpha = 0.5$ . (d)  $\epsilon + b + \alpha < \epsilon + a + \alpha < \mu$ :  $a = 3.0$ ,  $b = 1.0$ ,  $\mu = 5.0$ ,  $\epsilon = 0.5$ ,  $\alpha = 0.5$ . Plots in (a<sub>2</sub>) and (b<sub>2</sub>) are close ups of (a) and (b) respectively. In all cases  $H(0) = 100$ ,  $P(0) = 50$ . Hosts (—), parasites (---).

Biologically, and mathematically, this model is very simplistic and hence does not tell us a great deal of information about the salmon-*G. salaris* system. Moreover, given the fact that *G. salaris* infections are not currently present in the UK (Shinn *et al.*, 1995; OIE, 2003; Defra, 2008a) this model is not sufficient since it only predicts exponential growth of the parasites. Hence, we now look at building on these results and begin making the model more biologically relevant.

### 2.3 MODEL A: DENSITY DEPENDENT CONSTRAINTS ON HOST POPULATION

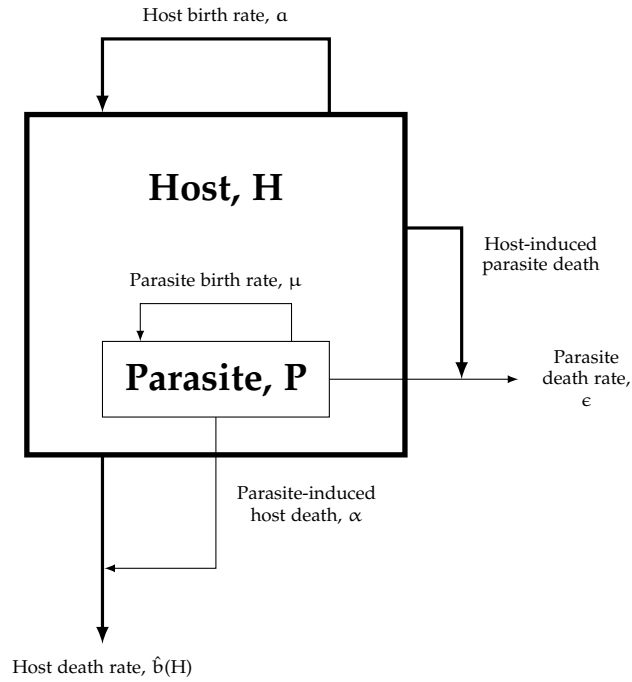


Figure 2.4: A schematic representation of a simplified Atlantic salmon-*G. salaris* interaction with density dependence in the host population.

In order to make the salmon - *G. salaris* model more realistic we begin by including density dependent constraints on the salmon population (Figure 2.4). These constraints, such as predation, resource limitation, fishing, *etc.*, make our model more biologically sound.

The density dependent constraint is added to the natural host mortality rate  $b$  and is linearly proportional to host density such that

$$\hat{b}(H) = b + sH \quad (2.14)$$

Thus, substituting  $\hat{b}$  for  $b$  in the basic model means equations (2.1) and (2.6) become

$$\frac{dH}{dt} = (a - b - sH)H - \alpha P \quad (2.15)$$

$$\frac{dP}{dt} = P \left( \mu - (\epsilon + b + \alpha + sH) - \alpha \frac{P}{H} \right) \quad (2.16)$$

Having this density dependence in the model puts an end to exponential growth of salmon in the absence of parasitic infection ( $P = 0$ ). Instead, the host population now grows to a threshold,  $K$ , commonly referred to as the carrying capacity. The general form of the carrying capacity is defined by equation (2.17) below.

$$K = \frac{a - b}{s} \quad (2.17)$$

### 2.3.1 Equilibria and stability

#### Equilibrium analysis

Equations (2.15) and (2.16) readily yield equilibria by setting  $dH/dt = dP/dt = 0$  and solving in the usual way for H and P. Hence, we find two equilibria exist:

1.  $(H^*, P^*) = (0, 0)$ , the trivial equilibrium with no salmon or *G. salaris* ;
2.  $(H^*, P^*) = (K, 0)$ , the disease-free equilibrium with salmon growth in the absence of *G. salaris*.

#### Stability analysis

The standard methods of analysis are followed (available in Appendix C) to determine the stability of the two equilibria.

#### The zero equilibrium, $(0, 0)$

The Jacobian obtained at  $(0, 0)$  is the same as that obtained from the basic model and hence, yields the same result (condition 2.13). A stability analysis of the zero equilibrium here yields the same results found in Section 2.2.2. Hence,  $(0, 0)$  is locally stable (by Routh-Hurwitz) if and only if  $a < b$  and  $\mu < \epsilon + b + \alpha$ .

As before  $a < b$  is the condition on the hosts and  $\mu < \epsilon + b + \alpha$  is the condition on the parasites.

The inequalities in (2.13) give rise to two situations:  $\mu < \epsilon + a + \alpha < \epsilon + b + \alpha$  and  $\epsilon + a + \alpha < \mu < \epsilon + b + \alpha$ . Assigning values to the parameters in the model to meet the conditions in (2.13) and plotting the result gives the graphs found in Figure 2.5. As we would expect, if host births are less than host deaths then the host population quickly dies out and hence the parasite population also dies out as a parasite cannot survive for long without a host. This can be seen in both Figures 2.5a and 2.5b. As witnessed in Figure 2.5a when  $\mu < \epsilon + a + \alpha$  the parasite population decreases to zero faster than in Figure 2.5b, this is due to parasite births,  $\mu$ , being less than parasite deaths, host births and parasite induced host deaths.

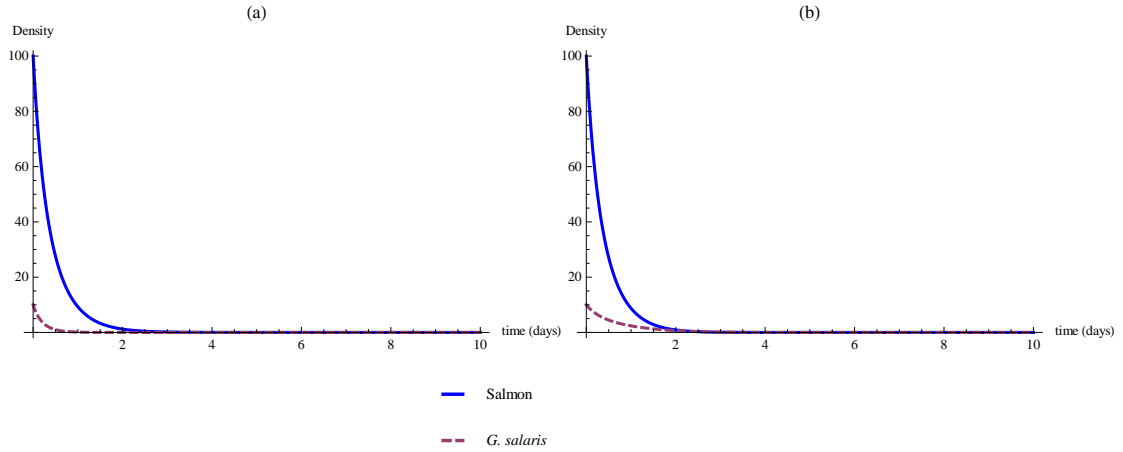


Figure 2.5: The zero equilibrium. Trajectories of host and parasite populations in time as predicted by the density dependent hosts model. With host birth rate less than host mortality rate ( $a < b$ ) the host population and hence the parasite population quickly decay to zero. (a)  $\mu < \epsilon + a + \alpha < \epsilon + b + \alpha$ :  $a = 3.0$ ,  $b = 5.0$ ,  $\mu = 2.0$ ,  $\epsilon = 0.5$ ,  $\alpha = 0.5$ ,  $s = 0.01$ ; (b)  $\epsilon + a + \alpha < \mu < \epsilon + b + \alpha$ :  $a = 3.0$ ,  $b = 5.0$ ,  $\mu = 5.0$ ,  $\epsilon = 0.5$ ,  $\alpha = 0.5$ ,  $s = 0.01$ . In both cases  $H(0) = 100$  and  $P(0) = 10$ . Hosts (—), parasites (---).

*The disease-free equilibrium,  $(K, 0)$*

A stability analysis of the Jacobian at  $(K, 0)$  (see Appendix C) yields the following:

$(K, 0)$  is locally stable (by the Routh-Hurwitz theorem) if and only if the inequalities in (2.18) are satisfied.

$$a > b, \quad \mu < \epsilon + a + \alpha \quad (2.18)$$

In biological terms this corresponds to salmon births being greater than deaths and *G. salaris* deaths outweighing births.

As with the conditions for the zero equilibrium to be stable, the inequalities in (2.18) for the disease-free case give two situations:  $\mu < \epsilon + b + \alpha < \epsilon + a + \alpha$  and  $\epsilon + b + \alpha < \mu < \epsilon + a + \alpha$ . Once again, assigning values to the parameters in the model to meet the conditions in (2.18) and plotting the result gives the graphs found in Figure 2.6.

However, when condition 2.18 is not satisfied two situations occur;

$$a < b, \quad \mu > b + \epsilon + \alpha \quad (2.19)$$

$$a > b, \quad \mu > a + \epsilon + \alpha \quad (2.20)$$

Using appropriate software to simulate the different scenarios the model might take we obtain the plots given in Figure 2.7.

The results seen in Figure 2.7 are similar to those described in Figure 2.3c and 2.3d from the basic model. Once again, with a negative salmon host growth rate  $a < b$  and large *G. salaris*

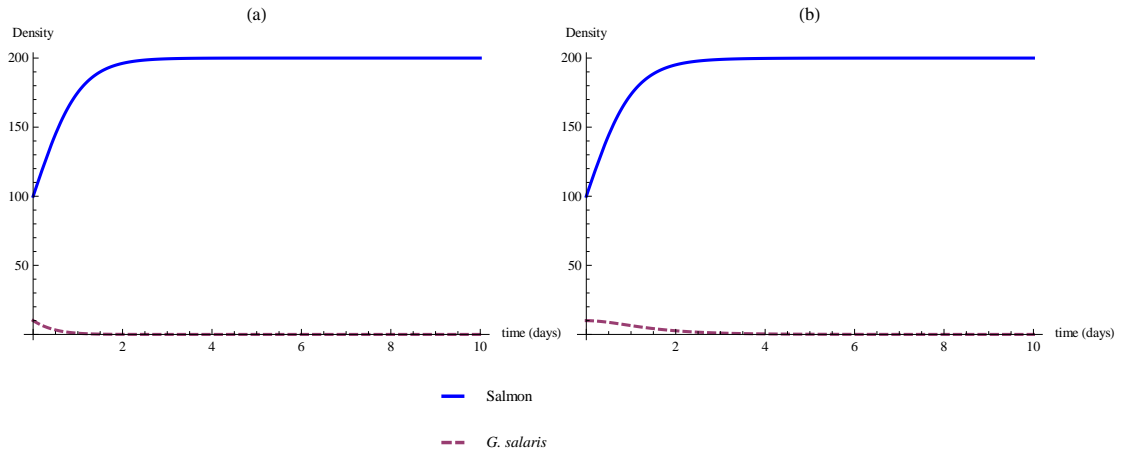


Figure 2.6: The disease-free equilibrium. Trajectories of host and parasite populations in time as predicted by the density dependent hosts model. With host birth rate greater than host mortality rate ( $a > b$ ) and parasite birth rate less than total parasite death ( $\mu < \epsilon + a + \alpha$ ) the parasite population quickly decays to zero and the host population is able to grow to carrying capacity  $K$ . Here (a)  $\mu < \epsilon + b + \alpha < \epsilon + a + \alpha$ , (b)  $\epsilon + b + \alpha < \mu < \epsilon + a + \alpha$ . In both cases  $H(0) = 100$ ,  $P(0) = 10$ ,  $a = 5.0$ ,  $b = 3.0$ ,  $\epsilon = 0.5$ ,  $\alpha = 0.5$ ,  $s = 0.01$ . The plots differ in the value of parasite birth:  $\mu = 3.0$  in (a) and  $\mu = 5.0$  in (b). Hosts (—), parasites (---).

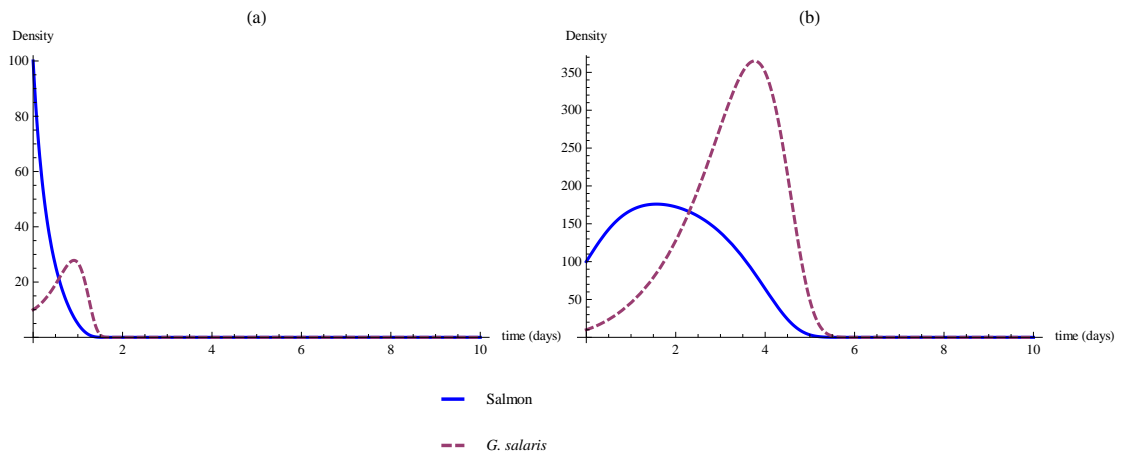


Figure 2.7: Model A: Other possible situations. Trajectories of host and parasite populations in time as predicted by the density dependent hosts model. (a)  $a = 3.0$ ,  $b = 5.0$ ,  $\mu = 8.0$ ,  $\epsilon = 0.5$ ,  $\alpha = 0.5$ ,  $s = 0.01$ ; (b)  $a = 5.0$ ,  $b = 3.0$ ,  $\mu = 8.0$ ,  $\epsilon = 0.5$ ,  $\alpha = 0.5$ ,  $s = 0.01$ . In both cases  $H(0) = 100$ ,  $P(0) = 10$ . Hosts (—), parasites (---).

parasite birth rate  $\mu > \epsilon + b + \alpha$  the *G. salaris* population is able to grow until the salmon population is depleted, after which the parasites die out (Figure 2.7a). If however salmon hosts have a positive growth rate ( $a > b$ ) and *G. salaris* parasite births are still large ( $\mu > \epsilon + a + \alpha$ ) then we observe a short epidemic before both salmon and *G. salaris* populations become extinct (Figure 2.7b). As before we observe a second zero equilibrium (when  $P/H > 0$ ) representing parasite induced host extinction that was not obtainable via our standard equilibrium analysis.

## 2.4 ESTIMATING PARAMETER VALUES

Using data and information readily available in the literature concerning both *G. salaris* and Atlantic salmon life-cycles allowed estimates for population parameters to be obtained. These estimates are collected in Table A.1, Appendix A.

### 2.4.1 Atlantic salmon

#### *Birth rate, a*

As discussed in Chapter 1, Section 1.4.1.1, salmon spawning is a seasonal process taking place between mid October and late February (Shearer, 1992). Due to this and the fact that seasonality is not explicitly modelled, and thus absent from models within this thesis, an estimate for salmon birth rate,  $a$ , is difficult to obtain. Taking this and the birth rate of parasites into consideration, a daily birth rate of 0.02 is chosen as a best estimate and added to Table A.1 in Appendix A.

#### *Mortality rate, b*

The natural weekly mortality rate of salmon parr was estimated by Hedger *et al.* (2013) as 0.004. Thus, this gives a daily mortality rate of 0.0006.

#### *Density-dependent constraint, s*

The density-dependent constraint for Atlantic salmon varies by river, and thus, estimations for  $s$  depend on the river being studied. Hedger *et al.* (2013) estimated parr carrying capacity as 7.5g per  $m^2$ , using this combined with the mean weight of parr (60g, N. McPherson, personal communication) the salmon carrying capacity can be estimated as 0.125 fish per  $m^2$ . This estimate is used as a guide when choosing a value for  $s$  and is consistent with parr densities previously estimated in the literature (12.5 fish per  $100m^2$ , ICES, 2001). Table 2.3 gives length and basin information for selected river systems across the UK.

Table 2.3: Examples of river systems from across the UK. The following rivers are known to contain populations of Atlantic salmon. Length and basin measurements are given.

<b>River, location</b>	<b>Length (km)</b>	<b>Basin (km<sup>2</sup>)</b>
River Tay, Scotland	188	4,970
River Tweed, Scotland	156	3,900
River Tyne, England	100	2,145
River Ribble, England	121	2,128
River Dee, Wales	110	1,817
River Wye, Wales	215	4,136

#### *Mortality rate due to infection, $\alpha$*

Data for salmon mortality due to infection is not readily available due to ethics involved with animal health such that experimental trials have to be ended as salmon hosts become too heavily infected. However, experimental trials conducted by Scott & Anderson (1984) concerning another *gyrodactylus* species (*G. turnbulli* infections on guppies *Poecilia reticulata*) estimated the daily rate of parasite induced host mortalities as 0.0012 (Table A.7, Appendix A). Thus, this value is used as an estimate for parasite induced host mortality in model simulations throughout this thesis.

#### 2.4.2 *Gyrodactylus salaris*

##### *Mortality rate, $\epsilon$*

The natural daily mortality rate of *G. salaris* parasites was calculated using data from Jansen & Bakke (1991). Using the average life-span of individual parasites given by Jansen & Bakke (1991) as 12.5 days (Table A.4, Appendix A), the natural daily mortality rate of *G. salaris* parasites was estimated as 0.008.

##### *Birth rate, $\mu$*

The daily birth rate of *G. salaris* parasites was calculated using the data from Bakke *et al.* (1990) (Table A.3, Appendix A) concerning *G. salaris* population growth on individual salmon hosts over time and the parasite mortality rate obtained from the data in Jansen & Bakke (1991). The data given by Bakke *et al.* (1990) allowed the calculation of parasite growth on the Atlantic strain of Atlantic salmon ( $r=0.103$ ) as well as the Baltic strain of Atlantic Salmon ( $r=0.085$ ). Further estimates of parasite growth were obtained using the data from Paladini *et al.* (in prep.) (Tables A.5 and A.6, Appendix A) on Norwegian salmon ( $r=0.116$ ) and UK salmon ( $r=0.091$ ). By fitting exponential best-fit curves to data (Bakke *et al.*, 1990; Paladini *et al.*, in prep.), the mean daily birth rate of *G. salaris* parasites was estimated as  $\mu=0.183$  (Norway Atlantic hosts, Bakke *et al.*, 1990),  $\mu=0.165$  (Russia Baltic hosts, Bakke *et al.*, 1990),  $\mu=0.196$  (Norway Atlantic hosts, Paladini *et al.*, in prep.),  $\mu=0.171$  (UK Atlantic hosts, Paladini *et al.*, in prep.).

## 2.5 SIMULATING THE MODEL FOR A UK RIVER SYSTEM

In a recent study by Paladini *et al.* (in prep.) Atlantic salmon parr originating from the Welsh River Dee (Afon Dyfrdwy) in the United Kingdom were used to study the effects and impact of *G. salaris* infections on UK salmon hosts. For consistency, the model in its current form (Equations 2.15 and 2.16) is used to simulate the long term dynamics of *G. salaris* infections

in the Welsh River Dee with parasite growth rates calculated using the data collected by Paladini *et al.* (in prep.). In order to remove the spatial component, the density dependent parameter,  $s$ , is calculated for an area of the river  $1000\text{m}^2$  in size with the assumption that the rest of the river behaves in a similar fashion. The remaining parameters in the model are given values according to the discussion in Section 2.4 above and Table A.1, Appendix A.

The model is simulated over a 10 year period (3650 days). Initially, Atlantic salmon are at their carrying capacity ( $H(0) = K = 125$ ) with no *G. salaris* infection ( $P(0) = 0$ ). After 2 years (730 days), 1 *G. salaris* parasite is introduced into the system ( $P(730) = 1$ ). The results obtained are seen in Figure 2.8 below.

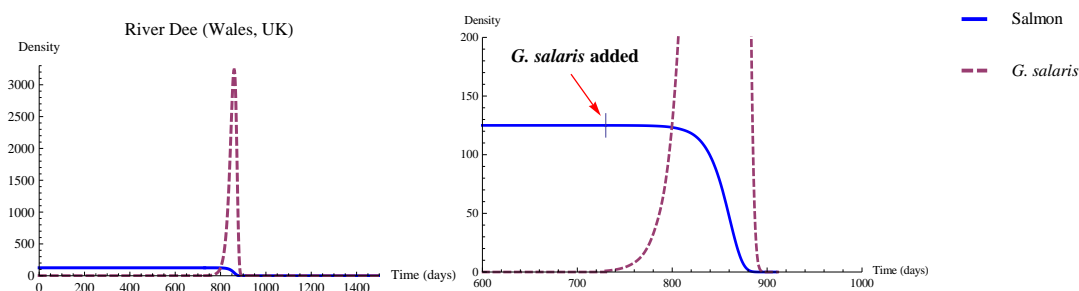


Figure 2.8: Model A: River Dee example. Trajectories of host and parasite populations in time as predicted by the density dependent hosts model and parameterised according to Table A.1 as follows  $a = 0.02$ ,  $b = 0.0006$ ,  $s = 0.00016$ ,  $\alpha = 0.0012$ ,  $\mu = 0.1708$ ,  $\epsilon = 0.08$ . Initially there is no infection present,  $H(0) = K = 125$ ,  $P(0) = 0$ . Infection is added (a single parasite) after 730 days,  $H(730) = K = 125$ ,  $P(730) = 1$ . Hosts (—), parasites (---).

By substituting parameter values for  $1000\text{m}^2$  of the River Dee into the conditions in (2.18), (2.19) and (2.20) the conditions for the parasite induced extinction equilibrium (2.20) are satisfied. Thus, in the case of the model in its current form, (2.15) and (2.16), we would expect the introduction (or emergence) of *G. salaris* to force salmon populations to extinction. This is confirmed when the model is simulated. As can be seen in Figure 2.8, in the absence of infection the salmon population maintains its carrying capacity, however, when infection is added to the system the *G. salaris* population exhibits rapid growth resulting in a short epidemic as predicted, quickly rendering the salmon population extinct.

## 2.6 SUMMARY

In using the deterministic macroparasite models of Anderson & May (1978) and May & Anderson (1978) as a foundation we have developed a simple two equation model to describe Atlantic salmon-*G. salaris* interactions.

We have set out a system such that salmon populations decay to zero under a negative growth rate and are able grow to carrying capacity under a positive growth rate in the

absence of *G. salaris* infection in a river. We have also shown that when the conditions for stability are not satisfied, with salmon and *G. salaris* populations exhibiting positive growth, a short epidemic occurs resulting in the salmon population becoming extinct. This event is quickly followed by the extinction of the *G. salaris* population.

The possibility of this scenario occurring in *G. salaris*-free territories was confirmed by simulating the model developed above and parameterising it for the River Dee in the UK. As mentioned earlier in the text, the model in its current form does not provide much detailed information of what is witnessed in the field due to its simplicity. However, these results do serve as a foundation and form a solid basis for the more complicated models that follow in the succeeding chapters.

## Detached parasites in the external environment

Until now we have been studying the dynamics of on-host (attached) *Gyrodactylus salaris* populations. However, when a *G. salaris* parasite becomes detached from a salmon host it is able to survive for a period of time, either drifting in the water column or settling on a substrate or dead host, before possibly infecting a new host. Parasite survival when off a host, or on a dead host, is considerably lower than survival when on a host.

If a parasite becomes detached from a host (either by being knocked off, washed off or due to a failed transfer attempt) then it is able to survive for a short period of time at low temperatures (60h, 45h and 27h at 3°C, 12°C and 18°C respectively, Olstad *et al.*, 2006) by settling on a substrate (Bakke *et al.*, 1992b). If this happens, the parasite will simply wait until a suitable host swims by and brushes over it. Gyrodactylids are capable of extending their bodies two or three times their normal length at right angles to the substrate and rapidly transfer to a new host (Bakke *et al.*, 1992b; Soleng *et al.*, 1999a; Bakke *et al.*, 2007).

Similarly, if the parasite becomes detached from the host but does not settle on the substrate it is able to survive by drifting in the water column, once again survival time is temperature dependent. In cases like this, the parasite will drift until a suitable host bumps into it (Bakke *et al.*, 1992b; Soleng *et al.*, 1999a). This route of transmission of the parasite was observed under experimental conditions by Soleng *et al.* (1999a). They placed a total of 160 uninfected fish into 160 individual small wire mesh cages suspended above the substrate (one fish per cage) in an infected river. After 24 hours the fish were tested and 10 out of 157 fish (6.4%) were found to be infected with *G. salaris* confirming that transmission via parasites drifting in the water column is possible but not as important as direct transmission via contact with an infected live/dead fish or indirect transmission via the substrate.

*Gyrodactylus salaris* can also survive on a dead host for a short period of time at low temperatures (Olstad *et al.*, (2006) found that after 3 days at 12°C there was still parasite activity on dead hosts). In this situation, the parasites may move short distances (on the dead host) during the first few hours to the first day after host death (temperature dependent) and continue to feed (Olstad *et al.*, 2006). Under experimental conditions Olstad *et al.* (2006) observed two

more distinctive modes: (i) stationary transmission mode (STM) - Parasites exhibiting this behaviour were motionless and extended their bodies at right angles to the dead host; (ii) search mode (SM) - Parasites exhibiting this behaviour extended their bodies to at least four times their normal length and constantly made circular movements and contractions around the motionless haptor. Olstad *et al.* (2006) also observed that parasites infecting dead hosts survive longer than those off a host and showed that transmission between live susceptible fish and dead infected fish is more important than was previously thought.

### 3.1 MAKING THE MODEL MORE REALISTIC

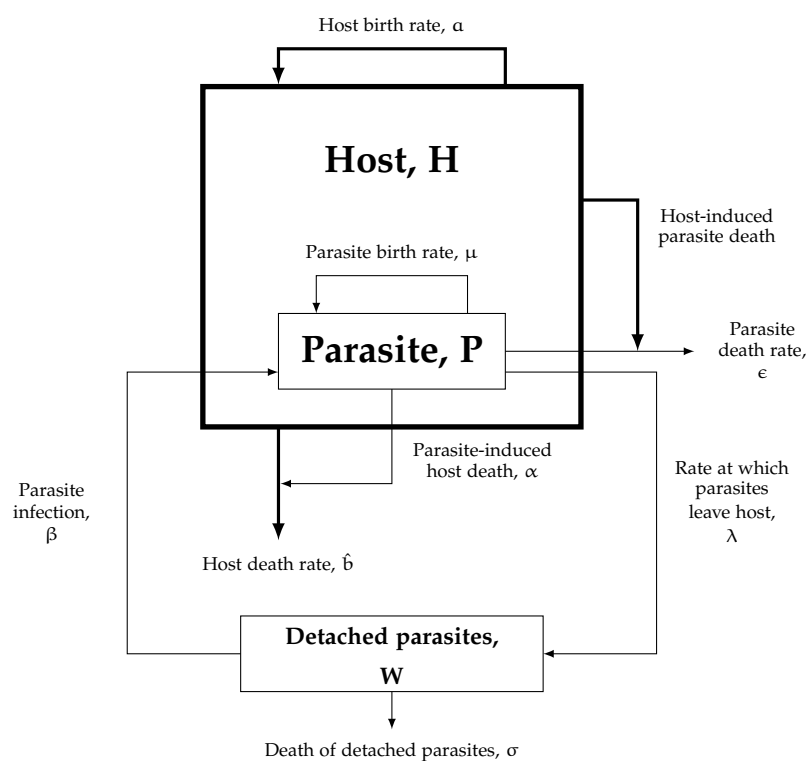


Figure 3.1: Schematic representation of Atlantic salmon-*Gyrodactylus salaris* interaction showing detached parasites. See Table A.1 (Appendix A) for a description of the parameters used.

Based on the information above we now consider a model that has detached *G. salaris* parasites. In this case “detached parasites” are defined as parasites that have become detached from a salmon host, either by a failed transfer to a new host or by being knocked/washed off, and are now present in the water column, on a substrate or on a dead host. From before our model (Model A - density dependent host population) was given by equations (2.15) and (2.16):

$$\begin{aligned}\frac{dH}{dt} &= (a - b - sH)H - \alpha P \\ \frac{dP}{dt} &= P \left( \mu - (\epsilon + b + \alpha + sH) - \alpha \frac{P}{H} \right)\end{aligned}$$

Now we add detached parasites into the model. Assume parasites become detached at rate  $\lambda$ , hence, leaving the on-fish (attached) parasite population. Detached parasites re-enter the attached parasite population by infecting hosts at rate  $\beta$ . Adding this new information for detached parasites means that equation (2.16) becomes:

$$\frac{dP}{dt} = P \left( \mu - (\epsilon + b + \alpha + sH + \lambda) - \alpha \frac{P}{H} \right) + \beta WH \quad (3.1)$$

We now add a third equation to our model to describe the way the detached parasite population interacts with the host and attached parasite populations. In this new equation parasites become detached at rate  $\lambda$ . These detached parasites then die at rate  $\sigma$  and infect hosts, via contact, at rate  $\beta$ . Thus, the equation for detached parasites is:

$$\frac{dW}{dt} = \lambda P - \sigma W - \beta WH \quad (3.2)$$

$\frac{dW}{dt}$  is the rate of change of the detached parasite population.

Hence, our model is now given by the equations in (3.3) below:

$$\begin{aligned}\frac{dH}{dt} &= (a - b - sH)H - \alpha P \\ \frac{dP}{dt} &= P \left( \mu - (\epsilon + b + \alpha + sH + \lambda) - \alpha \frac{P}{H} \right) + \beta WH \\ \frac{dW}{dt} &= \lambda P - \sigma W - \beta WH\end{aligned} \quad (3.3)$$

### 3.1.1 Equilibria and stability

#### Equilibrium analysis

The equations in (3.3) readily yield equilibria by setting  $dH/dt = dP/dt = dW/dt = 0$  and solving for  $H^*$ ,  $P^*$  and  $W^*$  (Appendix C). Hence, we find three equilibria exist at:

1.  $(H^*, P^*, W^*) = (0, 0, 0)$ , the trivial equilibrium with no salmon host or *G. salaris* parasites (neither on or off hosts);

2.  $(H^*, P^*, W^*) = (K, 0, 0)$ , the disease-free equilibrium with salmon population growth in the absence of *G. salaris* infection;
3.  $(H^*, P^*, W^*) = (H^*, P^*, W^*)$ , the coexistence equilibrium with both salmon and *G. salaris* (on and off hosts) populations present.

where,

$$K = \frac{a-b}{s}$$

$$H^* = \frac{\sigma(\Gamma - \mu)}{\beta(\mu - \Gamma + \lambda)} \quad (3.4)$$

$$P^* = \frac{\sigma(\Gamma - \mu)[r\beta(\mu - \Gamma + \lambda) - s\sigma(\Gamma - \mu)]}{\alpha\beta^2(\mu - \Gamma + \lambda)^2} \quad (3.5)$$

$$W^* = \frac{(\Gamma - \mu)[r\beta(\mu - \Gamma + \lambda) - s\sigma(\Gamma - \mu)]}{\alpha\beta^2(\mu - \Gamma + \lambda)} \quad (3.6)$$

with

$$\Gamma = \epsilon + a + \alpha + \lambda$$

### *Stability analysis*

#### 3.1.1.1 *The zero equilibrium, (0,0,0)*

A stability analysis of the zero equilibrium via the usual methods (Appendix C), yields the following result:  $(0,0,0)$  is locally stable (by Routh-Hurwitz conditions) if and only if:

$$a < b, \quad \mu < \epsilon + a + \alpha + \lambda \quad (3.7)$$

Assigning values to the parameters in the model so that they match condition (3.7) and plotting the result (see Figure 3.2) shows that all populations quickly die out. This is what we would expect as the inequalities in (3.7) correspond to host births being less than host deaths and parasite births being less than parasite deaths + host births + parasite induced host deaths + the rate at which parasites leave hosts. Also, if the host population decreases to zero then the parasite populations cannot survive and will quickly die out.

#### 3.1.1.2 *The disease-free equilibrium (K,0,0)*

As with the zero equilibrium, a stability analysis of the disease-free equilibrium using the usual methods yields the following result:  $(K,0,0)$  is locally stable (by Routh-Hurwitz conditions) if and only if:

$$a > b, \quad \mu < \epsilon + a + \alpha \quad (3.8)$$

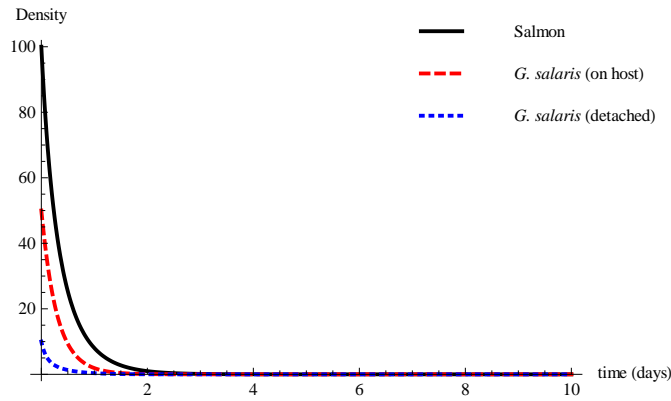


Figure 3.2: The zero equilibrium. Trajectories of host, attached parasite and detached parasite populations in time as predicted by Model B. As host birth rate is less than host mortality rate ( $a < b$ ) the host population and hence both parasite populations quickly decay to zero. Here,  $a = 2.0$ ,  $b = 4.0$ ,  $s = 0.01$ ,  $\mu = 4.0$ ,  $\epsilon = 2.0$ ,  $\alpha = 0.5$ ,  $\lambda = 0.5$ ,  $\sigma = 5.0$ ,  $\beta = 0.05$ . Initial population numbers are  $H(0) = 100$ ,  $P(0) = 50$ ,  $W(0) = 10$ . Hosts (—), parasites (---), detached parasites (···).

The inequalities in (3.8) tell us that  $(K, 0, 0)$  is stable if and only if host births are greater than host deaths and parasite births are less than parasite deaths + host births + parasite induced host deaths (Note also that  $\mu < \epsilon + a + \alpha \Rightarrow \mu < \epsilon + a + \alpha + \lambda$ ).

Assigning values to the model parameters to match condition (3.8) and plotting the result gives Figure (3.3). In this case, the parasite populations quickly die out due to parasite births being less than parasite deaths. As host births are greater than host deaths and there is no disease due to the parasite populations dying out, the host population grows following a logistic trajectory until reaching carrying capacity (in this case  $K = (a - b)/s = (4 - 2)/0.01 = 200$ ).

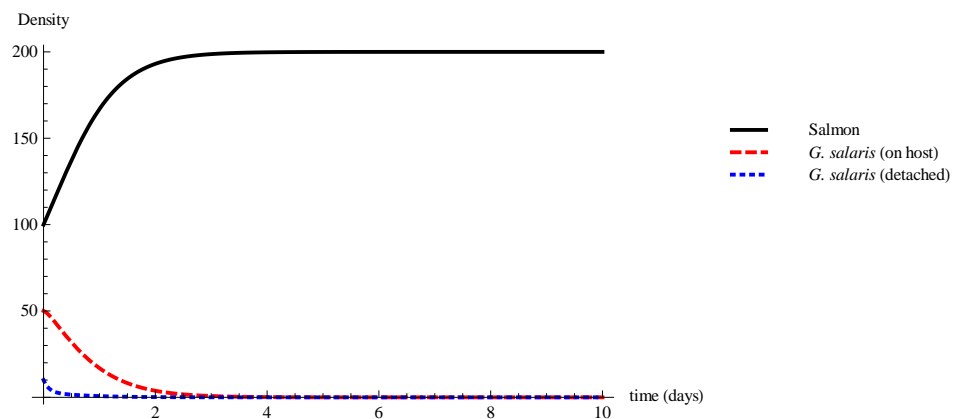


Figure 3.3: The disease-free equilibrium. Trajectories of host, attached parasite and detached parasite populations in time as predicted by Model B. As host birth rate is greater than host mortality rate ( $a > b$ ) and parasite birth rate is less than total parasite mortalities ( $\mu < \epsilon + a + \alpha$ ) the host population grows to carrying capacity  $K$  whilst both parasite populations decay to zero. Here,  $a = 4.0$ ,  $b = 2.0$ ,  $s = 0.01$ ,  $\mu = 5.0$ ,  $\epsilon = 0.5$ ,  $\alpha = 0.5$ ,  $\lambda = 2.0$ ,  $\sigma = 5.0$ ,  $\beta = 0.05$ . Initial population numbers are  $H(0) = 100$ ,  $P(0) = 50$ ,  $W(0) = 10$ . Hosts (—), attached parasites (---), detached parasites (···)

### 3.1.1.3 The coexistence equilibrium, $(H^*, P^*, W^*)$

A stability analysis of the coexistence equilibrium, where  $H^*$ ,  $P^*$  and  $W^*$  are defined as in equations (3.4), (3.5) and (3.6) respectively yields the following:

$(H^*, P^*, W^*)$  is locally stable (by the Routh-Hurwitz theorem) if and only if:

$$a > b, \quad \epsilon + a + \alpha + \frac{\sigma s \lambda}{\beta r + \sigma s} < \mu < \epsilon + a + \alpha + \lambda \quad (3.9)$$

The inequalities in (3.9) result in the following four scenarios:

1.  $a < b$  and  $\mu < \epsilon + a + \alpha + \frac{\sigma s \lambda}{\beta r + \sigma s}$ , salmon and *G. salaris* extinction;
2.  $a > b$  and  $\mu < \epsilon + a + \alpha + \frac{\sigma s \lambda}{\beta r + \sigma s}$ , salmon growth, *G. salaris* extinction;
3.  $a > b$  and  $\epsilon + a + \alpha + \frac{\sigma s \lambda}{\beta r + \sigma s} < \mu < \epsilon + a + \alpha + \lambda$ , salmon and *G. salaris* coexistence;
4.  $a > b$  and  $\epsilon + a + \alpha + \lambda < \mu$ , *G. salaris* induced salmon extinction.

1. If salmon births occur at a rate that is greater than that of salmon mortalities then both salmon and *G. salaris* populations decay to zero (Figure 3.4a).

2. When parasite birth rate is low *G. salaris* populations cannot sustain themselves. This results in *G. salaris* populations decaying to zero, and hence, with salmon births greater than mortalities the salmon parr population is able to grow to carrying capacity,  $K$  (Figure 3.4b).

3. When parasite birth rate is greater than total parasite mortalities but less than total parasite losses we observe salmon-*G. salaris* coexistence (3.4c). In this case the parasite population is able to regulate that of the hosts. As  $\mu$  is increased ever closer to the value of  $\epsilon + a + \alpha + \lambda$  we observe that the system begins to oscillate before settling to equilibrium (Figure 3.5). This results in parasites being able to regulate the host population at lower levels.

4. The final scenario that can occur is when parasite birth are high, in excess of total parasite losses (Figure 3.4d). In this case *G. salaris* exhibit rapid population growth resulting in a short epidemic forcing salmon populations into extinction. As the salmon population begins to decay *G. salaris* parasites are released into the external environment causing a short increase in detached *G. salaris* density. Salmon extinction is quickly followed by the extinction of *G. salaris* populations, and thus, we arrive at a second zero equilibrium,  $(0, 0, 0)_2$ . This equilibrium is similar to the situation witnessed in the basic and density dependent models in Chapter 2. As before, this equilibrium did not present itself during the original equilibrium analysis in Section 3.1.1 and represents disease-induced host extinction. We require a method of analysis to understand this equilibrium fully.

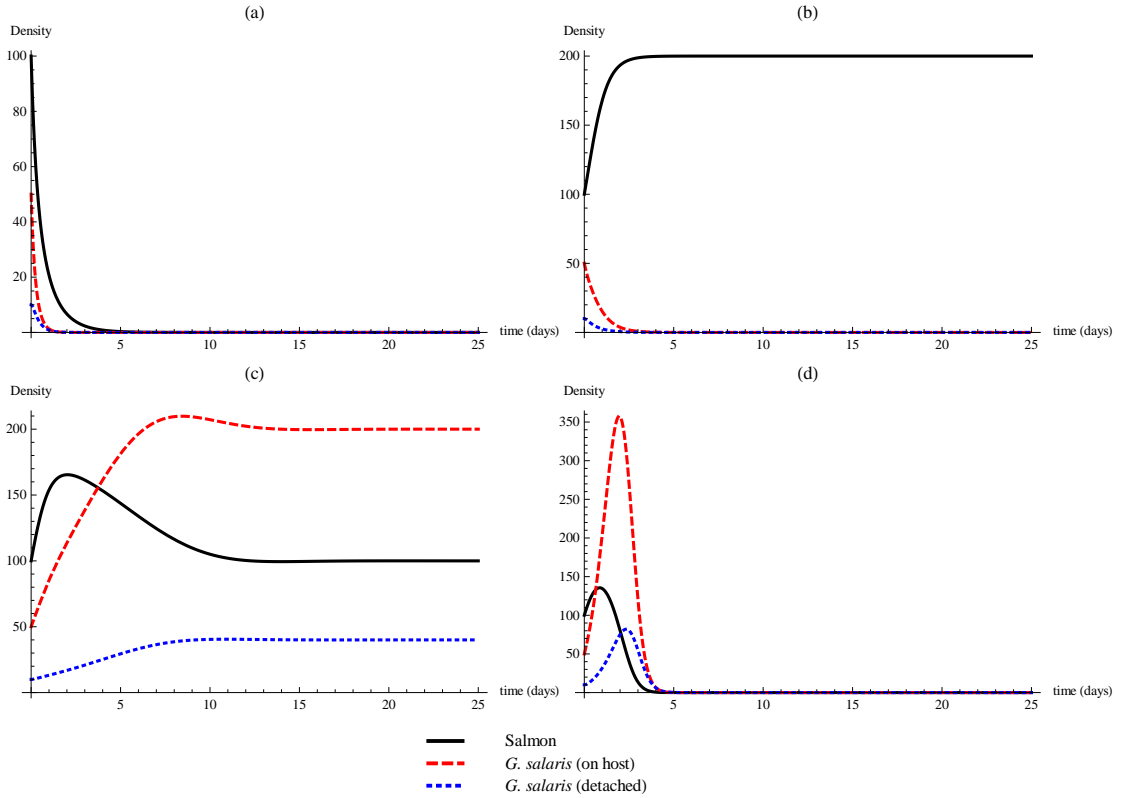


Figure 3.4: The possible scenarios that result from the conditions of the coexistence equilibrium. Trajectories of salmon host, attached *G. salaris* parasite and detached *G. salaris* parasite populations in time as predicted by Model B. (a) A negative salmon population growth rate combined with a negative *G. salaris* population growth rate results in all populations decaying to zero. (b) Positive salmon population growth combined with negative *G. salaris* population growth results in the salmon population growing to carrying capacity. (c) With host births greater than host mortalities and parasite births greater than total parasite mortalities but less than total parasite losses, the parasite population is able to regulate the host population resulting in host-parasite coexistence. (d) Once parasite the parasite birth rate exceeds the total parasite loss rates ( $\epsilon + a + \alpha + \lambda < \mu$ ) we arrive at a new zero equilibrium. In this case the host population begins to grow and the attached parasite population quickly increases to epidemic levels, killing the hosts and reducing the population to zero. When this happens the parasite population quickly die out due to lack of resources (hosts). In all plots  $a = 4.0$ ,  $b = 2.0$ ,  $s = 0.01$ ,  $\epsilon = 0.5$ ,  $\alpha = 0.5$ ,  $\lambda = 2.0$ ,  $\sigma = 5.0$ ,  $\beta = 0.05$ , with initial conditions  $H(0) = 100$ ,  $P(0) = 50$ ,  $W(0) = 10$ . The only parameter that varies is  $\mu$ .  $\mu = 4.0, 4.0, 6.0, 7.1$  in (a), (b), (c) and (d) respectively. Salmon (—), attached *G. salaris* (---), detached *G. salaris* (···).

### 3.2 RE-EVALUATING THE MODEL

As was mentioned in Chapter 2, and above, we now turn our attention to the investigation of the parasite induced host extinction equilibrium. In order to do this we begin by re-evaluating the model in its current form, given by the equations in (3.3) above, in terms of the mean number of parasites per host ( $P/H$ ). This approach is adopted in order to gain a greater understanding of the scenario that arises when  $\mu$  is large such that

$$a > b, \quad \epsilon + a + \alpha + \lambda < \mu \quad (3.10)$$

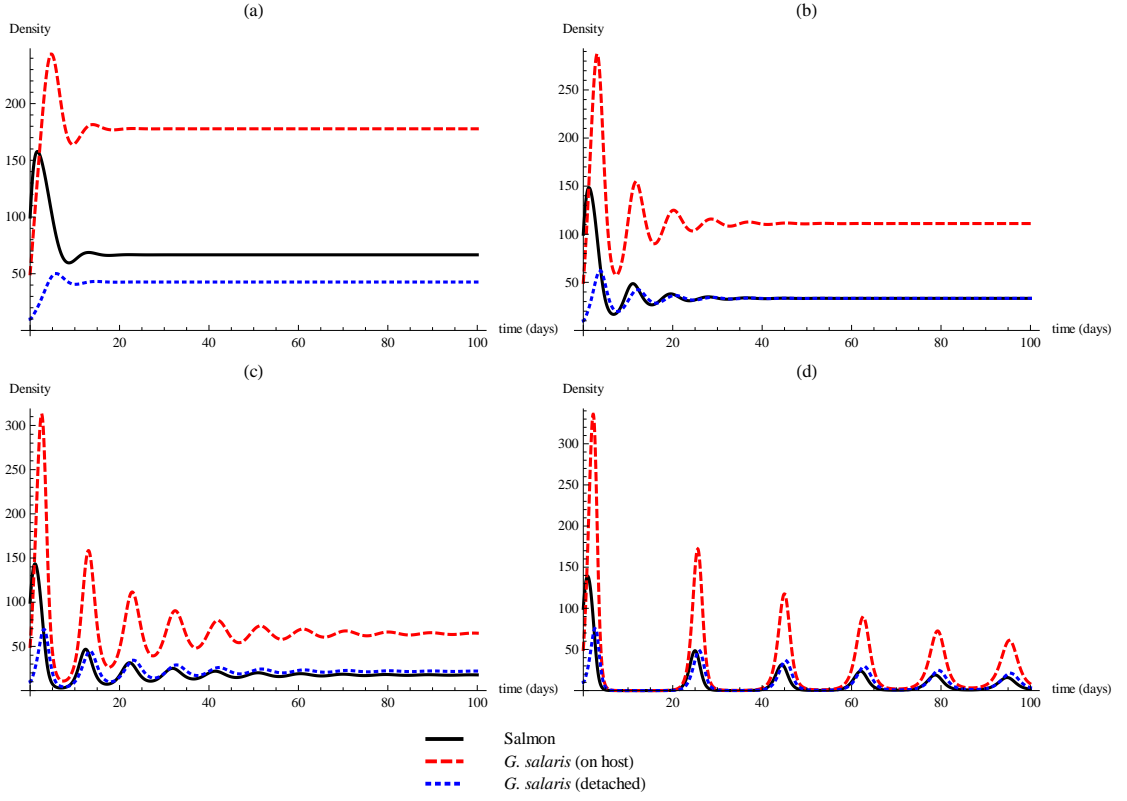


Figure 3.5: The coexistence equilibrium. Trajectories of salmon host, attached *G. salaris* parasite and detached *G. salaris* parasite populations in time as predicted by Model B. By varying parasite birth rate  $\mu$  such that it is increased closer to  $\epsilon + a + \alpha + \lambda$  the *G. salaris* population is able to regulate the salmon population at increasingly lower levels. In all plots  $a = 4.0$ ,  $b = 2.0$ ,  $s = 0.01$ ,  $\epsilon = 0.5$ ,  $\alpha = 0.5$ ,  $\lambda = 2.0$ ,  $\sigma = 5.0$ ,  $\beta = 0.05$ , with initial conditions  $H(0) = 100$ ,  $P(0) = 50$ ,  $W(0) = 10$ . The only parameter that varies is  $\mu$  such that (a)  $\mu = 6.2$ , (b)  $\mu = 6.5$ , (c)  $\mu = 6.7$ , and (d)  $\mu = 6.9$ . Salmon (—), attached *G. salaris* (---), detached *G. salaris* (···).

In this case (Equation 3.10) all densities are 0 but  $P/H$  exhibits positive growth.

Now,

$$\begin{aligned} \frac{d \frac{P}{H}}{dt} &= \frac{H \frac{dP}{dt} - P \frac{dH}{dt}}{H^2} \\ &= \frac{1}{H} \frac{dP}{dt} - \frac{P}{H^2} \frac{dH}{dt} \end{aligned} \quad (3.11)$$

$$\begin{aligned} (3.1) \quad \Rightarrow \quad \frac{1}{H} \frac{dP}{dt} &= \frac{1}{H} \left( P(\mu - (\epsilon + b + sH + \alpha + \lambda)) - \frac{\alpha P}{H} + \beta HW \right) \\ &= \frac{P}{H} (\mu - (\epsilon + b + sH + \alpha + \lambda)) - \frac{\alpha P^2}{H^2} + \beta W \end{aligned} \quad (3.12)$$

$$\begin{aligned} (2.15) \quad \Rightarrow \quad \frac{P}{H^2} \frac{dH}{dt} &= \frac{P}{H^2} ((a - b - sH)H - \alpha P) \\ &= \frac{P}{H} (a - b - sH) - \frac{\alpha P^2}{H^2} \end{aligned} \quad (3.13)$$

Hence

$$\frac{1}{H} \frac{dP}{dt} - \frac{P}{H^2} \frac{dH}{dt} = \frac{P}{H} (\mu - \Gamma) + \beta W \quad (3.14)$$

with  $\Gamma = \epsilon + a + \alpha + \lambda$

Hence, the model is now given by the equations in (3.15) below.

$$\begin{aligned}\frac{dH}{dt} &= (a - b - sH)H - \alpha P \\ \frac{d\frac{P}{H}}{dt} &= \frac{P}{H}(\mu - \Gamma) + \beta W \\ \frac{dW}{dt} &= \lambda P - \sigma W - \beta WH\end{aligned}\tag{3.15}$$

Now, if we substitute  $M = P/H$  into the equations in (3.15) our model becomes

$$\frac{dH}{dt} = (a - b - sH)H - \alpha MH\tag{3.16}$$

$$\frac{dM}{dt} = M(\mu - \Gamma) + \beta W\tag{3.17}$$

$$\frac{dW}{dt} = \lambda MH - \sigma W - \beta WH\tag{3.18}$$

where  $dH/dt$ ,  $dM/dt$  and  $dW/dt$  are the rates of change of hosts, mean number of parasites per host and detached parasites respectively.

### 3.2.1 Equilibria and stability

#### Equilibrium analysis

As before, setting  $dH/dt = dM/dt = dW/dt = 0$  we find the following equilibria exist:

1.  $(H^*, M^*, W^*) = (0, 0, 0)$ , the trivial equilibrium with no salmon host or *G. salaris* parasites (neither on or off hosts);
2.  $(H^*, M^*, W^*) = (K, 0, 0)$ , the disease-free equilibrium with salmon population growth in the absence of *G. salaris* infection;
3.  $(H^*, M^*, W^*) = (H^*, M^*, W^*)$ , the coexistence equilibrium with both salmon and *G. salaris* (on and off hosts) populations present.

where,

$$H^* = -\frac{\sigma(\mu - \Gamma)}{\beta(\mu + \lambda - \Gamma)}\tag{3.19}$$

$$M^* = \frac{r\beta(\mu + \lambda - \Gamma) + s\sigma(\mu - \Gamma)}{\alpha\beta(\mu + \lambda - \Gamma)}\tag{3.20}$$

$$W^* = -\frac{(\mu - \Gamma)(r\beta(\mu + \lambda - \Gamma) + s\sigma(\mu - \Gamma))}{\alpha\beta^2(\mu + \lambda - \Gamma)}\tag{3.21}$$

### *Stability analysis*

A stability analysis of these equilibria yield the same conditions for stability as found in Section 3.1.1.1 as expected and hence validates the consistency of the re-evaluated model.

Keeping parameter values consistent with those assigned in Section 3.1.1.1 and simulating the model for the zero, disease-free and coexistence equilibria respectively we arrive at the same outcomes (and hence conclusions) as before. Since the results here agree with those obtained in Section 3.1.1 we can conclude that the model and our stability analysis are sound. We now turn our attention to the fourth equilibrium  $(0,0,0)_2$ .

#### *3.2.2 The second zero equilibrium - Parasite induced extinction*

As discussed above the reason for re-evaluating Model B using the mean number of parasites per host was to gain a greater understanding of the model dynamics when the *G. salaris* birth rate is large (given by inequalities in 3.10). Using consistent parameter values and plotting the result we arrive at Figure 3.6. As was seen earlier (Figure 3.4d), the parasites cause the extinction of the host population, however, comparing Figure 3.6 with Figure 3.4d we see that the mean number of parasites per host increase exponentially once the host population (and hence, detached parasite population) has decayed to zero. In a biological sense the behaviour that occurs after the salmon have died out due to *G. salaris* infection is improbable, however, mathematically possible. When the inequalities in (3.10) are satisfied (*i.e.*,  $a > b$ ,  $\mu > \epsilon + a + \alpha + \lambda$ ) equation (3.17) is always positive (since  $(\mu - \Gamma) + \beta W > 0$ ), thus,  $\frac{dM}{dt}$  exhibits exponential growth. Consequently, as  $M$  increases this has a negative impact on the host equation which decays to zero due to the  $-\alpha MH$  term in equation (3.16). Hence, this leads to the conclusion that the second zero equilibrium, the parasite induced host extinction equilibrium, is in fact stable.

### 3.3 INVESTIGATING THE OCCURRENCE OF PARASITE INDUCED HOST EXTINCTION

The parasite induced host extinction equilibrium discussed above is not often witnessed in macroparasite models but is more commonly encountered when investigating the dynamics of microparasitic infections. The appearance of such behaviour in the model was investigated to determine whether this scenario occurs as a result of the probability function used to model the distribution of parasites or is a result of the parasites ability to give birth directly on the skin of its salmon host, and hence, removing the requirement of a free-living stage. In the previous model, the distribution of the *G. salaris* parasites is given by a Poisson

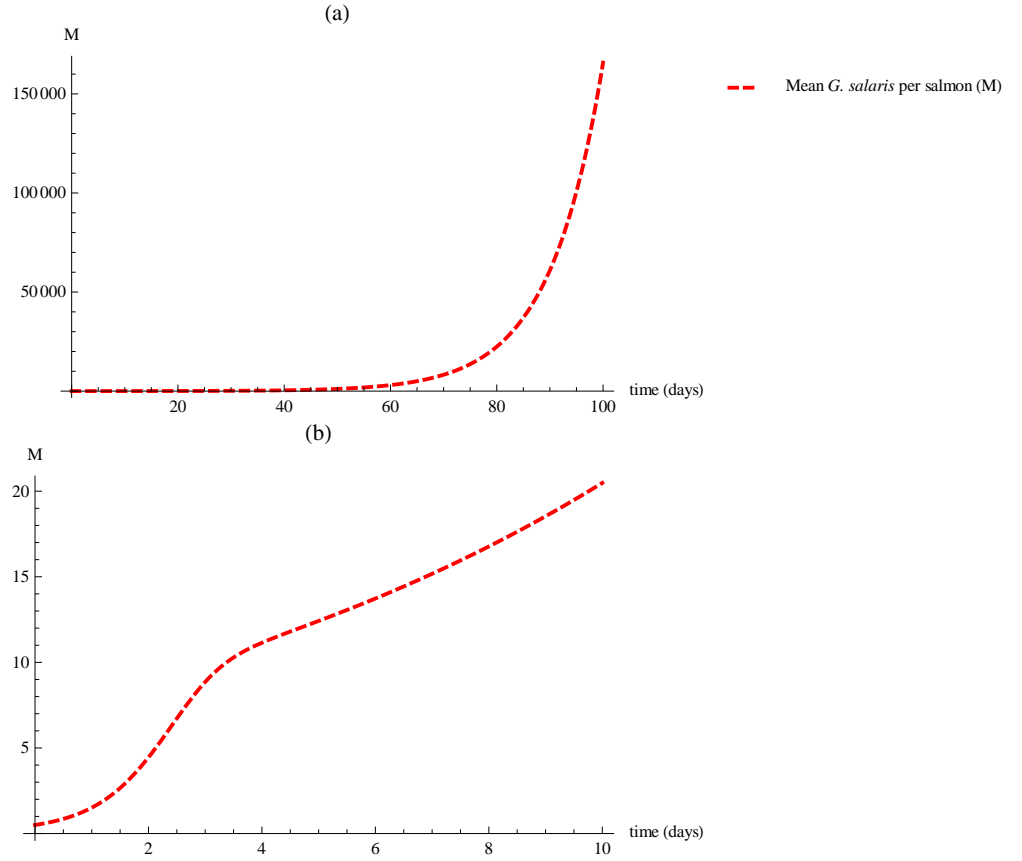


Figure 3.6: Parasite induced extinction. Trajectories for mean *G. salaris* per salmon host in time as predicted by Model B re-evaluated. As with Model B evaluated using density dependent transmission the parasites reduce the host population to zero, this occurs when  $a > b$  and  $\mu > \epsilon + a + \alpha + \lambda$ . However, the mean number of parasites per host now grows exponentially. Hence, the parasite induced equilibrium is stable. Here  $a = 4.0$ ,  $b = 2.0$ ,  $s = 0.01$ ,  $\mu = 7.1$ ,  $\epsilon = 0.5$ ,  $\alpha = 0.5$ ,  $\lambda = 2.0$ ,  $\sigma = 5.0$ ,  $\beta = 0.05$ ;  $H(0) = 100$ ,  $M(0) = 0.5$ ,  $W(0) = 10$ . Mean number of attached parasites per host (—). Plot (b) is a magnification of the behaviour in plot (a) over the first 10 days.

distribution, meaning the parasites are independently randomly distributed throughout the host population. Another distribution that is commonly used is the negative binomial distribution. This distribution is used when the parasite population is overdispersed. In this case at low densities parasites are aggregated and at high densities all hosts are highly infected. We now consider a model with *G. salaris* parasites following a negative binomial distribution. The system is now described by the following equations:

$$\begin{aligned}
 \frac{dH}{dt} &= (a - b - sH)H - \alpha P \\
 \frac{dP}{dt} &= P \left( \mu - (\epsilon + b + \alpha + sH + \lambda) - \alpha \frac{P(k+1)}{Hk} \right) + \beta WH \\
 \frac{dW}{dt} &= \lambda P - \sigma W - \beta WH
 \end{aligned} \tag{3.22}$$

Here the parameter  $k$  in (3.22) is the negative binomial parameter which measures the degree of parasite aggregation. If  $k$  is low then aggregation is high and if  $k$  is high then there is very little aggregation.

Following the usual methods of analysis we find equilibria exist at  $(0,0,0)$ ,  $(K,0,0)$ ,  $(H_+^*, P_+^*, W_+^*)$  and  $(H_-^*, P_-^*, W_-^*)$ , where  $(H_{\pm}^*, P_{\pm}^*, W_{\pm}^*)$  corresponds to the sign of  $\pm\sqrt{\Theta}$  with:

$$H^* = \frac{-\beta(r + k(\Gamma - \mu - \lambda)) + \sigma s \pm \sqrt{\Theta}}{-2\beta s} \quad (3.23)$$

$$P^* = \frac{(r - sH)H}{\alpha} \quad (3.24)$$

$$W^* = \frac{P(\mu + \lambda - \Gamma + r - sH - (r - sH)(\frac{k+1}{k}))}{\sigma} \quad (3.25)$$

and

$$\Gamma = \epsilon + a + \alpha + \lambda$$

$$\Theta = (\beta(r + k(\Gamma - \mu - \lambda)) - \sigma s)^2 + 4\beta s \sigma (r + k(\Gamma - \mu))$$

$$K = \frac{r}{s} \text{ and } r = a - b$$

$K$  is the carrying capacity.

Now, assigning values to the parameters in (3.22) and plotting the result gives the plots found in Figure 3.7.

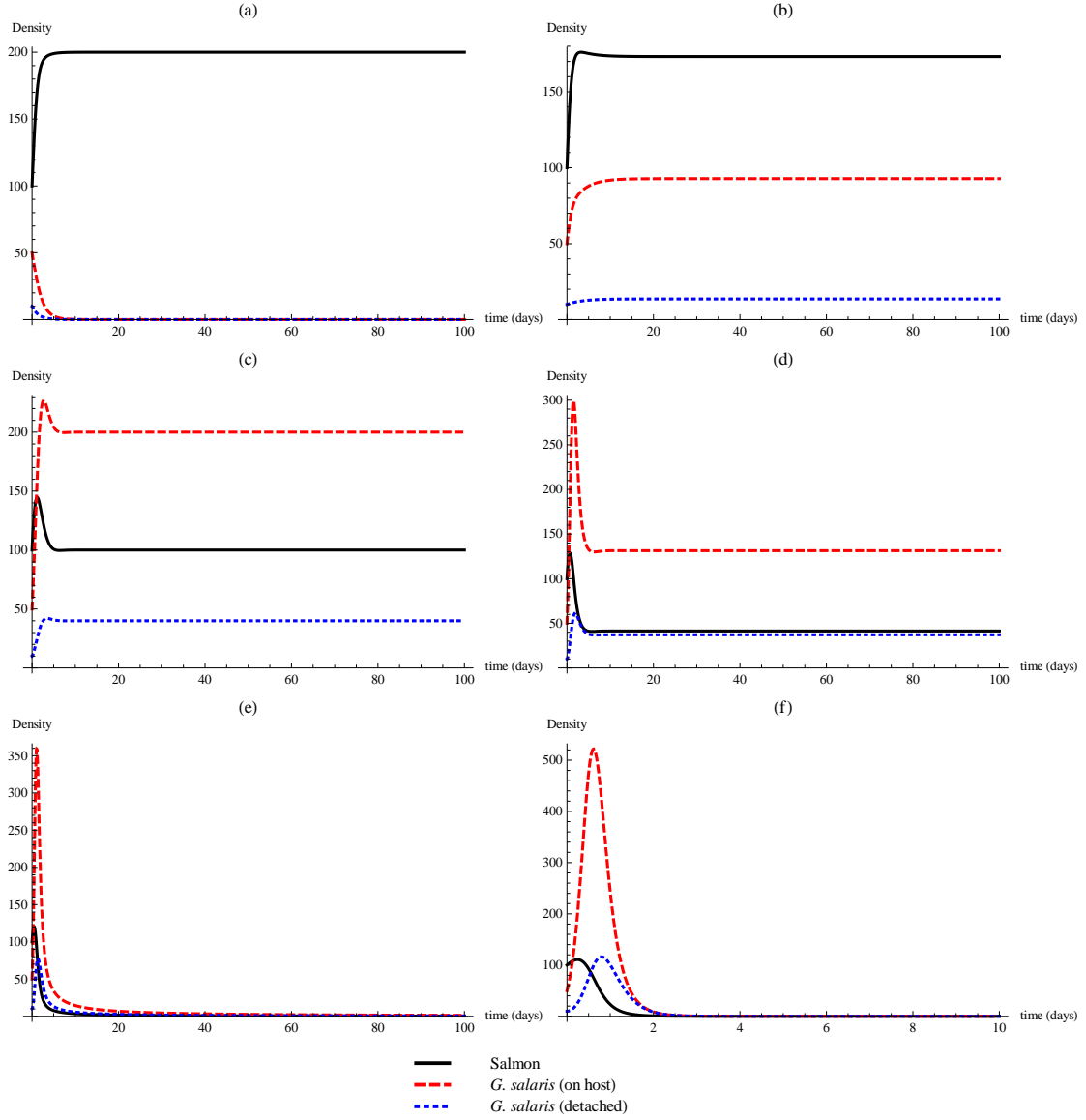


Figure 3.7: Trajectories for host, attached parasite and detached parasite populations in time as predicted by Model B re-evaluated using a negative binomial distribution. Starting at the disease-free scenario (a) and increasing the parasite birth rate  $\mu$  we arrive at coexistence, (b)-(e). Increasing  $\mu$  further we move into parasite induced extinction, (f). Here  $a = 4.0$ ,  $b = 2.0$ ,  $s = 0.01$ ,  $\epsilon = 0.5$ ,  $\alpha = 0.5$ ,  $\lambda = 2.0$ ,  $\sigma = 5.0$ ,  $\beta = 0.05$ ;  $H(0) = 100$ ,  $P(0) = 50$ ,  $W(0) = 10$ .  $\mu = 5.0, 6.0, 7.0, 8.0, 9.0, 12.0$  in (a), (b), (c), (d), (e) and (f) respectively. Hosts (—), mean number of attached parasites per host (---), detached parasites (···).

As can be seen in Figure 3.7, starting at the disease-free scenario, (a), and increasing the parasite birth rate  $\mu$ , we move into coexistence, (b)-(e). With  $\mu$  still increasing the parasite is able to regulate the host population at lower levels similar to what we seen in our previous model. Finally, parasite births get so large that the host population becomes extinct and we are once again at the parasite-induced extinction equilibrium, (f).

Changing the distribution of the parasite has allowed us to confirm that the cause of the parasite-induced extinction equilibrium is due to parasites giving birth directly on the hosts. This means the occurrence of parasite induced host extinction is not a consequence of using the Poisson distribution in the model. Hence, we have shown that whether a Poisson or negative binomial distribution is used the parasites can still reduce the host population to zero if its birth rate is high enough.

### 3.4 MODEL B: DETACHED PARASITES IN THE EXTERNAL ENVIRONMENT

According to the model above when a salmon host dies the parasites that it harboured also die. In reality the death of a salmon host does not necessarily cause the mortality of the *G. salaris* parasites it harboured. It is well documented that not only can *G. salaris* survive on a substrate and in the water column for a period of time, it can also survive on a dead host (Bakke *et al.*, 1992a; Soleng *et al.*, 1998; Olstad *et al.*, 2006). With this in mind, we change our model to incorporate this piece of information. We return to using the Poisson distribution for the parasite population and note that since hosts die due to natural and parasite induced causes, equation (3.2) becomes:

$$\frac{dW}{dt} = \left( b + sH + \lambda + \alpha + \frac{\alpha P}{H} \right) P - \sigma W - \beta WH \quad (3.26)$$

Hence our model is now given by equations (2.15), (3.1) and (3.26):

$$\begin{aligned} \frac{dH}{dt} &= (a - b - sH)H - \alpha P \\ \frac{dP}{dt} &= P \left( \mu - (\epsilon + b + \alpha + sH + \lambda) - \alpha \frac{P}{H} \right) + \beta WH \\ \frac{dW}{dt} &= \left( b + sH + \lambda + \alpha + \frac{\alpha P}{H} \right) P - \sigma W - \beta WH \end{aligned} \quad (3.27)$$

Once again, in the absence of disease ( $P = 0, W = 0$ ), the host population follows logistic growth to carrying capacity  $K$ , where  $K = \frac{a-b}{s}$ .

### Equilibria and stability

The equations in (3.27) readily yield equilibria by setting  $dH/dt = dP/dt = dW/dt = 0$  and solving in the usual way as above. Hence, we find equilibria exist at  $(0, 0, 0)$ ,  $(K, 0, 0)$  and  $(H^*, P^*, W^*)$ , where:

$$H^* = \frac{\sigma(\mu - (\epsilon + \alpha + \lambda))}{\beta(\epsilon - \mu)} \quad (3.28)$$

$$P^* = \frac{\sigma(\mu - (\epsilon + \alpha + \lambda))[\beta r(\epsilon - \mu) - s\sigma(\mu - (\epsilon + \alpha + \lambda))]}{\alpha\beta^2(\epsilon - \mu)^2} \quad (3.29)$$

$$W^* = -\frac{(\mu - (\epsilon + \alpha + \lambda))[\beta r(\epsilon - \mu) - s\sigma(\mu - (\epsilon + \alpha + \lambda))]}{\alpha\beta^2(\epsilon - \mu)} \quad (3.30)$$

In this model, the conditions for stability of the zero equilibrium are the same as the conditions for the original model in Section 3.1.1.1, that is the inequalities in (3.7). Assigning values to parameters in the equations in (3.27) and plotting as before we obtain the plot in Figure 3.8.

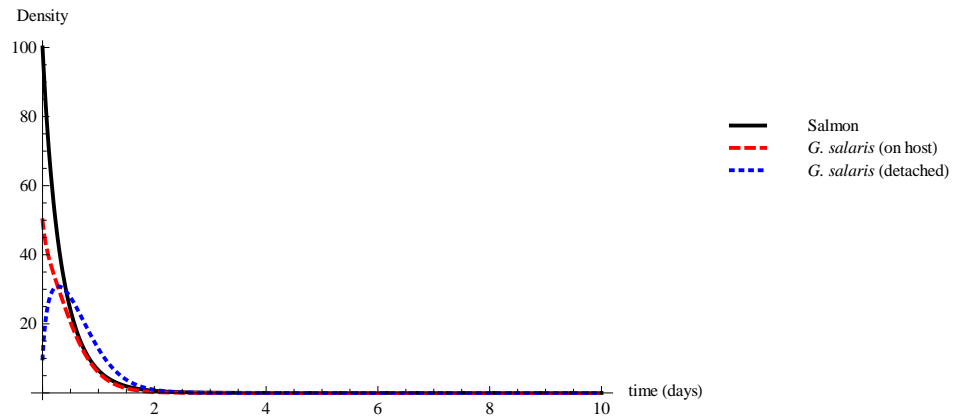


Figure 3.8: Zero equilibrium. Trajectories for host, attached parasite and detached parasite populations in time as predicted by Model B re-evaluated using equation (3.26). As before, at the zero equilibrium all populations decay to zero, however, in this case as the host population dies out the detached population now grows slightly before decaying to zero as expected. Here  $\alpha = 2.0$ ,  $b = 4.0$ ,  $s = 0.01$ ,  $\mu = 4.0$ ,  $\epsilon = 0.5$ ,  $\alpha = 0.5$ ,  $\lambda = 2.0$ ,  $\sigma = 5.0$ ,  $\beta = 0.05$ ;  $H(0) = 100$ ,  $P(0) = 50$ ,  $W(0) = 10$ . Hosts (—), parasites (---), detached parasites (···).

As expected, at the zero equilibrium (where salmon and *G. salaris* birth rates are less than their respective mortality rates) all populations quickly die out. This matches the results in Section 3.1.1.1. Closer examination of Figure 3.8, however, also shows a small increase in the numbers of detached parasites before the population decays to zero. This happens because hosts are dying and releasing their parasites into the detached environment which was not the case in results in Figure 3.2.

Moving forward, we now consider the disease-free equilibrium. The conditions for  $(K, 0, 0)$  to be stable are similar to the inequalities in (3.8) found in Section 3.1.1.2. However, due to

the addition of a dead host's parasites becoming detached instead of dying the conditions for stability in this case are:

$$a > b, \quad \mu < \epsilon \quad (3.31)$$

Now all we require for stability is (i) salmon births greater than salmon deaths and (ii) *G. salaris* births less than *G. salaris* deaths. Assigning values to the parameters in the model so that (3.31) holds true and plotting gives Figure 3.9.

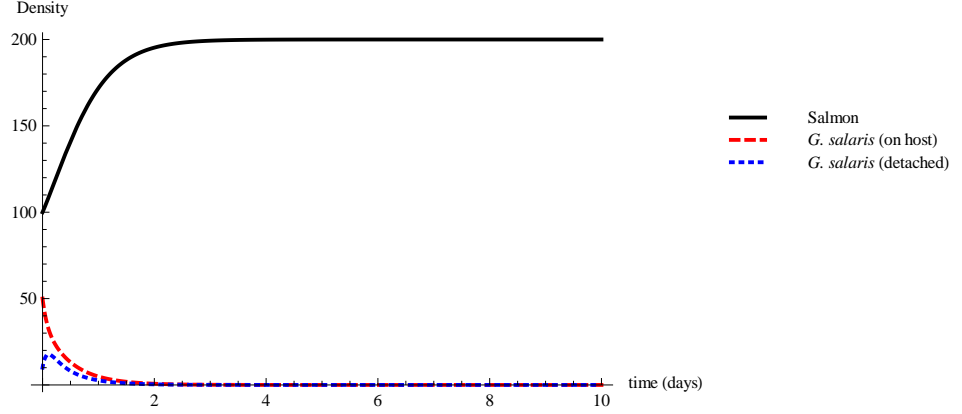


Figure 3.9: Disease-free equilibrium. Trajectories for host, attached parasite and detached parasite populations in time as predicted by Model B re-evaluated using equation (3.26). As expected, at the disease-free equilibrium the host population ( $a > b$ ) grows to carrying capacity as the parasite populations decay to zero. Here  $a = 4.0$ ,  $b = 2.0$ ,  $s = 0.01$ ,  $\mu = 0.1$ ,  $\epsilon = 0.5$ ,  $\alpha = 0.5$ ,  $\lambda = 2.0$ ,  $\sigma = 5.0$ ,  $\beta = 0.05$ ;  $H(0) = 100$ ,  $P(0) = 50$ ,  $W(0) = 10$ . Hosts (—), parasites (---), detached parasites (···).

As expected we get a similar result to that in Section 3.1.1.2. In the absence of disease (with host births greater than host mortality) the host population exhibits logistic growth to carrying capacity  $K$  whilst both parasite populations quickly decay to zero.

Next we consider the coexistence equilibrium. Using the expressions for  $H^*$ ,  $P^*$  and  $W^*$  given by equations (3.28), (3.29) and (3.30) respectively and following the usual methods of analysis we find that the coexistence equilibrium is stable (by Routh-Hurwitz) if and only if the following conditions are satisfied:

$$a > b, \quad \epsilon + \frac{s\sigma(a + \alpha + \lambda)}{\beta r + s\sigma} < \mu < \epsilon + a + \alpha + \lambda \quad (3.32)$$

Assigning values to the model's parameters to match the inequalities in (3.32) we get the results found in Figure 3.10 below.

As with the previous model, increasing the parasite birth rate  $\mu$  allows the parasites to regulate the host population at lower levels. With the condition  $\epsilon + \frac{s\sigma(a + \alpha + \lambda)}{\beta r + s\sigma} < \mu < \Gamma$  (where  $\Gamma = \epsilon + a + \alpha + \lambda$ ) it is now easier for the parasite to survive. In the previous model in order for the parasite population to persist parasite births,  $\mu$ , had to be greater than natural parasite deaths,  $\epsilon$ , + host births,  $a$ , + parasite induced host deaths,  $\alpha$ , + a proportion of the parasites that become detached,  $\frac{s\sigma\lambda}{\beta r + s\sigma}$ , but now all that is required is  $\mu > \epsilon + \frac{s\sigma(a + \alpha + \lambda)}{\beta r + s\sigma}$ .

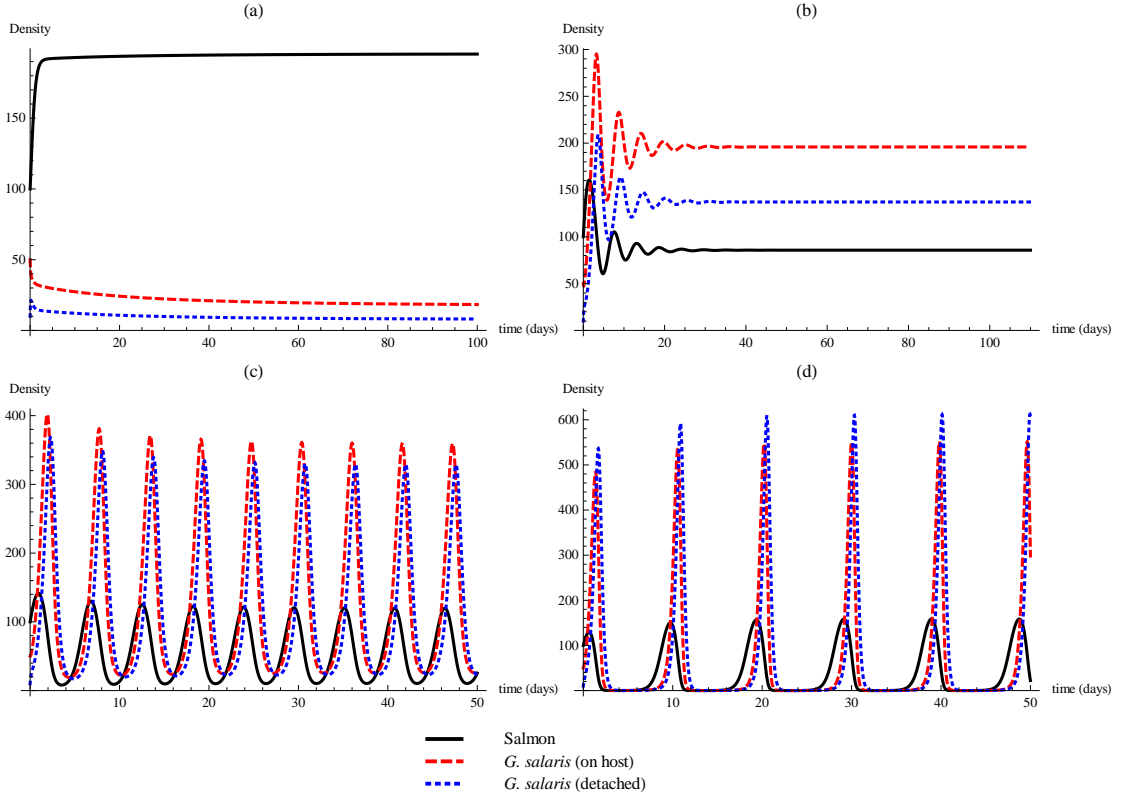


Figure 3.10: Coexistence equilibria. Trajectories for host, attached parasite and detached parasite populations in time as predicted by Model B re-evaluated using equation (3.26). With the addition of equation (3.26) it is now easier for the parasite to grow and regulate the host population. This is because the condition for coexistence is now  $\epsilon + \frac{s\sigma(a+\alpha+\lambda)}{\beta r+s\sigma} < \mu < \epsilon + a + \alpha + \lambda$ . In all plots  $a = 4.0$ ,  $b = 2.0$ ,  $s = 0.01$ ,  $\epsilon = 0.5$ ,  $\alpha = 0.5$ ,  $\lambda = 2.0$ ,  $\sigma = 5.0$ ,  $\beta = 0.05$ ;  $H(0) = 100$ ,  $P(0) = 50$ ,  $W(0) = 10$ . The only parameter that varies is parasite birth rate  $\mu$ .  $\mu = 2.7, 4.0, 5.0, 6.0$  in (a), (b), (c) and (d) respectively. Hosts (—), parasites (---), detached parasites (···).

If however, we have  $\epsilon < \mu < \epsilon + \frac{s\sigma(a+\alpha+\lambda)}{\beta r+s\sigma}$ , the host population grows to carrying capacity and the parasite populations quickly decay to zero and we are at the disease-free equilibrium.

Finally, if we take  $\mu$  greater than  $\Gamma$ ;

$$a > b, \quad \mu > \epsilon + a + \alpha + \lambda \quad (3.33)$$

we once again arrive at a second zero equilibrium, the parasite induced extinction equilibrium (see Figure 3.11).

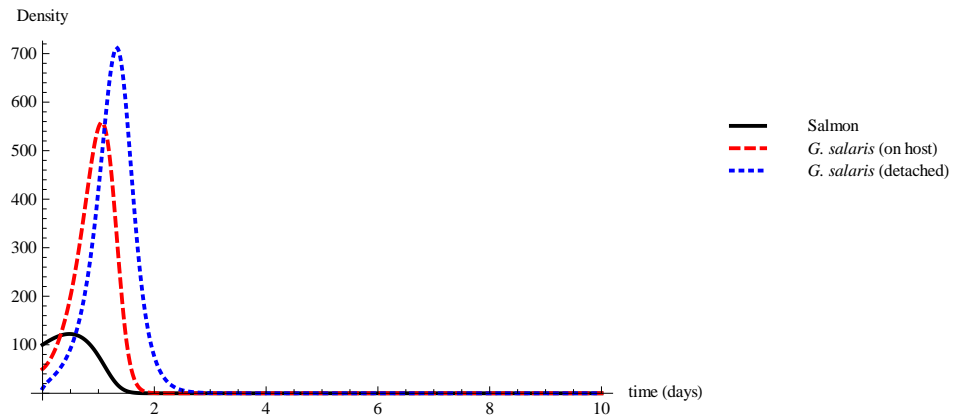


Figure 3.11: Parasite induced extinction. Trajectories for host, attached parasite and detached parasite populations in time as predicted by Model B re-evaluated using equation (3.26). As can be seen, the attached parasite population grows to an epidemic level and hence kills the host population. With the addition of equation (3.26), the detached parasite population now quickly increases. This is because attached parasites join the detached parasite population when a host dies. Here  $a = 4.0$ ,  $b = 2.0$ ,  $s = 0.01$ ,  $\epsilon = 0.5$ ,  $\alpha = 0.5$ ,  $\lambda = 2.0$ ,  $\sigma = 5.0$ ,  $\beta = 0.05$ ;  $H(0) = 100$ ,  $P(0) = 50$ ,  $W(0) = 10$ . Here the parasite birth rate  $\mu = 2.7$ . Hosts (—), parasites (---), detached parasites (···).

Looking at Figure 3.11 we see that the parasite population grows to an epidemic level and behaves similar to the results in Figure 3.4d. As the host population decays more parasites are released into the detached environment which continues to increase. Finally, when the host population has reached zero both parasite populations cannot persist and quickly decay to zero.

### 3.5 ESTIMATING PARAMETER VALUES

Three new parameters ( $\lambda$ ,  $\sigma$ ,  $\beta$ ) have been added to the models in this chapter. As was done in Chapter 2, estimates for population parameters were obtained using data and information available in the literature. These estimates are collected in Table A.1, Appendix A.

#### *Detachment rate, $\lambda$*

The rate at which *G. salaris* parasite become detached from a salmon host was estimated using unpublished experimental trials by Paladini and Denholm (see Tables A.8, A.9, A.10, A.11, Appendix A). However, the value obtained ( $\lambda = 0.14$ ) seemed rather high. It is possible that the high leave-host rate obtained was due to the fact that only one individual salmon host was present in the container. Thus, a lower value of  $\lambda = 0.06$  was taken as a more realistic estimate.

Off-host mortality rate,  $\sigma$

Mo (1987), as cited by Peeler *et al.* (2006), gave the maximum survival rate of *G. salaris* parasites off a salmon host as 6-7 days in ideal conditions. Thus, the daily mortality rate of *G. salaris* parasites when off a salmon host is estimated as 0.17-0.14.

Attach rate,  $\beta$

Data concerning the rate at which *G. salaris* parasites attach to a salmon host was not readily available, however, unpublished experimental trials by Paladini and Denholm (see Table A.10, Appendix A) allowed the estimation of this parameter. An infected Atlantic salmon parr and an uninfected Atlantic salmon parr were placed in a bucket of clean water in order to determine the rate at which *G. salaris* parasites leave a live salmon host and infect a new host. The experiment was run for eight hours after which both fish were removed from the bucket and the number of *G. salaris* parasites infecting each host counted. The *G. salaris* parasites remaining in the bucket were also counted. At the end of the trial the initially uninfected salmon had 57 parasites. Thus, the daily rate at which *G. salaris* parasites attach to a host is estimated as 0.006.

### 3.6 SIMULATING THE MODEL FOR A UK RIVER SYSTEM

Once again, for consistency, the model in its current form (the equations in 3.27) is parameterised and simulated for the Welsh River Dee according to Table A.1, Appendix A.

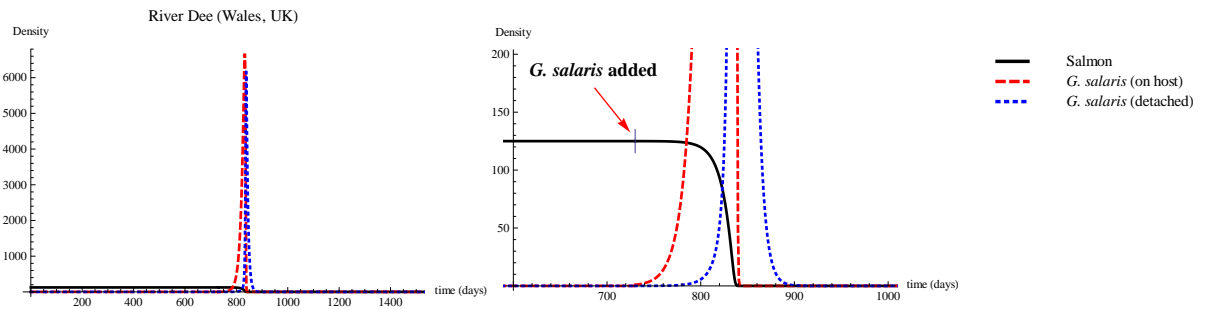


Figure 3.12: Model B: River Dee example. Trajectories of host, attached parasite and detached parasite populations in time as predicted by the detached parasites in the external environment model and parameterised according to Table A.1 as follows:  $a = 0.02$ ,  $b = 0.0006$ ,  $s = 0.00016$ ,  $\alpha = 0.0012$ ,  $\mu = 0.1708$ ,  $\epsilon = 0.08$ ,  $\lambda = 0.06$ ,  $\beta = 0.006$ ,  $\sigma = 0.16$ . Initially there is no infection present,  $H(0) = K = 125$ ,  $P(0) = 0$ ,  $W(0) = 0$ . Infection is added (a single attached parasite) after 730 days,  $H(730) = K = 125$ ,  $P(730) = 1$ ,  $W(730) = 0$ . Hosts (—), parasites (---).

As was the case in Chapter 2, Section 2.5, the conditions for the parasite induced extinction equilibrium (3.33) are satisfied when the model (in its current form, *i.e.*, the equations in 3.27) is parameterised for the River Dee. Looking at Figure 3.12 a short epidemic is observed after the introduction of *G. salaris*. This forces the salmon hosts to extinction, quickly followed

by the extinction of the *G. salaris* populations, as predicted by earlier results in the sections above. Once again the model simulations predict salmon extinction in the UK in the event of the emergence of *G. salaris* infections.

### 3.7 SUMMARY

The results contained within this chapter have contributed to the construction of the baseline model (Model B). The results obtained from Model B are consistent with observations made both experimentally and in the wild as well as what one would expect mathematically, *i.e.*, (i) if host births are less than host deaths both host and parasite populations die out; (ii) in the absence of disease the host population grows exponentially to carrying capacity; (iii) parasites regulate the host population until the parasite population is so large that the host population is forced into decay, and ultimately, extinction. Through equilibrium and stability analysis we have found if and where equilibria exist and under what conditions these equilibria are stable.

The analysis also highlighted a second zero equilibrium that occurs when the *G. salaris* population forces the salmon to extinction, an equilibrium not commonly witnessed in macroparasite models, and shown that this parasite induced host extinction equilibrium is stable. We have also determined that parasite induced host extinction will occur if and only if the parasite birth rate is greater than the rate of total parasite losses ( $\epsilon + a + \alpha + \lambda$ ) and, by varying the probability distribution function used to describe parasite distribution, that this equilibrium does not depend on the probability distribution function chosen but the ability of the parasite to reproduce on directly on the skin of a host.

Finally, we have extended equations (2.15), (3.1) and (3.2) to include the fact that individual *G. salaris* parasites do not generally die when the salmon host they are infecting dies. This adds biological realism to the the baseline model, and in turn, to the more complicated models that follow.

Biologically, the results obtained from the models above demonstrate that without any form of resistance or immune response, and if the parasite birth rate is high, *G. salaris* populations will grow to epidemic levels causing salmon populations to become extinct followed then by the parasite until both salmon and *G. salaris* populations are gone. However, if the parasite birth rate is low enough then populations of salmon and *G. salaris* should (in theory) be able to coexist, this however has not been witnessed in the field. Parameterising the model above for a UK river system (River Dee, Wales) predicts salmon extinction in the event of *G. salaris* emergence.

## Mechanisms for resistance in *Salmo salar* L.

### 4.1 INTRODUCTION

As discussed in Chapter 1, *Gyrodactylus salaris* has caused catastrophic damage to wild Atlantic salmon (*Salmo salar*, L.) stocks since its accidental introduction to Norway in 1975 (Johnsen, 1978; Johnsen & Jensen, 1986, 1991) resulting in a significant, continued, economic impact. In the years post introduction, *G. salaris* has spread to 48 rivers, 13 Atlantic salmon hatcheries and 26 rainbow trout hatcheries in Norway (Sviland *et al.*, 2012). It is estimated that *G. salaris* has cost the Norwegian salmon industry more than \$655 M (Bakke *et al.*, 2004) with an annual loss of 250 - 500 metric tonnes of salmon due to the average density of salmon parr in infected rivers being reduced by 86% (Bakke *et al.*, 2004). Such annual loss costs the Norwegian economy of over \$50 M per annum through the costs of surveillance and eradication (circa US \$23 million per annum), and losses to fisheries associated industries and tourism (circa US \$34 million per annum) (Bakke *et al.*, 2007). Hence, *G. salaris* poses a serious threat if it establishes in the UK and other potentially *G. salaris* free areas of Europe (Paladini *et al.*, *subm.*).

As discussed earlier *G. salaris* is highly pathogenic to populations of juvenile Atlantic salmon parr. However, different strains of the parasite have varying effects and hence these strains must be taken into consideration. Hansen *et al.* (2003) outlined the three currently known clades of *G. salaris* :

1. Clade I, this strain was only found on Atlantic salmon and is highly pathogenic;
2. Clade II, this strain was found on salmon from the river Göta älv in Sweden;
3. Clade III, this strain was found on salmon from the rivers Lærdalselva, Drammenselva and Lierelva in Norway and on rainbow trout from a fish farm in Lake Bullaren, Sweden.

Another strain of *G. salaris* has been found on rainbow trout in Denmark (Buchmann & Bresciani, 1997; Nielsen & Buchmann, 2001). This variant of the *G. salaris* parasite shows

low virulence towards Atlantic salmon and under experimental conditions, on isolated hosts, this strain showed limited reproduction or no establishment at all (Lindenstrom *et al.*, 2003). However, Lindenstrom *et al.* (2003) observed high susceptibility to this strain in rainbow trout and noted that this strain of the parasite greatly resembles *G. salaris sensu stricto*.

*Gyrodactylus salaris sensu stricto* (Clade I) is the strain of *G. salaris* that is highly pathogenic to Atlantic salmon. The Atlantic salmon is highly susceptible to this strain of *G. salaris* with infection resulting in death. Within five years of introduction, *G. salaris* can reduce a salmon population by approximately 98% as has been observed throughout much of Norway (Johnsen & Jensen, 1991). As mentioned above (and discussed in Chapter 1), *G. salaris* can survive and reproduce on Atlantic salmon but cannot survive full strength salinity, hence, the parasite mainly infects juvenile salmon (*e.g.*, fry and parr) since they are more likely to make contact with the substrate, resulting in fewer smolts migrating to the sea.

In terms of Atlantic salmon strains, Bakke *et al.* (2004) showed that some stocks of the Baltic strain of Atlantic salmon are susceptible to *G. salaris* but not to the same degree as the Atlantic strain. It is the current belief that relative immunity of the Baltic strain is due to the presence of the parasite in the Baltic watershed since the last glacial period (Bakke *et al.*, 2002). This supports the hypothesis that *G. salaris* is a recent introduction to Norwegian rivers and demonstrates why Norwegian Atlantic salmon are particularly susceptible to the parasite. The different strains of *G. salaris* have been shown to have varying effects on salmon as mentioned above, in particular the rainbow trout strain was shown to have no effect on Scottish Conon salmon (Lindenstrom *et al.*, 2003).

#### 4.1.1 *The biology of Gyrodactylus*

As discussed earlier, the Atlantic strain of Atlantic salmon, examples of which occur naturally in Norway and the UK, does not appear to have any resistance to *G. salaris* infections (Bakke *et al.*, 1990; Bakke & MacKenzie, 1993; Hansen *et al.*, 2003), hence, on juvenile hosts the parasite population is able to increase in size rapidly and cause substantial mortality. The rapid growth of the *G. salaris* population on a salmon host is due to progenic parasites giving birth to fully grown pregnant offspring (a process known as hyperviviparity) as well as generally short generation times. This “Matryoshka” (Russian doll) method of reproduction means the parasite population is able to grow exponentially to epidemic levels within the host population, resulting in mass salmon mortality. In contrast, the Baltic strain of Atlantic salmon, examples of which occur naturally in Sweden and Russia, does exhibit some form of resistance (Bakke *et al.*, 2002, 2004) to attacks and the parasite is unable to persist and parasite numbers are kept at low levels (Bakke *et al.*, 1990; Cable *et al.*, 2000). Understanding

the differences in these responses to the parasite is critical to understanding how salmon in *G. salaris* free territories such as the UK would respond to infection.

This chapter concerns the use of two different mathematical methods to investigate the possible differences in the *G. salaris* life-cycle which could cause the differences in parasite population numbers on Baltic and Atlantic strains of Atlantic salmon. Until now it has been assumed that the parasites are either less fecund or have a lower survival rate on the Baltic strain. Here both Leslie matrices and individual based models are used to determine the effect of another mechanism - timing of parasite first birth. In this chapter the relative importance of timing of parasite first birth, total number of offspring and parasite survival are compared.

#### 4.2 DATA

The dynamics of a population of *G. salaris* infecting a single fish host were studied using data from Cable *et al.* (2000) for one strain of *G. salaris* infecting three strains of Atlantic salmon. Of the three Atlantic salmon strains two were susceptible Atlantic strains (originating from the Rivers Alta and Lier, Norway) and the third was the resistant Baltic strain (originating from the River Neva, Russia). From their study Cable *et al.* (2000) showed at 12.5°C ( $\pm 0.2$ ) individual *G. salaris* parasites had a maximum longevity of 26, 24 and 17 days (median survival of 7.9, 5.2 and 3.5 days) on Alta, Lier and Neva hosts respectively. Median survival of parasites was low due to high parasite mortality on both Atlantic and Baltic hosts, however, mortality was significantly higher in parasites infecting Baltic hosts (Cable *et al.*, 2000).

Their study highlighted differences in fecundity exist between parasites on Atlantic and Baltic hosts with 4 births occurring on Alta and Lier hosts (confirming the results of an earlier study by Jansen & Bakke, 1991) compared to 2 birth occurring on Neva hosts. They also observed the timing of parasite first birth was more variable on Neva hosts compared to that on Alta and Lier hosts with parasite first birth occurring after 1.85, 1.88 and 2.34 days on Alta, Lier and Neva hosts respectively.

#### 4.3 MODELLING TECHNIQUES

Two different modelling techniques were used to simulate the data. Due to our interest in *G. salaris* population growth on a single fish host only, Leslie matrix population models were used because they allow the use of daily fertility rates and fit well with the biology of the parasite (*e.g.* parasite's method of reproduction, in particular, an individual parasite only gives birth to one female offspring at any one time). In order to verify that results

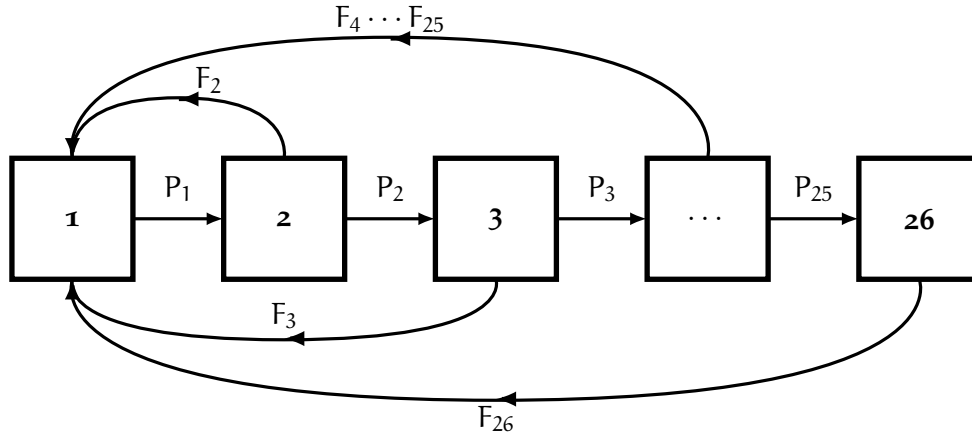


Figure 4.1: A schematic representation of the general form of the Leslie matrix and individual based models for *G. salaris* infecting a single salmon host. The model is age structured (in days) with parameters F and P indicating fertility and survival respectively. Models are parameterised for Alta (susceptible), Lier (susceptible) and Neva (resistant) salmon stocks according to Table 4.1 in the main text.

obtained were not a consequence of the modelling method used a stochastic approach was also developed in the form of individual based models. All models were simulated using Mathematica and selected code is available in Appendix D.

#### 4.3.1 Leslie matrix models

$$\begin{pmatrix} n_0 \\ n_1 \\ n_2 \\ \vdots \\ n_\omega \end{pmatrix}_{t+1} = \begin{pmatrix} F_0 & F_1 & \dots & F_{\omega-1} & F_\omega \\ P_0 & 0 & \dots & 0 & 0 \\ 0 & P_1 & \dots & 0 & 0 \\ \vdots & \vdots & \ddots & \vdots & \vdots \\ 0 & 0 & \dots & P_{\omega-1} & 0 \end{pmatrix} \begin{pmatrix} n_0 \\ n_1 \\ n_2 \\ \vdots \\ n_\omega \end{pmatrix}_t \quad (4.1)$$

Leslie matrix population models are discrete, age or stage-dependent models that are widely used in the fields of mathematics and biology for predicting population growth (Leslie, 1945). The Leslie matrix itself, Equation (4.1), is a square matrix that is closed to migration and only considers the females of a population. Only females are considered due to the convention that only the females of a population can reproduce. All elements in the Leslie matrix are zero except those found in the first row, representing fertility rates  $F_i \geq 0$ , and sub-diagonal, representing survival rates from one generation to the next  $0 \leq P_i \leq 1$ . Finally,  $n_i(t)$  is the number of individuals in age class  $i$  at time  $t$ .

#### 4.3.2 Parameterising Leslie matrix models

Under experimental conditions the maximum longevity of parasites was extended to 26, 24 and 17 days for parasites on Alta, Lier and Neva fish respectively to allow births to occur (Cable *et al.*, 2000). Since maximum longevity of parasites observed on all three salmon stocks was less than or equal to 26 days, a  $26 \times 26$  Leslie matrix model was constructed to predict the growth of a *G. salaris* population on a single fish host. Experiments were undertaken for a period of 5 weeks, likewise, models were simulated for 35 days (time step = 1 day). Equation (4.2) and Figure 4.1 give the general form of our model.

$$A = \begin{pmatrix} F_1 & F_2 & F_3 & \dots & F_{26} \\ P_1 & 0 & 0 & \dots & 0 \\ 0 & P_2 & 0 & \dots & 0 \\ \vdots & \vdots & \ddots & \vdots & \vdots \\ 0 & 0 & \dots & P_{25} & 0 \end{pmatrix} \quad (4.2)$$

Models were parameterised for the two stocks of Atlantic salmon (Alta, Lier) and one stock of Baltic salmon (Neva) and simulated such that each of the three salmon stocks were initially infected with one single *G. salaris* parasite at time  $t = 0$ .

##### 4.3.2.1 Parasite survival

Parasite daily survival rates were estimated using the 50% survival times determined and given by Cable *et al.* (2000). The 50% survival time is the time taken for the population to decrease to 50% (median survival) and was given as 7.9 days on Alta fish, 5.2 days on Lier fish and 3.5 days on Neva fish. Survival rates ( $P_t$ ) for the Leslie models were calculated as follows:

$$N_{t+1} = bN_t \quad (4.3)$$

$$N_t = b^t N_0 \quad (4.4)$$

$$\frac{1}{2} N_0 = b^t N_0 \quad (4.5)$$

$$\frac{1}{2} = b^{50\% \text{ life span}} \quad (4.6)$$

where  $N_0$  is the number of parasites at time  $t = 0$  (here  $N_0 = 1$ ),  $t$  is time (in days) and  $N_t$  is the proportion of parasites surviving to time  $t$ . Here,  $N_0 = 1$  due to all simulations initially starting with 1 parasite. Since the 50% survival times found in the literature are used,  $\frac{1}{2} N_0$  is used as above. Hence, survival rates for Alta, Lier and Neva are respectively:

$$b_{\text{Alta}} = \left(\frac{1}{2}N_0\right)^{\frac{1}{50\% \text{ Alta life span}}} = \left(\frac{1}{2}\right)^{\frac{1}{7.9}} = 0.92 \quad (4.7)$$

$$b_{\text{Lier}} = \left(\frac{1}{2}N_0\right)^{\frac{1}{50\% \text{ Lier life span}}} = \left(\frac{1}{2}\right)^{\frac{1}{5.2}} = 0.88 \quad (4.8)$$

$$b_{\text{Neva}} = \left(\frac{1}{2}N_0\right)^{\frac{1}{50\% \text{ Neva life span}}} = \left(\frac{1}{2}\right)^{\frac{1}{3.5}} = 0.82 \quad (4.9)$$

Survival rates were kept constant throughout the three Leslie models such that  $P_1 = P_2 = \dots = P_{25}$ .

#### 4.3.2.2 Parasite fecundity and fertility

With maximum longevity extended, Cable *et al.* (2000) observed 4 births occurring on Atlantic hosts (Alta and Lier) and only 2 births on Baltic hosts (Neva). Thus, models were developed such that individual *G. salaris* parasite gave birth to either 4 or 2 offspring in its lifetime depending on whether it was infecting an Atlantic or Baltic strain of salmon host respectively (see Appendix A, Table A.2).

Parasite fertility rates  $F_i$  were calculated using the average time taken for parasite offspring to be born on the different salmon hosts. Probabilistic distribution of births was included in order to allow part day differences in birth timing to occur. Allowing part day differences in fertility made it possible for an offspring to be born on fractions of days as is the case in the literature. Thus, fertility rates were calculated via the following:

Let  $F_1, \dots, F_{26} = \text{day } 1, \dots, 26$  respectively.

Then  $F_1 + F_2 = 1$  etc.

Therefore, for an offspring born between day 1 and day 2, e.g. on day 1.85 let  $F_1 + 2F_2 = 1.85$ .

Now  $F_1 + F_2 = 1 \Rightarrow F_1 = 1 - F_2$ .

Therefore,  $1 - F_2 + 2F_2 = 1.85$

$F_2 = 0.85$

$F_1 = 0.15$

Hence, 0.15 births on day 1 and 0.85 on day 2. Table 4.1 gives descriptions of the parameters used throughout this chapter.

Table 4.1: Parameter values used in Leslie matrix and individual based models calculated using data from Cable *et al.* (2000) for one strain of *G. salaris* infecting two susceptible salmon stock (from the Rivers Alta and Lier, Norway) and one resistant salmon stock (from the River Neva, Russia).

$i = 1, \dots, 26$	Lier	Alta	Neva
$P_i$	0.875	0.916	0.820
$F_1$	0.12	0.15	0
$F_2$	0.88	0.85	0.66
$F_3$	0	0	0.34
$F_4$	0	0	0
$\vdots$	$\vdots$	$\vdots$	$\vdots$
$F_8$	0.65	0	0
$F_9$	0.35	0.95	0
$F_{10}$	0	0.05	1
$F_{11}$	0	0	0
$\vdots$	$\vdots$	$\vdots$	$\vdots$
$F_{16}$	1	0.6	0
$F_{17}$	0	0.4	0
$F_{18}$	0	0	0
$\vdots$	$\vdots$	$\vdots$	$\vdots$
$F_{22}$	0	0.5	0
$F_{23}$	1	0.5	0
$F_{24}$	0	0	0
$F_{25}$	0	0	0
$F_{26}$	0	0	0

#### 4.3.3 Individual based models

In addition to the Leslie matrix modelling approach, an individual based stochastic model was also developed for the reason stated in Section 4.3 above. As with the Leslie matrix models, the individual based models consisted of 26 stages representing the maximum longevity of individual parasites (26 days).

#### 4.3.4 Parameterising individual based models

##### 4.3.4.1 Parasite survival

At each time step each parasite could either die or progress to the next stage. To determine whether a parasite progressed to the next stage or died, a random number (between 0 and 1) was generated and compared to the probability of mortality per day of parasites,  $p_b$ . If this random number was less than the mortality probability the parasite died and was removed from the simulation, otherwise it survived and moved to the next stage. The probability of mortality per day of parasites ( $p_b$ ) in the individual based models was calculated as follows:

$$pb = 1 - b \quad (4.10)$$

Hence,

$$pb_{Alta} = 1 - b_{Alta} = 0.08 \quad (4.11)$$

$$pb_{Lier} = 1 - b_{Lier} = 0.12 \quad (4.12)$$

$$pb_{Neva} = 1 - b_{Neva} = 0.18 \quad (4.13)$$

The probability of mortality per day of parasites was kept constant throughout each of the 26 stages in model simulations.

#### 4.3.4.2 Parasite fecundity and fertility

Models were once again parameterised to allow 4 or 2 births to occur depending on the host strain being infected. To determine if and when a parasite gives birth, a second random number was generated (again between 0 and 1) and compared to the probability of a parasite giving birth in that stage. The probability of a parasite giving birth in a stage was determined using the day on which offspring were born according to Table 3 in Cable *et al.* (2000). For example, in the case of Alta parasites, 1st birth occurs after 1.85 days, thus, there is a 0.15 probability the birth will occur on day 1 and a 0.85 probability the birth will occur on day 2. Hence, at certain stages parasite would do one of four things:

1. Give birth to an offspring before moving to the next stage;
2. Give birth to an offspring before dying;
3. Move to the next stage without giving birth;
4. Die without giving birth.

New born parasites entered the model at stage 1. The model followed individual parasites through time and kept track of the number of parasites in each stage throughout the simulation. Individual based models were simulated for 35 days of infection and repeated 50 times. The results shown are the average of the 50 simulations.

## 4.4 MECHANISMS FOR RESISTANCE

### 4.4.1 Baseline simulations

Initially the Leslie matrix model was used to simulate the data directly in order to compare model outputs with experimental data. Figure 4.2 shows the results obtained from the Leslie matrix models.

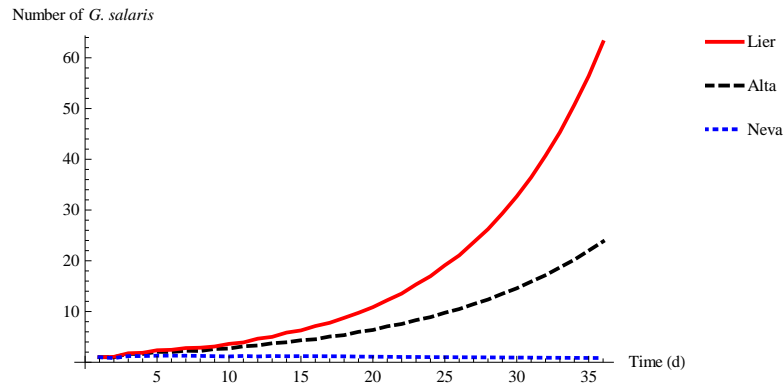


Figure 4.2: Leslie baseline simulation. Change in parasite numbers over time (days) from model simulation of *G. salaris* on three strains of *Salmo salar*, two susceptible Atlantic strains (Alta —, Lier —) and one resistant Baltic strain (Neva ···). As can be seen, with no changes to parameters, *G. salaris* populations on the Atlantic strains exhibit exponential-like growth whereas those on the Baltic strain decay to zero.

As can be seen in Figure 4.2, *G. salaris* populations on both Atlantic strains exhibit positive growth whereas those on the Baltic strain decay to zero. This is what one would expect from the biology and matches the experimental results obtained by Bakke *et al.* (1990). The data was then simulated using the individual based model. For comparison purposes outputs from the individual based model were plotted along with results from the Leslie matrix model and those obtained experimentally by Bakke *et al.* (1990) and are shown in (Figure 4.3).

Comparing the baseline simulation results from both modelling techniques to the experimental data from literature (Bakke *et al.*, 1990; Jansen & Bakke, 1991; Cable *et al.*, 2000) one can see that both models give a reasonable fit to data in susceptible Atlantic hosts initially but under predict *G. salaris* numbers by the end of the 5 week period. Additionally, some of the stochastic simulations were in fact able to capture the dynamics of parasites infecting resistant Baltic hosts. However, the majority of individual based simulations and all Leslie matrix simulations for *G. salaris* on Baltic hosts were unable to accurately provide such a fit. The individual based models also enabled the calculation of extinction probabilities of parasites where 0.00 indicates the population will never become extinct and 1.00 indicates the opposite. Extinction probabilities were estimated as 0.22 for *G. salaris* populations on Atlantic hosts and 0.9 for *G. salaris* populations on Neva hosts. The extinction probabilities obtained from model

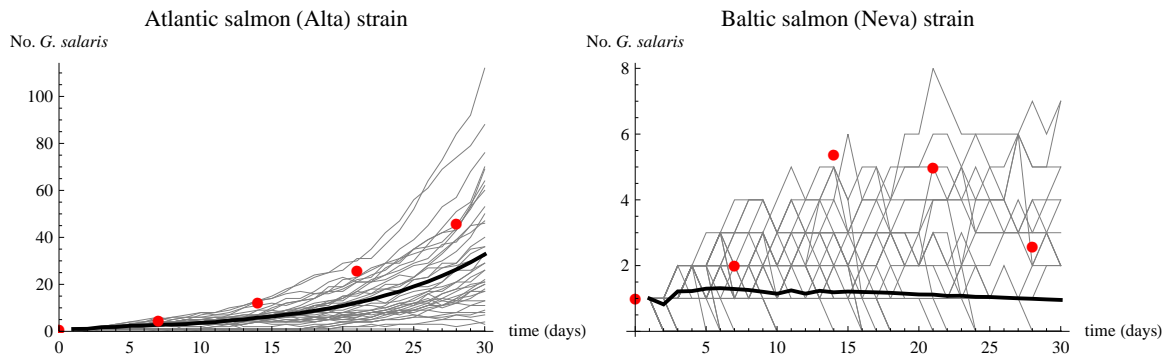


Figure 4.3: Baseline simulation results showing change in parasite numbers over time (days) for *G. salaris* on one susceptible (Alta) and one resistant (Neva) strain of *S. salar* obtained via the Leslie model (thick, black trajectory) and individual based model (thin, grey trajectories). The trajectory of parasite growth obtained from the literature via experimentation (Bakke *et al.*, 1990) is given in red (red plot markers). As can be seen in the case of the susceptible Alta salmon both modelling techniques give a reasonable fit to the data, however, in the resistant Neva case neither model is capable of providing an accurate fit to data.

simulations further confirmed the observations by Bakke *et al.* (1990) were populations of *G. salaris* grow exponentially on Atlantic hosts but decay to zero on Baltic hosts.

From the literature it is clear that that Baltic hosts are able to mount some form of immune response to *G. salaris* infections (Bakke *et al.*, 1990; Cable *et al.*, 2000). In order to try and explain these different responses comparisons were made between the parameters for the parasites on the different strains of salmon.

#### 4.4.2 Delayed parasite first birth

One of the differences immediately noted between parasites infecting Atlantic hosts and Baltic hosts is the fact that the first born offspring occurs after 1.9 days on Atlantic salmon and 2.3 days on their Baltic counterparts. Approximately there was a 0.49 day difference between the first born offspring on Alta and Neva stocks and a 0.46 day difference between Lier and Neva stocks. The possible consequences of this slight delay in initial birthing times was investigated. This was achieved by altering the birth rates in both the Leslie matrix and individual based models. It was decided that a delay in first birth would be more informative than a delay in all births since the timing of second births did not appear to vary much on either Atlantic or Baltic hosts (Cable *et al.*, 2000). Simulations were performed for *G. salaris* on the two stocks of susceptible salmon and compared the resulting outcomes with the baseline simulations in obtained on Section 4.4.1 to determine whether this difference alone can explain the resistance to *G. salaris* witnessed in Baltic salmon.

Figure 4.4 shows the impact on the parasite population when first birth occurs after 2.34 days on both Alta and Lier stocks (with all other parameters as in Figure 4.2). As can be

seen, delaying the first birth by only half a day has caused the parasite populations on both Norwegian stocks to reduce by around 50%.

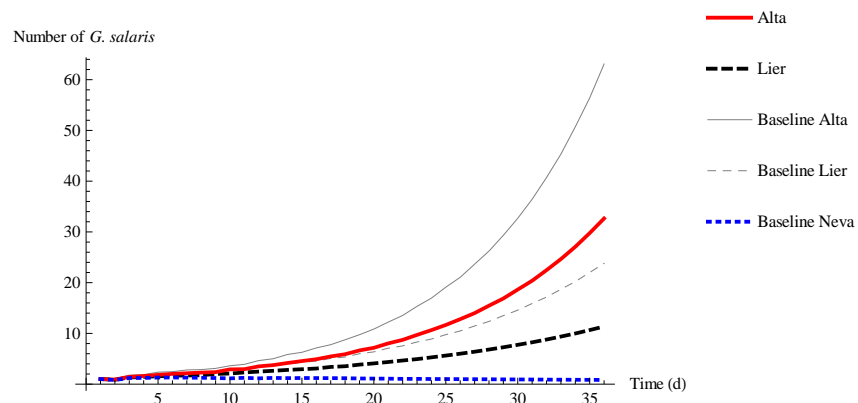


Figure 4.4: Parasite first birth delayed by 0.5 days. Trajectories of *G. salaris* populations infecting two Atlantic strains of *S. salar* (Alta —, Lier ---) over time (days) as predicted by the Leslie matrix model with delayed first birth. Delaying parasite first birth by 0.5 days on Alta and Lier salmon and comparing the results to the baseline simulation a 50% reduction in parasite numbers is witnessed. Baseline Alta (—), Lier (---) and Neva (···) trajectories given for comparison.

As with the baseline simulations in Section 4.4.1, simulations were performed using the individual based model and the results plotted with those obtained using the Leslie matrix model (see Figure 4.5). As can be seen in Figure 4.5 for *G. salaris* on Alta and Lier fish the individual based model results agree with those obtained using the Leslie matrix model.

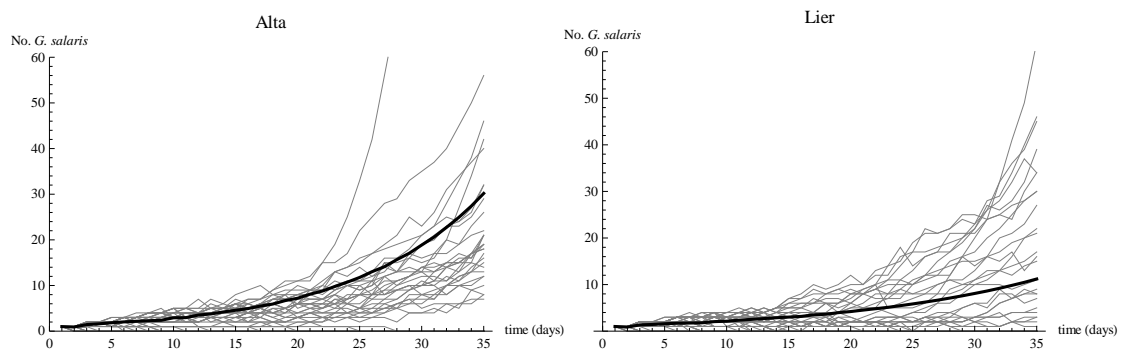


Figure 4.5: Parasite first birth delayed by 0.5 days. Trajectories of *G. salaris* populations infecting two Atlantic strains of *S. salar* as predicted by the individual based model (thin, grey) with delayed parasite first birth. Results from the Leslie matrix model (thick, black) are given for comparison of model outputs.

Taking this approach further, parasite first birth was then delayed by one whole day with offspring first birth occurring after 2.85 and 2.88 days on Alta and Lier stocks respectively using the Leslie matrix model (Figure 4.6) and individual based model (Figure 4.7). Importantly it was found, via both modelling methods, that the *G. salaris* population on the two Atlantic fish stocks is reduced by approximately 75%. However, the parasite populations on both Alta and Lier hosts still exhibit positive growth. Hence, a delay in the timing of parasite first birth

alone has an important impact on the dynamics but does not give hosts an adequate form of defence against infection.

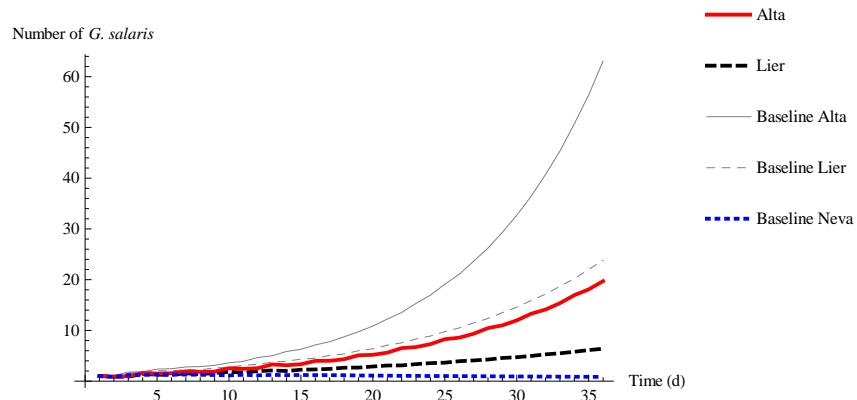


Figure 4.6: Parasite first birth delayed by 1 day. Trajectories of *G. salaris* populations infecting two Atlantic strains of *S. salar* (Alta —, Lier ---) over time (days) as predicted by the Leslie matrix model with delayed parasite first birth. Delaying parasite first birth by 1 day on Alta and Lier salmon and comparing the results to the baseline simulation a 75% reduction in parasite numbers is witnessed. Baseline Alta (—), Lier (---) and Neva (···) trajectories given for comparison.

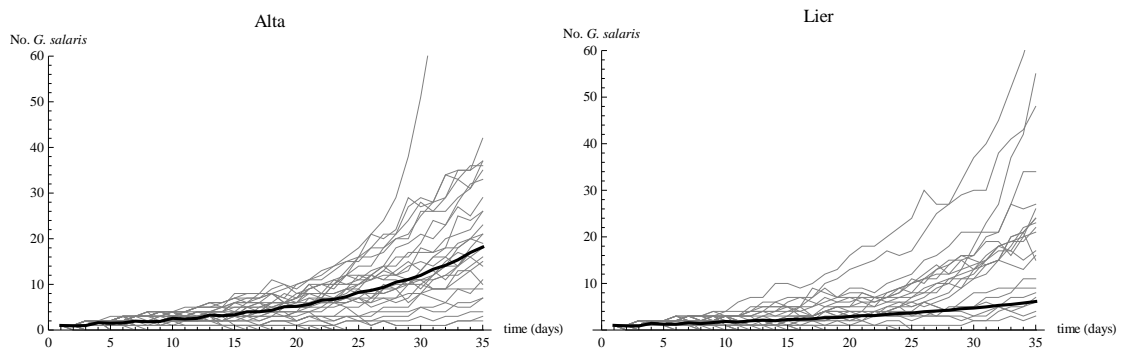


Figure 4.7: Parasite first birth delayed by 1 day. Trajectories of *G. salaris* populations infecting two Atlantic strains of *S. salar* as predicted by the individual based model (thin, grey) with delayed parasite first birth. Results from the Leslie matrix model (thick, black) are given for comparison of model outputs.

#### 4.4.3 Reduced number of parasite births

Another possible manifestation of resistance of Baltic salmon to rapid *G. salaris* population growth is a reduction in the number of births that may occur in a parasite's life-cycle. As demonstrated by Cable *et al.* (2000), *G. salaris* parasites infecting Baltic hosts only achieve two births in their lifetime compared to the four births that occur for those parasites infecting Atlantic hosts. Looking at the parasite populations on both Atlantic and Baltic hosts over a period of two weeks in the baseline simulation (Figure 4.2), population numbers at this point are not significantly different. Moreover, after this period observations of parasites on

Baltic hosts begin to decay (Bakke *et al.*, 1990). In the first two weeks parasites on Atlantic and Baltic hosts give birth to two offspring, after the two week period parasites on Atlantic hosts can give birth to up to two more parasites giving a maximum of four offspring in its life time. Therefore, the Leslie and individual based models were re-parameterised to determine whether reducing the number of times that a single parasite, infecting Alta and Lier fish, gives birth in its lifetime will cause the overall parasite population to decline. All other parameter values remained consistent with the baseline simulations as in Figure 4.2.

Running simulations via the Leslie matrix model and comparing output with individual based simulations gives the results in Figures 4.8 and 4.9 respectively. In both Alta and Lier cases with individual parasite giving birth only twice (1.85 and 9.05 days on Alta and 1.88 and 8.35 days on Lier), the size of the parasite population is not significantly reduced and is still able to grow (approximately a 20% reduction in *G. salaris* numbers on both Alta and Lier hosts was observed). This behaviour is in contrast to that of *G. salaris* populations on Baltic hosts which decay to zero. Our results highlight the fact that a reduced number of births alone does not explain the Baltic salmon's innate resistance to *G. salaris* infections. Output from both modelling methods remained consistent (See Figure 4.9).

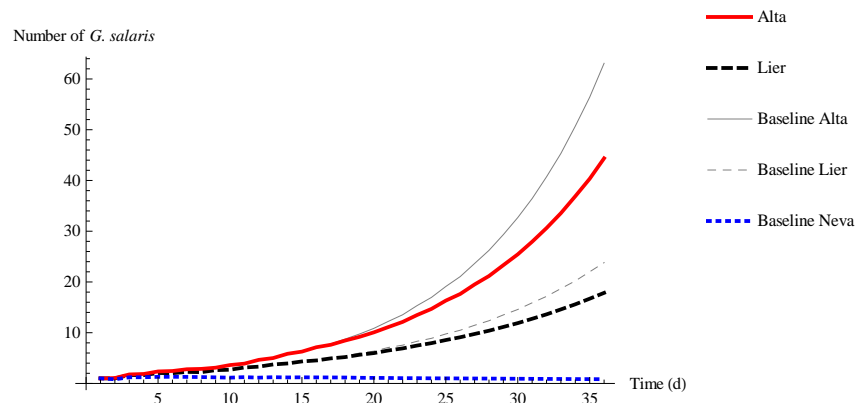


Figure 4.8: Reduced parasite births. Trajectories of *G. salaris* populations infecting two Atlantic strains of *S. salar* (Alta —, Lier ---) over time (days) as predicted by the Leslie matrix model with reduced number of parasite offspring. Reducing the total number of births per parasite on Alta and Lier hosts from four offspring to two offspring has very little effect on the parasite population dynamics with only a 20% reduction over the 35 day period. Baseline Alta (—), Lier (---) and Neva (···) trajectories given for comparison.

#### 4.4.4 Reduced parasite survival

The third notable difference between parasites infecting Atlantic and Baltic salmon is their survival rate. To study this, the rate at which *G. salaris* parasites survive from one age class to the next was reduced in both the Leslie matrix and individual based models.

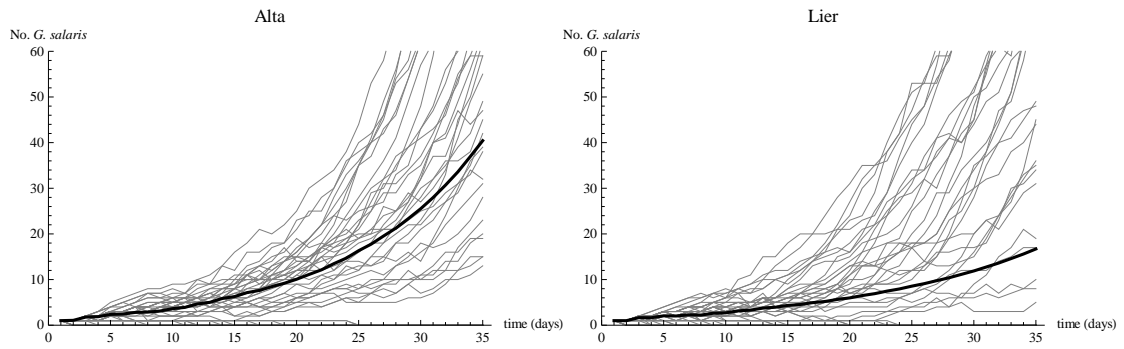


Figure 4.9: Reduced parasite births. Trajectories of *G. salaris* populations infecting two Atlantic strains of *S. salar* as predicted by the individual based model (thin, grey) with reduced number of parasite offspring. Results from the Leslie matrix model (thick, black) are given for comparison of model outputs.

As mentioned earlier, the literature gives the median lifespan of parasites (7.9, 5.2 and 3.5 days) (Cable *et al.*, 2000) this information yields survival rates of 0.92, 0.88 and 0.82 on Alta, Lier and Neva salmon respectively. Reducing the survival rates of those parasites infecting Atlantic stocks to equal those on the Baltic (with all other parameters as in Figure 4.2) yields the results in Figures 4.10 and 4.11.

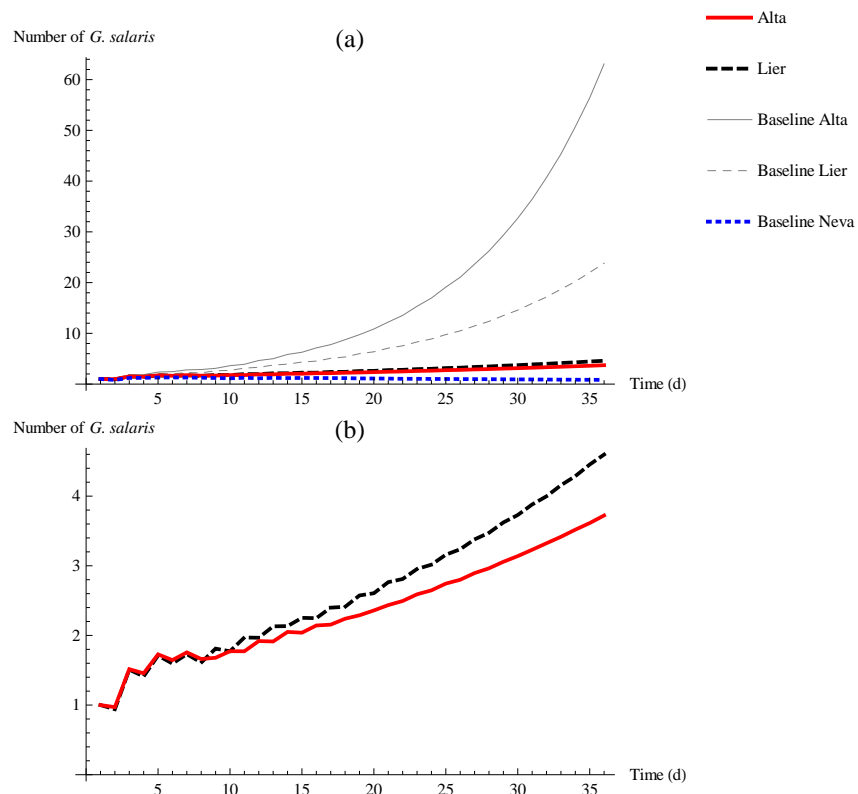


Figure 4.10: Reduced parasite survival. Trajectories of *G. salaris* populations infecting two Atlantic strains of *S. salar* (Alta —, Lier —) over time (days) as predicted by the Leslie matrix model. Reducing parasite survival on Alta and Lier salmon to equal that of parasites infecting the Neva salmon (a survival rate of ) has the largest impact on the dynamics. As can be seen the *G. salaris* populations on both Atlantic strains is now very low, however, they are still not decaying to zero as in the Baltic Neva case. Plot (b) is a close-up of (a) and shows only *G. salaris* numbers on Alta (—) and Lier (—) hosts.

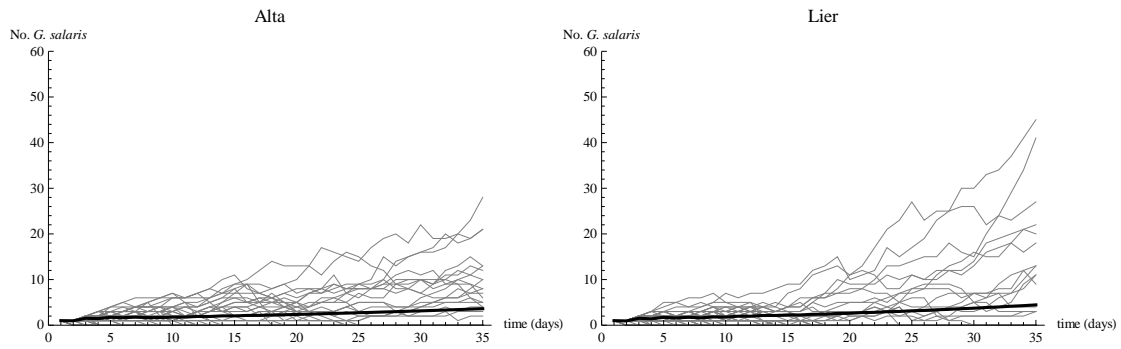


Figure 4.11: Reduced parasite survival. Trajectories of *G. salaris* populations infecting two Atlantic strains of *S. salar* as predicted by the individual based model (thin, grey) with increased parasite death. Results from the Leslie matrix model (thick, black) are given for comparison of model outputs.

Here both Atlantic stocks still do not decay to zero and exhibit positive growth, albeit at a slower rate than in previous simulations; this is an intuitively obvious result. If individual parasites have an increased death rate then the parasite population grows more slowly. As with the previous mechanisms studied, the results gained from the two modelling techniques allow us to deduce that this mechanism alone, *i.e.* reduced parasite survival, does not explain the Baltic's ability to fight *G. salaris* infections. Model outputs were not as consistent between the two modelling methods as in previous results, however, as seen in Figure 4.11 the individual based model predicted similar *G. salaris* numbers in a handful of simulations.

#### 4.4.5 Combination of mechanisms

Finally, the impact that a combination of the three mechanisms studied above has on the parasite population was considered. The results in Sections 4.4.1 - 4.4.4 above were compared with those obtained via the Leslie matrix model parameterised using a combination of:

1. Delayed first birth with reduced number of births;
2. Delayed first birth with reduced parasite survival; and,
3. Delayed first birth with reduced number of births and reduced parasite survival.

Figure 4.12 shows the results obtained for *G. salaris* parasites on Atlantic (Alta) salmon hosts allowing comparisons to be made with the baseline Atlantic (Alta) and Baltic (Neva) results. As can be seen, all three combinations reduce the parasite population to levels lower than the results in the previous sections. Combination (1) has the least significant impact on the dynamics with combination (2) significantly lowering parasite numbers close to the baseline Neva trajectory. However, combination (2) still results in low-level parasite growth. Only combination (3) actually results in parasites decaying to extinction. Combination (3) is what is witnessed in parasites infecting the Baltic strain of Atlantic salmon. Hence, in

addition to single mechanisms, a combination of two mechanisms is also not adequate in explaining the immune response of Baltic salmon to infection. Moreover, in order to beat infection and force parasites to extinction strains of Atlantic salmon must exhibit all three of the mechanisms, and thus, evolve to be more like the Baltic strain.

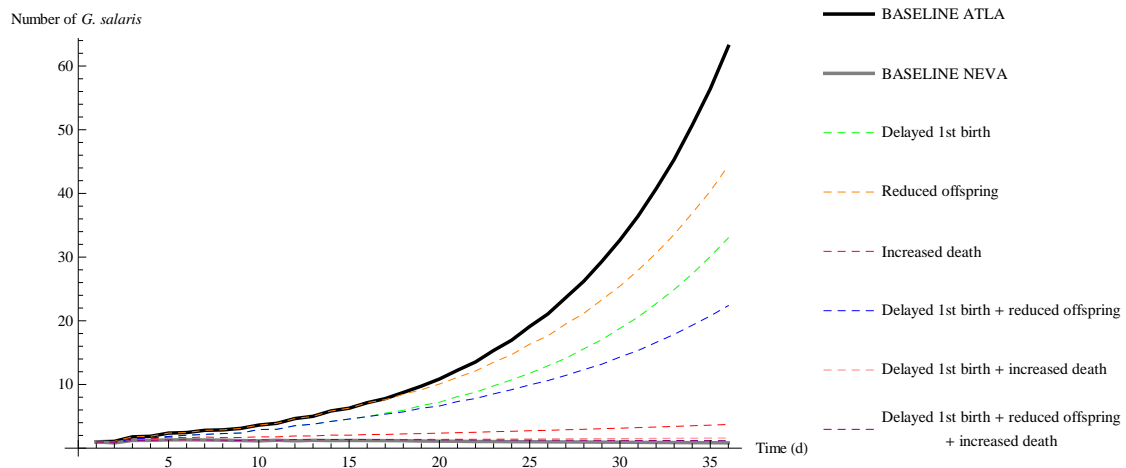


Figure 4.12: Combination of mechanisms for resistance to *G. salaris* infections (Leslie model simulations). Trajectories of *G. salaris* populations infecting one Atlantic strain of *S. salar* (Alta) between the baseline trajectories of parasites on Alta and Neva salmon with a combination of the mechanisms studied in this work and simulated using Leslie matrix models. Combinations are baseline Alta, reduced number of offspring, delayed parasite first birth, delayed parasite first birth and reduced number of offspring, increased death, increased death and delayed parasite first birth, baseline Neva.

#### 4.5 SUMMARY

Each of the three possible mechanisms of resistance exhibited by Baltic salmon hosts when infected by *G. salaris* were studied in depth using both Leslie matrix and individual based models. The outputs obtained via both modelling techniques gave similar *G. salaris* population sizes against time (in days) and the results from baseline simulations for Atlantic hosts were reasonably consistent (both techniques under predicted the data slightly) with previous experimental data presented in Bakke *et al.* (1990) and Jansen & Bakke (1991). Unfortunately, neither the Leslie matrix or individual based model were able to accurately fit the behaviour of parasites on Baltic hosts. It is known that *G. salaris* populations on Baltic salmon do not increase at the same rate as those on Atlantic stocks and in most cases decay to zero or co-exist at low levels of infection. This could be caused by three possible mechanisms, two of which have been suggested in the literature (decreased number of offspring, increased death rate) (Bakke *et al.*, 1990; Jansen & Bakke, 1991; Cable *et al.*, 2000) and a third which has not (delayed first birth). From the data set used it is clear that all three of these occur.

Our aim here was to use a simple mathematical model to determine which factor is most important. Our most surprising finding was that, with all else equal, altering the timing of the first born offspring of a *G. salaris* parasite by 0.5 days can cause a 50% reduction in parasite numbers over a 35 day period and altering it by 1 day can cause a 75% reduction. On the other hand, decreasing only the number of offspring per parasite from four to two had very little effect on the size of parasite population. Less surprisingly, decreasing the survival rate of parasites on Atlantic stocks to that of those parasites on the Baltic stock has the largest impact on the dynamics, however, parasite populations on both Atlantic stocks are still capable of surviving and exhibit positive growth, albeit at rates that are reduced immensely.

Finally, the model results highlight that a combination of delayed first birth with either reduced number of births or reduced survival is still not sufficient to force parasites into decay. Hence, in order for Atlantic hosts to beat *G. salaris* infections they must evolve all three of the mechanisms. In the chapters that follow these results are used to predict whether Atlantic salmon might evolve to coexist with *G. salaris* in the long-term.

## Adding immunity and trade-offs to the system

The literature states that not all strains of Atlantic salmon are as susceptible to *G. salaris* as the Atlantic strain (Cable *et al.*, 2000; Bakke *et al.*, 2002, 2004). As discussed in Chapter 4 the Baltic strain of Atlantic salmon is able to coexist with low levels of parasite infection and in some cases beat parasite infection altogether. This is achieved through the ability of the Baltic strain to exhibit some form of resistance (Bakke *et al.*, 1990; Cable *et al.*, 2000; Bakke *et al.*, 2002, 2004). In Chapter 4 Leslie matrix and individual based stochastic models were employed to investigate the ways in which the Baltic's resistance manifests itself. In this chapter we study this resistance, and the possibility of evolving such a mechanism, through the use of a multiple strain deterministic model.

### 5.1 EXTENDING MODEL B FOR TWO HOST STRAINS

As a basis we begin by extending the equations in (3.27) (Model B: the detached parasites in the external environment model, Chapter 3, Section 3.4) to study one strain of parasite and two strains of salmon host. The 2-strain model is given by equations (5.1) to (5.5) below.

$$\frac{dH_1}{dt} = [a - b - s(H_1 + H_2)]H_1 - \alpha P_1 \quad (5.1)$$

$$\frac{dH_2}{dt} = [a - b - s(H_1 + H_2)]H_2 - \alpha P_2 \quad (5.2)$$

$$\frac{dP_1}{dt} = P_1 \left[ \mu_1 - (\epsilon_1 + b + s(H_1 + H_2) + \alpha + \lambda) - \alpha \frac{P_1}{H_1} \right] + \beta W H_1 \quad (5.3)$$

$$\frac{dP_2}{dt} = P_2 \left[ \mu_2 - (\epsilon_2 + b + s(H_1 + H_2) + \alpha + \lambda) - \alpha \frac{P_2}{H_2} \right] + \beta W H_2 \quad (5.4)$$

$$\frac{dW}{dt} = \Omega_1 P_1 + \Omega_2 P_2 - \sigma W - \beta W H_1 - \beta W H_2 \quad (5.5)$$

Where

$$\Omega_1 = \left[ b + s(H_1 + H_2) + \lambda + \alpha + \frac{\alpha P_1}{H_1} \right]$$

$$\Omega_2 = \left[ b + s(H_1 + H_2) + \lambda + \alpha + \frac{\alpha P_2}{H_2} \right]$$

Equations (5.1) to (5.5) describe a system where two strains of Atlantic salmon host (e.g. Atlantic and Baltic)  $H_1$  and  $H_2$  interact with one another via the density dependent term and one strain of *G. salaris* that behaves differently depending on the strain of salmon host it is infecting ( $P_1$  and  $P_2$ ). This approach keeps the investigation consistent with the situation in the literature (Bakke *et al.*, 1990; Cable *et al.*, 2000) and is discussed in Chapter 4. We assume salmon hosts from both strains share the same birth, natural and parasite induced mortality rates,  $a$ ,  $b$  and  $\alpha$  respectively. When infection is present we assume no difference in the transmission rate of parasites,  $\beta$ , or the rate parasites leave hosts,  $\lambda$ . Additionally, parasites exhibit differing birth and mortality rates ( $\mu_i$  and  $\epsilon_i$  respectively for  $i = 1, 2$ ) on different salmon strains in keeping with the mechanisms of resistance highlighted in Chapter 4. In the absence of parasitic infection ( $P_i = 0, i = 1, 2$ )  $H_1$  and  $H_2$  are indistinguishable such that they share the same per capita growth rate, carrying capacity  $H_1 + H_2 \rightarrow K = \frac{(a-b)}{s}$ , growing to densities with proportions dependent on initial conditions.

The model proposed above acts as a basis for studying interactions between susceptible and resistant hosts of salmon. However, it does not explicitly model immunity. We now go about including immunity in the model and will return to the 2-strain model in Chapter 6.

## 5.2 MODEL C: ADDING IMMUNITY TO MODEL B

In Chapter 4 mechanisms for salmon resistance to *G. salaris* infections were discussed in depth with the impact of such mechanisms modelled using Leslie matrix and individual based models. Until now our deterministic models have yet to include any mechanism of resistance to *G. salaris*. We now go about adding an explicit mechanism to account for the differences in parasite births,  $\mu_i$ , for *G. salaris* on susceptible and resistant hosts. To do this we return to the single host deterministic model (3.27, Chapter 3, Section 3.4). Thus, the immune response to infection is added to the system as follows:

- When an infection is present an immune response is mounted by the host.
- As the parasite infection level increases, the level of immunity also increases.
- The rate of change of parasites is negatively correlated with the rate of change of immunity in that the immune response causes an additional death rate in parasites.
- The immune response decays at a continuous rate.

Putting all of this together, the rate of change of the parasite population and the immune response,  $\frac{dP}{dt}$  and  $\frac{dI}{dt}$  respectively, are given by equations (5.6) and (5.7) below.

$$\frac{dP}{dt} = P \left( \mu - (\epsilon + mI + b + \alpha + sH + \lambda) - \alpha \frac{P}{H} \right) + \beta WH \quad (5.6)$$

$$\frac{dI}{dt} = \gamma \frac{P}{H} - \zeta I \quad (5.7)$$

Three new parameters have been introduced into the model,  $m$ ,  $\gamma$   $\zeta$ . When an immune response is mounted against infection this happens at a rate proportional to parasites per host,  $\gamma$ , and in turn decays at rate  $\zeta$  (approx 6 months - N. Taylor, personal communication). This immune response by the host results in a negative effect on the rate of change of the parasite population via  $m$ .

Hence, our single host model with immunity is now given by:

$$\begin{aligned} \frac{dH}{dt} &= (a - b - sH)H - \alpha P \\ \frac{dP}{dt} &= P \left( (\mu - \epsilon - mI) - (b + \alpha + sH + \lambda) - \alpha \frac{P}{H} \right) + \beta WH \\ \frac{dW}{dt} &= \left( b + sH + \lambda + \alpha + \frac{\alpha P}{H} \right) P - \sigma W - \beta WH \\ \frac{dI}{dt} &= \gamma \frac{P}{H} - \zeta I \end{aligned} \quad (5.8)$$

We simplify the model above by normalising and re-writing the the immunity and attached parasite equations. This approach is taken since it is not possible to estimate values for all the immunity parameters in (5.8).

Let

$$i = mI \quad (5.9)$$

then (5.9)  $\Rightarrow$

$$\frac{dP}{dt} = P \left( (\mu - \epsilon - i) - (b + \alpha + sH + \lambda) - \alpha \frac{P}{H} \right) + \beta WH \quad (5.10)$$

Now,

$$\frac{dI}{dt} = \gamma \frac{P}{H} - \zeta I \quad (5.11)$$

$$\Rightarrow \frac{1}{m} \frac{di}{dt} = \gamma \frac{P}{H} - \zeta \frac{i}{m} \quad (5.12)$$

$$\frac{di}{dt} = \gamma m \frac{P}{H} - \zeta i \quad (5.13)$$

$$(5.14)$$

Thus, now we are only dealing with one term,  $\tilde{m}$ . Hence, re-writing Equations (5.10) and (5.14) with  $i \rightarrow I$  yields the following:

$$\begin{aligned}
\frac{dH}{dt} &= (a - b - sH)H - \alpha P \\
\frac{dP}{dt} &= P \left( \mu - (\epsilon + I + b + \alpha + sH + \lambda) - \alpha \frac{P}{H} \right) + \beta WH \\
\frac{dW}{dt} &= \left( b + sH + \lambda + \alpha + \frac{\alpha P}{H} \right) P - \sigma W - \beta WH \\
\frac{dI}{dt} &= \tilde{m} \frac{P}{H} - \zeta I
\end{aligned} \tag{5.15}$$

where,

$$\tilde{m} = \gamma m \tag{5.16}$$

Simulating (5.15) for a *G. salaris* population on a single salmon host ( $H=1$  with  $a = b = \alpha = 0$  and no detached parasite population,  $W=0$ ) gives the results in Figure 5.1. In the absence of immunity in the host ( $\tilde{m} = 0$ , Figure 5.1 a) the *G. salaris* population exhibits rapid exponential growth. In reality this behaviour would result in mortality of the infected host, however, our interest lies in the impact of a host immune response on *G. salaris* density. Figure 5.1 b shows the impact of including immunity ( $\tilde{m} > 0$ ). As can be seen, initially the *G. salaris* population once again increases quickly, however, when this happens the immune response activates and the level of immunity increases and forces the *G. salaris* population into decay. With parasite density decreasing the level of immunity also decreases. Hence, the parasite population eventually decays to zero as does the level of immunity. This behaviour is similar to that observed by Bakke *et al.* (1990) in *G. salaris* on Baltic salmon with parasites reaching a peak density after approximately 10-15 days before decaying to zero after a further 10 – 15 days (see Figure 5.2). Through this single host simulation we have been able to demonstrate that the immune response in (5.15) is indeed capable of defending a host from infection.

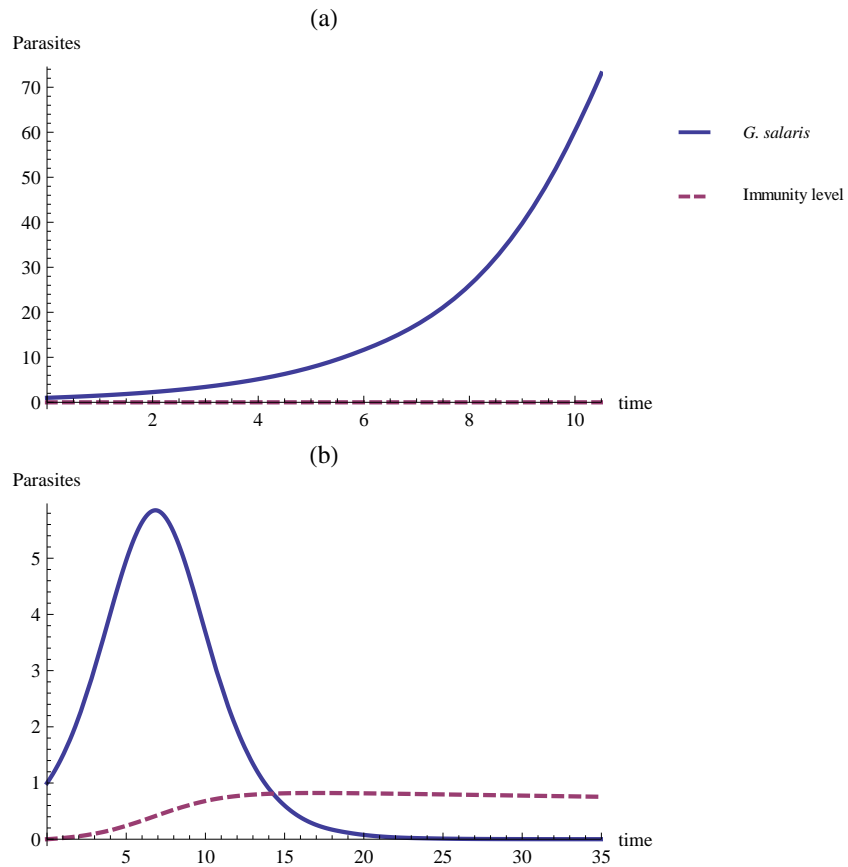


Figure 5.1: Impact of a host immune response to *G. salaris* infection. Trajectories of parasite density on an individual salmon host ( $H(0) = 1$  with  $a = 0$ ,  $b = 0$  and  $\alpha = 0$ ) with (a) immunity absent ( $\tilde{m} = 0$ ) and (b) immunity present ( $\tilde{m} > 0$ ). In both plots initial parasite density is 1,  $P(0) = 1$ , and no free living parasites are present,  $W(0) = 0$ .

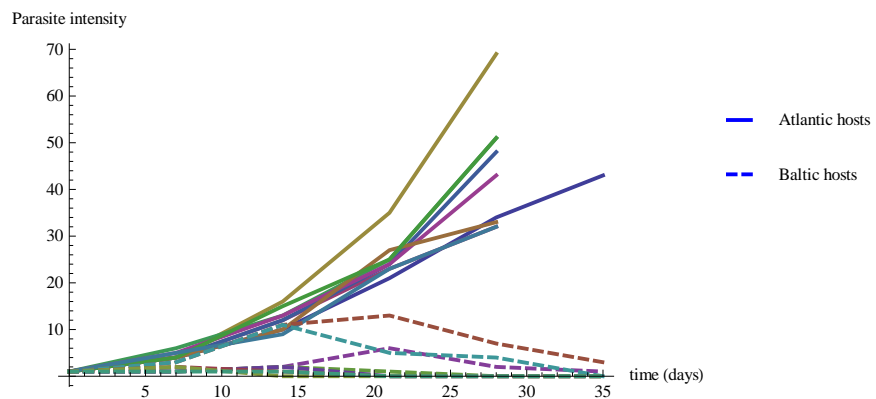


Figure 5.2: Data from Bakke *et al.* (1990). Trajectories of parasite development on individual Atlantic salmon parr hosts (solid trajectories) from the River Lone, Norway, and Baltic salmon parr hosts (dashed trajectories) from the River Neva, Russia. Salmon hosts kept individually in small aquaria at  $12^{\circ}\text{C}$ .

At this point we have a model that includes immunity when *G. salaris* infection is present in the environment ( $P, W > 0$ ). As expected, if we set the immune response to zero ( $\tilde{m} = 0$ ,  $I = 0$ ) then we have the equations for Model B as it appears in Chapter 3, Section 3.4. We

now go about finding estimations for  $\tilde{m}$  and  $\zeta$  before simulating (5.15) for a population of salmon hosts.

### 5.2.1 Estimating parameter values

At this stage we require values for  $\tilde{m}$  and  $\zeta$ .

#### *Decay rate of immune response, $\zeta$*

As highlighted above the decay rate of the immune response is approximately 6 months (N. Taylor, personal communication), converting this into a daily rate we obtain an estimate for  $\zeta$  and hence set  $\zeta = 0.005$ .

#### *Rate of increase of immune response, $\tilde{m}$*

As discussed in Chapter 2, Section 2.4, by fitting exponential best-fit curves to data from Bakke *et al.* (1990) concerning *G. salaris* population growth on individual hosts of Atlantic and Baltic salmon and taking the mean, daily parasite growth rate is estimated to be  $\mu_A - \epsilon = 0.103$  and  $\mu_B - \epsilon = 0.085$  for Atlantic and Baltic strains respectively (the data used is reproduced and collected in Table A.3, Appendix A). Recent experimental trials of *G. salaris* growth on Atlantic salmon reared in the UK by Paladini *et al.* (in prep.) gave growth rates consistent with those obtained using the Bakke *et al.* (1990) data (see Table 5.1). Parasite death rate was calculated using the available data from Jansen & Bakke (1991). This allowed the estimation of the birth rate,  $\mu$ , for parasites on Atlantic and Baltic hosts as 0.183 and 0.165 respectively. Data for salmon immunity to *G. salaris* infections is not readily available, hence,  $\tilde{m}$  is currently unknown. However,  $\tilde{m}$  can be estimated to an extent in order to give a reasonable guess that can be used in the model.

Assume that in the absence of an immune response to infection, parasites infecting Atlantic and Baltic host strains have the same growth rate,  $\rho = \mu - \epsilon$ . A comparison of the estimates for parasite growth on Baltic and Atlantic hosts calculated from the literature can then be made. Considering the equations in (5.8), we set  $\rho = \mu_A - \epsilon = \mu_B - \epsilon = 0.103$ . Thus, when an immune response is present in the system  $\rho = \mu - \epsilon - mI$ . Now, since Atlantic hosts have no immunity to *G. salaris* infections ( $I = 0$ ) parasite growth on Atlantic hosts is given as  $\rho_A - mI = 0.103 - m * 0 = 0.103$ . This implies that for *G. salaris* on Baltic hosts, where an immune response is present ( $I = 1$ , the maximum level reached - see in Figure 5.1b), we have  $\rho_B - mI = 0.103 - m * 1 = 0.085$  giving  $m = 0.103 - 0.085 = 0.0175$ . Hence, setting  $\gamma$  to unity in (5.16) gives an estimate for  $\tilde{m}$  as  $\tilde{m} = 0.0175$ . Sensitivity analysis (see Appendix D) shows that the model is not particularly sensitive to the value chosen for  $\tilde{m}$ .

Table 5.1: *Gyrodactylus salaris* growth rates on Atlantic and Baltic strains of Atlantic salmon estimated by fitting exponential best fit curves to data for *G. salaris* population growth on individual fish hosts. Estimations were made using data readily available in the literature from experimental trials by Bakke *et al.* (1990); Jansen & Bakke (1991); Paladini *et al.* (in prep.). Here parasite growth rates on Atlantic and Baltic hosts is given by  $\rho_A$  and  $\rho_B$  respectively. Note,  $\rho_A = \mu_A - \epsilon$  and  $\rho_B = \mu_B - \epsilon$ .

Parameter	Description	Salmon host, origin	Estimate	Source
$\rho_A$	Parasite growth	Atlantic, Norway	0.103	Bakke <i>et al.</i> (1990)
$\rho_B$	Parasite growth	Baltic, Russia	0.085	Bakke <i>et al.</i> (1990)
$\rho_A$	Parasite growth	Atlantic, Norway	0.116	Paladini <i>et al.</i> (in prep.)
$\rho_A$	Parasite growth	Atlantic, UK	0.091	Paladini <i>et al.</i> (in prep.)
$\epsilon$	Parasite death	Atlantic, Norway	0.080	Jansen & Bakke (1991)

Running simulations in Mathematica with a range of values for  $\tilde{m}$  gives the results in Figure 5.3. As can be seen, with no immunity  $\tilde{m} = 0$ , the parasite population quickly grows to epidemic levels. This in turn puts the host population into extinction. As always, with no hosts to sustain the *G. salaris* population, the parasites decay to zero. As  $\tilde{m}$  is increased the system begin to oscillate and settle into cycles. When  $\tilde{m}$  finally reaches the estimated value of 0.0175 salmon density is close to carrying capacity with low parasite coexistence. Finally, when a high enough level is reached ( $\tilde{m} > 0.02$ ) salmon density reach just under carrying capacity and coexist with the parasite population with very low level parasite infection. The simulations have highlighted the ability of the salmon to coexist with low levels of *G. salaris* infection. We highlight one final observation for scenarios where  $\tilde{m}$  is unrealistically large. In such cases the *G. salaris* population decays to zero becoming extinct, hence, enabling the salmon host population to grow to carrying capacity.

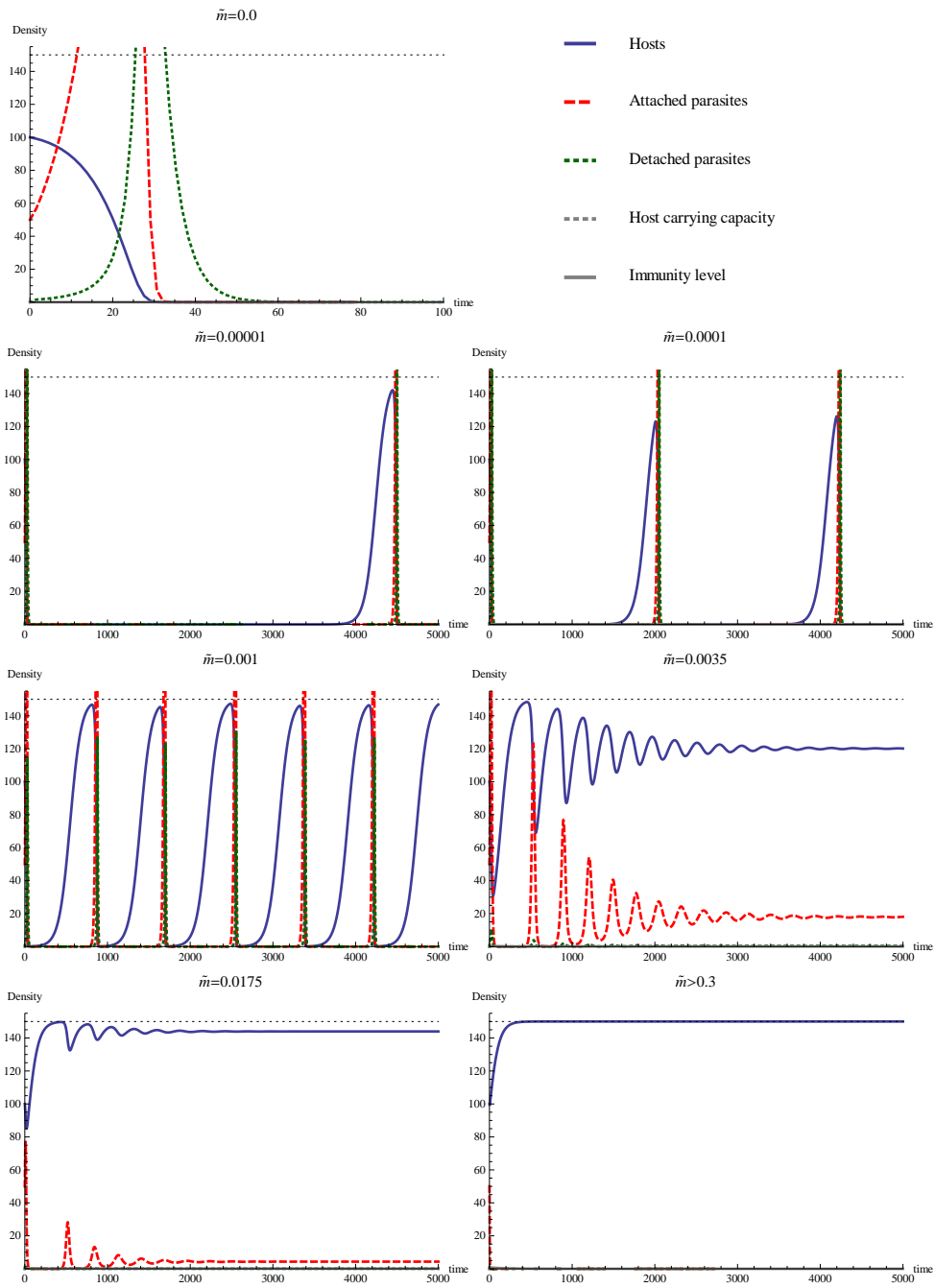


Figure 5.3: Plots showing trajectories of hosts, parasites and detached parasites with an immune response from the host against time (in days). From left to right  $\tilde{m} = 0; 0.00001; 0.0001; 0.001; 0.0035; 0.0175$ ; and finally  $> 0.3$  respectively. In all plots  $a = 0.02; b = 0.005; s = 0.0001; \mu = 0.19; e = 0.08; \alpha = 0.02; \lambda = 0.1; \sigma = 0.24; \beta = 0.05; \zeta = 0.005$ .

### 5.2.2 Investigating the impact of immunity on salmon density

The effect of varying the value of  $\tilde{m}$  in regard to equilibrium salmon density was investigated. Plotting salmon density against  $\tilde{m}$  (Figure 5.4) we observe that  $\tilde{m}$  is positively correlated with host density such that an increase in immunity results in an increase in salmon density as one would expect. Thus we observe rapid growth followed by a plateau. However, for very small values of  $\tilde{m}$ , *i.e.*,  $\tilde{m} < 0.01$ , salmon density exhibits cyclic behaviour as seen earlier in Figure 5.3. Importantly, Figure 5.4 highlights the fact that only a small amount of immunity is required in order to cause a large impact on the equilibrium density of the salmon population.

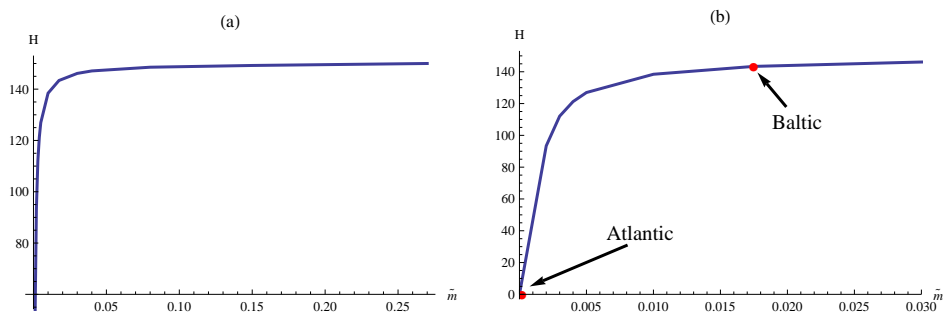


Figure 5.4: Plot of salmon density against the immunity parameter  $\tilde{m}$ . Trajectory of salmon density following logistic growth to carrying capacity (a) highlighting a positive relationship between host population size and  $\tilde{m}$ . Importantly, only a small amount of immunity is required in order to cause a large impact on the dynamics of the salmon population. Plot (b) shows the result from (a) on a magnified scale showing the positions of the fully susceptible Atlantic strain of Atlantic salmon and the resistant Baltic strain of Atlantic salmon.

### 5.3 MODEL D: ADDING A TRADE-OFF

*...as Goethe expressed it, 'in order to spend on one side, nature is forced to economise on the other side.' I think this holds true to a certain extent with our domestic productions: if nourishment flows to one part or organ in excess, it rarely flows, at least in excess, to another part...* (Darwin, 1872).

By adding an immune response into the model, the cost to the host due to evolving such a mechanism must also be taken into consideration. Moreover, without the addition of a cost, salmon hosts would evolve to  $\tilde{m} \rightarrow \infty$ . Such consequences of evolving an immune response to infection is achieved by adding a trade-off into the model via the host equation.

Trade-offs can be added to the system in a number of ways such as via death, growth, birth, *etc.* Due to the lack of evidence of trade-offs in salmon another system is considered. A study of furunculosis in brook trout by Cipriano *et al.* (2002) demonstrated that an increase in immunity had a negative effect on the host's birth rate. In this study they observed ap-

proximately a 7 to 12% decrease in the birth rate of the trout that had exhibited an immune response to infection. If we assume a similar situation is true in the case of Atlantic salmon and *G. salaris* we can go about adding a trade-off to the host birth rate  $a$ . Starting at the Atlantic strain of Atlantic salmon with a birth rate equal to 0.02 we find the results in Table 5.2 for the new birth rate  $\hat{a}(\tilde{m})$  following the equation of a line.

Table 5.2: Values for salmon birth rate with trade-off,  $\hat{a}(\tilde{m})$ , assuming a similar situation to that observed by Cipriano *et al.* (2002) in their study of furunculosis resistance in brook trout. Values estimated using an initial salmon birth rate of 0.02 and via the equation of a line.

% decrease from Atlantic birth rate	Baltic birth rate	$\hat{a}(\tilde{m})$
7	0.0186	$-0.008 \tilde{m} + 0.02$
8	0.0184	$-0.094 \tilde{m} + 0.02$
9	0.0182	$-0.106 \tilde{m} + 0.02$
10	0.0180	$-0.118 \tilde{m} + 0.02$
11	0.0178	$-0.129 \tilde{m} + 0.02$
12	0.0176	$-0.141 \tilde{m} + 0.02$
mean (9.5)	0.0181	$-0.112 \tilde{m} + 0.02$

Figure 5.5 shows the theoretical values of birth rates for Atlantic and Baltic strains of Atlantic salmon with respect to the rate of the immune response,  $\tilde{m}$ . These positions are calculated using the information in Table 5.2 and values of  $\tilde{m}$  for Atlantic and Baltic populations, assuming as above, that Atlantic hosts have no immunity to infection and the opposite true of Baltic hosts.

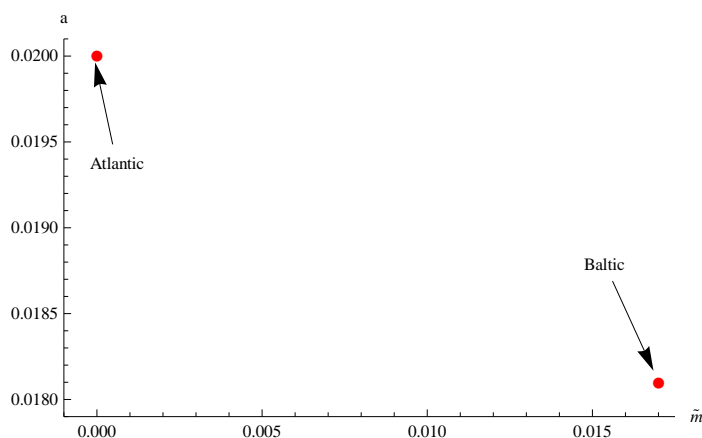


Figure 5.5: Plot of the theoretical positions of birth rates of Atlantic and Baltic strains of *S. salar* against  $\tilde{m}$  assuming Baltic strains have a birth rate that is 9.5% less than that of Atlantic strains. This is due to the ability of Baltic hosts to fight infection via an evolved immune response to infection.

Using the results in Table 5.2 for a 9.5% decrease in host birth rate and the equation of a line we obtain Figure 5.6 for salmon birth rate,  $a$ , versus the rate of the immune response,  $\tilde{m}$ .

By adding a trade-off on host birth in the form of the equation of a line (Figure 5.6) such that host birth rate is negatively correlated with immunity, *i.e.* as an individual's immunity

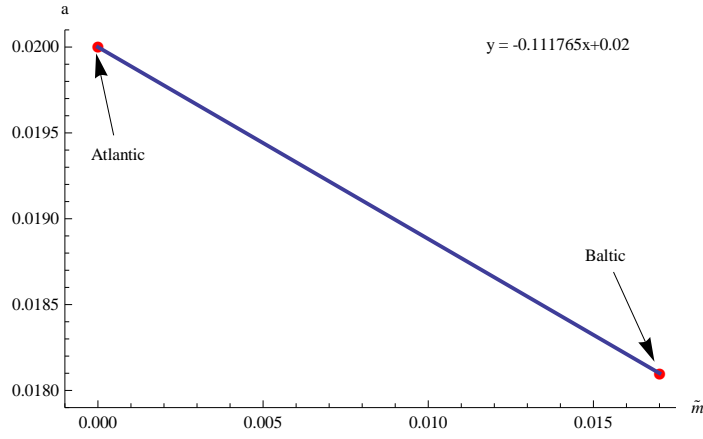


Figure 5.6: Plot of host birth rate against  $\tilde{m}$  following a the trajectory of a straight line. The trade-off trajectory was calculated assuming birth rates of 0.020 and 0.018 for Atlantic Atlantic and Baltic Atlantic salmon strains respectively.

to infection increases its birth rate decreases, the model is now described by the equations in (5.17):

$$\begin{aligned}
 \frac{dH}{dt} &= (\hat{a}(\tilde{m}) - b - sH)H - \alpha P \\
 \frac{dP}{dt} &= P \left( \mu - (\epsilon + I + b + \alpha + sH + \lambda) - \alpha \frac{P}{H} \right) + \beta WH \\
 \frac{dW}{dt} &= \left( b + sH + \lambda + \alpha + \frac{\alpha P}{H} \right) P - \sigma W - \beta WH \\
 \frac{dI}{dt} &= \tilde{m} \frac{P}{H} - \zeta I
 \end{aligned} \tag{5.17}$$

where  $\hat{a}(\tilde{m}) = -0.112\tilde{m} + a$ .

As was done previously, we now investigate the effect that varying  $\tilde{m}$  has on salmon density, the results of which are found in Figure 5.7.

As can be seen, as immunity increases the size of the salmon host population also increases. However, in contrast to when the model only included immunity (see Figure 5.4), now when the immunity reaches too great a level the host population begins to decay due to the effect of the trade-off. Hence, the cost of evolving an immune response to too high a level has a negative impact on host density. Figure 5.7 also highlights the Baltic's  $\tilde{m}$  value, estimated earlier as 0.017. Importantly, looking at where the Baltic strain of salmon sit on the curve in Figure 5.7 we note that Baltic hosts appear to have evolved their  $\tilde{m}$  to a value close to that which maximizes their population size.

In the model above we added a trade-off such that the benefit and resulting cost increase at the same rate, *i.e.* a linear trade-off (Hoyle *et al.*, 2008). However, it is not always the case that we have a linear trade-off. Costs may also increase at a rate that is faster than the benefit

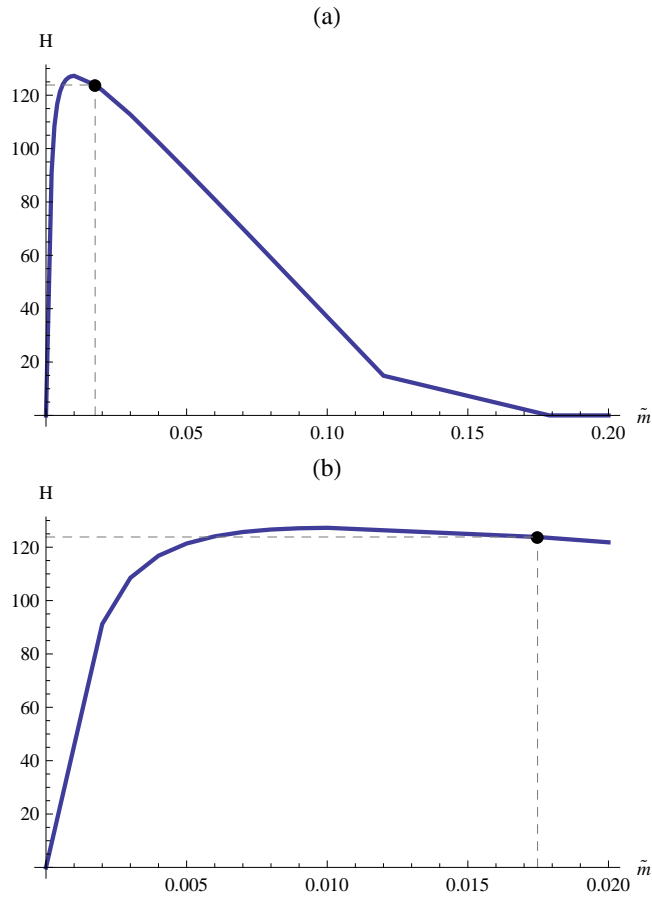


Figure 5.7: Trajectory of salmon density against  $\tilde{m}$  with trade-off on salmon births. Plot (a) shows the impact on host density of increasing  $\tilde{m}$  from 0 to 0.2. Plot (b) gives a magnification of the trajectory in (a) for between 0 and 0.02. The Baltic salmon's  $\tilde{m}$  value is represented by the black plot marker and grey dashed lines.

(an acceleratingly costly trade-off) or increase at a rate slower than that of the benefit (a deceleratingly costly trade-off) (Hoyle *et al.*, 2008). The importance of shape in regards to trade-offs has been the subject of much study (Levins, 1962, 1968; Boots & Haraguchi, 1999; Boots & Bowers, 2004; De Mazancourt & Dieckmann, 2004; Rueffler *et al.*, 2004; Hoyle *et al.*, 2008). Thus, we now turn attention and take into consideration what effect the shape of the trade-off has on the dynamics of the salmon population.

### 5.3.1 Investigating the effect of trade-off shape

In the results above (Figure 5.7) the equation of a straight line was used to implement a trade-off on host birth rate. This method is extended to study the impact on the host dynamics when the trade-off is estimated by following a concave or convex curve and whether or not such an approach gives a better fit for  $\hat{a}(\tilde{m})$ . Using Equation (5.18) the trade-off was estimated.

$$\hat{a}(\tilde{m}) = a_{As} - \left( \frac{(a_{As} - a_{Bs}) \left( 1 - \frac{\tilde{m} - \tilde{m}_{Bs}}{\tilde{m}_{As} - \tilde{m}_{Bs}} \right)}{1 + \frac{\theta(\tilde{m} - \tilde{m}_{Bs})}{\tilde{m}_{As} - \tilde{m}_{Bs}}} \right) \quad (5.18)$$

Where  $a_{As}$  is Atlantic birth rate,  $a_{Bs}$  is Baltic birth rate,  $\tilde{m}_{As}$  is Atlantic immune response rate,  $\tilde{m}_{Bs}$  is Baltic immune response rate and  $\theta$  is the “shape” parameter, determining if the trade-off takes the form of a straight, concave or convex trajectory.

When  $\theta = 0$  we are at the equation for a straight line, and hence, the results in Figures 5.6 and 5.7. We now observe what happens when  $-1 < \theta < 0$  and  $\theta > 0$ , the general behaviour of which is represented by Figure 5.8.

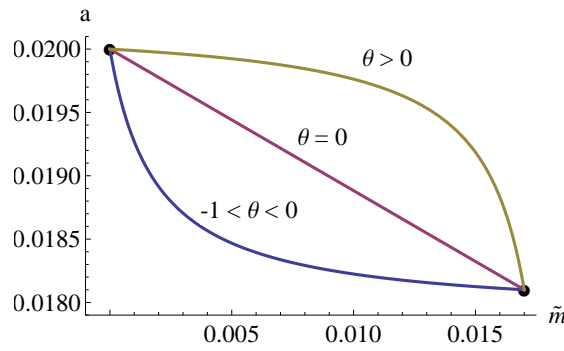


Figure 5.8: Plot showing the possible trajectories used to estimate the trade-off on host birth. If  $\theta = 0$  the trade-off follows the trajectory of a straight line. If  $-1 < \theta < 0$  the trade-off follows a concave trajectory representing a deceleratingly costly trade-off. If  $\theta > 0$  the trade-off follows a convex trajectory representing an acceleratingly costly trade-off.

Plotting birth rate,  $a$ , against  $\tilde{m}$  using various values of  $\theta$ , (a)  $\theta = -0.5, 0, 0.5$ ; (b)  $\theta = -0.6, 0, 1$ ; (c)  $\theta = -0.7, 0, 9$ ; (d)  $\theta = -0.9, 0, 20$ ; (e)  $\theta = -0.99, 0, 100$ , the results in Figure 5.9 are obtained.

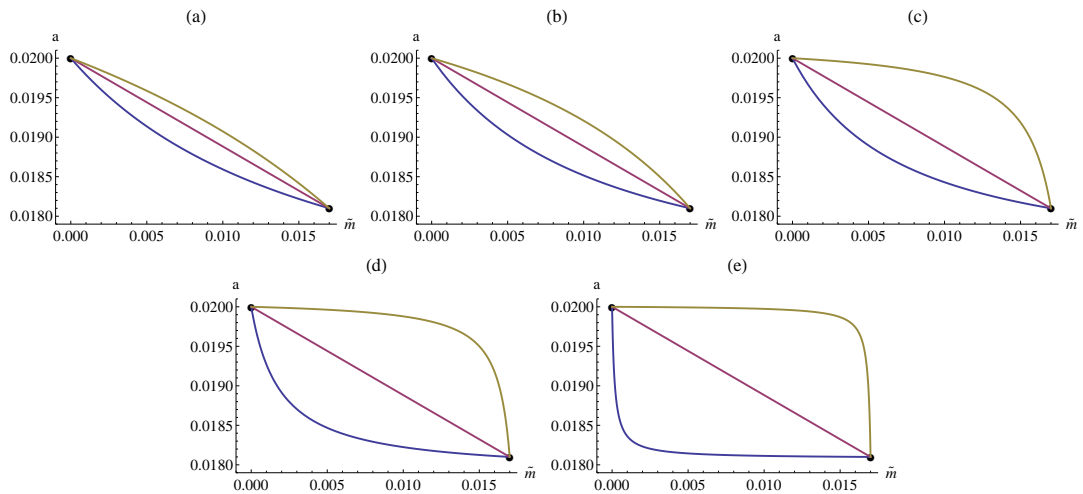


Figure 5.9: Results of plotting Equation (5.18) for a range of values of  $\theta$ . From left to right the values of  $\theta$  are as follows: (a)  $\theta = -0.5, 0, 0.5$ ; (b)  $\theta = -0.6, 0, 1$ ; (c)  $\theta = -0.7, 0, 9$ ; (d)  $\theta = -0.9, 0, 20$ ; (e)  $\theta = -0.99, 0, 100$ ;

As was done for the case when  $\theta = 0$  we now vary the value of  $\tilde{m}$  and observe the impact this has on the salmon population, the results of which are found in Figures 5.10, 5.11 and 5.12.

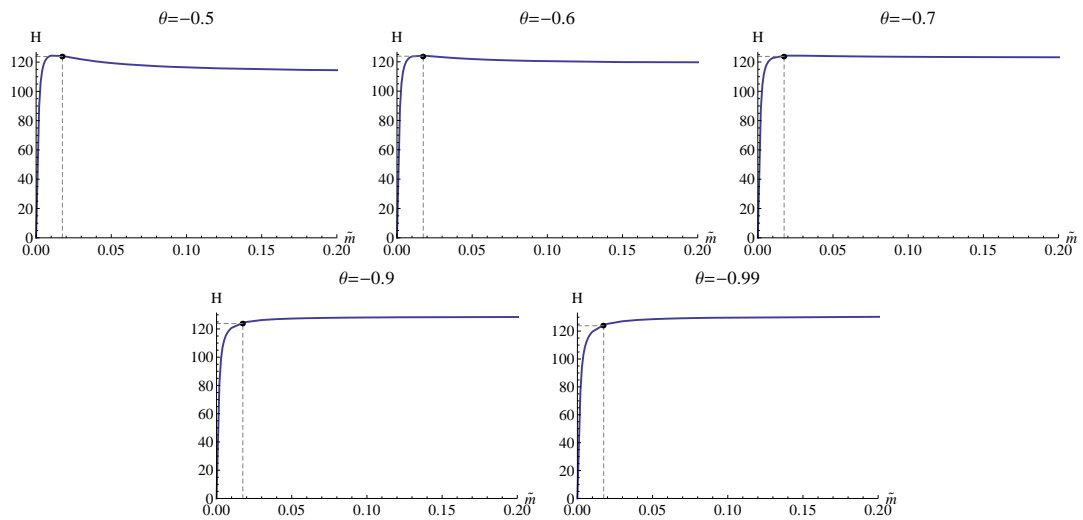


Figure 5.10: Trajectory of salmon density against  $\tilde{m}$  with trade-off on salmon births for varying values of  $1 < \theta < 0$ . The Baltic salmon's  $\tilde{m}$  value is represented by the black plot marker and grey dashed lines.

Figure 5.11 shows the results of plotting Equation (5.18) against  $\tilde{m}$ . As can be seen, plotting  $\hat{a}(\tilde{m})$  for  $\theta > 0$  highlights where vertical asymptotes occur. Only the behaviour to the left of the asymptote is of interest since this is the part that is biologically relevant. Using this new information combined with ending plots before the asymptote is reached gives the results contained within Figure 5.12.

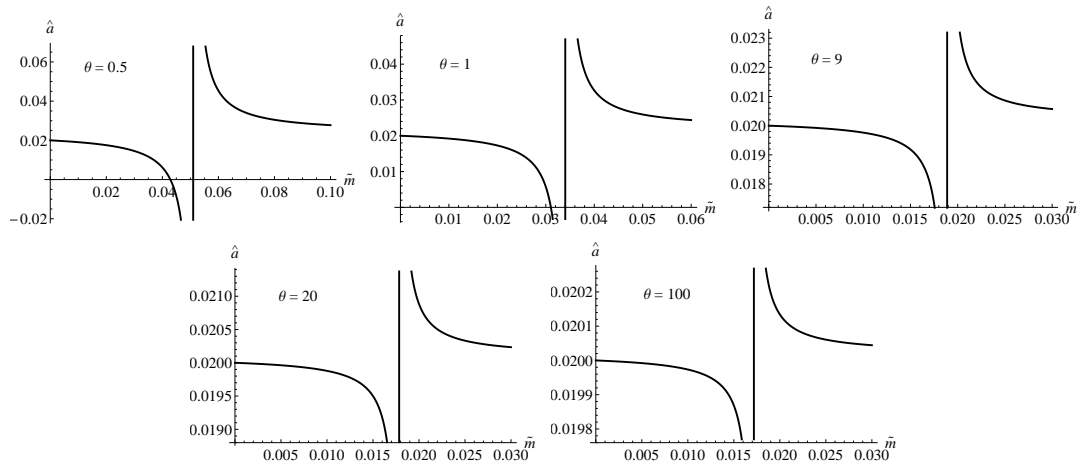


Figure 5.11: The occurrence of asymptotes when  $\theta > 0$ . Plotting host birth rate ( $\hat{a}(\tilde{m})$ , given by Equation (5.18) in the main text) against immunity ( $\tilde{m}$ ) when  $\theta > 0$  shows where vertical asymptotes occur. The upper right area of each plot occurs after the asymptote and is not biologically relevant, hence, only the behaviour in the bottom left of each plot is of interest.

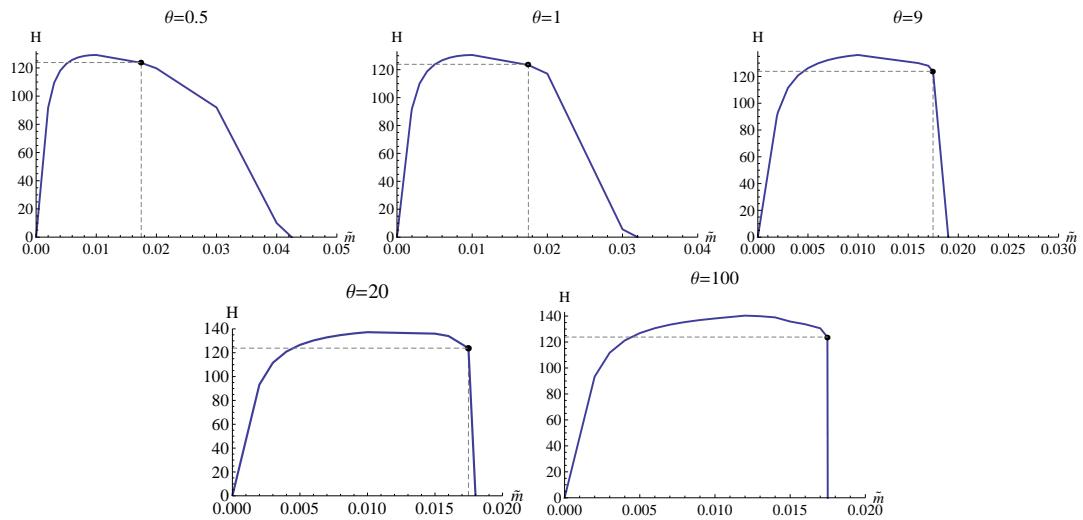


Figure 5.12: Trajectory of salmon density against  $\tilde{m}$  with trade-off on salmon births for varying values of  $\theta > 0$ . Following the results from Figure 5.11, only the biologically relevant trajectory is considered and plotted. The Baltic salmon's  $\tilde{m}$  value is represented by the black plot marker and grey dashed lines.

Comparing the results in Figures 5.7, 5.10 and 5.12 we conclude that the best fit comes from a trade-off following a convex trajectory, *i.e.*, when  $-1 < \theta < 0$ . In all cases, an initially small increase in  $\tilde{m}$  from zero causes a large positive impact on salmon density. However, in cases with  $-1 < \theta < 0$ , as  $\tilde{m}$  increases further from zero, the salmon eventually reach their carrying capacity. A  $\theta$  value equal to  $-0.7$ , *i.e.*, a deceleratingly costly trade-off, is selected allowing salmon populations to reach their maximum density and a  $\tilde{m}$  value as close as possible to the estimated value for the Baltic's immunity.

#### 5.4 SUMMARY

The models above illustrate the effect, and consequences, of adding a host immune response to infection into the salmon - *G. salaris* system. The results in the previous chapters have shown, for individual host strains, that in the absence of immunity salmon density quickly decays to extinction when faced with infection by *G. salaris*. This is the case as witnessed in Atlantic strains in the field (e.g. Norway). Previous models (see Chapter 4) also allowed us to determine that the Baltic's acquired resistance is not present from the first day of infection but occurs some days after infection takes hold and is consistent with behaviour observed in the literature (Bakke *et al.*, 1990; Kania *et al.*, 2007).

The results in this chapter have shown the effect of adding an immune response and resulting trade-off into the host equation. They have also highlighted the fact that only a small amount of immunity is required to cause a substantial impact on the dynamics with salmon population density being significantly increased or, for extremely small levels of immunity, settling into cycles. We also note that model simulations and resulting output suggests the Baltic strain appear to have evolved an immune response so as to maximize their population size. This would go in some way as to confirm what has been witnessed experimentally (Bakke *et al.*, 1990; Cable *et al.*, 2000; Bakke *et al.*, 2002, 2004). Through an investigation concerning the equation used to estimate the value of the trade-off we have also determined that the most accurate fit comes from a concave trajectory (deceleratingly costly trade-off) with a  $\theta$  value equal to -0.7, such a value gives a fit close to that of the Baltic strain.

The model in its current form (Model D, *i.e.*, equations in 5.17 with 5.18) now serves as the basis for the final area of interest, answering the question of whether or not Atlantic strains will follow their Baltic counterparts and evolve an immune response to *G. salaris* infections.

## Models with multiple host strains

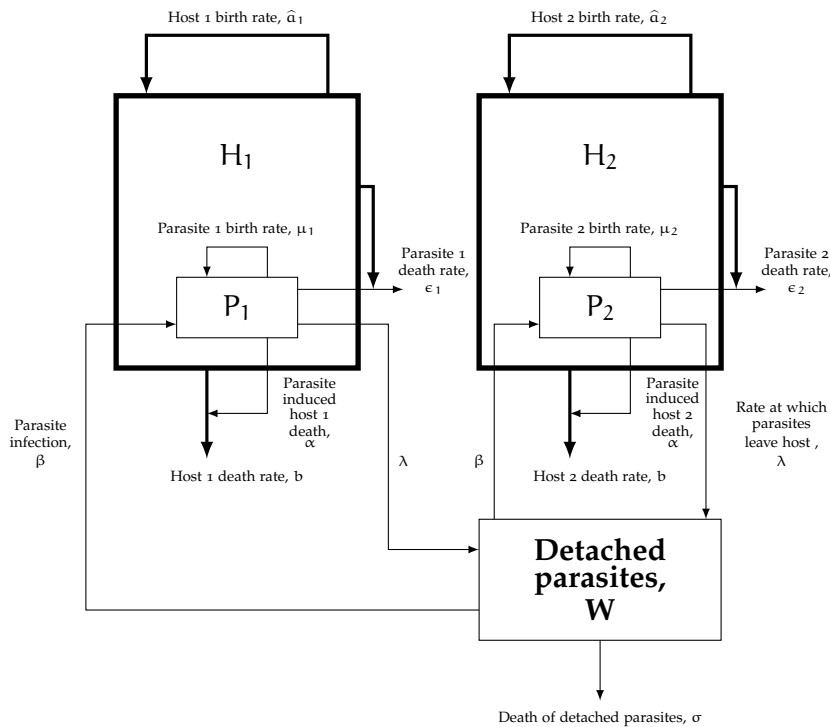


Figure 6.1: Schematic representation of Atlantic salmon-*Gyrodactylus salaris* interactions with 2 Atlantic salmon strains and one strain of *G. salaris* that exhibits different behaviour on each host strain. See Table A.1 (Appendix A) for a description of the parameters used.

## 6.1 RETURN TO THE TWO-STRAIN MODEL

The models in Chapter 5 included the addition of both an immune response to parasite infection and a trade-off, that impacts host birth rate, resulting from evolving such a mechanism. However, in order to study the effects of immunity and whether or not a susceptible strain of salmon host is capable of evolving into a more immune strain we require a model that consists of more than one strain of host. We now return and consider the two-strain model from Chapter 5 that deals with two different salmon strains (*e.g.* Atlantic Atlantic and Baltic Atlantic salmon) and one *G. salaris* strain that behaves differently on the two host strains.

Incorporating the immunity and trade-off into Equations (5.1) to (5.5) we obtain the model described by Equations (6.1) to (6.7) below and schematically in Figure 6.1.

$$\frac{dH_1}{dt} = [\hat{a}(\tilde{m}_1) - b - s(H_1 + H_2)]H_1 - \alpha P_1 \quad (6.1)$$

$$\frac{dH_2}{dt} = [\hat{a}(\tilde{m}_2) - b - s(H_1 + H_2)]H_2 - \alpha P_2 \quad (6.2)$$

$$\frac{dP_1}{dt} = P_1 \left[ \mu_1 - (\epsilon_1 + I_1 + b + s(H_1 + H_2) + \alpha + \lambda) - \alpha \frac{P_1}{H_1} \right] + \beta W H_1 \quad (6.3)$$

$$\frac{dP_2}{dt} = P_2 \left[ \mu_2 - (\epsilon_2 + I_2 + b + s(H_1 + H_2) + \alpha + \lambda) - \alpha \frac{P_2}{H_2} \right] + \beta W H_2 \quad (6.4)$$

$$\frac{dW}{dt} = \Omega_1 P_1 + \Omega_2 P_2 - \sigma W - \beta W H_1 - \beta W H_2 \quad (6.5)$$

$$\frac{dI_1}{dt} = \tilde{m}_1 \frac{P_1}{H_1} - \zeta I_1 \quad (6.6)$$

$$\frac{dI_2}{dt} = \tilde{m}_2 \frac{P_2}{H_2} - \zeta I_2 \quad (6.7)$$

Where

$$\hat{a}(\tilde{m}_1) = \frac{0.006 + 0.711765\tilde{m}_1}{0.3 + 41.1765\tilde{m}_1}$$

$$\hat{a}(\tilde{m}_2) = \frac{0.006 + 0.711765\tilde{m}_2}{0.3 + 41.1765\tilde{m}_2}$$

$$\Omega_1 = \left[ b + s(H_1 + H_2) + \lambda + \alpha + \frac{\alpha P_1}{H_1} \right]$$

$$\Omega_2 = \left[ b + s(H_1 + H_2) + \lambda + \alpha + \frac{\alpha P_2}{H_2} \right]$$

Note: fish to fish transmission of parasites is not explicitly modelled the reasons for which are discussed in Chapter 2.

Simulation of the two-strain model was carried out using Mathematica™. The system is simulated with no immunity present in Atlantic salmon hosts ( $H_1$ ) and an immune response present in Baltic salmon hosts ( $H_2$ ), hence we set  $\tilde{m}_1 = 0$  and  $\tilde{m}_2 = 0.017$  for Atlantic and Baltic hosts respectively. Assuming that Atlantic and Baltic hosts have the same death rate in the absence of infection, and the only difference in parameter values between the two strains is the hosts ability to mount an immune response to *G. salaris* infection, gives the result found in Figure 6.2.

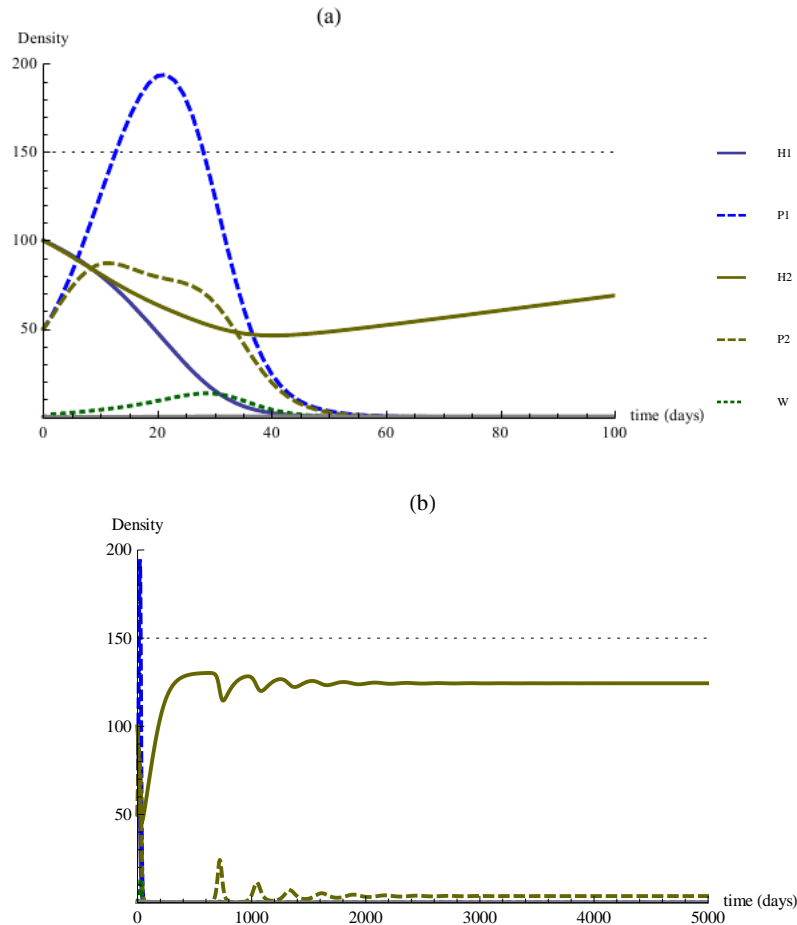


Figure 6.2: Plots showing trajectories of two salmon host strains and one *G. salaris* strain that exhibits differing behaviour on each host. The first salmon strain, H<sub>1</sub>, has no immunity to infection whereas the second salmon strain, H<sub>2</sub>, is able to mount an immune response. Plot (a) shows the trajectories of salmon, attached *G. salaris* and detached *G. salaris* (H<sub>1</sub>, H<sub>2</sub>, P<sub>1</sub>, P<sub>2</sub> and W respectively) over a 100 day period. Plot (b) shows the trajectories of salmon, attached *G. salaris* and detached *G. salaris* from (a) over an extended period of time (5000 days) allowing the H<sub>2</sub> population to settle to an equilibrium level.

As can be seen in Figure 6.2 (a) the Atlantic host population with zero immunity (H<sub>1</sub>) quickly decays to zero due to the rapid growth of *G. salaris* to an epidemic level (P<sub>1</sub>). In contrast the Baltic hosts begin to decay initially with a small increase in parasite numbers due to parasites from the Atlantic population being released into the environment and picked up by Baltic hosts. However, Baltic hosts soon mount an immune response to infection, causing the *G. salaris* population (P<sub>2</sub>) to decay. Increasing the time period, Figure 6.2 (b), it can be seen that the Baltic's immunity allows positive growth with the Baltic population eventually reaching a density that is 83% of the original carrying capacity (*i.e.* a density of 150 in the absence of a trade-off). The trade-off on host birth means that the original host carrying capacity can never be reached. In this case the Baltic's new carrying capacity due to the trade-off is reduced by approximately 13% to a density of 130. Thus, looking at the results in Figure 6.2 (b) the Baltic population is able to beat *G. salaris* infection, growing to 95.18% of their new carrying capacity, and coexist with low parasite numbers (a parasite density of 3.7 at the end of the simulation).

## 6.2 EXTENDING THE MODEL FOR N-SALMON STRAINS

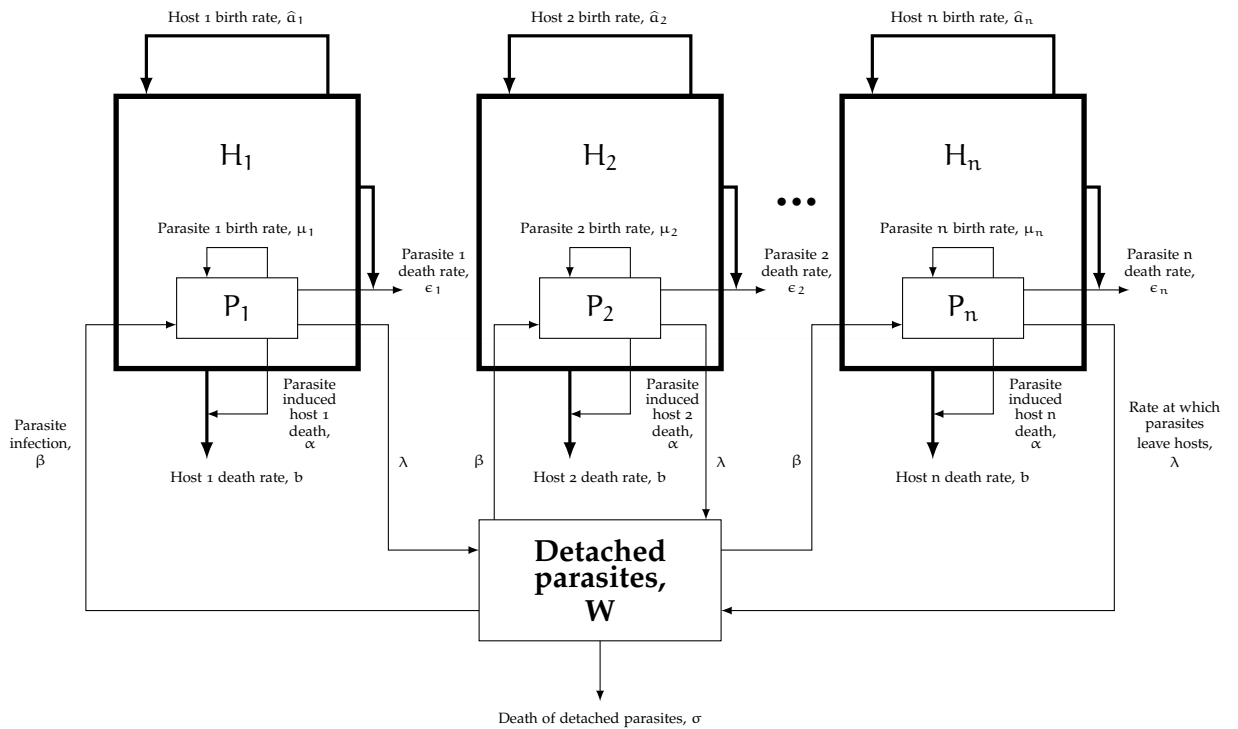


Figure 6.3: Schematic representation of Atlantic salmon-*Gyrodactylus salaris* interactions with  $n$  Atlantic salmon strains and one strain of *G. salaris* that exhibits different behaviour on each host strain. See Table A.1 (Appendix A) for a description of the parameters used.

Simulating the two-strain model gives results that one would expect to receive when considering the Atlantic and Baltic strains and does not really add any new information. However, the model does confirm the impact that an immune response has on both salmon and *G. salaris* populations and is consistent with experimental data (Bakke *et al.*, 1990; Jansen & Bakke, 1991; Cable *et al.*, 2000; Paladini *et al.*, in prep.). The two-strain model and the results obtained provide a solid foundation for investigations into the possibility of susceptible salmon strains evolving into a more resistant strain. Hence, the two-strain model is now extended to consider a system with  $n$  salmon strains interacting with one *G. salaris* strain exhibiting  $n$  different behaviours and  $n$  levels of immunity starting at a fully susceptible state to resistance to infection.

The model has the general form for  $n$  strains given by Equations (6.8)-(6.11) and represented schematically in Figure 6.3.

$$\frac{dH_n}{dt} = \left( \hat{a}(\tilde{m}_n) - b - s \sum_{j=1}^n H_j \right) H_n - \alpha P_n \quad (6.8)$$

$$\frac{dP_n}{dt} = P_n \left( \mu_n - \left( \epsilon_n + I_n + b + \alpha + s \sum_{j=1}^n (H_j) + \lambda \right) - \alpha \frac{P_n}{H_n} \right) + \beta W H_n \quad (6.9)$$

$$\frac{dW}{dt} = \sum_{i=1}^n \left( P_i \left( b + s \sum_{j=1}^n (H_j) + \lambda + \alpha + \frac{\alpha P_i}{H_i} \right) - \beta W H_i \right) - \sigma W \quad (6.10)$$

$$\frac{dI_n}{dt} = \tilde{m}_n \frac{P_n}{H_n} - \zeta I \quad (6.11)$$

where,

$$\hat{a}(\tilde{m}_n) = \frac{0.006 + 0.711765\tilde{m}_n}{0.3 + 41.1765\tilde{m}_n}$$

Due to the complexity of the system the model is simulated as before using Mathematica™ (an example of the source code can be found in Appendix D).

### 6.2.1 Baseline simulations in the absence of infection

We begin by simulating the model for four salmon strains with no *G. salaris* infection present and levels of immunity given as in Table 6.1.

Table 6.1: Values for  $\tilde{m}$  in baseline simulations. Simulating the model (Equations 6.8-6.11) for four salmon host strains with  $\tilde{m}$  values equally spread from fully susceptible to resistant.

Host strain	$\tilde{m}$
Salmon host strain 1 (e.g. Atlantic)	0.0
Salmon host strain 2	0.0058
Salmon host strain 3	0.0117
Salmon host strain 4 (e.g. Baltic)	0.0175

As Figure 6.4 shows, in the absence of infection, over a 100 year period, the salmon strain that is highly susceptible to infection (no immunity) wins and grows to carrying capacity whereas the other salmon strains present in the system decay to zero. This is due to the  $H_1$  population having the largest birth rate resulting from the absence of immunity, and hence, trade-off.

### 6.2.2 Adding *G. salaris* infection

Extending the results above we now investigate the impact of adding *G. salaris* into the system via the detached parasite class. As above the model is simulated to allow populations of salmon reach equilibrium in the absence of infection, then after 100 years, 0.1 detached

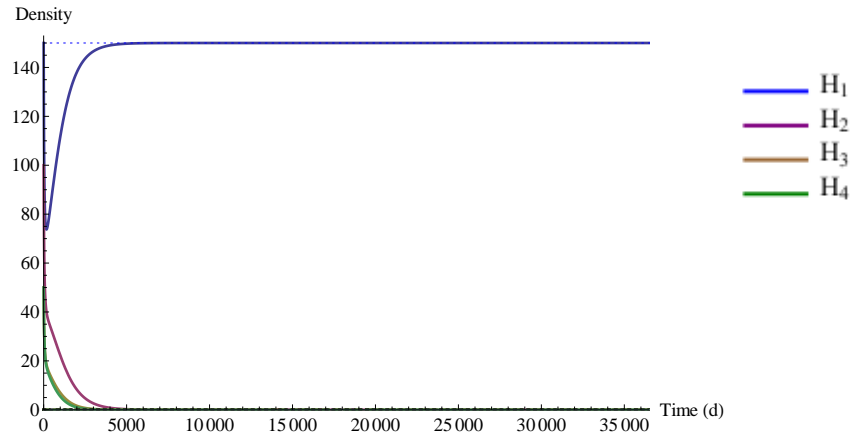


Figure 6.4: Simulating the multiple host strain model for 4 salmon host strains in the absence of infection. Trajectories for populations of host strains ( $H_1, \dots, H_4$ ). When *G. salaris* is not present in the environment the salmon strain with the highest birth rate, in this case the fully susceptible  $H_1$  population, out competes the other host strains and grows to carrying capacity.

parasites are added and the model simulated for a further 900 years to study the effects of infection over a long time period. As was seen in Figure 6.4 the salmon strains exhibiting varying levels of resistance die out as the fully susceptible strain grows to carrying capacity, hence, the model is kept seeded with resistant salmon at the point of *G. salaris* introduction. The results obtained are found in Figure 6.5.

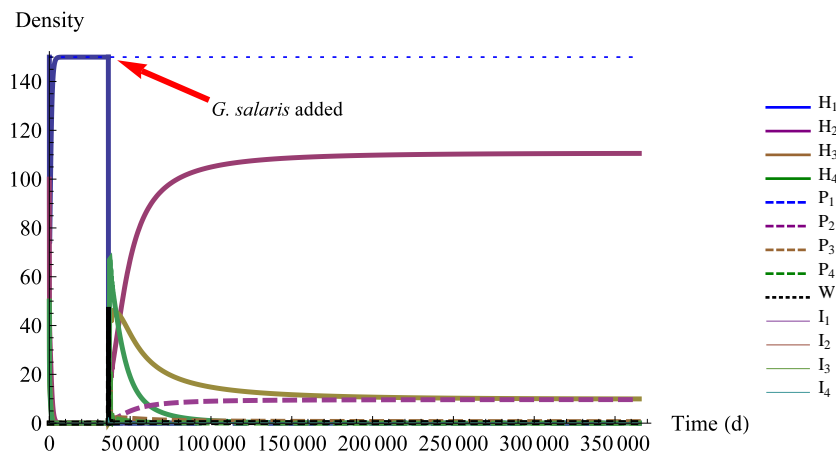


Figure 6.5: Simulating the multiple host strain model for four salmon host strains with varying levels of resistance and *G. salaris* infection added after 100 years. Trajectories for populations of host strains ( $H_1, \dots, H_4$ ), attached *G. salaris* ( $P_1, \dots, P_4$ ) and detached *G. salaris* ( $W$ ) are shown. In the absence of *G. salaris* the salmon strain with the highest birth rate grows to carrying capacity. After the introduction of *G. salaris* (highlighted in the plot) the fully susceptible hosts are forced to extinction resulting in an increase in density of the three remaining resistant host strains. Coexistence with low levels of *G. salaris* infection is observed.

As can be seen, at the point *G. salaris* infection is added (highlighted in Figure 6.5) the highly susceptible host strain with no immunity to infection immediately begins to decay. On closer inspection (see Figures 6.6 (a) and (b) below) it can be seen that as a result of adding infection the host 1 (fully susceptible) population becomes extinct after approximately 100 days. After the fully susceptible host strain population reaches zero the three host strains

remaining, each with increasing levels of resistance to the parasite, begin to increase in density. Due to having the highest level of immunity host strain 4 exhibits quicker and stronger growth than strains 2 and 3 forcing the parasite population into decay. However, after a short period of time (approx 4 years), and with a low level of infection present, strain 4 begins to be replaced by strains 2 and 3 due to hosts in these populations having a higher birth rate. We observe that over time the strain that wins is in fact host strain 2, with only a small level of *G. salaris* resistance and hence smallest impact on host birth rate. Host 2 is able to recover and coexist with a low level of *G. salaris* infection as well as a low level of the strain 3 hosts.

It is interesting that in a system with multiple populations of host strains present, each with a differing level of immunity, it is the strain with the highest level of resistance to infection that becomes extinct like the fully susceptible strain. This could be due to the resistant strain bringing the *G. salaris* population down to a low enough level such that the more susceptible strains can exhibit positive growth. Consequently, due to the less resistant strain having a more efficient birth rate, hosts are able to grow to a higher density and hence beat and replace the resistant strain that is less efficient at reproducing.

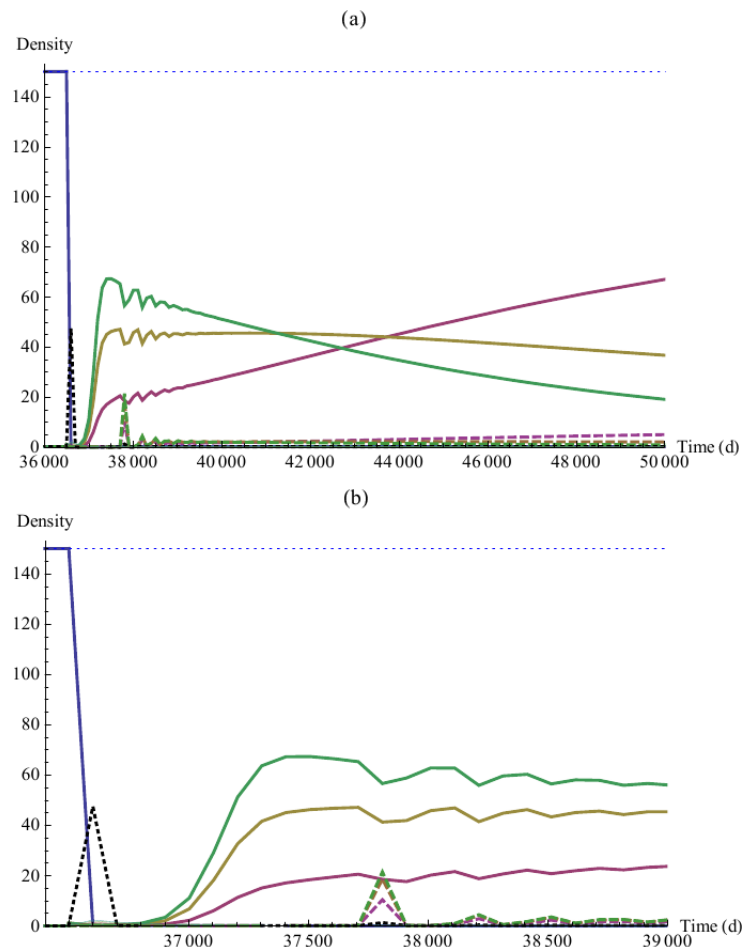


Figure 6.6: Simulating the multiple host strain model for four salmon host strains with infection added after 100 years. Trajectories for populations of host strains ( $H_1, \dots, H_4$ ), attached *G. salaris* ( $P_1, \dots, P_4$ ) and detached *G. salaris* ( $W$ ) 6 to 36 years after introduction of *G. salaris*.

## 6.3 MODEL E: MULTIPLE HOST STRAINS

### 6.3.1 Adding mutations

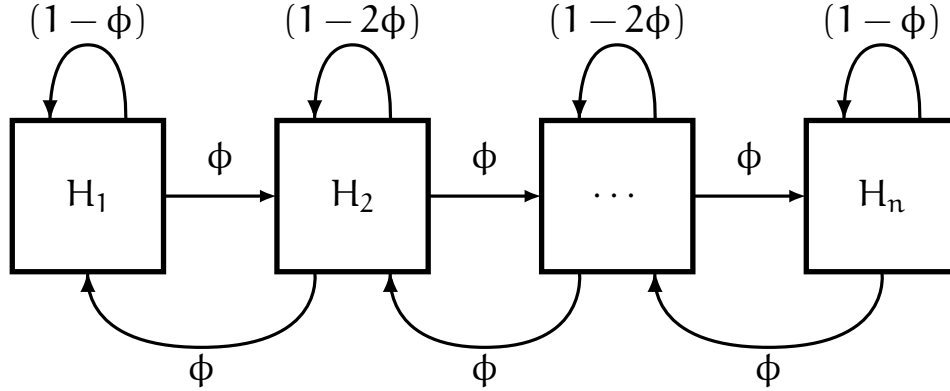


Figure 6.7: Adding mutations to the multiple host strain model. Mutations are added to the system via the parameter  $\phi$  host equations.  $\phi$  determines the number of mutated hosts that are born such that a host from strain  $j$  can do one of three things: 1) give birth to an offspring that shares traits with its parent, this occurs at rate  $(1-\phi)$  for  $j = 1, n$  and  $(1-2\phi)$  for  $2 < j < n - 1$ ; 2) give birth to a mutated offspring that has evolved traits similar to hosts in strain  $j+1$  at rate  $\phi$ ; 3) give birth to a mutated offspring that has devolved traits similar to hosts in strain  $j-1$  at rate  $\phi$ . Fully susceptible hosts cannot give birth to mutant offspring that are less evolved, likewise, hosts in the final strain that have the highest level of resistance cannot give birth to mutant offspring that are more evolved.

The model and results above do not take into consideration the possibility of a hosts reproducing and giving birth to mutated offspring. Hence, we now add such mutations to the system such that it is possible for a host from strain  $j$  to give birth to a mutated offspring further along the evolutionary line that shares traits with hosts in strain  $j+1$ , Equation (6.13). Similarly, there is also the chance that a host might give birth to a mutated offspring that is not as evolved as its parent and actually shares traits with hosts in strain  $j-1$ , Equation (6.13). The ability of a host strain to give birth to mutant offspring into the previous and next strain in the evolutionary line is implemented into the model via the parameter  $\phi$ . This new parameter  $\phi$  determines the number of mutated hosts that are born, for example say for every 1000 salmon offspring born 2 of these said offspring are mutants, and are added to the rate of change of the hosts (Equation 6.8). It is assumed that hosts in the first strain, with zero immunity, cannot give birth to mutant offspring that are less resistant, Equation (6.12), and hosts in the final strain, with the highest level of immunity, cannot give birth to mutant offspring that are more resistant, Equation (6.14). The model now has general form given by Equations (6.12) to (6.17).

$$\frac{dH_1}{dt} = (1 - \phi)\hat{a}(\tilde{m}_1)H_1 + \phi\hat{a}(\tilde{m}_2)H_2 - \left( b + s \sum_{j=1}^n H_j \right) H_1 - \alpha P_n \quad (6.12)$$

$$\begin{aligned} \frac{dH_i}{dt} &= \phi\hat{a}(\tilde{m}_{i-1})H_{i-1} + (1 - 2\phi)\hat{a}(\tilde{m}_i)H_i + \phi\hat{a}(\tilde{m}_{i+1})H_{i+1} \\ &\quad - \left( b + s \sum_{j=1}^n H_j \right) H_i - \alpha P_n \quad \text{for } 2 \leq i < n \end{aligned} \quad (6.13)$$

$$\frac{dH_n}{dt} = \phi\hat{a}(\tilde{m}_{n-1})H_{n-1} + (1 - \phi)\hat{a}(\tilde{m}_n)H_n - \left( b + s \sum_{j=1}^n H_j \right) H_n - \alpha P_n \quad (6.14)$$

$$\frac{dP_l}{dt} = P_l \left( \mu_l - \left( \epsilon_l + I_l + b + \alpha + s \sum_{j=1}^n (H_j) + \lambda \right) - \alpha \frac{P_l}{H_l} \right) + \beta W H_l \quad (6.15)$$

$$\frac{dW}{dt} = \sum_{q=1}^n \left( P_q \left( b + s \sum_{j=1}^n (H_j) + \lambda + \alpha + \frac{\alpha P_q}{H_q} \right) - \beta W H_q \right) - \sigma W \quad (6.16)$$

$$\frac{dI_l}{dt} = \tilde{m}_l \frac{P_l}{H_l} - \zeta I \quad (6.17)$$

$$\hat{a}(\tilde{m}_l) = \frac{0.006 + 0.711765\tilde{m}_l}{0.3 + 41.1765\tilde{m}_l} \quad (6.18)$$

The approach that was taken in the previous sections is now repeated in order to compare model outputs. Once again we begin by observing the dynamics in the absence of infection.

### 6.3.2 Baseline simulations in the absence of infection

As mentioned above we simulate the model (Equations 6.12 to 6.17) in Mathematica™ with no *G. salaris* infection present. In order to compare the results with those obtained in the absence of the ability for hosts to give birth to mutant offspring we once again simulate the model for 4 salmon host strains (by setting  $n = 4$ ), starting at a fully susceptible salmon strain with zero immunity and ending at resistant salmon strain with the highest level of immunity. We observe the dynamics over a 25 year period. The mutation rate  $\phi$  is set to 0.0001, allowing a mutant to occur in every 2 out of 1000 offspring births. The immunity parameter,  $\tilde{m}$ , is varied equally between the 4 salmon strains starting at  $\tilde{m} = 0$  and ending with  $\tilde{m} = 0.0175$ . Figure 6.8 shows the results obtained.

As can be seen, within 25 years in an environment with no *G. salaris* infection the fully susceptible strain of salmon is able to out-compete the three other strains. This is consistent with the results observed in Section 6.2.1. In the previous model the more resistant strains died out, however, in this case these lesser strains are maintained at low levels with the fully susceptible strain reaching a level just under carrying capacity.

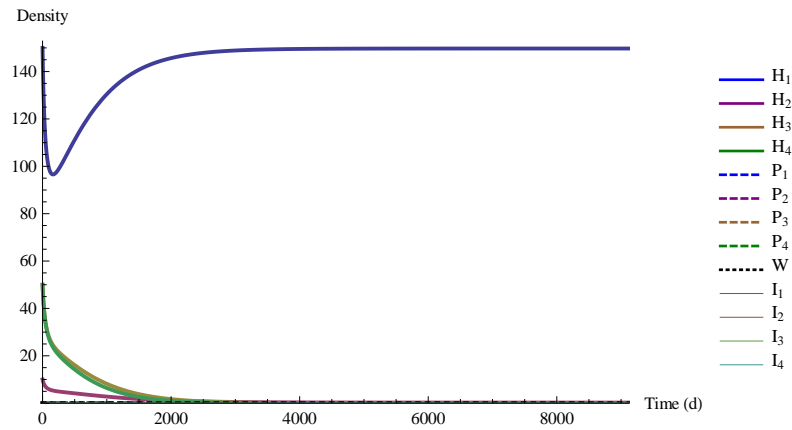


Figure 6.8: Simulating the multiple host strain model for four salmon host strains in the absence of *G. salaris* infection where host strains are capable of giving birth to mutant offspring that share traits with other host strains in the system. Mutants are born such that every 1 in 1000 offspring produced is a mutant. Trajectories for populations of host strains ( $H_1, \dots, H_4$ ), attached *G. salaris* ( $P_1, \dots, P_4$ ) and detached *G. salaris* ( $W$ ). As in the case with no mutant births, when *G. salaris* is not present the host strain with no immunity ( $H_1$ ), and hence strongest birth rate, out competes the other less susceptible host strains and grows to carrying capacity.

### 6.3.3 Adding *G. salaris* infection

As was done in Section 6.2.2 the investigation is now focused on the impact of adding *G. salaris* into the system via the detached parasite class. Initially, the model is simulated to allow populations of salmon strains to reach equilibrium in the absence of infection and using  $\phi = 0.0001$ . After 25 years 0.1 detached parasites are added and the model simulated for a further 975 years to study the dynamics over a 1000 year period. Values for  $\tilde{m}$  are as in Table 6.1. The results obtained are found in Figures 6.9 and 6.10.

The results in Figures 6.9 and 6.10 give results similar to those obtained in Section 6.2.2 with the final outcome being consistent. As in Section 6.2.2 strain 2 is capable of out-competing the other strains resulting in low level parasite coexistence with a small population of strain 3 hosts present. As before the fully susceptible hosts (strain 1) and the hosts with the highest level of resistance (strain 4) both decay to zero. As can be seen in Figure 6.9 (a) and (b) the population of strain 2 hosts is able to increase due to low levels of parasite infection and quickly grows to high levels eventually reaching carrying capacity. However, as the strain 2 population increases so to does the number of *G. salaris* present in the strain 2 population, lowering the number of strain 2 hosts and allowing the strain 3 host population, with its slightly higher level of immunity, to grow and over the course of the simulation coexist with host strain 2. As discussed, once again the host strain with the highest level of immunity cannot compete with the host strains that exhibit a lower resistance but higher birth rate.

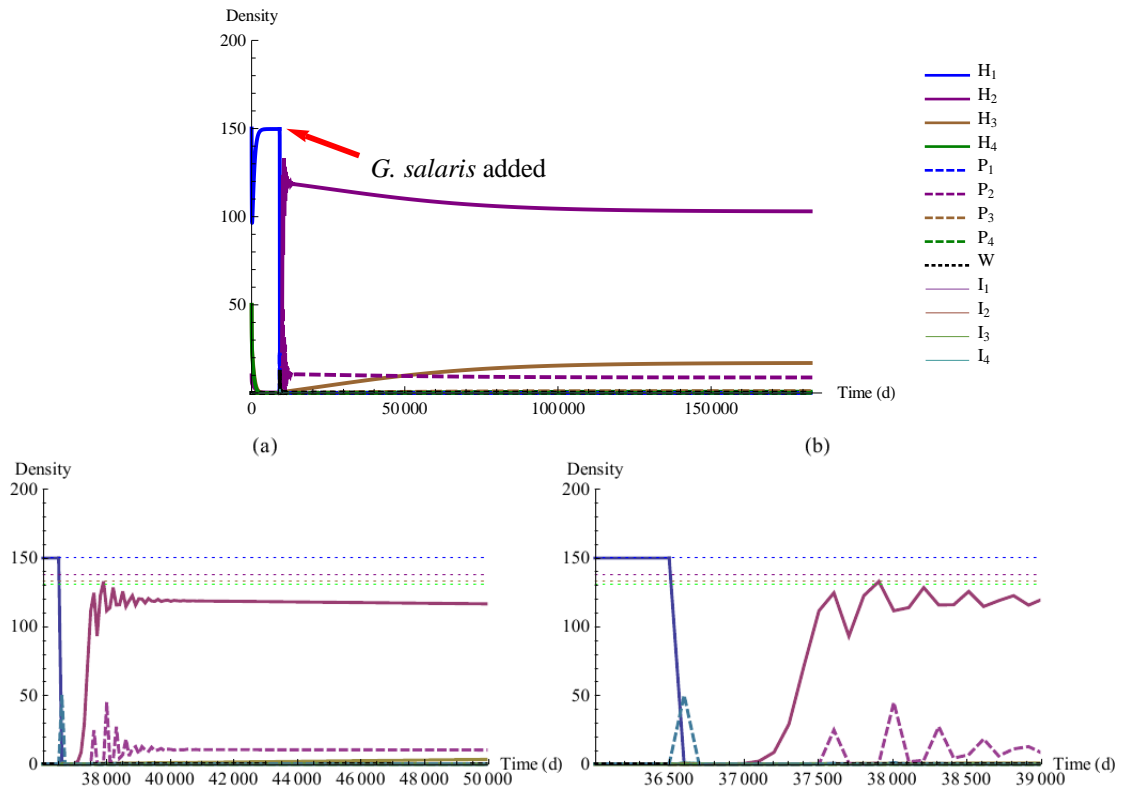


Figure 6.9: Simulating the multiple host strain model for 4 salmon host strains (*G. salaris* infection added after 25 years) such that host strains are capable of giving birth to mutant offspring that share traits with other host strains in the system. Mutants are born such that every 1 in 1000 offspring produced is a mutant. Trajectories for populations of host strains ( $H_1, \dots, H_4$ ), attached *G. salaris* ( $P_1, \dots, P_4$ ) and detached *G. salaris* ( $W$ ) are observed. Under these conditions the  $H_1$  strain decays to zero and it is the  $H_2$  strain that beats infection and outcompetes the two remaining host strains. Plots (a) and (b) show the trajectories magnified in order to show behaviour at the point *G. salaris* infection is introduced.

Figure 6.10 shows the trajectory of the total number of hosts from all strains. As can be seen the total number of hosts present in the reaches and settles at 80% of the original carrying capacity.

#### 6.4 INVESTIGATING TIME TO SALMON POPULATION RECOVERY

We have seen the impact of introducing *G. salaris* to a system that has at most four strains. Increasing the number of host strains present in the system gives results in Figures 6.11 and 6.12.

Looking at Figure 6.11 we see that the results are consistent with those obtained in the previous sections such that as the number of host strains is increased so to is the length of time taken for the fully susceptible strain to beat the more resistant strains and reach carrying capacity in the absence of *G. salaris* infections. Once again after 100 years *G. salaris* infection is added to the system via the detached parasite class and the impact simulated over 1000 years.

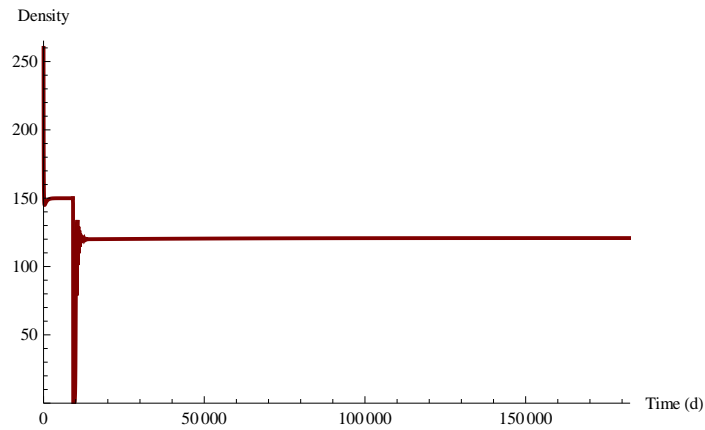


Figure 6.10: Simulating the multiple host strain model for four salmon host strains (*G. salaris* infection added after 25 years and  $\phi = 0.0001$ ) where host strains are capable of giving birth to mutant offspring that share traits with other host strains in the system. The trajectory of total host density (all salmon strains) is plotted.

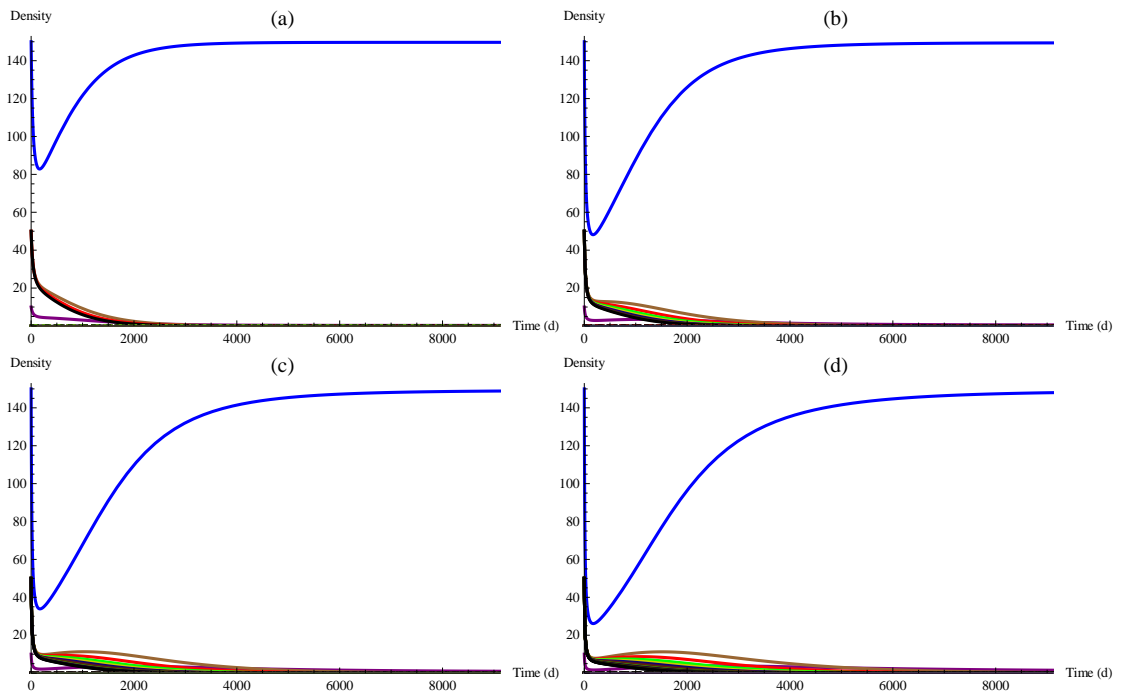


Figure 6.11: Simulating the  $n$ -strain model for a)  $n = 5$ , b)  $n = 10$ , c)  $n = 15$  and d)  $n = 20$  salmon strains over 25 years in the absence of infection with mutations occurring in all simulations at rate  $\phi = 0.0001$ . As the number of host strains present in the system is increased, so too is the length of time taken for an equilibrium state to be reached with the fully susceptible strain out-competing the more resistant host strains.

The behaviour witnessed after infection is added follows that observed in the four-strain case. As before, the fully susceptible host population (strain 1) immediately begins to decay which quickly results in strain 1 becoming extinct. At this point the *G. salaris* population, that was present in the strain 1 salmon population, begins to decrease as they become detached and search for new hosts. Due to the low number of hosts in the system, and the fact that all hosts present now exhibit some level of resistance to infection, the *G. salaris* population continues to decay, and hence, hosts begin to recover. The results also show that an increased

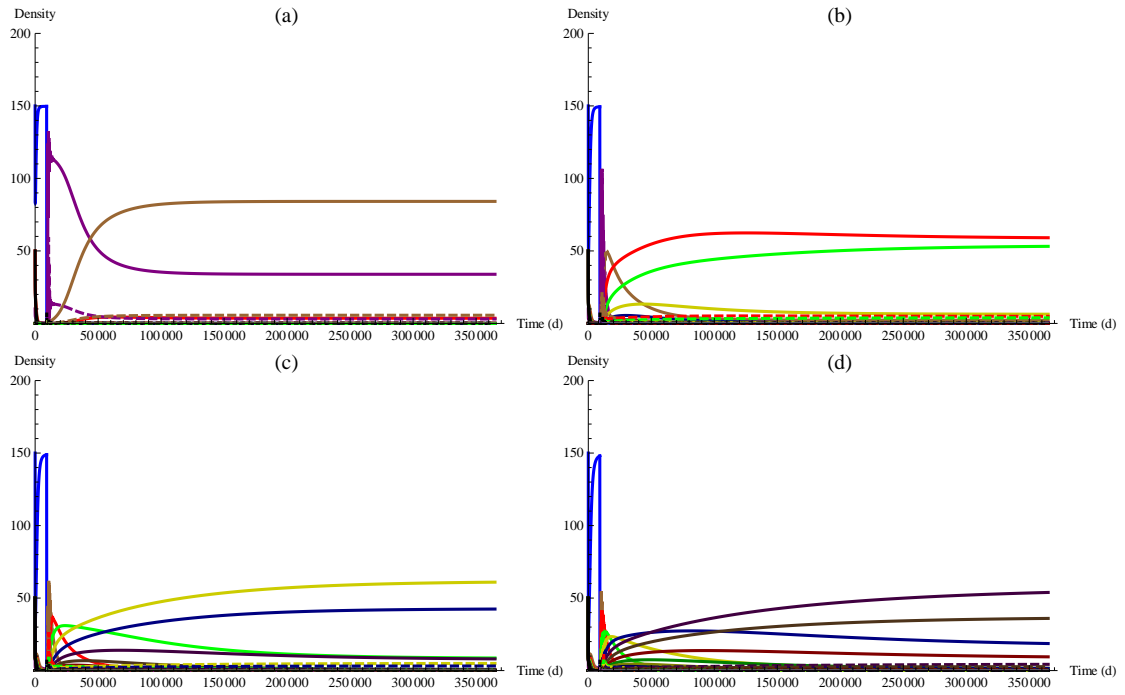


Figure 6.12: Simulating the  $n$ -strain model for  $n = 5, 10, 15$  and  $20$  salmon strains over 1000 years with infection added after 25 years. From left to right  $n = 5, 10, 15, 20$  in (a), (b), (c) and (d) respectively with mutations occurring in all simulations at rate  $\phi = 0.0001$ . As the number of host strains present in the system is increased, so too is the length of time taken for an equilibrium state to be reached, as is the number of strains coexisting with each other and the parasite at the end of the simulation.

number of host strains also means an increased number of strains that can beat infection and coexist with each other as well as low levels of parasite infection. In such cases *G. salaris* populations are present in each of the remaining salmon strain populations. The highest density of parasites is present in the dominant salmon strain population. Table 6.2 gives a summary of the way in which salmon strains coexist with each other for an increasing number of strain populations.

Looking at the results in Table 6.2 it can be seen that the dominant strain in each of the simulations (*i.e.*, the strain with the highest density) is the strain that is approximately half way between the fully susceptible strain and the strain with the highest level of resistance. It is also worth highlighting that as the number of initial host strains present in the system is increased, the percentage of host strains remaining actually decreases, for example when  $n = 4$ , 60% of original strains survive whereas when  $n = 50$  only 20% of the original salmon strains survive. Thus, a lower number of salmon host strains initially present in a system would be advantageous.

Table 6.2: Host strain coexistence after recovery from infection. Simulating the n-strain model ( $\phi = 0.0001$ ) for an increasing number of salmon host strains ( $n \geq 5$ ) over a 1000 year period with *G. salaris* infection added after 25 years. Dominant host strain and host strains remaining at end of simulation are given. Strains are considered extinct at the end of a simulation if they have a density that is less than 0.5. As the number of host strains present in the system is increased, so too is the number of host strains coexisting with each other and the parasite at the end of the simulation.

Number of host strains present at start of simulation	Number of strains present at end of simulation	Dominant host strain (highest density)	Other strains present (highest - lowest density)
5	3	Host strain 3	Host strain 2 & 4
10	4	Host strain 5	Host strain 4, 6 & 3
15	4	Host strain 6	Host strain 7, 5 & 8
20	6	Host strain 8	Host strain 9, 7, 10, 6 & 11
25	6	Host strain 10	Host strain 11, 9, 12, 8 & 13
30	7	Host strain 12	Host strain 11, 13, 14, 10, 15 & 9
50	10	Host strain 19	Host strain 18, 20, 21, 17, 22, 16, 23, 24 & 15

#### 6.4.1 Mutation rate

As discussed earlier the mutations that occur in the models above are determined by  $\phi$ . Until now we have been using a  $\phi$  value that results in two mutant being born in every one thousand births. We now investigate the effect that varying the mutation rate has on time to salmon recovery. Here we consider the salmon population as sufficiently recovered when the total of all salmon strains reaches a density that is at least 60% of the carrying capacity of the most resistant salmon strain, in other words the strain with the lowest carrying capacity. We study the implications of varying  $\phi$  for 2, 3, 4, 5, 10 and 25 salmon strains respectively.

Looking at the results in Figure 6.13 we observe that increases in mutation rate,  $\phi$ , results in faster salmon recovery. In the absence of infection a higher mutation rate allows more host strains to coexist, hence, lowering the total density that the fully susceptible salmon strain can grow to. After *G. salaris* infection is introduced into the system salmon populations recover initially with densities oscillating for some years, sometimes above and below the 60% threshold (Tables 6.3 and 6.4 give times in years to first occurrence of 60% recovery). Finally population densities stabilise resulting in coexistence of host strains and low level *G. salaris* infections. However, in the case where the number of salmon strains is 25, the time to salmon recovery begins to oscillate after the mutation rate reaches values greater than 0.04 and the system settles into cycles thereafter.

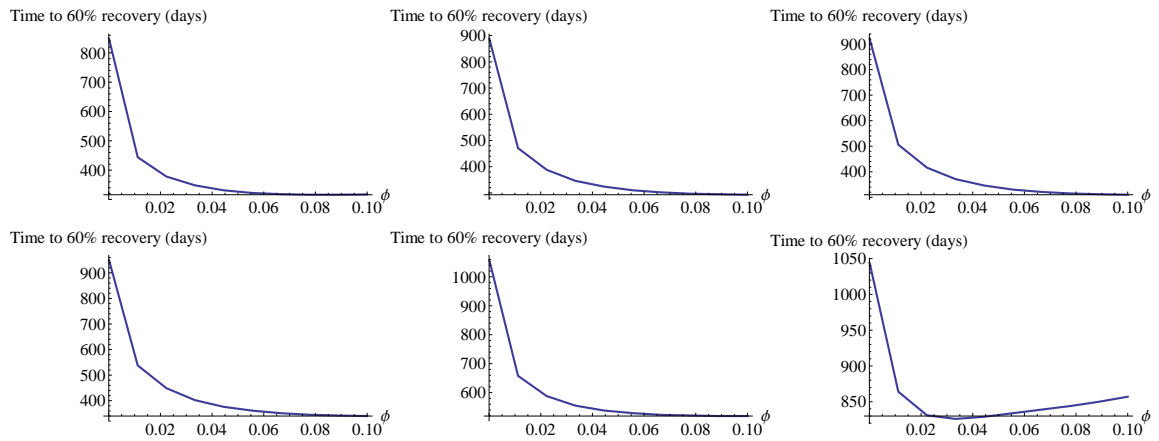


Figure 6.13: Simulating the  $n$ -strain model for 2, 3, 4, 5, 10 and 25 host strains for differing levels of mutation,  $\phi$ , against the time it takes for the total salmon population to recover. The salmon population is considered as recovered when the total number of salmon from all strains reaches a density that is at least 60% of carrying capacity.

Biologically, larger values of  $\phi$  (e.g.,  $\phi = 0.1$ ) are not plausible as mutations are rare. With this in mind our original mutation rate of 0.0001 would appear to be a reasonable estimate. Taking into consideration the fact that *G. salaris* infections are not present in the system until 25 years into the simulation, Tables 6.3 and 6.4 give a comparison of the time taken in years for salmon to initially recover from infection for different  $\phi$  values. Moreover, model simulations demonstrated whether or not salmon recovery to a stable level occurred (see Tables 6.5 and 6.6). The majority of simulations predicted salmon populations would recover from *G. salaris* infections 10 to 15 years post introduction (for  $0.0001 \leq \phi \leq 0.1$ ,  $n < 25$ ).

Table 6.3: Mutation rate versus time to initial salmon population recovery (60% of  $K_{min}$ ). Models simulated using differing levels of mutation rate,  $0.0001 \leq \phi \leq 0.1$ , for 2, 3, 4, 5, 10 and 25 salmon host strains. Results were used to determine the amount of time taken for the total salmon population to initially recover to a level that is at least 60% of the carrying capacity of the most resistant salmon strain. Occurrences of salmon populations oscillating above and below the 60% threshold are represented by \* with  $*^+$  and  $*^-$  representing oscillations settling to a level above and below the threshold respectively. Models simulated for a 1000 year period with *G. salaris* infection added after 25 years.

Number of host strains present at start of simulation	Time to 60% ( $K_{min}$ ) salmon population recovery (in years)									
	$\phi = 0.0001$	$\phi = 0.0112$	$\phi = 0.0223$	$\phi = 0.0334$	$\phi = 0.0445$	$\phi = 0.0556$	$\phi = 0.0667$	$\phi = 0.0778$	$\phi = 0.0889$	$\phi = 0.1$
2	2.32	1.22	1.04	0.95	0.93	0.88	0.87*	0.87*	0.87*	0.87*
3	2.43	1.29	1.06	0.95	0.89*	0.85	0.83	0.81*	0.81*	0.80*
4	2.52	1.39	1.14	1.02	0.95*	0.90*	0.88	0.86*	0.85*	0.85*
5	2.60*	1.47*	1.23*	1.10	1.03*	0.99*	0.96*	0.95*	0.94*	0.93*
10	2.90*	1.80*	1.61*	1.52*	1.47*	1.45*	1.43*	1.43*	1.43*	1.42*
25	2.86*	2.37*	2.28*	2.26*	2.27* <sup>-</sup>	2.28* <sup>+</sup>	2.30* <sup>+</sup>	2.31	2.33	2.35

Table 6.4: Mutation rate versus time to initial salmon population recovery (60% of  $K_{max}$ ). Models simulated using differing levels of mutation rate,  $0.0001 \leq \phi \leq 0.1$ , for 2, 3, 4, 5, 10 and 25 salmon host strains. Results were used to determine the amount of time taken for the total salmon population to initially recover to a level that is at least 60% of the carrying capacity of the fully susceptible salmon strain. Occurrences of salmon populations oscillating above and below the 60% threshold are represented by \* with  $*^+$  and  $*^-$  representing oscillations settling to a level above and below the threshold respectively. Models simulated for a 1000 year period with *G. salaris* infection added after 25 years.

Number of host strains present at start of simulation	Time to 60% ( $K_{max}$ ) salmon population recovery (in years)									
	$\phi = 0.0001$	$\phi = 0.0112$	$\phi = 0.0223$	$\phi = 0.0334$	$\phi = 0.0445$	$\phi = 0.0556$	$\phi = 0.0667$	$\phi = 0.0778$	$\phi = 0.0889$	$\phi = 0.1$
2	2.40	1.30	1.12	1.04	0.99*	0.97*	0.96*	0.96*	0.96*	0.98*
3	2.51	1.36	1.14*	1.03	0.97*	0.93*	0.91*	0.90*	0.89*	0.89*
4	2.59	1.46*	1.21*	1.09*	1.02*	0.98*	0.96*	0.95*	0.94*	0.93*
5	2.67*	1.54*	1.30*	1.18*	1.10*	1.06*	1.04*	1.02*	1.02*	1.01*
10	2.96*	1.87*	1.68*	1.59*	1.55*	1.52*	1.51*	1.50*	1.50*	1.50*
25	2.92*	2.43*	2.35*	2.33*	2.35* <sup>-</sup>	2.36* <sup>+</sup>	2.39* <sup>+</sup>	5.28* <sup>-</sup>	Never	Never

Table 6.5: Stable salmon population recovery. Models simulated using differing levels of mutation rate,  $0.0001 \leq \phi \leq 0.1$ , for 2, 3, 4, 5, 10 and 25 salmon host strains. Results were used to determine whether or not salmon recover to a stable level within 10 to 15 years post introduction. Models simulated for a 1000 year period with *G. salaris* infection added after 25 years.

Number of host strains present at start of simulation	Salmon recover to a stable level within 10-15 years post introduction									
	$\phi = 0.0001$	$\phi = 0.0112$	$\phi = 0.0223$	$\phi = 0.0334$	$\phi = 0.0445$	$\phi = 0.0556$	$\phi = 0.0667$	$\phi = 0.0778$	$\phi = 0.0889$	$\phi = 0.1$
2	Yes	Yes	Yes	Yes	Yes	Yes	Yes	Yes	Yes	Yes
3	Yes	Yes	Yes	Yes	Yes	Yes	Yes	Yes	Yes	Yes
4	Yes	Yes	Yes	Yes	Yes	Yes	Yes	Yes	Yes	Yes
5	Yes	Yes	Yes	Yes	Yes	Yes	Yes	Yes	Yes	Yes
10	No	Yes	Yes							
25	No	No	No	No	Never	Never	Never	Never	Never	Never

Table 6.6: Level of salmon population recovery. Models simulated using differing levels of mutation rate,  $0.0001 \leq \phi \leq 0.1$ , for 2, 3, 4, 5, 10 and 25 salmon host strains. Results were used to determine the level of salmon recovery (percentage of  $K_{\max}$ ) after 1000 years. Models simulated for a 1000 year period with *G. salaris* infection added after 25 years.

Number of host strains present at start of simulation	% of maximum K salmon population recovered after 1000 years									
	$\phi = 0.0001$	$\phi = 0.0112$	$\phi = 0.0223$	$\phi = 0.0334$	$\phi = 0.0445$	$\phi = 0.0556$	$\phi = 0.0667$	$\phi = 0.0778$	$\phi = 0.0889$	$\phi = 0.1$
2	83.07	78.61	75.22	72.08	69.08	66.19	63.35	60.59	57.87	55.21
3	82.13	79.47	76.92	74.57	72.33	70.19	68.12	66.11	64.15	62.23
4	80.52	79.01	76.63	74.37	72.23	70.17	68.17	66.23	64.33	62.49
5	81.15	78.21	75.71	73.35	71.10	68.95	66.87	64.85	62.88	60.95
10	80.86	74.70	70.47	66.98	63.89	61.05	58.37	55.83	53.39	51.05
25	80.72	67.13	59.05	52.68	oscillates 40 - 50	oscillates 17 - 67	oscillates 12 - 63	oscillates 10 - 60	oscillates 6 - 57	oscillates 4 - 50

The behaviour of salmon populations for 10 strains (Figure 6.14) and 25 strains (Figures 6.15 and 6.16) is found below.

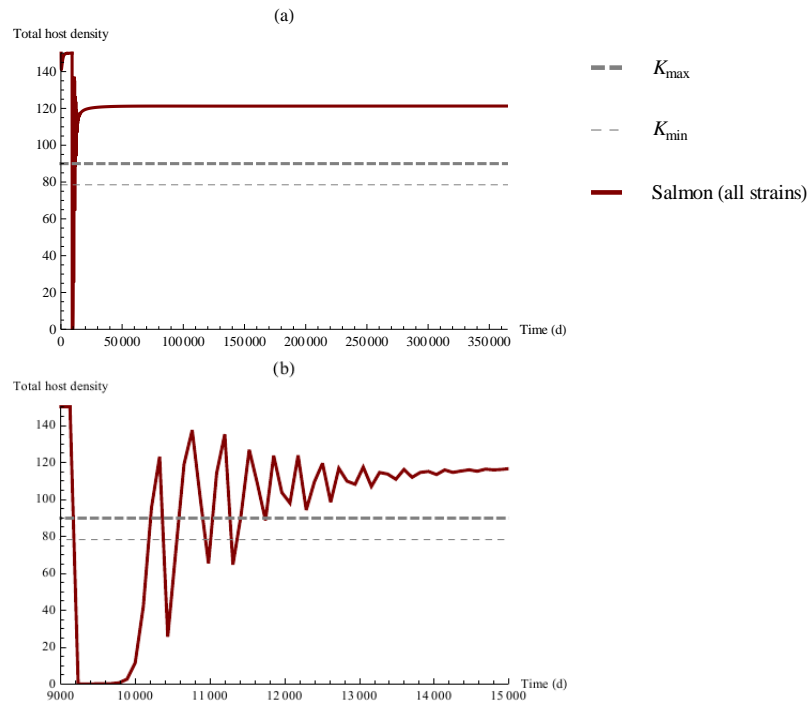


Figure 6.14: Total salmon density over time. Trajectories for total salmon density over a 1000 year period obtained via simulations of the n-strain model for 10 salmon host strains and  $\phi = 0.0001$ . Plots (a) and (b) show the results in full and over a shorter range respectively. Maximum carrying capacity and minimum carrying capacity are given by  $K_{max}$  (Thick, dashed, grey line) and  $K_{min}$  (Thin, dashed, grey line) respectively.

As can be seen in Figure 6.14a for 10 salmon strains and  $\phi = 0.0001$  the total salmon population takes approximately 7300 days, *i.e.*, 20 years, to reach a level of recovery that is stable. On closer inspection, Figure 6.14b, total salmon density oscillates above and below the 80% and 60% recovery thresholds for approximately 8 years post parasite introduction.

The results in Figure 6.15 for 25 salmon host strains in the absence of *G. salaris* infection is consistent with similar simulations for <25 strains given previously in this chapter. Once again, with no *G. salaris* parasites present the salmon strain with the highest birth rate is the dominant strain.

Figure 6.16 shows the impact of adding *G. salaris* infection to the system in Figure 6.15 for an increasing  $\phi$ .

As can be seen, as the value of  $\phi$  is increased from 0.0001 to 0.1 the total salmon population becomes less and less stable to the point that when  $\phi$  is too high salmon density can no longer reach the minimum recovery threshold (60% carrying capacity) and oscillates between 4% - 50% of carrying capacity.

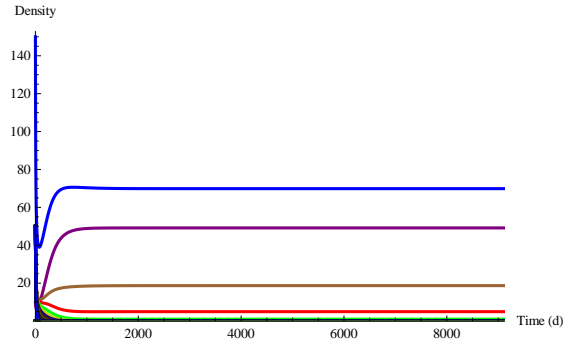


Figure 6.15: Simulating the n-strain model for 25 host strains in the absence of *G. salaris* infection. Trajectories of 25 salmon host strains over a 25 year period obtained via simulations of the n-strain model with  $\phi = 0.0001$ .

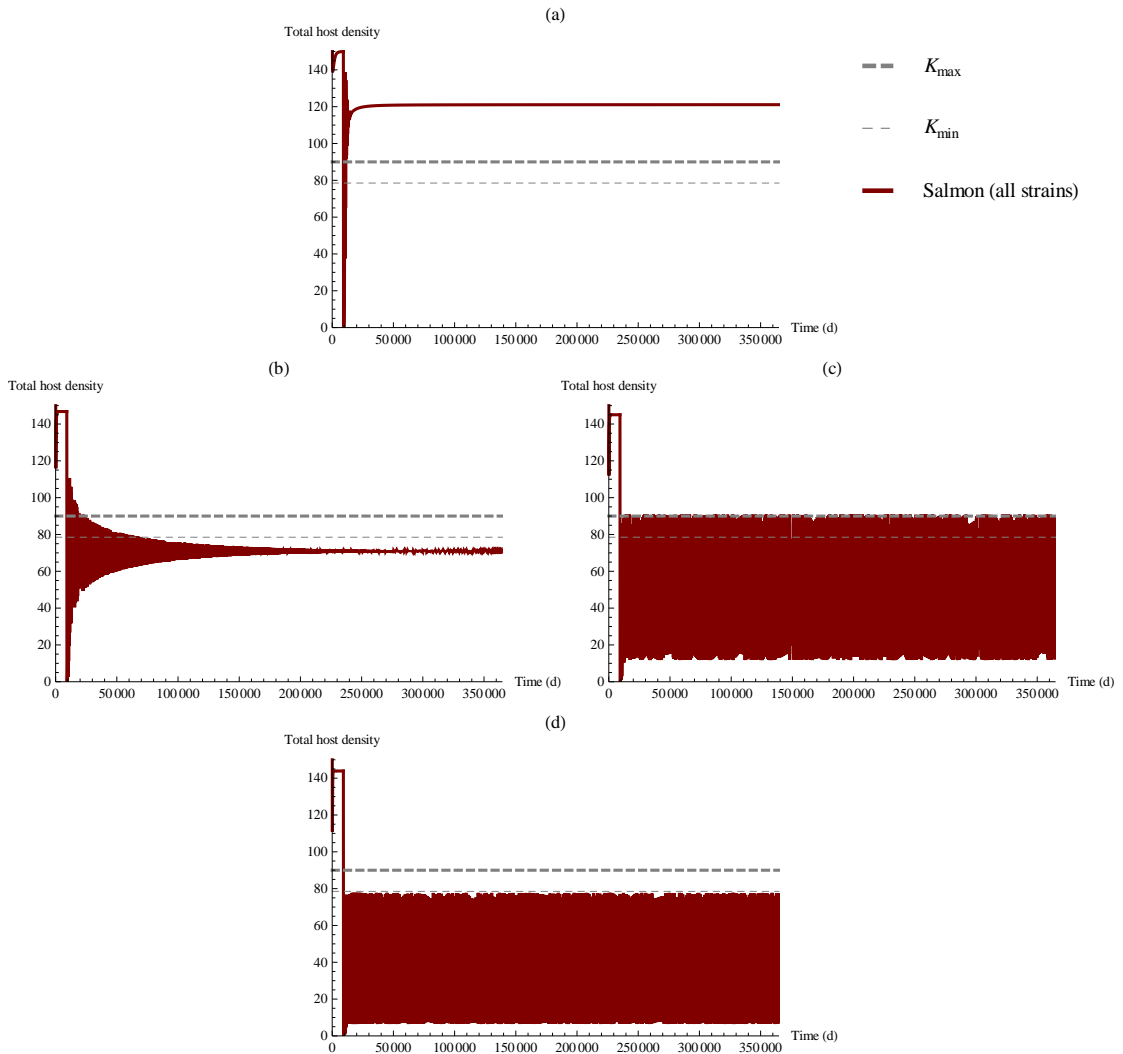


Figure 6.16: Total salmon density over time. Trajectories for total salmon density over a 1000 year period obtained via simulations of the n-strain model for 25 salmon host strains. The parameter  $\phi$  was varied as follows: (a)  $\phi = 0.0001$ ; (b)  $\phi = 0.0445$ ; (c)  $\phi = 0.0778$ ; (d)  $\phi = 0.1$ . Maximum carrying capacity and minimum carrying capacity are given by  $K_{\max}$  (Thick, dashed, grey line) and  $K_{\min}$  (Thin, dashed, grey line) respectively.

## 6.5 SIMULATING THE MODEL FOR A UK RIVER SYSTEM

For the final time a theoretical outbreak of *G. salaris* infection in the Welsh River Dee is studied. The model in its final form (Equations 6.12 to 6.17) is simulated to study the impact of *G. salaris* in the UK using the parameter estimates obtained in Sections 2.4, 3.5, 5.2.1 and 5.3.1 (see Table A.1, Appendix A).

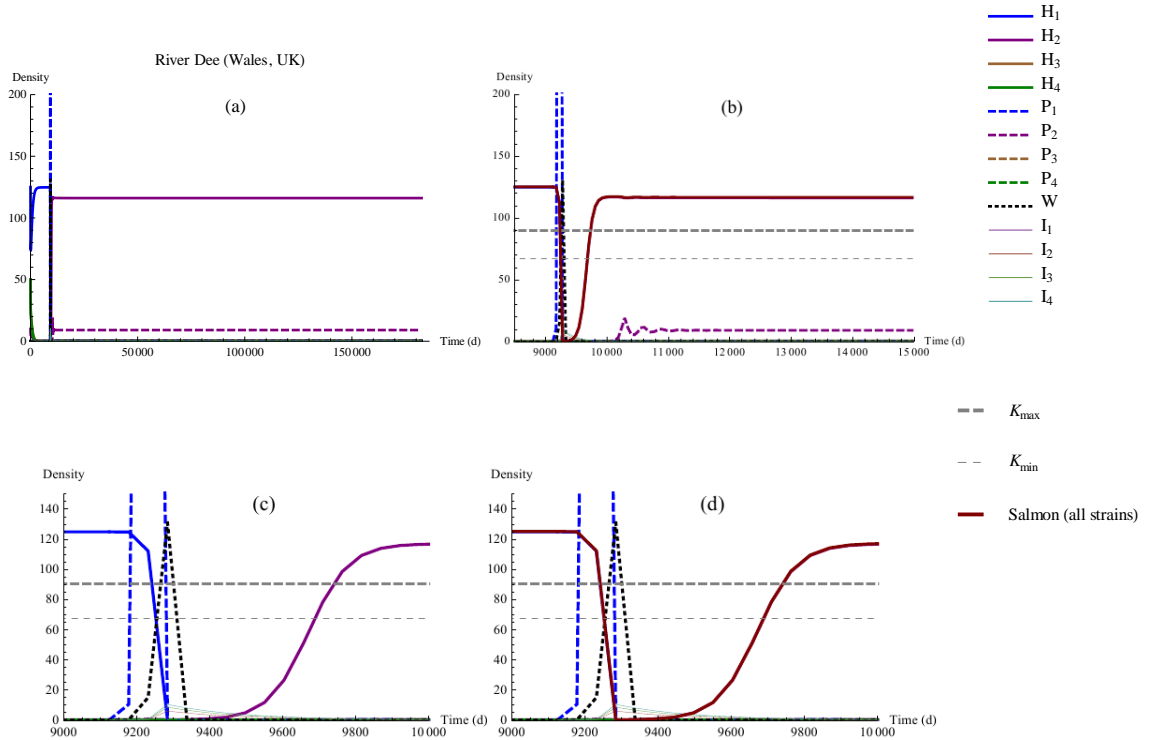


Figure 6.17: Model E: River Dee example. Trajectories of host, attached parasite and detached parasite populations in time as predicted by the  $n$ -host strain (with mutations) model and parameterised according to Table A.1 as follows:  $\alpha = 0.02$ ,  $b = 0.0006$ ,  $s = 0.00016$ ,  $\alpha = 0.0012$ ,  $\mu = 0.1708$ ,  $\epsilon = 0.08$ ,  $\lambda = 0.06$ ,  $\beta = 0.006$ ,  $\sigma = 0.155$ . Initially there is no infection present,  $H(0) = K = 125$ ,  $P(0) = 0$ ,  $W(0) = 0$ . Infection is added (a single attached parasite) after 730 days,  $H(7300) = K = 125$ ,  $P(730) = 1$ ,  $W(730) = 0$ . Hosts (—), parasites (---). Plot (a) highlights the trajectories of individual host strains whereas plot (b) highlights the trajectory of the total number of hosts (all strains). Plots (c) and (d) are magnifications of (a) and (b) respectively.

Figure 6.17 highlights the results obtained by simulating the model in its final format, Equations (6.12) to (6.17), for 4 salmon strains parameterised for a UK river, in this case the River Dee, Wales. Looking at Figure 6.17a and 6.17b it can be seen that the model predicts salmon recovery with low level *G. salaris* coexistence. The results gained are consistent with those found earlier in this chapter (Section 6.3.3 onwards) in that with initially 4 salmon strains it is salmon strain 2 that is the dominant one with very low densities of salmon strain 3. In this example the total density of salmon (i.e., from all strains) recovers to a level that is approximately 94% of the original carrying capacity. Figure 6.17c and 6.17d show that initial 60% recovery is reached 730 days post introduction with stable recovery following a short

time after. These results highlight the fact that salmon in the UK may in fact recover from *G. salaris* infections in the long run, however, time to recovery is likely to be much longer than predicted due to limitations of the model as mentioned below and discussed in more detail in Chapter 7.

## 6.6 SUMMARY

In this chapter we started by building on the immunity and trade-off work in Chapter 4 by adding an immune response and resulting trade off into a two host strain model. This allowed us to confirm model output is consistent with the literature such that, in terms of Atlantic and Baltic strains of Atlantic salmon, fully susceptible Atlantic salmon strains decay to zero when *G. salaris* is present whereas resistant Baltic salmon strains can beat infection and survive.

The two strain model was then extended to study a system with  $n$  host strains. This approach enabled the study of how salmon strains exhibiting differing levels of immunity from 0 (fully susceptible) to 0.017 (resistant) interact with each other and infections by *G. salaris*. These models showed that initially the resistant salmon strain out competes the remaining strains. However, with low parasite numbers the less resistant salmon with greater birthing potential replace the resistant salmon and coexist with low levels of *G. salaris* infection.

The final model had the addition of hosts having the ability to give birth to an offspring with a higher or lower level of resistance. This was determined by a mutation rate given by the parameter  $\phi$ . In the absence of infection the mutation rate determined the density to which strains grow with higher values of  $\phi$  resulting in more strains coexisting. The output from model simulations, with *G. salaris* infection present, was consistent in the long run with the results obtained from the  $n$  host strain model with no mutations such that the fully susceptible and highest resistant salmon strains becoming extinct and strains with less immunity but higher birth rate coexisting with each other and low levels of *G. salaris* infection. At the end of the 1000 year simulation the total number of salmon hosts remaining was not significantly different against the number of strains initially used.

Increasing the mutation rate from 0.0001 to 0.1 caused the time to population recovery to decrease. Whereas increasing the number of salmon strains caused the time for population recovery to increase. However, when the number of strains reached 25 the dynamics changed and instead of settling to an equilibrium with parasite coexistence the system settles into cycles.

The results obtained via model simulations, depending on the number of salmon strains present in an environment, allows us to conclude that if *G. salaris* is introduced into a river then we can expect fully susceptible salmon strains, such as those that occur naturally in the UK and Norway, to become extinct. However, in a system where multiple salmon strains are present with varying levels of immunity then salmon - *G. salaris* coexistence is possible with salmon reaching initial recovery (60%) occurring within one to three years. In the majority of cases with more than 3 salmon strains, see Tables 6.3 and 6.4, the salmon population oscillates above and below the 60% level reaching a constant stable level within 10 to 15 years after introduction (Table 6.5).

The results from the n-host strain model are in contrast with the hypothesis that salmon in infected rivers, if left untreated, will eventually decline to extinction. However, through experimental trials on salmon from the Drammen River in Norway, Salte *et al.* (2010) showed that wild salmon stocks have the genetic capacity to adapt to *G. salaris* infection, and hence, increase their chances of survival from infection (Salte *et al.*, 2010). Our results agree with the observations of Salte *et al.* (2010) in that if natural selection was left to occur then the model predicts salmon would adapt and become more resistant to *G. salaris* infections. Salte *et al.* (2010) conclude by theorizing that improving the genetic capacity to survive infection will not be enough to completely eradicate the parasite from infected rivers but may go in some way to control infections to the point that it is no longer a threat, this is another result that is predicted by the multiple strain model in that the remaining host strains at the end of simulations coexist with low *G. salaris* parasite numbers. Model simulations also suggest that Atlantic strains of Atlantic salmon will not evolve to a resistant level equal to that of the Baltic strain of Atlantic salmon but evolve to become more of an intermediate strain somewhere between the highly susceptible (Atlantic strain) and the resistant (Baltic).

In the field, Atlantic salmon leave freshwater for a life in saltwater, spending anything from 1 to 4+ years there maturing into adults before returning to their natal river to spawn (Crisp, 2000), hence, this time delay will impact our results adding years to our predictions. With this information in mind we can estimate salmon recovery could take anything from approximately 15 to 25 years after the introduction of *G. salaris*.

Part III

RESULTS AND CONCLUSIONS

## Discussion

The aim of this thesis was to explore interactions between populations of Atlantic salmon and the monogenean parasite *Gyrodactylus salaris* in order to make predictions on the possible consequences of introducing such an infection into an environment containing susceptible salmon host populations such as the United Kingdom. As discussed in the introduction, the majority of previous mathematical work concerning the salmon-*G. salaris* system is centred on risk and statistical analysis highlighting areas such as routes of infection, hence, there was much scope for a mathematical modelling approach to be developed in order to allow predictions of infection dynamics to be made.

In addition to studying interactions via macroparasite distributional models, contrasting modelling techniques such as Leslie matrix population models and individual based models were also used throughout this research. Models were used to study the possible differences between strains of Atlantic salmon to determine the mechanisms evolved by the Baltic strain in order to be able to beat infection and in some cases coexist with low levels of *G. salaris* infection. Models were also used to investigate the possibility of Atlantic strains of Atlantic salmon evolving traits and resulting trade-offs to become more like their Baltic counterparts.

As discussed in Chapter 6 the models showed that if *G. salaris* is introduced into a river system containing  $n$ -strains of salmon ( $n > 2$ ), such that birth rate is negatively correlated with resistance, salmon will evolve to a more resistant state and therefore be able to recover from infection. Such recovery would result in host coexistence with low parasite densities as well as other host strains of varying immunity.

Model simulations in Chapter 6 predicted rapid salmon decline after the introduction of *G. salaris* with susceptible salmon populations declining to extinction within 2 years. It is well established that *G. salaris* is able to reduce salmon populations in a river by 98%, this decline has been observed and occurred within 5 years after the emergence of the parasite (Johnsen & Jensen, 1991). One of the possible reasons as to why the model predicts salmon will decline faster than the time witnessed by Johnsen & Jensen (1991) could be due to the absence, in the model, of salmon returning from the sea each year to spawn (and similarly

salmon running to sea). This behaviour would add a steady stream of uninfected hosts to the system each year, and hence, increase the time taken for the salmon population in a river to decline.

## 7.1 MODEL DEVELOPMENT

### *Model basis and the baseline model*

Due to the absence of an existing model of salmon-*G. salaris* dynamics the first stage of this research was to develop a baseline model that would act as a foundation for the more complicated work. Chapter 2 highlighted the characteristics *G. salaris* shares with both macro and micro parasitic diseases and introduced the initial model. This model used the distributional models of Anderson and May (Anderson & May, 1978; May & Anderson, 1978) as a basis. This work was extended to include a detached parasite class as individual parasites can survive off a host for a limited time period (Mo, 1987; Bakke *et al.*, 2007).

When investigating the stability of the coexistence equilibrium a second zero equilibrium was discovered that resulted from parasites forcing the salmon population to extinction. Such equilibria do not commonly occur in distributional models but are more akin to compartmental models used to study microparasite dynamics. An investigation showed that this parasite induced extinction was not a result of the probability distribution of the parasites but as a result of short generation times and ability of *G. salaris* to give birth to pregnant offspring directly onto the skin of a salmon host (Bakke *et al.*, 2007), and hence, removing the requirement of a free-living infectious stage.

### *A new mechanism for resistance to *G. salaris**

In Chapter 4 a different approach was taken in order to estimate parasite growth rate on a single salmon host from data found in the literature (Cable *et al.*, 2000) and check that the parameter estimates obtained gave parasite numbers consistent with those obtained experimentally (Bakke *et al.*, 1990; Jansen & Bakke, 1991). Here Leslie matrix population models were used and an interesting observation was made. We noticed that a delay in the time taken for a parasite to achieve first birth had a noticeable impact on parasite numbers, a difference that exists between Atlantic and Baltic salmon strains (Cable *et al.*, 2000). Hence, an investigation into the possible mechanisms for resistance to *G. salaris* in salmon was undertaken. We were able to determine, through the use of both discrete and stochastic methods, a new mechanism of resistance to *G. salaris* infection existed. Until this point it was believed that the Baltic's acquired immunity was due to parasites infecting Baltic hosts giving birth

to fewer offspring and having a lower survival rate (Bakke *et al.*, 1990; Jansen & Bakke, 1991; Bakke & MacKenzie, 1993; Cable *et al.*, 2000).

We highlighted the fact that parasites on Baltic hosts give birth to their first offspring 0.5 days later than those parasites on Atlantic. Our results showed that delaying parasite first birth on Atlantic hosts caused parasite numbers to decrease by 50% and a 75% decrease observed if a 1 day delay is implemented. The results also highlighted that reducing the number of offspring birthed by an individual parasite from 4 (on Atlantic) to 2 (on Baltic) had little effect on the dynamics.

#### *Immunity, trade-offs and multiple salmon strains*

The final aim of this thesis was to have a model that incorporated multiple strains of salmon host. Following on from the work in Chapter 4 the baseline model was first extended for 2 salmon host strains, such as Atlantic and Baltic, and one strain of *G. salaris* parasite that exhibits a different behaviour on each salmon host strain. In order to investigate whether or not salmon would recover if *G. salaris* was to be introduced into a susceptible host population the model had to first be extended to include an immune response and resulting trade-off. The trade-off was determined assuming a similar situation in salmon to that observed by Cipriano *et al.* (2002) in their study of furunculosis in trout, in which trout exhibiting a tolerance to infection had lower birth rates than the fully susceptible individuals. Hence, the trade-off was implemented into the model via host birth rate.

Our results demonstrated that only a small amount of immunity is required to allow substantial host growth. Finally, the 2 strain model was extended for  $n$  salmon host strains with levels of immunity ranging from 0, fully susceptible - *e.g.*, Atlantic salmon, to 0.017, resistant - *e.g.*, Baltic salmon, with salmon hosts having the ability to give birth to mutant offspring with an increased or decreased immune response. The results highlighted the fact that, in a system with hosts of varying resistance, salmon with a small amount of immunity, and hence a higher birth rate, can out compete the salmon strain with the highest immunity and coexist with low *G. salaris* infection as well as with other salmon strains exhibiting similar immune/birth rates. The models predict that salmon recovery to at least 60% of carrying capacity is possible within one to three years after infection is introduced if susceptible hosts evolve to be more resistant.

## 7.2 MODEL LIMITATIONS

### *Parasite behaviour*

One of first limitations of the models proposed in the preceding chapters is they do not give number of parasites per host but the rate of change of total salmon and *G. salaris* populations, and hence, they do not explicitly model those *G. salaris* parasites that transfer between hosts, either from infected fish to uninfected fish or infected fish to infected fish. As discussed in Chapter 2, this was not explicitly modelled since we were working at the population level and not the individual level.

It is well established that parasites become more active after they have given birth to their first offspring and tend to move around the host or attempt to transfer to a new host (Bakke *et al.*, 2007). Our models are also limited with respect to parasite behaviour in that there is no spatial aspect present. This is also true with salmon hosts in that their territorial behaviour (Keenlyside & Yamamoto, 1962; Crisp, 2000), as discussed in Chapter 1, is not modelled.

### *Salmon births and run to sea*

Another limitation of the models proposed in this thesis is the assumption that new salmon hosts are born at a constant rate. This approach was taken in order to simplify models somewhat. However, in reality salmon spawning is a discrete process taking place once a year between mid October and late February (Shearer, 1992). Hence, the models developed throughout this work lack such seasonal variation.

Similarly, our models do not consider the fact that salmon run to sea and do not spend their entire life in a river, though it is possible for some salmon parr to mature sexually in a river without the need to run to sea, and hence, stay to participate in spawning (Crisp, 2000). Once smolts reach the sea they spend anything between one and four winters at sea before returning to their natal river to spawn (Crisp, 2000). This behaviour will have an important impact on the length of time it would take for a population of salmon to recover from *G. salaris* infections due to the possibility of immune salmon escaping an infected river leaving more susceptible salmon hosts to take the brunt of infection. This means there will also be a one to four year (or more) delay in possible immune salmon giving birth to offspring with a heightened resistance to disease by which time *G. salaris* infections may have forced the susceptible population to extinction. Another problem is the fact that not all salmon are successful in returning from the sea to their natal river. In these cases salmon from a *G. salaris*

infected river may not make it back, hence, any acquired resistance to infection will not be passed on to subsequent generations.

### *Evolution*

The final model, dealing with multiple salmon strains with the possibility of giving birth to offspring with more/less resistance to *G. salaris* infections, assumes mutations continuously occur, *e.g.*, if  $\phi$  is set to 0.0001 then we will always get 1 mutant in every 1000 offspring. Biologically this is not the case, in reality mutations are more stochastic in nature with the possibility that a mutant is born or not born.

All these limitation will have an impact on the results obtained in this this thesis and hence increase the length of time required for salmon population recover from infection by *G. salaris*.

### 7.3 FUTURE WORK

The population dynamics of *G. salaris* are still not fully understood, however, the work contained within the chapters of this thesis forms a solid basis for future salmon-*G. salaris* modelling. Our results thus far have highlighted the fact that after the introduction of *G. salaris* into a susceptible host population, salmon population recovery in an infected river is in fact possible, resulting in low level host-parasite coexistence.

If more time were available there is much scope for the accuracy of estimates of time to salmon population recovery to be improved. The inclusion of seasonality in host births as mentioned above as well as the inclusion of an extra host class, where salmon run to sea and spend one to four winters there before returning to their river, to the multiple host strain model would greatly improve predictions of salmon recovery and salmon - *G. salaris* coexistence. Seasonality would also be of benefit in regards to the *G. salaris* life cycle since parasites demonstrate seasonal dynamics with respect to water temperature, becoming more active when rivers are colder (Mo, 1987, as cited by Peeler *et al.*, 2006, Soleng *et al.*, 1998, Winger *et al.*, 2008).

The models we have proposed consider the total densities of a *G. salaris* population within a salmon host population, It would also be worthwhile taking an approach looking into the density of *G. salaris* populations on individual hosts within a host population with particular focus on the impact that fish to fish transmission has on the dynamics of infection.

Even though the literature concerning *Gyrodactylus salaris* infections in salmon is vast, models would greatly benefit from more accurate and up to date parameter estimates. Experimental studies undertaken exclusively for this reason would be worthwhile in order to obtain estimates for currently unknown parameters. Through our research we have determined that more data is required in order to accurately parameterise the rate at which parasites leave, attach to and kill hosts.

The results obtained from the individual based stochastic model in Chapter 4 gave a reasonably good fit to the current data available and could be extended from an individual host up to the population level. Adding stochasticity to the multiple strain model would also be a useful way forward in order to gain further insights into the dynamics of *G. salaris* infections. Recent work by van Oosterhout *et al.* (2008) and Ramírez *et al.* (2012), highlighted in Chapter 1, Section 1.5.3, also emphasize and provide confirmation of the usefulness of adding stochasticity to models in regards to *G. salaris* infections.

Moreover the way in which evolution is handled in the multiple strain model could be improved by adding stochasticity or through the use of techniques such as that of adaptive dynamics. Through the use of adaptive dynamics the continuous mutations that are present in the current model (Equations 6.12 to 6.17) would be replaced by the assumption that mutations are rare and discrete events. The (rare) mutant and (established) resident strains would then compete, in a manner similar to that in Equations (6.12) to (6.17), to determine whether the mutant strain will grow in number, replacing the resident, or die out; or in the rarer case, co-exist. By modelling a series of these mutation and replacement events it is possible to determine the evolutionary stable level of immunity and, given appropriate data on mutation rate/size, the time until it occurs.

It would also be practical to re-evaluate the multi-strain model for multiple *G. salaris* strains as well as multiple host strains in order to investigate the co-evolutionary response from parasites (also possible through the use of adaptive dynamics). It is well documented in the literature that differing strains of *G. salaris* have varying effects on a range of salmonid hosts (Bakke *et al.*, 1990; Johnsen & Jensen, 1991; Bakke & MacKenzie, 1993; Hansen *et al.*, 2003; Lindenstrom *et al.*, 2003; Bakke *et al.*, 2002, 2004) and that importation of rainbow trout has been identified as posing the greatest threat of introducing *G. salaris* infection into UK water systems (Peeler *et al.*, 2004; Peeler & Thrush, 2004).

## 7.4 CONCLUSIONS

Atlantic salmon populations the world over are currently threatened with numbers in some regions in decline (WWF, 2001). The catastrophic impact that infections by *G. salaris* can have on susceptible salmon populations, and the consequential financial implications, has already been witnessed in Norway (Johnsen, 1978; Johnsen & Jensen, 1986, 1991). In the years post the parasites accidental introduction to Norway it has since spread to many river systems throughout Europe (Buchmann & Bresciani, 1997; Nielsen & Buchmann, 2001; OIE, 2003; Cunningham *et al.*, 2003; Ziętara *et al.*, 2007; Rokicka *et al.*, 2007; OIE, 2009; Paladini *et al.*, 2009).

In terms of both mathematics and biology *Gyrodactylus salaris* is a very interesting area of study. Through the use of different mathematical techniques we have proposed and developed models capable of capturing the dynamics of salmon-*G. salaris* interactions, and where possible, we have compared model outputs with experimental and observed data from the literature. Hence, we have been able to make predictions regarding the possible consequences of *G. salaris* infection in the long-term. Of the results obtained via our research and recorded in this thesis, the most illuminating were those concerning the impact that timing of parasite first birth has on parasite population growth and the results obtained in Chapters 5 and 6 concerning salmon recovery from *G. salaris* infections.

Firstly, we were able to show that by delaying parasite first birth by as little as 0.5 days the total parasite density becomes significantly decreased (by approximately 50%). Thus if first birth is delayed further, for example by a whole day, parasite numbers decrease further. Through experimental studies we know that *G. salaris* survival is temperature dependent (Soleng *et al.*, 1998) with first birth occurring later at colder water temperatures (Jansen & Bakke, 1991). In regards to water temperature we must also consider the impact of climate change. Based on the study by Jansen & Bakke (1991) we can assume that rising temperatures in rivers will cause parasites to give birth to their first offspring earlier resulting in faster population growth. Hence, it may be possible to manage *G. salaris* infections through lowering water temperature, delaying the first birth of individual parasites and therefore reducing parasite numbers.

Secondly, through simulation of the multiple host strain model (for a varied number of strains) we were able to predict salmon populations will recover from *G. salaris* infection and reach a stable level within 15 to 25 years after introduction. However, such recovery is only possible if hosts evolve to a more resistant state. Importantly, we showed small increases in resistance resulted in large positive changes in salmon density and in a system with many

salmon strains present a low level of resistance and a consequently high birth rate is more beneficial than a high resistance to infection and hence a low birth rate. In all model simulations which result in salmon recovery, *G. salaris* populations never actually decay to zero and disappear from the system but in fact exhibit low-level coexistence with the remaining salmon host strains present in the environment.

The results we have obtained are important as they highlight populations of Atlantic salmon should recover from *G. salaris* infections in the long-term even if unaided by human intervention. This means that the current practice of treating rivers and restocking with salmon from the original genetic pool of that river, as is the method adopted in Norway, may in fact be lengthening the time required for salmon to evolve a mechanism of resistance to infection and thus recover naturally.

As discussed in the main text, to date the United Kingdom and Ireland are the only known countries to officially establish freedom from *G. salaris* infections (Shinn *et al.*, 1995; OIE, 2003; Defra, 2008a). This is confirmed and supported by the European Commission, EC decision 2004/453/EC (Peeler *et al.*, 2004). The current consensus is that Atlantic salmon populations in the UK are believed to be just as susceptible as those found in Norway (Bakke & MacKenzie, 1993; Paladini *et al.*, *subm.*), hence, if *G. salaris* is introduced a similar environmental and economic impact to that of Norway can be expected. Due to this, *G. salaris* and its impact on susceptible hosts must continue to be the subject of further study in order to aid in contingency planning and defence against introduction and emergence.

Part IV

**BIBLIOGRAPHY**

## BIBLIOGRAPHY

---

- Anderson RM, May RM (1978) Regulation and stability of host-parasite population interactions. I: Regulatory processes. *Journal of Animal Ecology*, **47**, 219–247.
- Anderson RM, May RM (1981) The population dynamics of microparasites and their invertebrate hosts. *Philosophical Transactions of the Royal Society of London. Series B, Biological Sciences*, **291**, 451–524.
- Anderson RM, May RM (1991) *Infectious diseases of humans: Dynamics and control*. Oxford University Press, Oxford.
- Bakke TA, Cable J, Harris PD (2007) The biology of gyrodactylid monogeneans: The “Russian-doll killers”. *Advances in Parasitology*, **64**, 161–460.
- Bakke TA, Harris PD, Cable J (2002) Host specificity dynamics: observations on gyrodactylid monogeneans. *International Journal for Parasitology*, **32**, 281–308.
- Bakke TA, Harris PD, Hansen H, Cable J, Hansen LP (2004) Susceptibility of Baltic and East Atlantic salmon *Salmo salar* stocks to *Gyrodactylus salaris* (Monogenea). *Diseases of Aquatic Organisms*, **58**, 171–177.
- Bakke TA, Harris PD, Jansen PA (1992a) The susceptibility of *Salvelinus fontinalis* (Mitchill) to *Gyrodactylus salaris* Malmberg (Platyhelminthes; Monogenea) under experimental conditions. *Journal of Fish Biology*, **41**, 499–507.
- Bakke TA, Harris PD, Jansen PA, Hansen LP (1992b) Host specificity and dispersal strategy in gyrodactylid monogeneans, with particular reference to *Gyrodactylus salaris* (Platyhelminthes, Monogenea). *Diseases of Aquatic Organisms*, **13**, 63–74.
- Bakke TA, Jansen PA, Hansen LP (1990) Differences in the host resistance of Atlantic salmon, *Salmo salar* L., stocks to the monogenean *Gyrodactylus salaris* Malmberg, 1957. *Journal of Fish Biology*, **37**, 577–587.
- Bakke TA, Jansen PA, Hansen LP (1991a) Experimental transmission of *Gyrodactylus salaris* Malmberg, 1957 (Platyhelminthes, Monogenea) from the Atlantic salmon (*Salmo salar*) to the European eel (*Anguilla anguilla*). *Canadian Journal of Zoology*, **69**, 733–737.
- Bakke TA, Jansen PA, Harris PD (1996) Differences in susceptibility of anadromous and resident stocks of Arctic charr to infections of *Gyrodactylus salaris* under experimental conditions. *Journal of Fish Biology*, **49**, 341–351.

- Bakke TA, Jansen PA, Kennedy CR (1991b) The host specificity of *Gyrodactylus salaris* Malmberg (Platyhelminthes, Monogenea): susceptibility of *Oncorhynchus mykiss* (Walbaum) under experimental conditions. *Journal of Fish Biology*, **39**, 45–57.
- Bakke TA, MacKenzie K (1993) Comparative susceptibility of native Scottish and Norwegian stocks of Atlantic salmon, *Salmo salar* L., to *Gyrodactylus salaris* Malmberg: Laboratory experiments. *Fisheries Research*, **17**, 69–85.
- Bakke TA, Soleng A, Harris PD (1999) The susceptibility of Atlantic salmon (*Salmo salar* L.) x brown trout (*Salmo trutta* L.) hybrids to *Gyrodactylus salaris* Malmberg and *Gyrodactylus derjavini* Mikailov. *Parasitology*, **119**, 467–481.
- Boots M, Bowers RG (2004) The evolution of resistance through costly acquired immunity. *Proceedings of the Royal Society London*, **B 271**, 715–723.
- Boots M, Haraguchi Y (1999) The evolution of costly resistance in host-parasite systems. *American Naturalist*, **153**, 359–370.
- Buchmann K, Bresciani J (1997) Parasitic infections in pond-reared rainbow trout *Oncorhynchus mykiss* in Denmark. *Diseases Of Aquatic Organisms*, **28**, 125–138.
- Cable J, Harris PD, A BT (2000) Population growth of *Gyrodactylus salaris* (Monogenea) on Norwegian and Baltic Atlantic salmon (*Salmo salar*) stocks. *Parasitology*, **121**, 621–629.
- Cipriano RC, Marchant D, Jones TE, Schachte JH (2002) Practical application of disease resistance: a brook trout fishery selected for resistance to furunculosis. *Aquaculture*, **206**, 1–17.
- Crisp D (2000) *Trout and Salmon: Ecology, Conservation and Rehabilitation*. Fishing News Books, London.
- Crisp DT (1981) A desk study of the relationship between temperature and hatching time for the eggs of five species of salmonid fishes. *Freshwater Biology*, **11**, 361–368.
- Cunningham CO, Collins CM, Malmberg G, Mo TA (2003) Analysis of ribosomal RNA intergenic spacer (IGS) sequences in species and populations of *Gyrodactylus* (Platyhelminthes: Monogenea) from salmonid fish in northern Europe. *Diseases of Aquatic Organisms*, **57**, 237–246.
- Cusack R, Cone DK (1986) *Gyrodactylus salmonis* (Yin and Sproston, 1948) parasitizing fry of *Salvelinus fontinalis* (Mitchel). *Journal of Wildlife Diseases*, **22**, 209–213.
- Darwin C (1872) *On the Origin of Species by Means of Natural Selection, or the Preservation of Favoured Races in the Struggle for Life*. John Murray, London.
- Defra (2008a) *Contingency Plan for Combating Gyrodactylus salaris in England*. Department for Environment, Food and Rural Affairs. Crown copyright.

- Defra (2008b) Publication of *Gyrodactylus salaris* contingency plan for England - Information Bulletin. <http://www.defra.gov.uk/news/2008/080414.htm>. Date of access 12/02/2010.
- des Clers S (1993) Modelling the impact of disease-induced mortality on the population size of wild salmonids. *Fisheries Research*, **17**, 237–248.
- De Mazancourt C, Dieckmann U (2004) Trade-off geometries and frequency-dependent selection. *American Naturalist*, **164**, 765–778.
- Dietz K, Heesterbeek JAP (2002) Daniel Bernoulli's epidemiological model revisited. *Mathematical Biosciences*, **180**, 1–21.
- Dobson AP, Hudson PJ (1992) Regulation and stability of a free-living host-parasite system: *Trichostrongylus tenuis* in red grouse. II. Population models. *Journal of Animal Ecology*, **61**, 487–498.
- FAO (2004-2013) Fishery and Aquaculture Country profiles. United Kingdom. Fishery and Aquaculture Country Profiles. In: FAO Fisheries and Aquaculture Department [online]. Rome. Updated 5 August 2004. [http://www.fao.org/fishery/countrysector/FI-CP\\_GB/en](http://www.fao.org/fishery/countrysector/FI-CP_GB/en). Date of access 25/02/2013.
- FRS (2004) Fisheries Research Services leaflet. *Gyrodactylus salaris*. Crown copyright. Available at <http://www.marlab.ac.uk>.
- Gani J (2009) Mathematical models of epidemics. *The Mathematical Intelligencer*, **3**, 41–43.
- Hamer WH (1906) Epidemic disease in England - The evidence of variability and of persistency of type. *The Lancet*, **1**, 733–739.
- Hansen H, Bachmann L, Bakke TA (2003) Mitochondrial DNA variation of *Gyrodactylus* spp. (Monogenea, Gyrodactylidae) populations infecting Atlantic salmon, grayling, and rainbow trout in Norway and Sweden. *International journal for Parasitology*, **33**, 1471–1478.
- Harris PD (1986) Species of *Gyrodactylus* von Nordmann, 1832 (Monogenea Gyrodactylidae) from poeciliid fishes, with a description of *G. turnbulli* sp. nov. from the guppy, *Poecilia reticulata* Peters. *Journal of Natural History*, **20**, 183–191.
- Harris PD, Jansen PA, Bakke TA (1994) The population age structure and reproductive biology of *Gyrodactylus salaris* Malmberg (Monogenea). *Parasitology*, **108**, 167–173.
- Harris PD, Shinn AP, Cable J, Bakke TA (2004) Nominal species of the genus *Gyrodactylus* von Nordmann 1832 (Monogenea: Gyrodactylidae), with a list of principal host species. *Systematic Parasitology*, **59**, 1–27.
- Hedger RD, Sundt-Hansen LE, Forseth T, Diserud OH, Ugedal O, Finstad AG (2013) Modelling the complete life-cycle of Atlantic salmon (*Salmo salar* L.) using a spatially explicit individual-based approach. *Ecological Modelling*, **248**, 119–129.

- Hendry K, Cragg-Hine D (2003) *Ecology of the Atlantic Salmon*. Conserving Natura 2000 Rivers Ecology Series No. 7. English Nature, Peterborough.
- Hogasen HR, Brun E (2003) Risk of inter-river transmission of *Gyrodactylus salaris* by migrating Atlantic salmon smolts, estimated by Monte Carlo simulation. *Diseases of Aquatic Organisms*, **57**, 247–254.
- Holm A, Molander P, Lundanes E, Greibrokk T (2003) Determination of rotenone in river water utilizing packed capillary column switching liquid chromatography with UV and time-of-flight mass spectrometric detection. *Journal of Chromatography A*, **983**, 43–50.
- Hoyle A, Bowers RG, White A, Boots M (2008) The influence of trade-off shape on evolutionary behaviour in classical ecological scenarios. *Journal of Theoretical Biology*, **250**, 498–511.
- ICES (2001) *Report of the Baltic Salmon and Trout Assessment Working Group*. ICES CM 2001/ACFM:14, Pärnu, Estonia.
- IPCS-INCHEM (1992) International Programme on Chemical Safety - Rotenone: health and safety guide. Geneva (Health and safety guide; No. 73). ISBN 9241510730. ISSN 0259-7268. <http://www.inchem.org/documents/hsg/hsg/hsg073.htm>. Date of access 26/01/2010.
- Jansen PA, Bakke TA (1991) Temperature-dependant reproduction and survival of *Gyrodactylus salaris* Malmberg, 1957 (Platyhelminthes - Monogenea) on Atlantic salmon (*Salmo salar* L.). *Parasitology*, **102**, 105–112.
- Jansen PA, Bakke TA (1995) Susceptibility of brown trout to *Gyrodactylus salaris* (Monogenea) under experimental conditions. *Journal of Fish Biology*, **46**, 415–422.
- Jansen PA, Matthews L, Toft N (2007) Geographic risk factors for inter-river dispersal of *Gyrodactylus salaris* in fjord systems in Norway. *Diseases of Aquatic Organisms*, **2**, 139–149.
- Johnsen BO (1978) The effect of an attack by the parasite *Gyrodactylus salaris* on the population of salmon parr in the river Lakselva, Misvær in northern Norway. *Astarte*, **11**, 7–9.
- Johnsen BO (2006) NOBANIS - Invasive Alien Species Fact Sheet - *Gyrodactylus salaris*. From: Online Database of the North European and Baltic Network on Invasive Alien Species. NOBANIS <http://www.nobanis.org>. Date of access 27/11/2009.
- Johnsen BO, Jensen AJ (1986) Infestations of Atlantic salmon, *Salmo salar*, by *Gyrodactylus salaris* in Norwegian rivers. *Journal of Fish Biology*, **29**, 233–241.
- Johnsen BO, Jensen AJ (1991) The *Gyrodactylus* story in Norway. *Aquaculture*, **98**, 289–302.
- Johnsen BO, Jensen AJ (1992) Infection of Atlantic salmon, *Salmo salar* L., by *Gyrodactylus salaris*, Malmberg 1957, in the river Lakselva, Misvær in northern Norway. *Journal of Fish Biology*, **40**, 433–444.

- Jones J (1959) *The Salmon*. Collins, London.
- Kalleberg H (1958) Observations in a stream tank of territoriality and competition in juvenile salmon and trout (*Salmo salar* L. and *S. trutta* L.). *Report Institute of Freshwater Research Drottningholm*, **39**, 55–98.
- Kania P, Jørgensen TR, Buchmann K (2007) Differentiation between a pathogenic and a non-pathogenic form of *Gyrodactylus salaris* using PCR-RFLP. *Journal of Fish Diseases*, **30**, 123–126.
- Keenleyside MHA, Yamamoto FT (1962) Territorial behaviour of juvenile Atlantic salmon (*Salmo salar* L.). *Behaviour*, **19**, 139–169.
- Kennedy CEJ, Endler JA, Poynton SL, H M (1987) Parasite load predicts mate choice in guppies. *Behavioral Ecology and Sociobiology*, **21**, 291–295.
- Kermack WO, McKendrick AG (1927) A contribution to the mathematical theory of epidemics. *Proceedings of the Royal Society of London*, **115**, 700–721.
- Lautraite A, Blanc G, Thiery R, Daniel P, M V (1999) Gyrodactylids parasitizing salmonids in Brittany and Western Pyrenees water basins: Epidemiological features of infection and species composition. *Bulletin Français de la Pêche et de la Pisciculture*, **355**, 305–325.
- Leberg PL, Vrijenhoek RC (1994) Variation among desert topminnows in their susceptibility to attack by exotic parasites. *Conservation Biology*, **8**, 419–424.
- Leslie PH (1945) On the use of matrices in certain population mathematics. *Biometrika*, **33**, 183–212.
- Levins R (1962) Theory of fitness in heterogeneous environment. 1. The fitness set and the adaptive function. *American Naturalist*, **96**, 361–373.
- Levins R (1968) *Evolution in changing environments*. Princeton University Press, Princeton.
- Lindenstrom T, Collins CM, Bresciani J, Cunningham CO, Buchmann K (2003) Characterization of a *Gyrodactylus salaris* variant: infection biology, morphology and molecular genetics. *Parasitology*, **127**, 165–177.
- Malmberg G (1957) On the occurrence of *Gyrodactylus* on Swedish fishes. *Skrifter utgivna av Södra Sveriges Fiskeriförening Årsskrift*, **1956**, 19–76. [in Swedish, summary in English].
- Malmberg G, Malmberg M (1993) Species of *Gyrodactylus* (Platyhelminthes, Monogenea) on salmonids in Sweden. *Fisheries Research*, **17**, 59–68.
- Mathematica Research, Inc (2008) Mathematica, Version 7.0, Wolfram Research, Inc., Champaign, Illinois.

- May RM, Anderson RM (1978) Regulation and stability of host-parasite population interactions. II: Destabilizing processes. *Journal of Animal Ecology*, **47**, 249–267.
- Mills D (1999) *The ocean life of Atlantic salmon: Environmental and biological factors influencing survival*. Fishing News Books, Oxford.
- Mo TA (1987) *Taksonomiske og biologiske undersøkelser, virksomheten i 1986 og forslag til virksomhet i 1987*. University of Oslo, Oslo.
- Mo TA, Norheim K, Jansen PA (2008) The surveillance and control programme for *Gyrodactylus salaris* in Atlantic salmon and rainbow trout in Norway. In: Brun, E., Jordsmyr, H.M., Hellberg, H., Mørk, T. (editors). *Surveillance and control programmes for terrestrial and aquatic animals in Norway. Annual report 2007*. Oslo: National Veterinary Institute, pp. 143–148.
- Murray JD (2002) *Mathematical Biology: I. An Introduction (3rd Ed)*. Interdisciplinary Applied Mathematics. Springer, 551 pp.
- Murray JD (2003) *Mathematical Biology II: Spatial Models and Biomedical Applications (3rd Ed)*. Interdisciplinary Applied Mathematics. Springer, 811 pp.
- Nielsen CV, Buchmann K (2001) Occurrence of *Gyrodactylus* parasites in Danish fish farms. *Bulletin European Association of Fish Pathology*, **21**, 19–25.
- OIE (2003) *Office International des Epizooties. International manual of diagnostic tests for aquatic animals, 4th edn*. Paris.
- OIE (2009) *Office International des Epizooties. Manual of Diagnostic Tests for Aquatic Animals 2009. Chapter 2.3.3: Gyrodactylosis (Gyrodactylus salaris). Dr T.A Mo (contributor)*. Paris. Available at <http://www.oie.int>.
- Olstad K, Cable J, Robertsen G, Bakke TA (2006) Unpredicted transmission strategy of *Gyrodactylus salaris* (Monogenea : Gyrodactylidae): survival and infectivity of parasites on dead hosts. *Parasitology*, **133**, 33–41.
- Oxford Dictionaries (2007) *New Shorter Oxford English Dictionary, Sixth Edition*. Oxford University Press, Oxford.
- Paisley LG, Karlsen E, Jarp J, Mo TA (1999) A Monte Carlo simulation model for assessing the risk of introduction of *Gyrodactylus salaris* to the Tana river, Norway. *Diseases of Aquatic Organisms*, **37**, 145–152.
- Paladini G, Bron JE, Taylor NGH, Shinn AP (subm.) Geographical distribution of *Gyrodactylus salaris* Malmberg, 1957 (Monogenea, Gyrodactylidae) throughout Europe. *Veterinary Research*.

- Paladini G, Gustinelli A, Fioravanti ML, Hansen H, Shinn AP (2009) The first report of *Gyrodactylus salaris* Malmberg, 1957 (Platyhelminthes, Monogenea) on Italian cultured stocks of rainbow trout (*Oncorhynchus mykiss* Walbaum). *Veterinary Parasitology*, **165**, 290–297.
- Paladini G, Williams CF, Hansen H, Taylor NGH, Rubio OL, Denholm SJ, Hytterød S, Bron JE, Shinn AP (in prep.) The experimental susceptibility of English and Welsh salmonids to *Gyrodactylus salaris* (Platyhelminthes, Monogenea).
- Peeler EJ, Gardiner R, Thrush MA (2004) Qualitative risk assessment of routes of transmission of the exotic fish parasite *Gyrodactylus salaris* between river catchments in England and Wales. *Preventative Veterinary Medicine*, **64**, 175–189.
- Peeler EJ, Thrush M, Paisley L, Rodgers C (2006) An assessment of the risk of spreading the fish parasite *Gyrodactylus salaris* to uninfected territories in the European Union with the movement of live Atlantic salmon (*Salmo salar*) from coastal waters. *Aquaculture*, **258**, 187–197.
- Peeler EJ, Thrush MA (2004) Qualitative analysis of the risk of introducing *Gyrodactylus salaris* into the United Kingdom. *Diseases of Aquatic Organisms*, **62**, 103–113.
- Ramírez R, Harris PD, Bakke TA (2012) An agent-based modelling approach to estimate error in gyrodactylid population growth. *International Journal for Parasitology*, **42**, 809–817.
- Richards GR, Chubb JC (1996) Host response to initial and challenge infections, following treatment, of *Gyrodactylus bullatarudis* and *G. turnbulli* (Monogenea) on the guppy (*Poecilia reticulata*). *Parasitology Research*, **82**, 242–247.
- Rokicka M, Lumme J, Ziętara MS (2007) Identification of *Gyrodactylus* ectoparasites in Polish salmonid farms by PCR-RFLP of the nuclear ITS segment of ribosomal DNA (Monogenea, Gyrodactylidae). *Acta Parasitologica*, **52**, 185–195.
- Rueffler C, Van Dooren TJM, Metz JAJ (2004) Adaptive walks on changing landscapes: Levin's approach. *Theoretical Population Biology*, **65**, 165–178.
- Salte R, Bentsen HB, Moen T, Tripathy S, Bakke TA, Ødegård J, Omholt S, Hansen LP (2010) Prospects for a genetic management strategy to control *Gyrodactylus salaris* infection in wild Atlantic salmon (*Salmo salar*) stocks. *Canadian Journal of Fisheries and Aquatic Sciences*, **67**, 121–129.
- Scott JP, Fredericson E (1951) The causes of fighting in mice and rats. *Physiological Zoology*, **24**, 273–309.
- Scott ME (1985) Experimental epidemiology of *Gyrodactylus bullatarudis* (Monogenea) on guppies (*Poecilia reticulata*): short and long-term studies. *Ecology and Genetics of Host-Parasite Interactions*, pp. 21–38.

- Scott ME, Anderson RM (1984) The population dynamics of *Gyrodactylus bullatarudis* (Monogenea) within laboratory populations of the fish host *Poecilia reticulata*. *Parasitology*, **89**, 159.
- Shearer W (1992) *The Atlantic salmon : natural history, exploitation and future management*. Fishing News Books, Oxford.
- Shinn AP, Sommerville C, Gibson DI (1995) Distribution and characterization of species of *Gyrodactylus* Nordmann, 1832 (Monogenea) parasitizing salmonids in the UK, and their discrimination from *Gyrodactylus salaris* Malmberg, 1957. *Journal of Natural History*, **29**, 1383–1402.
- Soleng A, Bakke TA (2001) The susceptibility of grayling (*Thymallus thymallus*) to experimental infections with the monogenean *Gyrodactylus salaris*. *International Journal for Parasitology*, **31**, 793–797.
- Soleng A, Bakke TA, Hansen LP (1998) Potential for dispersal of *Gyrodactylus salaris* (Platyhelminthes, Monogenea) by sea-running stages of the Atlantic salmon (*Salmo salar*): field and laboratory studies. *Canadian Journal of Fisheries and Aquatic Sciences*, **55**, 507–514.
- Soleng A, Jansen PA, Bakke TA (1999a) Transmission of the monogenean *Gyrodactylus salaris*. *Folia Parasitologica*, **46**, 179–184.
- Soleng A, Poleo ABS, Alstad NEW, Bakke TA (1999b) Aqueous aluminium eliminates *Gyrodactylus salaris* (Platyhelminthes, Monogenea) infections in Atlantic salmon. *Parasitology*, **119**, 19–25.
- Sviland C, Hansen H, Mo TA, Moen A, Jensen BB (2012) The surveillance and control programme for *Gyrodactylus salaris* in Atlantic salmon and rainbow trout in Norway 2011. In: Brun, E., Jordsmyr, H.M., Hellberg, H., Mørk, T. (editors). *Surveillance and control programmes for terrestrial and aquatic animals in Norway. Annual report 2011*. Oslo: National Veterinary Institute, pp. 143–148.
- van Oosterhout C, Harris PD, J C (2003) Marked variation in parasite resistance between two wild populations of the Trinidadian guppy, *Poecilia reticulata* (Pisces: Poeciliidae). *Biological Journal of the Linnean Society*, **79**, 645–651.
- van Oosterhout C, Potter R, Wright H, Cable J (2008) Gyro-scope: An individual-based computer model to forecast gyrodactylid infections on fish hosts. *International Journal For Parasitology*, **38**, 541–548.
- Verspoor E, Stradmeyer L, Nielsen J (2007) *The Atlantic salmon : genetics, conservation, and management*. Blackwell Publishing, Oxford.

- Watts EJ, Palmer SCF, Bowman AS, Irvine RJ, Smith A, J TJM (2009) The effect of host movement on viral transmission dynamics in a vector-borne disease system. *Parasitology*, **136**, 1221–1234.
- Winger AC, Kanck M, Kristoffersen R, Knudsen R (2008) Seasonal dynamics and persistence of *Gyrodactylus salaris* in two riverine anadromous Arctic charr populations. *Environmental Biology of Fishes*, **83**, 117–123.
- WWF (2001) *The status of wild Atlantic salmon: a river by river assessment*. 174 pp. Available at <http://www.assets.panda.org/downloads/salmon2.pdf>. Date of access 25/02/2013,.
- Ziętara MS, Rokicka M, Stojanovski S, Skorkowski EF, Lumme J (2007) Alien mitochondrial DNA in variant clones of *Gyrodactylus salaris* indicates a complex hybrid history in salmonid farms. *Parassitologia*, **49**, 119.

Part V

APPENDICES

## Data

Contained within this appendix is a collection of data sources taken from the literature. These data have been used for estimation of model parameters and comparison of model output throughout the work in the main chapters of this thesis.

Table A.1 gives the parameter estimations used in model simulations throughout the entirety of this thesis.

Table A.1: Parameter estimations. Estimations for the population parameters used in the models using data available in the literature. Unpublished experimental trials were also used to estimate some unknown parameters. The data from these trials is collected in Appendix A.

Parameter	Description	Estimate/day	Source
$\alpha$	Salmon birth rate	0.02	See Chapter 1, Section 2.4
$b$	Salmon death rate due to natural causes	0.0006	Hedger <i>et al.</i> (2013)
$s$	Density dependent constraint	$1.55 \times 10^{-4}$	Estimated using salmon carrying capacity for $1000\text{m}^2$
$K$	Salmon carrying capacity	0.125 fish per $\text{m}^2$	Hedger <i>et al.</i> (2013)
$\mu$	<i>G. salaris</i> birth rate (Noway)	0.1825	Bakke <i>et al.</i> (1990)
	<i>G. salaris</i> birth rate (UK)	0.1708	Paladini <i>et al.</i> (in prep.)
$\epsilon$	<i>G. salaris</i> death rate (natural)	0.08	Jansen & Bakke (1991)
$\alpha$	Salmon death rate due to infection (depends on parasite)	0.0012	Scott & Anderson (1984)
$\lambda$	Rate that <i>G. salaris</i> parasites leave hosts	0.06	See Chapter 3, Section 3.5
$\sigma$	Detached <i>G. salaris</i> death rate (natural)	0.14 - 0.17	Peeler <i>et al.</i> (2006)
$\beta$	Transmission rate of detached <i>G. salaris</i> parasites to new hosts	0.006	Paladini and Denholm (unpublished)
$\tilde{m}$	immune response rate of increase	0.0175	Estimated using Atlantic and Baltic growth rates
$\zeta$	Decay rate of immune response	0.005	N. Taylor (per. comm.)
$\theta$	Trade-off shape parameter	-0.7	See Chapter 5
$\phi$	Mutation rate	0.0001	See Chapter 6

Cable et al. (2000)

The data in Table A.2 is a reproduction of the results found in Cable *et al.* (2000) for one strain of *G. salaris* infecting two susceptible salmon stocks (from the Rivers Alta and Lier, Norway) and one resistant salmon stock (from the River Neva, Russia). These results were used in Chapter 4 in order to parameterise the Leslie matrix and individual based models.

Table A.2: Results from Cable *et al.* (2000) for one strain of *G. salaris* infecting two susceptible salmon stocks (from the Rivers Alta and Lier, Norway) and one resistant salmon stock (from the River Neva, Russia). Experiment was run at a water temperature of 12.5°C with an individual parasite infecting each of the three salmon strains. Parasite offspring were killed and number of births that occurred were recorded, as was the life-span of the original parasite.

Salmon stock	1st birth	2nd birth	3rd birth	4th birth
Lier	1.88 ( $\pm 0.52$ )	8.35 ( $\pm 1.06$ )	16.0 ( $\pm 1.00$ )	23.0
Alta	1.85 ( $\pm 0.49$ )	9.05 ( $\pm 0.99$ )	16.4 ( $\pm 0.99$ )	22.5 ( $\pm 0.5$ )
Neva	2.34 ( $\pm 0.89$ )	10.0 ( $\pm 1.90$ )	-	-

Bakke et al. (1990)

The data from Figure 5 by Bakke *et al.* (1990) showing *G. salaris* growth on individual Atlantic and Baltic salmon parr is reproduced here in Table A.3. These results by Bakke *et al.* (1990) were used to estimate *G. salaris* growth rates on Atlantic (Norwegian) and Baltic strains of Atlantic salmon (see Chapter 2, Section 2.4) for use in the deterministic models. This data was also used to compare parasite densities from model outputs.

Table A.3: Data from the results given by Bakke *et al.* (1990) Figure 5. Development of the intensity of *G. salaris* infection on individual Atlantic salmon parr of both the Norwegian Lone and the Baltic Neva stocks. Salmon hosts kept individually in small aquaria at 12.0°C starting with 1 parasite on day 0.

Atlantic							Baltic						
Host	0h	7d	14d	21d	28d	35d	Host	0h	7d	14d	21d	28d	35d
1	1	4	10	21	34	43	1	1	1	2	6	2	1
2	1	4	12	23	32	-	2	1	3	11	13	7	3
3	1	4	16	35	69	-	3	1	1	2	1	0	0
4	1	6	13	25	51	-	4	1	3	11	5	4	0
5	1	4	12	24	48	-	5	1	1	2	0	0	0
6	1	5	13	24	43	-	6	1	2	1	0	0	0
7	1	4	10	27	33	-	7	1	2	0	0	0	0
8	1	4	15	25	51	-	8	1	1	1	0	0	0
9	1	5	9	23	32	-							

The data found in Table A.4 is reproduced from Jansen & Bakke (1991) for isolated *G. salaris* infecting isolated Atlantic salmon hosts at different water temperatures. The results for a water temperature of 13.0°C were used to estimate natural parasite death rate (discussed in Chapter 2, Section 2.4) for use in the deterministic models.

Table A.4: Results from Jansen & Bakke (1991) (Experiment 1, Table 1). Isolated *G. salaris* infecting isolated Atlantic salmon hosts at different water temperatures. Parasite offspring were killed and number of births that occurred were recorded, as was the life-span of the original parasite.  $R_0$ , net reproductive rate (/parasite); G, generation time in days;  $r_m$ , innate capacity for increase (/parasite/day); s.e., standard error; s.d., standard deviation.

	Temperature (°C)				
	19.1	16.5	13.0	6.6	2.6
Average lifespan	4.5	5.8	12.5	31.4	33.7
± s.e.	0.7	0.6	0.8	4.6	3.6
Mean number of offspring	1.5	1.67	2.38	2.4	1.4
± s.e.	0.16	0.14	0.12	0.29	0.21
age at 1st birth	1.1	1.3	2.0	5.1	9.3
± s.d.	0.3	0.4	0.5	0.5	0.9
age at 2nd birth	4	5.4	7.5	19.4	36.6
± s.d.	0	0.5	0.8	0.9	2.6
age at 3rd birth	-	-	13.6	35.2	-
± s.d.	-	-	1.4	1.2	-
age at 4th birth	-	-	21.5	49	-
± s.d.	-	-	0.5	-	-
$R_0$	1.50	1.67	2.38	2.40	1.40
G	2.1	2.9	6.5	18.0	19.0
$r_m$	0.22	0.21	0.17	0.06	0.02

Paladini et al. (in prep.)

The data collected by Paladini *et al.* (in prep.) is reproduced in Tables A.5 and A.6 for *G. salaris* infections on Norwegian and UK Atlantic salmon parr hosts respectively. These data were used to estimate *G. salaris* growth rate on UK Atlantic salmon for use in the River Dee simulations in Chapters 2, 3 and 6. The data in Paladini *et al.* (in prep.) was also used to compare model outputs and check the consistency of growth rates calculated using the data in Bakke *et al.* (1990).

Table A.5: Results from Paladini *et al.* (in prep.) for *G. salaris* population growth on Norwegian Atlantic salmon. Trials were run for a period of 40 days on 10 salmon parr originating in Norway. *Gyrodactylus salaris* parasites were added at time t=0. Trials were conducted using freshwater with a temperature of 13.0°C.

Fish no.	0h	24h	5d	12d	19d	26d	33d	40d
A-1	0	76	158	316	679	1206	1114	2055
A-2	0	102	291	544	657	960	2165	2300
A-3	0	104	199	430	477	781	1180	1850
A-4	0	80	172	344	563	860	1275	1950
A-5	0	82	190	338	661	1217	1414	2152
A-6	0	46	114					
A-7	0	59	165					
A-8	0	81	168	288	501	1284	1575	2045
A-9	0	58	126	184	385	714	1495	1570
A-10	0	108	251					
average	0	79.6	183.4	349.1	560.4	1003.1	1459.7	1988.9

Table A.6: Results from Paladini *et al.* (in prep.) for *G. salaris* population growth on UK Atlantic salmon. Trials were run for a period of 40 days on 30 salmon parr originating in the UK. The salmon were separated into three buckets each containing groups of 10 parr. *Gyrodactylus salaris* parasites were added at time t=0. Trials were conducted using freshwater with a temperature of 13.0°C.

Fish no.	oh	24h	5d	12d	19d	26d	33d	40d
A-1	0	115	207	310	719	1007	1484	3670
A-2	0	77	131	405	498	945	1223	4020
A-3	0	36	81	175	200	700	1368	3500
A-4	0	47	76	151	405	511	1770	5110
A-5	0	113	168	364	699	1278	2510	4840
A-6	0	47	104	239	608	664	1198	3555
A-7	0	131	175	308	469	1017	1112	4680
A-8	0	51	110	231	680	1287	2102	4960
A-9	0	78	102	193	528	1134	2890	5805
A-10	0	56	83	238	350	799	1770	3790
B-1	0	28	88	208	321	544	810	2210
B-2	0	85	207	338	629	752	1395	3420
B-3	0	120	193	412	566	901	1855	4880
B-4	0	61	150	317	573	1650	2600	4850
B-5	0	109	200	374	677	965	1680	4480
B-6	0	66	151	464	588	905	1590	2460
B-7	0	63	97	265	542	1031	1810	3420
B-8	0	91	162	387	628	880	1570	4210
B-9	0	47	122	463	923	1812	2520	5300
B-10	0	78	133	329	604	889	1240	3145
C-1	0	32	88	200	388	857	965	3326
C-2	0	146	246	584	705	1212	2370	3500
C-3	0	128	230	468	662	1108	1805	3240
C-4	0	81	176	317	586	1119	1566	3090
C-5	0	147	221	615	877	1051	1390	4080
C-6	0	35	115	300	539	1029	1435	2780
C-7	0	51	132	336	785	1326	2092	2650
C-8	0	160	274	485	618	1387	2030	3960
C-9	0	215	314	388	434	1413	2190	3200
C-10	0	116	185	444	648	1132	1906	3390
average	0.0	87.0	157.4	343.6	581.6	1043.5	1741.5	3850.7

Scott & Anderson's 1984 study of *G. turnbulli* infecting *Poecilia reticulata* was used to fill in gaps in such cases that parameter estimates could not be obtained. The table of parameter estimations used in the models proposed by Scott & Anderson (1984) is reproduced in Table A.7.

Table A.7: Estimates of host and parasite population parameters for populations of *Gyrodactylus turnbulli* infecting laboratory populations of *Poecilia reticulata* from Scott & Anderson (1984).

	Parameter	Symbol	Value/day	units
Host	Immigration rate	I	0.14 (low) 0.64 (medium) 1.43 (high)	/population/time unit
	Natural mortality rate	b	0.0045	/host/time unit
	Infection-induced mortality rate (prevalence framework)	$\hat{\alpha}$	0.0701	/host/time unit
	Parasite-induced mortality rate (density framework)	$\alpha$	0.0012	/parasite/host/time unit
	Recovery rate from infection (prevalence framework)	$\gamma$	0.0873	/host/time unit
	Infection rate (prevalence framework)	$\Lambda$	0.0272	/host/5 l water/time unit
Parasite	Birth rate (density framework)	$\lambda$	0.43-0.49	/parasite/time unit
	Death rate on live fish (density framework)	$\mu$	0.24	/parasite/time unit
	Proportion of parasites successful in transfer between live hosts	q	0.24	-
	Negative binomial parameter	k	0.42	/parasite/time unit
	Transmission rate from live fish to live fish (density framework)	$\beta_2$	0.0052	/parasite/host/5 l water/time unit
	Death rate on dead fish (density framework)	w	2.07	/parasite/time unit
	Transmission rate from dead fish to live fish (density framework)	$\beta_1$	0.052	/parasite/host/5 l water/time unit
	Logarithmic parameter	a	0.06-0.95	-

*Field work - Paladini and Denholm (unpublished)*

In order to obtain parameter estimations for some of the unknown parasite parameters, in particular  $\beta$  and  $\lambda$ , four experimental trials were conducted using *G. salaris*, originating from Norway, and UK Atlantic salmon parr originating from the River Dee, Wales. Four experimental trials were run: two trials using dead salmon hosts, Tables A.8 and A.9, and

two using live salmon hosts, Tables A.10 and A.11. All experimental trials were conducted using freshwater with a temperature of 13.0°C.

Table A.8: Behaviour of *G. salaris* on a dead salmon host. An infected salmon parr was killed and placed in a bucket of clean water in order to determine the rate at which *G. salaris* parasites leave a dead salmon host. At one hour intervals the dead host was removed from the bucket and the number of *G. salaris* parasites remaining in the bucket were counted. The salmon host was immediately placed into clean water in a new bucket. This was repeated and the experiment was run for eight hours.

Dead Hap A1	
Time	Number of <i>G. salaris</i> off fish host (in Bucket)
10.45	-
11.45	121
12.45	238
13.45	312
14.45	350
15.45	328
16.45	248
Total <i>G. salaris</i> on fish host at end of trial	>4720
Dorsal fin	540
Adipose fin	60
Caudal fin	200
Anal fin	320
Pelvic fins	280
Pectoral fins	320
Body	>3000

Table A.9: Behaviour of *G. salaris* on a dead salmon host. An infected salmon parr was killed and placed in a bucket of clean water in order to determine the rate at which *G. salaris* parasites leave a dead salmon host. At one hour intervals the dead host was removed from the bucket and the number of *G. salaris* parasites remaining in the bucket were counted. The salmon host was immediately placed into clean water in a new bucket. This was repeated and the experiment was run for eight hours.

Dead Hap A1	
Time	Number of <i>G. salaris</i> off fish host (in Bucket)
10.45	-
11.45	101
12.45	218
13.45	303
14.45	286
15.45	253
16.45	250
Total <i>G. salaris</i> on fish host at end of trial	>3700
Dorsal fin	540
Adipose fin	60
Caudal fin	200
Anal fin	320
Pelvic fins	280
Pectoral fins	320
Body	>2000

Table A.10: Behaviour of *G. salaris* on a live salmon host. An infected Atlantic salmon parr was placed in a bucket of clean water in order to determine the rate at which *G. salaris* parasites leave a live salmon host. The experiment was run for eight hours after which the fish was removed from the bucket and the number of *G. salaris* parasites infecting the it were counted. The *G. salaris* parasites remaining in the bucket were also counted.

Alive 1 (after 8 hours)	
Number of <i>G. salaris</i> on fish host	2360
Number of <i>G. salaris</i> off fish host (in bucket)	112
Breakdown of total <i>G. salaris</i> on fish host at end of trial	
Dorsal fin	400
Adipose fin	40
Caudal fin	760
Anal fin	200
Pelvic fins	240
Pectoral fins	620
Body	>100

Table A.11: Behaviour of *G. salaris* on live salmon hosts. An infected Atlantic salmon parr and an uninfected salmon parr were placed in a bucket of clean water in order to determine the rate at which *G. salaris* parasites leave a live salmon host and infect a new host. The experiment was run for eight hours after which both fish were removed from the bucket and the number of *G. salaris* parasites infecting each host counted. The *G. salaris* parasites remaining in the bucket were also counted.

Alive 2 (after 8 hours)		
Number of <i>G. salaris</i> on initially infected fish host	4040	
Number of <i>G. salaris</i> on initially uninfected fish host	57	
Number of <i>G. salaris</i> off fish hosts (in bucket)	191	
Breakdown of total <i>G. salaris</i> at end of trial on:	initially infected fish	initially uninfected fish
Dorsal fin	700	3
Adipose fin	120	2
Caudal fin	1140	18
Anal fin	260	6
Pelvic fins	620	8
Pectoral fins	1000	18
Body	>200	2

## The models

Where possible, models were analysed using the standard algebraic methods (Anderson & May, 1978; May & Anderson, 1978; Anderson & May, 1981; Murray, 2002, 2003). These analyses can be found in Appendix C. In cases where solutions could not be found analytically, numerical solutions were obtained using appropriate mathematical computer software. Wolfram Mathematica version 8 (2008) was the package used for simulating the various models contained in this work. Solutions in Mathematica were obtained via the 'NDSolve' function. The 'NDSolve' function is used to find numerical solutions to ordinary differential equations.

### CHAPTER 2: THE INITIAL MODELS

#### *The basic model*

Following the framework set out in Anderson & May (1978) and May & Anderson (1978) the basic model is constructed using the following assumptions:

#### *Salmon growth*

The growth of the salmon populations is determined by the reproductive rate,  $a$ , minus the natural mortality rate,  $b$ . Both rates are assumed to be constants and density dependence is omitted at this stage.

#### *Gyrodactylus salaris induced salmon mortalities*

If the rate of *G. salaris* induced salmon deaths is assumed to be linearly proportional to the number of *G. salaris* parasites a salmon host harbours, with  $\alpha$  a constant representing the pathogenicity of parasites to hosts, then the number of salmon mortalities in a small interval of time,  $\delta t$ , among salmon hosts with  $i$  parasites can be given as  $\alpha i \delta t$ . Thus, for a population of salmon of size  $H(t)$ , the total rate of loss of salmon hosts due to infection is:

$$\alpha H(t) \sum_{i=0}^{\infty} ip(i)$$

where  $p(i)$  = the probability that a given host has  $i$  parasites. Now,

$$\begin{aligned} \sum_{i=0}^{\infty} ip(i) &\equiv E_t(i) = \frac{P(t)}{H(t)} = \text{mean parasite load} \\ \Rightarrow \alpha H(t) \sum_{i=0}^{\infty} ip(i) &= \alpha H(t) \frac{P(t)}{H(t)} \\ &= \alpha P(t) \end{aligned}$$

#### *Gyrodactylus salaris* births

The reproductive rate of parasites is defined as  $\mu$ . This gives the net rate for the total *G. salaris* population as:

$$\begin{aligned} \mu H(t) \sum_{i=0}^{\infty} ip(i) &= \mu H(t) \frac{P(t)}{H(t)} \\ &= \mu P(t) \end{aligned}$$

#### *Gyrodactylus salaris* mortality

As mentioned in the text (Chapter 2) parasites can die due to natural host deaths, parasite induced host deaths and natural parasite deaths.

Via natural host deaths: Net rate of *G. salaris* mortality due to natural salmon mortality is defined as:

$$\begin{aligned} bH(t) \sum_{i=0}^{\infty} ip(i) &= bH(t) \frac{P(t)}{H(t)} \\ &= bP(t) \end{aligned}$$

Via parasite induced host deaths: Net rate of *G. salaris* mortality due to *G. salaris* induced salmon mortality is defined as:

$$\begin{aligned} \alpha H(t) \sum_{i=0}^{\infty} i^2 p(i) &= \alpha H(t) E_t(i^2) \\ &= \alpha \frac{(P(t))^2}{H(t)} + \alpha P(t) \end{aligned}$$

(Note: this is determined using the Poisson distribution and is discussed in Chapter 2)

Via natural parasite deaths: Net rate of *G. salaris* mortality due to natural causes is defined as:

$$\epsilon P(t)$$

Hence, using the information above the basic model is defined as:

$$\begin{aligned}\frac{dH}{dt} &= (a - b)H - \alpha P \\ \frac{dP}{dt} &= P \left( \mu - \epsilon - b - \alpha - \alpha \frac{P}{H} \right)\end{aligned}$$

*The density dependent hosts model*

$$\begin{aligned}\frac{dH}{dt} &= (a - b - sH)H - \alpha P \\ \frac{dP}{dt} &= P \left( \mu - (\epsilon + b + \alpha + sH) - \alpha \frac{P}{H} \right)\end{aligned}$$

### CHAPTER 3: THE DETACHED PARASITES MODELS

*The detached parasites baseline model*

$$\begin{aligned}\frac{dH}{dt} &= (a - b - sH)H - \alpha P \\ \frac{dP}{dt} &= P \left( \mu - (\epsilon + b + \alpha + sH + \lambda) - \alpha \frac{P}{H} \right) + \beta WH \\ \frac{dW}{dt} &= \lambda P - \sigma W - \beta WH\end{aligned}$$

*The detached parasites baseline model with mean parasites per host*

$$\begin{aligned}\frac{dH}{dt} &= (a - b - sH)H - \alpha MH \\ \frac{dM}{dt} &= M(\mu - \Gamma) + \beta W \\ \frac{dW}{dt} &= \lambda MH - \sigma W - \beta WH\end{aligned}$$

*The detached parasites baseline model with a negative binomial parasite distribution*

$$\begin{aligned}\frac{dH}{dt} &= (a - b - sH)H - \alpha P \\ \frac{dP}{dt} &= P \left( \mu - (\epsilon + b + \alpha + sH + \lambda) - \alpha \frac{P}{H} \frac{(k+1)}{k} \right) + \beta WH \\ \frac{dW}{dt} &= \lambda P - \sigma W - \beta WH\end{aligned}$$

*The detached parasites model*

$$\begin{aligned}\frac{dH}{dt} &= (a - b - sH)H - \alpha P \\ \frac{dP}{dt} &= P \left( \mu - (\epsilon + b + \alpha + sH + \lambda) - \alpha \frac{P}{H} \right) + \beta WH \\ \frac{dW}{dt} &= \left( b + sH + \lambda + \alpha + \frac{\alpha P}{H} \right) P - \sigma W - \beta WH\end{aligned}$$

#### CHAPTER 4: THE LESLIE AND IBM MODELS

*The Leslie model*

The general form of the Leslie model is given by

$$A = \begin{pmatrix} F_1 & F_2 & F_3 & \dots & F_{26} \\ P_1 & 0 & 0 & \dots & 0 \\ 0 & P_2 & 0 & \dots & 0 \\ \vdots & \vdots & \ddots & \vdots & \vdots \\ 0 & 0 & \dots & P_{25} & 0 \end{pmatrix}$$

The Model is parameterised for the three stocks of salmon using the values given in Chapter 4, Table 4.1.

*The immunity model*

$$\begin{aligned}\frac{dH}{dt} &= (\alpha - b - sH)H - \alpha P \\ \frac{dP}{dt} &= P \left( \mu - (\epsilon + I + b + \alpha + sH + \lambda) - \alpha \frac{P}{H} \right) + \beta WH \\ \frac{dW}{dt} &= \left( b + sH + \lambda + \alpha + \frac{\alpha P}{H} \right) P - \sigma W - \beta WH \\ \frac{dI}{dt} &= \tilde{m} \frac{P}{H} - \zeta I\end{aligned}$$

*The immunity model with trade-off on host birth*

$$\begin{aligned}\frac{dH}{dt} &= (\hat{\alpha}(\tilde{m}) - b - sH)H - \alpha P \\ \frac{dP}{dt} &= P \left( \mu - (\epsilon + I + b + \alpha + sH + \lambda) - \alpha \frac{P}{H} \right) + \beta WH \\ \frac{dW}{dt} &= \left( b + sH + \lambda + \alpha + \frac{\alpha P}{H} \right) P - \sigma W - \beta WH \\ \frac{dI}{dt} &= \tilde{m} \frac{P}{H} - \zeta I\end{aligned}$$

where

$$\hat{\alpha}(\tilde{m}) = \alpha_1 - \left( \frac{(\alpha_1 - \alpha_2) \left( 1 - \frac{\tilde{m} - \tilde{m}_2}{\tilde{m}_1 - \tilde{m}_2} \right)}{1 + \frac{\theta(\tilde{m} - \tilde{m}_2)}{\tilde{m}_1 - \tilde{m}_2}} \right)$$

*Multiple salmon strain model*

$$\begin{aligned}\frac{dH_n}{dt} &= \left( \hat{\alpha}(\tilde{m}_n) - b - s \sum_{j=1}^n H_j \right) H_n - \alpha P_n \\ \frac{dP_n}{dt} &= P_n \left( \mu_n - \left( \epsilon_n + I_n + b + \alpha + s \sum_{j=1}^n (H_j) + \lambda \right) - \alpha \frac{P_n}{H_n} \right) + \beta WH_n \\ \frac{dW}{dt} &= \sum_{i=1}^n \left( P_i \left( b + s \sum_{j=1}^n (H_j) + \lambda + \alpha + \frac{\alpha P_i}{H_i} \right) - \beta WH_i \right) - \sigma W \\ \frac{dI_n}{dt} &= \tilde{m}_n \frac{P_n}{H_n} - \zeta I\end{aligned}$$

$$\begin{aligned} \frac{dH_1}{dt} &= (1 - \phi)\hat{a}(\tilde{m}_1)H_1 + \phi\hat{a}(\tilde{m}_2)H_2 - \left( b + s \sum_{j=1}^n H_j \right) H_1 - \alpha P_n \\ \frac{dH_i}{dt} &= \phi\hat{a}(\tilde{m}_{i-1})H_{i-1} + (1 - 2\phi)\hat{a}(\tilde{m}_i)H_i + \phi\hat{a}(\tilde{m}_{i+1})H_{i+1} - \left( b + s \sum_{j=1}^n H_j \right) H_i - \alpha P_n \\ &\hspace{25em} \text{for } 2 \leq i < n \\ \frac{dH_n}{dt} &= \phi\hat{a}(\tilde{m}_{n-1})H_{n-1} + (1 - \phi)\hat{a}(\tilde{m}_n)H_n - \left( b + s \sum_{j=1}^n H_j \right) H_n - \alpha P_n \\ \frac{dP_l}{dt} &= P_l \left( \mu_l - \left( \epsilon_l + I_l + b + \alpha + s \sum_{j=1}^n (H_j) + \lambda \right) - \alpha \frac{P_l}{H_l} \right) + \beta W H_l \\ \frac{dW}{dt} &= \sum_{q=1}^n \left( P_q \left( b + s \sum_{j=1}^n (H_j) + \lambda + \alpha + \frac{\alpha P_q}{H_q} \right) - \beta W H_q \right) - \sigma W \\ \frac{dI_l}{dt} &= \tilde{m}_l \frac{P_l}{H_l} - \zeta I \end{aligned}$$

where

$$\hat{a}(\tilde{m}_l) = a_1 - \left( \frac{(a_1 - a_2) \left( 1 - \frac{\tilde{m}_1 - \tilde{m}_2}{\tilde{m}_1 - \tilde{m}_2} \right)}{1 + \frac{\theta(\tilde{m}_1 - \tilde{m}_2)}{\tilde{m}_1 - \tilde{m}_2}} \right)$$

## Algebraic analysis

This Appendix contains the algebraic stability analysis for the models in Chapter 3. As mentioned in the text, models were analysed using the standard algebraic methods (Anderson & May, 1978; May & Anderson, 1978; Anderson & May, 1981; Murray, 2002, 2003) and in cases where solutions could not be found analytically, numerical solutions were obtained using Wolfram Mathematica version 8 (2008).

### Equilibrium analysis

To determine whether equilibria exist for a system of equations the standard methods of analysis are followed (Anderson & May, 1978; May & Anderson, 1978; Anderson & May, 1981; Murray, 2002, 2003) with equilibria found by setting the equations in the model to zero and solving for H, P, W, I, *etc.*

### Stability of equilibria

The standard methods of analysis, as outlined by Anderson & May (1978); May & Anderson (1978); Anderson & May (1981), are employed to determine stability of equilibria. If small perturbations from equilibrium return to said equilibrium point (when certain conditions are met) then the system is locally stable. For each equilibrium value the resulting Jacobian matrix is calculated. From the Jacobian, the characteristic equation and eigenvalues are obtained. If the eigenvalues of the Jacobian have negative real parts then local stability of the equilibrium value is confirmed.

## CHAPTER 2

### *Model A: Density dependent hosts*

#### *Equilibrium analysis*

1.  $(H^*, P^*) = (0, 0)$ , the trivial equilibrium with no salmon or *G. salaris*.

2.  $(H^*, P^*) = (K, 0)$ , the disease-free equilibrium with salmon growth in the absence of *G. salaris*.

*Stability analysis*

General form of the Jacobian is as follows:

$$\begin{pmatrix} a - b - 2sH^* & -\alpha \\ \alpha \frac{P^{*2}}{H^{*2}} - sP^* & \mu - (\epsilon + b + \alpha + sH^*) - 2\alpha \frac{P^*}{H^*} \end{pmatrix}$$

1. Eigenvalues of Jacobian at  $(0, 0)$  are given by,

$$\begin{vmatrix} a - b - \Lambda & -\alpha \\ 0 & \mu - \epsilon - b - \alpha - \Lambda \end{vmatrix} = 0$$

$$\Lambda^2 + [\alpha + 2b + \epsilon - (a + \mu)]\Lambda + (a - b)(\mu - \epsilon - b - \alpha) = 0 \quad (C.1)$$

Hence (by the Routh-Hurwitz theorem),  $(0, 0)$  is locally stable if and only if the conditions in (C.2) are satisfied.

$$a < b, \quad \mu < \epsilon + b + \alpha \quad (C.2)$$

2. Eigenvalues of Jacobian at  $(K, 0)$  are given by,

$$\begin{vmatrix} a - b - sK - \Lambda & -\alpha \\ 0 & \mu - \epsilon - b - sK - \alpha - \Lambda \end{vmatrix} = 0$$

$$\Lambda^2 + (2a + \epsilon + \alpha - \mu - b)\Lambda + (b - a)(\mu - a - \epsilon - \alpha) = 0 \quad (C.3)$$

Therefore by the Routh-Hurwitz theorem  $(K, 0)$  is locally stable if and only if the inequalities in (C.4) are satisfied.

$$a > b, \quad \mu < \epsilon + a + \alpha \quad (C.4)$$

*Detached parasites baseline model**Equilibrium analysis*

$$(2.15) \quad \Rightarrow \quad 0 = (a - b - sH^*)H^* - \alpha P^*$$

$$\frac{P^*}{H^*} = \frac{a - b - sH^*}{\alpha} \quad (C.5)$$

$$(3.1) \quad \Rightarrow \quad 0 = P^* \left( \mu - (\epsilon + b + sH^* + \alpha + \lambda) - \alpha \frac{P^*}{H^*} \right) + \beta H^* W^*$$

$$(C.5) \quad \Rightarrow \quad 0 = P^* \left( \mu - (\epsilon + b + sH^* + \alpha + \lambda) - \alpha \frac{a - b - sH^*}{\alpha} \right) + \beta H^* W^*$$

$$0 = P^* (\mu - (\epsilon + a + \alpha + \lambda)) + \beta H^* W^*$$

$$\beta H^* W^* = (\Gamma - \mu) P^* \quad (C.6)$$

where  $\Gamma = \epsilon + a + \alpha + \lambda$

$$(3.2) \quad \Rightarrow \quad 0 = \lambda P^* - \sigma W^* - \beta H^* W^*$$

$$(C.6) \quad \Rightarrow \quad 0 = \lambda P^* - \sigma W^* - (\Gamma - \mu) P^*$$

$$0 = (\lambda + \mu - \Gamma) P^* - \sigma W^*$$

$$(\lambda + \mu - \Gamma) P^* = \sigma W^* \quad (C.7)$$

Using (C.5), (C.6) and (C.7) we find three equilibria exist:

1.  $(H^*, P^*, W^*) = (0, 0, 0)$ , the trivial equilibrium with no salmon host or *G. salaris* parasites (neither on or off hosts).
2.  $(H^*, P^*, W^*) = (K, 0, 0)$ , the disease-free equilibrium with salmon population growth in the absence of *G. salaris* infection.
3.  $(H^*, P^*, W^*) = (H^*, P^*, W^*)$ , the coexistence equilibrium with both salmon and *G. salaris* (on and off hosts) populations present.

where,

$$\begin{aligned} K &= \frac{a-b}{s} \\ H^* &= \frac{\sigma(\Gamma-\mu)}{\beta(\mu-\Gamma+\lambda)} \end{aligned} \quad (C.8)$$

$$P^* = \frac{\sigma(\Gamma-\mu)[r\beta(\mu-\Gamma+\lambda) - s\sigma(\Gamma-\mu)]}{\alpha\beta^2(\mu-\Gamma+\lambda)^2} \quad (C.9)$$

$$W^* = \frac{(\Gamma-\mu)[r\beta(\mu-\Gamma+\lambda) - s\sigma(\Gamma-\mu)]}{\alpha\beta^2(\mu-\Gamma+\lambda)} \quad (C.10)$$

and

$$\Gamma = \epsilon + a + \alpha + \lambda$$

### Stability analysis

The general form of the Jacobian for equations (2.15), (3.1) and (3.2) is given as follows:

$$\begin{pmatrix} a-b-2sH & -\alpha & 0 \\ P\left(\frac{\alpha P}{H^2} - s\right) + \beta W & \mu - (\epsilon + b + sH + \alpha + \lambda) - \frac{2\alpha P}{H} & \beta H \\ -\beta W & \lambda & -\sigma - \beta H \end{pmatrix}$$

1. Eigenvalues of Jacobian at  $(0,0,0)$  are given by,

$$\begin{vmatrix} a-b-\Lambda & -\alpha & 0 \\ 0 & \mu - (\epsilon + b + \alpha + \lambda) - \Lambda & 0 \\ 0 & \lambda & -\sigma - \Lambda \end{vmatrix} = 0$$

which yields the characteristic equation  $\Lambda^3 + A\Lambda^2 + B\Lambda + C = 0$ , where

$$A = \Gamma - \mu + \sigma - 2(a-b) \quad (C.11)$$

$$B = (a-b)(a-b-\Gamma+\mu-2\sigma) + \sigma(\Gamma-\mu) \quad (C.12)$$

$$C = \sigma(a-b)(a-b-\Gamma+\mu) \quad (C.13)$$

Hence,  $(0,0,0)$  is locally stable (by Routh-Hurwitz conditions) if and only if:

$$a < b, \quad \mu < \epsilon + a + \alpha + \lambda \quad (C.14)$$

2. Eigenvalues of Jacobian at  $(K,0,0)$  are given by,

$$\begin{vmatrix} -a+b-\Lambda & -\alpha & 0 \\ 0 & \mu - (\epsilon + a + \alpha + \lambda) - \Lambda & \beta K \\ 0 & \lambda & -\sigma - \beta K - \Lambda \end{vmatrix} = 0$$

With characteristic equation  $\Lambda^3 + A\Lambda^2 + B\Lambda + C = 0$  where

$$A = \Gamma - \mu + \sigma + (a - b) + \beta K \quad (C.15)$$

$$B = \sigma(\Gamma - \mu) + \beta K(\Gamma - \mu - \lambda) + (a - b)(\Gamma - \mu + \sigma + \beta K) \quad (C.16)$$

$$C = \sigma(a - b)(\sigma(\Gamma - \mu) + \beta K(\Gamma - \mu - \lambda)) \quad (C.17)$$

Hence,  $(K, 0, 0)$  is locally stable (by Routh-Hurwitz conditions) if and only if:

$$a > b, \quad \mu < \epsilon + a + \alpha \quad (C.18)$$

3. Eigenvalues of Jacobian at  $(H^*, P^*, W^*)$  are given by,

$$\begin{vmatrix} a - b - 2sH^* - \Lambda & -\alpha & 0 \\ P^* \left( \frac{\alpha P^*}{H^{*2}} - s \right) + \beta W^* & \mu - (\epsilon + b + sH^* + \alpha + \lambda) - \frac{2\alpha P^*}{H^*} - \Lambda & \beta H^* \\ -\beta W^* & \lambda & -\sigma - \beta H^* - \Lambda \end{vmatrix} = 0$$

with characteristic equation  $\Lambda^3 + A\Lambda^2 + B\Lambda + C = 0$  where

$$A = \frac{s\sigma(\Gamma - \mu) + \beta\sigma\lambda + \beta(\Gamma - \mu)(\mu + \lambda - \Gamma)}{\beta(\mu + \lambda - \Gamma)} \quad (C.19)$$

$$B = \frac{s\sigma(\Gamma - \mu)(\sigma\lambda + (\Gamma - \mu)(\mu + \lambda - \Gamma))}{\beta(\mu + \lambda - \Gamma)^2} \quad (C.20)$$

$$C = \frac{\sigma(\Gamma - \mu)(r\beta(\mu + \lambda - \Gamma) - s\sigma(\Gamma - \mu))}{\beta(\mu + \lambda - \Gamma)} \quad (C.21)$$

$$r = a - b$$

$$\Gamma = \epsilon + a + \alpha + \lambda$$

Hence,  $(H^*, P^*, W^*)$  is locally stable (by Routh-Hurwitz conditions) if and only if:

$$a > b, \quad \epsilon + a + \alpha + \frac{\sigma s \lambda}{\beta r + \sigma s} < \mu < \epsilon + a + \alpha + \lambda \quad (C.22)$$

*Detached parasites model with mean parasites per host*

*Equilibrium analysis*

Setting  $dH/dt = dM/dt = dW/dt = 0$  we find the following equilibria exist:

1.  $(H^*, M^*, W^*) = (0, 0, 0)$ , the trivial equilibrium with no salmon host or *G. salaris* parasites (neither on or off hosts).
2.  $(H^*, M^*, W^*) = (K, 0, 0)$ , the disease-free equilibrium with salmon population growth in the absence of *G. salaris* infection.
3.  $(H^*, M^*, W^*) = (H^*, M^*, W^*)$ , the coexistence equilibrium with both salmon and *G. salaris* (on and off hosts) populations present.

where,

$$H^* = -\frac{\sigma(\mu - \Gamma)}{\beta(\mu + \lambda - \Gamma)} \quad (\text{C.23})$$

$$M^* = \frac{r\beta(\mu + \lambda - \Gamma) + s\sigma(\mu - \Gamma)}{\alpha\beta(\mu + \lambda - \Gamma)} \quad (\text{C.24})$$

$$W^* = -\frac{(\mu - \Gamma)(r\beta(\mu + \lambda - \Gamma) + s\sigma(\mu - \Gamma))}{\alpha\beta^2(\mu + \lambda - \Gamma)} \quad (\text{C.25})$$

*Stability analysis*

The general form of Jacobian for the re-evaluated model, equations (2.15), (3.14) and (3.2), is given by:

$$\begin{pmatrix} a - b - 2sH - \alpha M & -\alpha H & 0 \\ 0 & \mu - (\epsilon + a + \alpha + \lambda) & \beta \\ \lambda M - \beta W & \lambda H & -\sigma - \beta H \end{pmatrix}$$

1. Eigenvalues of Jacobian at  $(0, 0, 0)$  are given by,

$$\begin{vmatrix} a - b - \Lambda & 0 & 0 \\ 0 & \mu - (\epsilon + a + \alpha + \lambda) - \Lambda & \beta \\ 0 & 0 & -\sigma - \Lambda \end{vmatrix} = 0$$

with characteristic equation  $\Lambda^3 + A\Lambda^2 + B\Lambda + C = 0$  where,

$$A = \Gamma - \mu + \sigma - r \quad (\text{C.26})$$

$$B = \sigma(\Gamma - \mu) - r(\Gamma + \sigma - \mu) \quad (\text{C.27})$$

$$C = r\sigma(\mu - \Gamma) \quad (\text{C.28})$$

2. Eigenvalues of Jacobian at  $(K, 0, 0)$  are given by,

$$\begin{vmatrix} a - b - 2sK - \Lambda & -\alpha K & 0 \\ 0 & \mu - (\epsilon + a + \alpha + \lambda) - \Lambda & \beta \\ 0 & \lambda K & -\sigma - \beta K - \Lambda \end{vmatrix} = 0$$

with characteristic equation  $\Lambda^3 + A\Lambda^2 + B\Lambda + C = 0$  where,

$$A = s(\Gamma - \mu + \sigma + r) + r\beta \quad (\text{C.29})$$

$$B = sr(\Gamma - \mu + \sigma) + r^2\beta + r\beta(\Gamma - \mu - \lambda) + s\sigma(\Gamma - \mu) \quad (\text{C.30})$$

$$C = r(s\sigma(\Gamma - \mu) + r\beta(\Gamma - \mu - \lambda)) \quad (\text{C.31})$$

3. Eigenvalues of Jacobian at  $(H^*, M^*, W^*)$  are given by,

$$\begin{vmatrix} a - b - 2sH^* - \alpha M^* - \Lambda & -\alpha H^* & 0 \\ 0 & \mu - (\epsilon + a + \alpha + \lambda) - \Lambda & \beta \\ \lambda M^* - \beta W^* & \lambda H^* & -\sigma - \beta H^* - \Lambda \end{vmatrix} = 0$$

with characteristic equation  $\Lambda^3 + A\Lambda^2 + B\Lambda + C = 0$  where,

$$A = \frac{\beta[\sigma\lambda + (\Gamma - \mu)(\mu - \Gamma + \lambda)] - s\sigma(\mu - \Gamma)}{\beta(\mu - \Gamma + \lambda)} \quad (\text{C.32})$$

$$B = \frac{-s\sigma(\mu - \Gamma)[\sigma\lambda + (\Gamma - \mu)(\mu - \Gamma + \lambda)]}{\beta(\mu - \Gamma + \lambda)^2} \quad (\text{C.33})$$

$$C = \frac{-\sigma(\mu - \Gamma)[r\beta(\mu - \Gamma + \lambda) + s\sigma(\mu - \Gamma)]}{\beta(\mu - \Gamma + \lambda)} \quad (\text{C.34})$$

*Model B: Detached parasites*

*Equilibrium analysis*

Equilibria exist at:

1.  $(H^*, P^*, W^*) = (0, 0, 0)$ , the trivial equilibrium with no salmon host or *G. salaris* parasites (neither on or off hosts).
2.  $(H^*, P^*, W^*) = (K, 0, 0)$ , the disease-free equilibrium with salmon population growth in the absence of *G. salaris* infection.
3.  $(H^*, P^*, W^*) = (H^*, P^*, W^*)$ , the coexistence equilibrium with both salmon and *G. salaris* (on and off hosts) populations present.

where:

$$H^* = \frac{\sigma(\mu - (\epsilon + a + \alpha + \lambda))}{\beta(\epsilon - \mu)} \quad (C.35)$$

$$P^* = \frac{\sigma(\mu - (\epsilon + a + \alpha + \lambda))[\beta r(\epsilon - \mu) - s\sigma(\mu - (\epsilon + a + \alpha + \lambda))]}{\alpha\beta^2(\epsilon - \mu)^2} \quad (C.36)$$

$$W^* = -\frac{(\mu - (\epsilon + a + \alpha + \lambda))[\beta r(\epsilon - \mu) - s\sigma(\mu - (\epsilon + a + \alpha + \lambda))]}{\alpha\beta^2(\epsilon - \mu)} \quad (C.37)$$

#### Stability analysis

1. The conditions for stability of the zero equilibrium are the same as the conditions for the original model in Section 3.1.1.1, that is the inequalities in (3.7).
2. The conditions for  $(K, 0, 0)$  to be stable are similar to the inequalities in (3.8) found in Section 3.1.1.2. However, due to the addition of a dead host's parasites becoming detached instead of dying the conditions for stability in this case are  $a > b$  and  $\mu < \epsilon$ .
3. Following the usual methods of analysis we find that the coexistence equilibrium is stable (by Routh-Hurwitz) if and only if the following conditions are satisfied:  $a > b$  and  $\epsilon + \frac{s\sigma(a+\alpha+\lambda)}{\beta r+s\sigma} < \mu < \epsilon + a + \alpha + \lambda$

## Sensitivity analysis

In order to determine the impact of the parameter estimations obtained for use in model simulations throughout the main chapters of this thesis (see Appendix A, Table A.1) the sensitivity of models to the parameter values chosen was investigated.

Due to the earlier, simplistic models serving as a basis for the final model in Chapter 6, the sensitivity to the parameter values is determined for the Leslie matrix model/individual based models and the Model E: Multiple hosts strains with mutations.

### **Chapter 4 - Leslie Matrix/individual based models**

For the Leslie matrix and individual based models the impact of timing of parasite 1st birth, number of parasite births and level of parasite survival is investigated and compared with the baseline simulations. For all simulations the dominant eigenvalue (from Leslie simulations), extinction probability (from IBM simulations) and parasite density at  $t=35$  (end of the simulation) is recorded.

### **Chapter 6 - Model E: Multiple hosts strains with mutations**

For the n-host strain model (Model E) the method used to determine sensitivity follows that by Watts *et al.* (2009) such as to assess the magnitude of effect that individual parameter values have on model behaviour. In order to do this each parameter value in the model is varied, in turn, by  $\pm 10\%$  and the resulting change in model output (given as a percentage) recorded.

Table D.1: Sensitivity analysis of parameters used in Leslie and individual based models.

	Dominant Eigenvalue	Extinction Probability	N at t=35
Baseline Alta	1.12	0.29	63.09
Baseline Lier	1.09	0.36	23.81
Baseline Neva	0.98	0.80	0.84
Delayed 1st birth (0.5 days)			
Alta	1.10	0.40	32.65
Lier	1.08	0.48	11.36
Delayed 1st birth (1 day)			
Alta	1.09	0.42	19.71
Lier	1.05	0.56	6.39
Final birth Removed			
Alta	1.12	0.32	59.69
Lier	1.08	0.36	21.33
Final 2 births Removed			
Alta	1.10	0.38	44.37
Lier	1.07	0.48	17.85
Final 3 births Removed			
Alta	0.96	0.45	2.03
Lier	0.94	0.82	0.79
Survival rate reduced by 10%			
Alta	1.03	0.62	4.21
Lier	1.01	0.76	1.67
Survival rate reduced to = Neva			
Alta (10.44%)	1.03	0.64	3.72
Lier (6.30%)	1.04	0.64	4.60

CHAPTER 6 - MODEL E - MULTIPLE HOST STRAINS (WITH MUTATIONS)

Table D.2: Sensitivity of  $\theta$  in time to initial 60% salmon recovery.  $\phi = 0.0001$ .

Number of Salmon strains	% change from baseline value. Time to initial 60% recovery.	
	$\theta = -0.63$ (baseline value + 10%)	$\theta = -0.77$ (baseline value - 10%)
2	0.00	0.00
3	-0.82	1.23
4	-1.19	1.58
5	-1.54	1.92
10	-2.76	2.41
25	-5.94	7.69

Table D.3: Sensitivity of  $\theta$  in time to initial 60% salmon recovery.  $\phi = 0.0001$ .

Number of Salmon strains	Time to initial 60% recovery (years). % change from baseline values	
	$\theta = -0.6$	$\theta = -0.8$
2	0.00	0.00
3	-1.23	1.65
4	-1.59	2.58
5	-1.92	2.38
10	-4.14	4.14
25	-8.04	11.53

Table D.4: Sensitivity analysis of the parameters used in Model E - Multiple host strains (with mutations). The percentage change in model predictions of Atlantic salmon (total all strains) and *G. salaris* (total attached and detached) densities after altering individual parameter estimations by  $\pm 10\%$  are given. The percentage change in model predictions of time to 60% recovery is also given.

Parameter	Change in salmon density	Change in attached <i>G. salaris</i> density	Change in time to recovery
a+	4.027	5.105	1.877
b+	-0.021	-0.021	0.171
$\mu$ +	-0.096	17.954	-2.048
$\epsilon$ +	0.043	-7.5331	1.195
$\alpha$ +	-0.051	-0.440	0.341
$\beta$ +	-0.001	0.068	0.512
$\lambda$ +	-0.001	0.444	0.000
$\sigma$ +	0.001	-0.188	-0.683
$\tilde{m}$ +	-0.308	-8.973	0.171
$\zeta$ +	-0.051	9.512	0.000
s+	-9.090	-9.159	2.218
a-	-3.469	-67.787	-70.137
b-	0.021	0.021	-0.341
$\mu$ -	-0.035	37.949	3.242
$\epsilon$ -	-0.045	8.340	-1.195
$\alpha$ -	0.051	0.526	-0.512
$\beta$ -	0.001	-0.083	-0.683
$\lambda$ -	-0.000	-0.108	-0.171
$\sigma$ -	-0.001	0.189	0.512
$\tilde{m}$ -	0.331	10.988	-0.341
$\zeta$ -	0.051	-9.523	-0.171
s-	11.110	11.194	-2.048

## Selected Mathematica code

This Appendix contains selected Mathematica source code written and used throughout the research in the main text. A working example of the code used in each chapter is provided. Notes and comments made within the Mathematica source code are highlighted by (\* \*).

### CHAPTER 2

The source code for models in Chapter 2 has been omitted as it follows the techniques used in the more complicated models in Chapter 3. Please refer to Chapter 3 source code for examples of zero and disease-free equilibria analysis and simulation.

### CHAPTER 3

Model B: Detached parasites in the external environment

(\* CODE USED FOR CHECKING ANALYSIS DONE BY HAND \*)

(\* Equations for hosts \*)

$$I1[H,P,W] = (a - b - s*H)*H - \alpha*P;$$

(\* Equations for parasites \*)

$$I2[H,P,W] = \beta*W*H + P*(\mu - (\epsilon + b + s*H + \alpha + \lambda) - (\alpha*P/H));$$

(\* Equations for detached parasites \*)

$$I3[H,P,W] = (b + s*H + \alpha + ((\alpha*P)/H) + \lambda)*P - \sigma*W - \beta*W*H;$$

(\* Find equilibria \*)

$$\text{eqmI} = \text{Solve}[\{I1[H,P,W] == 0, I2[H,P,W] == 0, I3[H,P,W] == 0\}, \{H, P, W\}];$$

$$\text{simpI} = \text{Simplify}[\text{eqmI}]$$

(\* Jacobian \*)

$$\text{jacI} = \{ \{ \partial_H I1[H,P,W], \partial_P I1[H,P,W], \partial_W I1[H,P,W] \}, \\ \{ \partial_H I2[H,P,W], \partial_P I2[H,P,W], \partial_W I2[H,P,W] \},$$

```

{∂HI3[H,P,W],∂PI3[H,P,W],∂WI3[H,P,W]}

(* Characteristic Equation *)
CPI=CharacteristicPolynomial[{jacI},∧];

(* Solve C.E for equilibria *)
Print["(0,0,0)"]
subscpi0=Collect[{CPI}/.{H→ 0,P→ 0,W→ 0},∧]
Print["(K,0,0)"]
subscpiKK=Collect[{CPI}/.{simpI[[1]]},∧]
Print["(H,P,W)"]
subscpiC1=Collect[{CPI}/.{simpI[[2]]},∧]

(* CODE USED FOR RUNNING SIMULATIONS *)

(* Parameter values *)
(* Alter depending on conditions for stability at (0,0,0), (K,0,0), (H,P,W) *)

a1=2.0; b1=4.0; ε1=0.5; μ1=4; α1=0.5; s1=0.01; λ1=2; β1=0.05; σ1=5; ans=.;

(* Simulate the model using NDSolve *)
ans=NDSolve[{
H1'[t1]==(a1-b1-s1*H1[t1])*H1[t1]-α1*P1[t1],
P1'[t1]==β1*W1[t1]*H1[t1]+P1[t1]*(μ1-(α1+b1+ε1+s1*H1[t1]+λ1)-α1*P1[t1]/H1[t1]),
W1'[t1]==(b1+s1*H1[t1]+α1+((α1*P1[t1])/H1[t1])+λ1)*P1[t1]-σ1*W1[t1]-β1*W1[t1]*H1[t1],
H1[0]==100,P1[0]==50,W1[0]==10},{H1,P1,W1},{t1,0,1000},Method→ StiffnessSwitching];

(* Plot results *)

(* Plot H results only *)
Plot[H1[t1]/.ans,{t1,0,5},PlotRange→ Full,AxesLabel→ {time,H},AxesOrigin→ {0,0}];
(* Plot P results only *)
Plot[P1[t1]/.ans,{t1,0,5},PlotRange→ Full,AxesLabel→ {time,P},AxesOrigin→ {0,0}];
(* Plot W results only *)
Plot[W1[t1]/.ans,{t1,0,5},PlotRange→ Full,AxesLabel→ {time,W},AxesOrigin→ {0,0}];
(* Plot H, P, W results together *)
Plot[{H1[t1]/.ans,P1[t1]/.ans,W1[t1]/.ans},{t1,0,10},PlotRange→ Full,AxesOrigin→
{0,0},AxesLabel→ {Time,Number of Hosts, Parasites},

```

```
PlotStyle->{Black,{Dashed,Red},{Dotted,Blue}}
```

```
(* Find number of hosts/parasites at a given time point (in days) *)
```

```
Print[H1[50]/.ans]
```

```
Print[P1[50]/.ans]
```

```
Print[W1[50]/.ans]
```

The code that follows allows the user to simulate the model then alter each parameter value independently via the use of sliding bars (see screenshot).

```
Manipulate[
```

```
With[{ans=
```

```
NDSolve[{
```

```
H'[t]==(a-b-s*H[t])*H[t]-α*P[t],
```

```
P'[t]== β*W[t]*H[t]+P[t]*(μ-(α+b+ε+s*H[t]+λ)-α*P[t]/H[t]),
```

```
W'[t]==(b+s*H[t]+α+((α*P[t])/H[t]+λ)*P[t]-σ*W[t]-β*W[t]*H[t],
```

```
H[0]==Evaluate@h,P[0]==Evaluate@p,W[0]==Evaluate@w},{H,P,W},{t,0,1000},
```

```
Method→ StiffnessSwitching}},
```

```
Plot[{H[t]/.ans,P[t]/.ans,W[t]/.ans},{t,0,Evaluate@d},PlotRange→ {{0,Evaluate@d},Full},
```

```
PlotStyle→{Thick,{Dashed,Thick,Red},{Dotted,Thick,Darker[Green,0.6]}},
```

```
AxesOrigin→ {0,0},AxesLabel→ {time,Hosts & Parasites}]],
```

```
(* Parameter values of the form {{parameter, initial value} min value, max value} *)
```

```
{{a,4},0,10},{b,2},0,10},{ε ,0.5},0,10},{μ,7},0,10},{α,0.5},0,10},
```

```
{{σ,5},0,10},{s,0.01},0,10},{λ,2},0,10},{β,0.05},0,10},
```

```
{{h,100},0,500},{p,1},0,500},{w,0},0,500},{d,10},0.1,1000}]
```

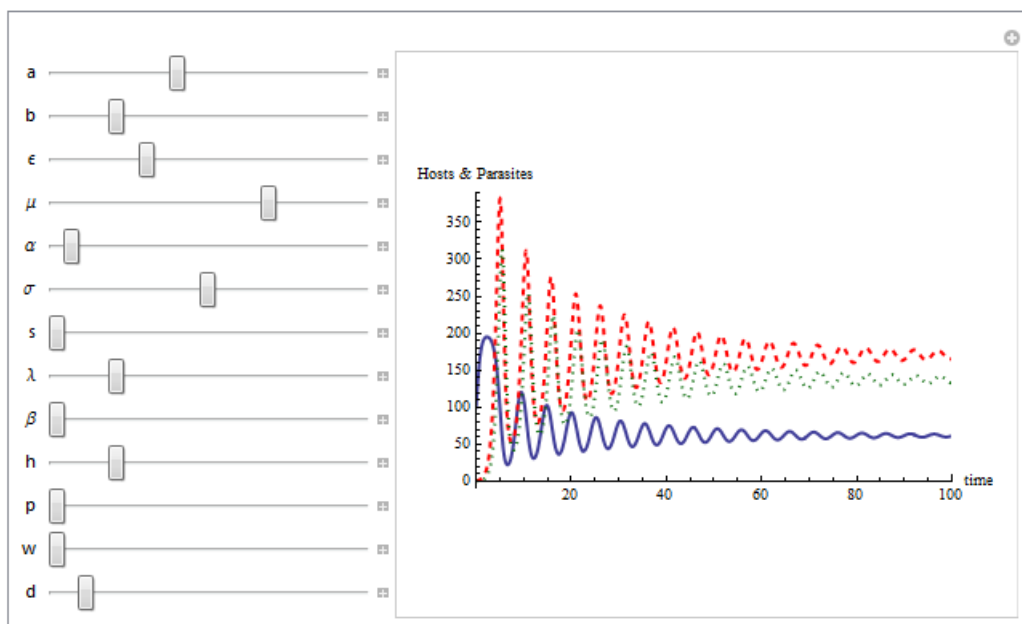


Figure E.1: Screenshot of plot generated with user alterable parameter values

## CHAPTER 4

This section includes Mathematica code for the Leslie and individual based model simulations for parasites infecting Alta stocks of Atlantic salmon. Both these methods were compiled in one notebook to allow comparison of results from the two methods.

```
(* Survival Rates*)
```

```
p2=(0.5)^(1/7.9); (* for Leslie sims *)
```

```
pb=1-p2; (* for IBM sims *)
```

```
(* INITIAL CONDITIONS *)
```

```
initialparasites=1;
```

```
(* for Leslie models *)
```

```
poptimepl=.;p0=1;
```

```
poptimepl0={{initialparasites},{0},{0},{0},{0},{0},{0},{0},
```

```
{0},{0},{0},{0},{0},{0},{0},{0},{0},{0},{0},{0},{0},{0},{0},{0},
```

```
{0},{0},{0},{0}};
```

```
(* for individual based models *)
```

```
stage1[0]=initialparasites;stage1b[0]=0;stage2[0]=0;stage2b[0]=0;stage3[0]=0;
```

```
stage4[0]=0;stage5[0]=0;stage6[0]=0;stage7[0]=0;stage8[0]=0;stage9[0]=0;
```

```
stage9b[0]=0;stage10[0]=0;stage10b[0]=0;stage11[0]=0;stage12[0]=0;stage13[0]=0;
```

```
stage14[0]=0;stage15[0]=0;stage16[0]=0;stage16b[0]=0;stage17[0]=0;stage17b[0]=0;
```

```
stage18[0]=0;stage19[0]=0;stage20[0]=0;stage21[0]=0;stage22[0]=0;
```

```
stage22b[0]=0;stage23[0]=0;stage23b[0]=0;stage24[0]=0;stage25[0]=0;
```

```
TOTALpop[0]=stage1[0]+stage2[0]+stage3[0]+stage4[0]+stage5[0]+stage6[0]+stage7[0]+
```

```
stage8[0]+stage9[0]+stage10[0]+stage11[0]+stage12[0]+stage13[0]+stage14[0]+
```

```
stage15[0]+stage16[0]+stage17[0]+stage18[0]+stage19[0]+stage20[0]+stage21[0]+
```

```
stage22[0]+stage23[0]+stage24[0]+stage25[0];
```

```
(* PARASITE BIRTHS *)
```

```
pa1=0;pa2=1;pa3=0;pa4=0;pa5=0;pa6=0;pa7=0;pa8=0;pa9=0;pa10=0;
```

```
pa11=0;pa12=0;pa13=0;pa14=0;pa15=0;pa16=0;pa17=0;pa18=0;pa19=0;pa20=0;
```

```
pa21=0;pa22=0;pa23=0;pa24=0;pa25=0;
```

```
(* PARASITE DEATHS *)
```

```

(* rb=(-log[1-P])/t1, pb=1-Exp[rb*t2],
where P is 50% (0.5) since after 7.9 days only 50% of the population is still alive,
t1 is the 50% survival time (7.9 days for Alta)
and t2 is 1 (to convert to a daily probability 1 day) *)

(* rb=(-Log[1-0.5])/7.9;Print["mortality rate per day rb= ",rb//N]
pb=(1-Exp[-rb*1])/N;Print["prob of mortality per day pb= ",pb//N] *)

Print["prob of mortality per day pb= " ,pb//N]

(* LENGTH & NUMBER OF SIMULATIONS *)
end=30; (* how long a single simulation lasts (in days) *)
LeslieEnd=end-1;
ender=50; (* Number of simulations for IBMs *)
(* BOUNDS - for IBM simulations *)
e0=1;e1=stage1[t-1];e2=e1+stage2[t-1];e3=e2+stage3[t-1];e4=e3+stage4[t-1];
e5=e4+stage5[t-1];e6=e5+stage6[t-1];e7=e6+stage7[t-1];e8=e7+stage8[t-1];
e9=e8+stage9[t-1];e10=e9+stage10[t-1];e11=e10+stage11[t-1];e12=e11+stage12[t-1];
e13=e12+stage13[t-1];e14=e13+stage14[t-1];e15=e14+stage15[t-1];e16=e15+stage16[t-1];
e17=e16+stage17[t-1];e18=e17+stage18[t-1];e19=e18+stage19[t-1];e20=e19+stage20[t-1];
e21=e20+stage21[t-1];e22=e21+stage22[t-1];e23=e22+stage23[t-1];e24=e23+stage24[t-1];
e25=e24+stage25[t-1];

(* IBM SIMULATIONS START HERE *)
Print[*START*];Print["-----"];
Do[
pa1=0;pa2=0;pa9=0;pa10=0;pa16=0;pa17=0;pa22=0;pa23=0;

Print["SIMULATION [",m,"] ✓"]

(* Print["stage1[0]=",stage1[0]];Print["***stage1b[0]=",stage1b[0]];
Print["stage2[0]=",stage2[0]];Print["stage3[0]=",stage3[0]];
Print["stage4[0]=",stage4[0]];Print["stage5[0]=",stage5[0]];
Print["stage6[0]=",stage6[0]];Print["stage7[0]=",stage7[0]];
Print["stage8[0]=",stage8[0]];Print["stage9[0]=",stage9[0]];
Print["stage10[0]=",stage10[0]];Print["stage11[0]=",stage11[0]];
Print["stage12[0]=",stage12[0]];Print["stage13[0]=",stage13[0]];
Print["stage14[0]=",stage14[0]];Print["stage15[0]=",stage15[0]];

```

```

Print["stage16[0]=",stage16[0]];Print["stage17[0]=",stage17[0]];
Print["stage18[0]=",stage18[0]];Print["stage19[0]=",stage19[0]];
Print["stage20[0]=",stage20[0]];Print["stage21[0]=",stage21[0]];
Print["stage22[0]=",stage22[0]];Print["stage23[0]=",stage23[0]];
Print["stage24[0]=",stage24[0]];Print["stage25[0]=",stage25[0]];

Print["TOTALpop[0]=",TOTALpop[0]];
Print["-----"]; *)

Do[(* Print["e0=",e0," e1=",e1," e2=",e2," e3=",e3," e4=",e4,"
e5=",e5," e6=",e6," e7=",e7," e8=",e8," e9=",e9," e10=",e10]; *)

Do[rndnod2[u]=RandomReal[];
(*Print["rndnod2["u,"]=",rndnod2[u]]*),{u,stage1[t-1]};
(*Print["-----"];*)
Do[rndnod3[u]=RandomReal[];
(*Print["rndnod3["u,"]=",rndnod3[u]]*),{u,stage9[t-1]};
(*Print["-----"];*)
Do[rndnod4[u]=RandomReal[];
(*Print["rndnod4["u,"]=",rndnod4[u]]*),{u,stage16[t-1]};
(*Print["-----"];*)
Do[rndnod5[u]=RandomReal[];
(*Print["rndnod5["u,"]=",rndnod5[u]]*),{u,stage22[t-1]};
(*Print["-----"];*)

Do[If[rndnod2[l]<0.15,pa1=1],{l,stage1[t-1]};
Do[If[rndnod2[l]>0.15,stage1b[t-1]=stage1b[t-1]-1],{l,stage1b[t-1]};
If[stage1[t]≤ 0,stage1[t]=0];
If[stage1b[t]≤ 0,stage1b[t]=0];
Do[If[rndnod2[l]>0.15,pa2=1],{l,stage1[t-1]};

Do[If[rndnod2[l]<0.15,stage2b[t-1]=stage2b[t-1]-1],{l,e1+1,e2}];
If[stage2b[t]≤ 0,stage2b[t]=0];

stage1[t]=pa1*stage1b[t-1]+pa2*stage2b[t-1]+pa3*stage3[t-1]+pa4*stage4[t-1]+
pa5*stage5[t-1]+pa6*stage6[t-1]+pa7*stage7[t-1]+pa8*stage8[t-1]+
pa9*stage9b[t-1]+pa10*stage10b[t-1]+pa11*stage11[t-1]+pa12*stage12[t-1]+
pa13*stage13[t-1]+pa14*stage14[t-1]+pa15*stage15[t-1]+pa16*stage16b[t-1]+

```

```

pa17*stage17b[t-1]+pa18*stage18[t-1]+pa19*stage19[t-1]+pa20*stage20[t-1]+
pa21*stage21[t-1]+pa22*stage22b[t-1]+pa23*stage23b[t-1]+pa24*stage24[t-1]+
pa25*stage25[t-1];

```

```

stage1b[t]=pa1*stage1b[t-1]+pa2*stage2[t-1]+pa3*stage3[t-1]+pa4*stage4[t-1]+
pa5*stage5[t-1]+pa6*stage6[t-1]+pa7*stage7[t-1]+pa8*stage8[t-1]+
pa9*stage9[t-1]+pa10*stage10[t-1]+pa11*stage11[t-1]+pa12*stage12[t-1]+
pa13*stage13[t-1]+pa14*stage14[t-1]+pa15*stage15[t-1]+pa16*stage16[t-1]+
pa17*stage17[t-1]+pa18*stage18[t-1]+pa19*stage19[t-1]+pa20*stage20[t-1]+
pa21*stage21[t-1]+pa22*stage22[t-1]+pa23*stage23[t-1]+pa24*stage24[t-1]+
pa25*stage25[t-1];

```

```

stage2[t]=stage1[t-1];stage2b[t]=stage1[t-1];stage3[t]=stage2[t-1];
stage4[t]=stage3[t-1];stage5[t]=stage4[t-1];stage6[t]=stage5[t-1];
stage7[t]=stage6[t-1];stage8[t]=stage7[t-1];stage9[t]=stage8[t-1];
stage9b[t]=stage8[t-1];stage10[t]=stage9[t-1];stage10b[t]=stage9[t-1];
stage11[t]=stage10[t-1];stage12[t]=stage11[t-1];stage13[t]=stage12[t-1];
stage14[t]=stage13[t-1];stage15[t]=stage14[t-1];stage16[t]=stage15[t-1];
stage16b[t]=stage15[t-1];stage17[t]=stage16[t-1];stage17b[t]=stage16[t-1];
stage18[t]=stage17[t-1];stage19[t]=stage18[t-1];stage20[t]=stage19[t-1];
stage21[t]=stage20[t-1];stage22[t]=stage21[t-1];stage22b[t]=stage21[t-1];
stage23[t]=stage22[t-1];stage23b[t]=stage22[t-1];stage24[t]=stage23[t-1];
stage25[t]=stage24[t-1];stage26[t]=stage25[t-1];

```

```

Do[rndnod[i]=RandomReal[];
(*Print["rndnod[" ,i,""]=" ,rndnod[i]]*),i,1,TOTALpop[t-1]];
(*Print["-----"];*)

```

```

Do[If[rndnod[j]<pb,stage2[t]=stage2[t]-1},{j,e0,e1}];
If[stage2[t]≤ 0,stage2[t]=0];
Do[If[rndnod[j]<pb,stage2b[t]=stage2b[t]-1},{j,e0,e1}];

```

```

Do[If[rndnod[j]<pb,stage3[t]=stage3[t]-1},{j,e1+1,e2}];
If[stage3[t]≤ 0,stage3[t]=0];

```

```

Do[If[rndnod[j]<pb,stage4[t]=stage4[t]-1},{j,e2+1,e3}];
If[stage4[t]≤ 0,stage4[t]=0];

```

```
Do[If[rndnod[j]<pb,stage5[t]=stage5[t]-1},{j,e3+1,e4}];
If[stage5[t]≤ 0,stage5[t]=0];
```

```
Do[If[rndnod[j]<pb,stage6[t]=stage6[t]-1},{j,e4+1,e5}];
If[stage6[t]≤ 0,stage6[t]=0];
```

```
Do[If[rndnod[j]<pb,stage7[t]=stage7[t]-1},{j,e5+1,e6}];
If[stage7[t]≤ 0,stage7[t]=0];
```

```
Do[If[rndnod[j]<pb,stage8[t]=stage8[t]-1},{j,e6+1,e7}];
If[stage8[t]≤ 0,stage8[t]=0];
```

```
Do[If[rndnod[j]<pb,stage9[t]=stage9[t]-1},{j,e7+1,e8}];
If[stage9[t]≤ 0,stage9[t]=0];
```

```
Do[If[rndnod3[l]<0.95,pa9=1},{l,stage9[t-1]}];
Do[If[rndnod3[l]>0.95,stage9b[t]=stage9b[t]-1},{l,e7+1,e8}];
Do[If[rndnod[j]<pb,stage9b[t]=stage9b[t]-1},{j,e7+1,e8}];
If[stage9b[t]≤ 0,stage9b[t]=0];
```

```
Do[If[rndnod[j]<pb,stage10[t]=stage10[t]-1},{j,e8+1,e9}];
If[stage10[t]≤ 0,stage10[t]=0];
```

```
Do[If[rndnod3[l]>0.95,pa10=1},{l,stage9[t-1]}];
Do[If[rndnod3[l]<0.95,stage10b[t]=stage10b[t]-1},{l,e8+1,e9}];
Do[If[rndnod[j]<pb,stage10b[t]=stage10b[t]-1},{j,e8+1,e9}];
If[stage10b[t]≤ 0,stage10b[t]=0];
```

```
Do[If[rndnod[j]<pb,stage11[t]=stage11[t]-1},{j,e9+1,e10}];
If[stage11[t]≤ 0,stage11[t]=0];
```

```
Do[If[rndnod[j]<pb,stage12[t]=stage12[t]-1},{j,e10+1,e11}];
If[stage12[t]≤ 0,stage12[t]=0];
```

```
Do[If[rndnod[j]<pb,stage13[t]=stage13[t]-1},{j,e11+1,e12}];
If[stage13[t]≤ 0,stage13[t]=0];
```

```
Do[If[rndnod[j]<pb,stage14[t]=stage14[t]-1},{j,e12+1,e13}];  
If[stage14[t]≤ 0,stage14[t]=0];
```

```
Do[If[rndnod[j]<pb,stage15[t]=stage15[t]-1},{j,e13+1,e14}];  
If[stage15[t]≤ 0,stage15[t]=0];
```

```
Do[If[rndnod[j]<pb,stage16[t]=stage16[t]-1},{j,e14+1,e15}];  
If[stage16[t]≤ 0,stage16[t]=0];
```

```
Do[If[rndnod4[l]>0.6,pa16=1},{l,stage16[t-1]}];  
Do[If[rndnod4[l]<0.6,stage16b[t]=stage16b[t]-1},{l,e14+1,e15}];  
Do[If[rndnod[j]<pb,stage16b[t]=stage16b[t]-1},{j,e14+1,e15}];  
If[stage16b[t]≤ 0,stage16b[t]=0];
```

```
Do[If[rndnod[j]<pb,stage17[t]=stage17[t]-1},{j,e15+1,e16}];  
If[stage17[t]≤ 0,stage17[t]=0];
```

```
Do[If[rndnod4[l]<0.6,pa17=1},{l,stage16[t-1]}];  
Do[If[rndnod4[l]>0.6,stage17b[t]=stage17b[t]-1},{l,e15+1,e16}];  
Do[If[rndnod[j]<pb,stage17b[t]=stage17b[t]-1},{j,e15+1,e16}];  
If[stage17b[t]≤ 0,stage17b[t]=0];
```

```
Do[If[rndnod[j]<pb,stage18[t]=stage18[t]-1},{j,e16+1,e17}];  
If[stage18[t]≤ 0,stage18[t]=0];
```

```
Do[If[rndnod[j]<pb,stage19[t]=stage19[t]-1},{j,e17+1,e18}];  
If[stage19[t]≤ 0,stage19[t]=0,stage19[t]=stage19[t]];
```

```
Do[If[rndnod[j]<pb,stage20[t]=stage20[t]-1},{j,e18+1,e19}];  
If[stage20[t]≤ 0,stage20[t]=0,stage20[t]=stage20[t]];
```

```
Do[If[rndnod[j]<pb,stage21[t]=stage21[t]-1},{j,e19+1,e20}];  
If[stage21[t]≤ 0,stage21[t]=0];
```

```
Do[If[rndnod[j]<pb,stage22[t]=stage22[t]-1},{j,e20+1,e21}];  
If[stage22[t]≤ 0,stage22[t]=0];
```

```

    Do[If[rndnod5[l]>0.5,pa22=1],{l,stage22[t-1]};
Do[If[rndnod5[l]<0.5,stage22b[t]=stage22b[t]-1],{l,e20+1,e21}];
Do[If[rndnod[j]<pb,stage22b[t]=stage22b[t]-1],{j,e20+1,e21}];
If[stage22b[t]≤ 0,stage22b[t]=0];

    Do[If[rndnod[j]<pb,stage23[t]=stage23[t]-1],{j,e21+1,e22}];
If[stage23[t]≤ 0,stage23[t]=0];

    Do[If[rndnod5[l]<0.5,pa23=1],{l,stage22[t-1]};
Do[If[rndnod5[l]>0.5,stage23b[t]=stage23b[t]-1],{l,e21+1,e22}];
Do[If[rndnod[j]<pb,stage23b[t]=stage23b[t]-1],{j,e21+1,e22}];
If[stage23b[t]≤ 0,stage23b[t]=0];

    Do[If[rndnod[j]<pb,stage24[t]=stage24[t]-1],{j,e22+1,e23}];
If[stage24[t]≤ 0,stage24[t]=0];

    Do[If[rndnod[j]<pb,stage25[t]=stage25[t]-1],{j,e23+1,e24}];
If[stage25[t]≤ 0,stage25[t]=0,stage25[t]=0];

TOTALpop[t]=stage1[t]+stage2[t]+stage3[t]+stage4[t]+stage5[t]+stage6[t]+
stage7[t]+stage8[t]+stage9[t]+stage10[t]+stage11[t]+stage12[t]+stage13[t]+
stage14[t]+stage15[t]+stage16[t]+stage17[t]+stage18[t]+stage19[t]+stage20[t]+
stage21[t]+stage22[t]+stage23[t]+stage24[t]+stage25[t]

(* Print["stage1[" ,t,"]=" ,stage1[t]];Print["***stage1b[" ,t,"]=" ,stage1b[t]];
Print["stage2[" ,t,"]=" ,stage2[t]];Print["stage3[" ,t,"]=" ,stage3[t]];
Print["stage4[" ,t,"]=" ,stage4[t]];Print["stage5[" ,t,"]=" ,stage5[t]];
Print["stage6[" ,t,"]=" ,stage6[t]];Print["stage7[" ,t,"]=" ,stage7[t]];
Print["stage8[" ,t,"]=" ,stage8[t]];Print["stage9[" ,t,"]=" ,stage9[t]];
Print["stage10[" ,t,"]=" ,stage10[t]];Print["stage11[" ,t,"]=" ,stage11[t]];
Print["stage12[" ,t,"]=" ,stage12[t]];Print["stage13[" ,t,"]=" ,stage13[t]];
Print["stage14[" ,t,"]=" ,stage14[t]];Print["stage15[" ,t,"]=" ,stage15[t]];
Print["stage16[" ,t,"]=" ,stage16[t]];Print["stage17[" ,t,"]=" ,stage17[t]];
Print["stage18[" ,t,"]=" ,stage18[t]];Print["stage19[" ,t,"]=" ,stage19[t]];
Print["stage20[" ,t,"]=" ,stage20[t]];Print["stage21[" ,t,"]=" ,stage21[t]];
Print["stage22[" ,t,"]=" ,stage22[t]];Print["stage23[" ,t,"]=" ,stage23[t]];
Print["stage24[" ,t,"]=" ,stage24[t]];Print["stage25[" ,t,"]=" ,stage25[t]];

```

```

Print["TOTALpop[" ,t,"]=",TOTALpop[t]];
Print["-----"]; *)

,{t,1,ender]];
gs[m]=Table[TOTALpop[t],{t,0,ender-1}]
(*;Print["Gyro[" ,m,"]=",gs[m]]*),
{m,1,ender}]];
Print["-----"];
Print["*END*"];(* END OF IBM SIMULATIONS *)

(* COMPILE SIMULATION RESULTS INTO A TABLE *)
GsTable=Table[gs[h],{h,1,ender}]];

(* GIVE SIMULATION RESULTS IN MATRIX FORM *)
GsMatrix=MatrixForm[%]; Print["GsMatrix=",GsMatrix];
Print["prob of mortality per day pb= ",pb//N]

(* PLOT IBM RESULTS *)
IBMSIM=ListPlot[GsTable,PlotRange→ {{0,Full},{0,(*60*)Full}},AxesOrigin→ {0,0},
Joined->True,PlotStyle→ Gray,AxesLabel→ {"time (days)","No. G. salaris"}]

avtot=Total[GsTable];
GsMean=avtot/ender;
Print[N[GsMean]];

(* PLOT MEAN IBM RESULT *)
ListPlot[GsMean,AxesOrigin→ {0,0},Joined→True,
AxesLabel→ {"time (days)","No. G. salaris"}]

(* LESLIE SIMULATIONS START HERE *)

Print["p2=",p2];
P=p2;

A=0.15;a=0.85;B=0.95;b=0.05;C=0.6;c=0.4;D=0.5;d=0.5;
lesALTA = {

```

```

{A, a, 0, 0, 0, 0, 0, 0, 0, B, b, 0, 0, 0, 0, 0, 0, C, c, 0, 0, 0, 0, 0, D, d, 0, 0, 0},
{P, 0, 0, 0, 0, 0, 0, 0, 0, 0, 0, 0, 0, 0, 0, 0, 0, 0, 0, 0, 0, 0, 0, 0, 0, 0},
{0, P, 0, 0, 0, 0, 0, 0, 0, 0, 0, 0, 0, 0, 0, 0, 0, 0, 0, 0, 0, 0, 0, 0, 0, 0},
{0, 0, P, 0, 0, 0, 0, 0, 0, 0, 0, 0, 0, 0, 0, 0, 0, 0, 0, 0, 0, 0, 0, 0, 0, 0},
{0, 0, 0, P, 0, 0, 0, 0, 0, 0, 0, 0, 0, 0, 0, 0, 0, 0, 0, 0, 0, 0, 0, 0, 0, 0},
{0, 0, 0, 0, P, 0, 0, 0, 0, 0, 0, 0, 0, 0, 0, 0, 0, 0, 0, 0, 0, 0, 0, 0, 0, 0},
{0, 0, 0, 0, 0, P, 0, 0, 0, 0, 0, 0, 0, 0, 0, 0, 0, 0, 0, 0, 0, 0, 0, 0, 0, 0},
{0, 0, 0, 0, 0, 0, P, 0, 0, 0, 0, 0, 0, 0, 0, 0, 0, 0, 0, 0, 0, 0, 0, 0, 0, 0},
{0, 0, 0, 0, 0, 0, 0, P, 0, 0, 0, 0, 0, 0, 0, 0, 0, 0, 0, 0, 0, 0, 0, 0, 0, 0},
{0, 0, 0, 0, 0, 0, 0, 0, P, 0, 0, 0, 0, 0, 0, 0, 0, 0, 0, 0, 0, 0, 0, 0, 0, 0},
{0, 0, 0, 0, 0, 0, 0, 0, 0, P, 0, 0, 0, 0, 0, 0, 0, 0, 0, 0, 0, 0, 0, 0, 0, 0},
{0, 0, 0, 0, 0, 0, 0, 0, 0, 0, P, 0, 0, 0, 0, 0, 0, 0, 0, 0, 0, 0, 0, 0, 0, 0},
{0, 0, 0, 0, 0, 0, 0, 0, 0, 0, 0, P, 0, 0, 0, 0, 0, 0, 0, 0, 0, 0, 0, 0, 0, 0},
{0, 0, 0, 0, 0, 0, 0, 0, 0, 0, 0, 0, P, 0, 0, 0, 0, 0, 0, 0, 0, 0, 0, 0, 0, 0},
{0, 0, 0, 0, 0, 0, 0, 0, 0, 0, 0, 0, 0, 0, P, 0, 0, 0, 0, 0, 0, 0, 0, 0, 0, 0},
{0, 0, 0, 0, 0, 0, 0, 0, 0, 0, 0, 0, 0, 0, 0, 0, P, 0, 0, 0, 0, 0, 0, 0, 0},
{0, 0, 0, 0, 0, 0, 0, 0, 0, 0, 0, 0, 0, 0, 0, 0, 0, 0, P, 0, 0, 0, 0, 0, 0, 0},
{0, 0, 0, 0, 0, 0, 0, 0, 0, 0, 0, 0, 0, 0, 0, 0, 0, 0, 0, 0, P, 0, 0, 0, 0},
{0, 0, 0, 0, 0, 0, 0, 0, 0, 0, 0, 0, 0, 0, 0, 0, 0, 0, 0, 0, 0, 0, P, 0}
};

```

```

total2={};stage1={};stage2={};stage3={};stage4={};stage5={};stage6={};
stage7={};stage8={};stage9={};stage10={};stage11={};stage12={};stage13={};
stage14={};stage15={};stage16={};stage17={};stage18={};stage19={};stage20={};
stage21={};stage22={};stage23={};stage24={};
stage25={};stage26={};

```

```

Do[poptime1=.;poptime1=MatrixPower[lesALTA,time].poptime10;

```

```

totalpop=poptime1[[1]]+poptime1[[2]]+poptime1[[3]]+poptime1[[4]]+
poptime1[[5]]+poptime1[[6]]+poptime1[[7]]+poptime1[[8]]+poptime1[[9]]+
poptime1[[10]]+poptime1[[11]]+poptime1[[12]]+poptime1[[13]]+poptime1[[14]]+
poptime1[[15]]+poptime1[[16]]+poptime1[[17]]+poptime1[[18]]+poptime1[[19]]+
poptime1[[20]]+poptime1[[21]]+poptime1[[22]]+poptime1[[23]]+poptime1[[24]]+

```

```

poptimep1[[25]]+poptimep1[[26]];total2=Append[total2,totalpop[[1]]];

stage1=Append[stage1,poptimep1[[1]]];stage2=Append[stage2,poptimep1[[2]]];
stage3=Append[stage3,poptimep1[[3]]];stage4=Append[stage4,poptimep1[[4]]];
stage5=Append[stage5,poptimep1[[5]]];stage6=Append[stage6,poptimep1[[6]]];
stage7=Append[stage7,poptimep1[[7]]];stage8=Append[stage8,poptimep1[[8]]];
stage9=Append[stage9,poptimep1[[9]]];stage10=Append[stage10,poptimep1[[10]]];
stage11=Append[stage11,poptimep1[[11]]];stage14=Append[stage14,poptimep1[[14]]];
stage15=Append[stage15,poptimep1[[15]]];stage12=Append[stage12,poptimep1[[12]]];
stage13=Append[stage13,poptimep1[[13]]];stage16=Append[stage16,poptimep1[[16]]];
stage17=Append[stage17,poptimep1[[17]]];stage18=Append[stage18,poptimep1[[18]]];
stage19=Append[stage19,poptimep1[[19]]];stage20=Append[stage20,poptimep1[[20]]];
stage21=Append[stage21,poptimep1[[21]]];stage22=Append[stage22,poptimep1[[22]]];
stage23=Append[stage23,poptimep1[[23]]];stage24=Append[stage24,poptimep1[[24]]];
stage25=Append[stage25,poptimep1[[25]]];stage26=Append[stage26,poptimep1[[26]]
,{time,0,LeslieEnd}];

(* PRINT OUT TOTAL PARASITES ALIVE IN EACH STAGE OF LESLIE SIMULATION *)
Print["Total2 = ",total2];
(* Print["stage1 ",stage1];Print["stage2 ",stage2];Print["stage3 ",stage3];
Print["stage4 ",stage4];Print["stage5 ",stage5];Print["stage6 ",stage6];
Print["stage7 ",stage7];Print["stage8 ",stage8];Print["stage9 ",stage9];
Print["stage10 ",stage10];Print["stage11 ",stage11];Print["stage12 ",stage12];
Print["stage13 ",stage13];Print["stage14 ",stage14];Print["stage15 ",stage15];
Print["stage16 ",stage16];Print["stage17 ",stage17];Print["stage18 ",stage18];
Print["stage19 ",stage19];Print["stage20 ",stage20];Print["stage21 ",stage21];
Print["stage22 ",stage22];Print["stage23 ",stage23];Print["stage24 ",stage24]; *)

(* END OF LESLIE SIMULATIONS *)
(* PLOT LESLIE RESULTS *)

LesSIM=ListPlot[total2,Joined→ True,PlotRange→ {{0,Full},{0,Full}},AxesOrigin→
{0,0},PlotStyle→ {Thick,Black},PlotRange→ Full(*,PlotLabel→ Mean IBM*),AxesLabel→
{"time (days)","No. G. salaris"}]

(* EIGENVALUES OF LESLIE MATRIX *)
Print["Eigenvalues=",Eigenvalues[lesALTA]]

```

```
(* PLOT LESLIE AND MEAN IBM TRAJECTORIES *)
```

```
Show[ListPlot[GsMean,AxesOrigin→ {0,0},Joined->True,PlotStyle→ {Thick,Gray,Dashed},
AxesLabel→ {"time (days)","No. G. salaris"},LesSIM]
```

```
(*PLOT LESLIE AND IBM RESULTS*)
```

```
Show[IBMSIM,LesSIM,PlotLabel→ "Atlantic salmon (Alta) strain"]
```

```
(* CALCULATE EXTINCTION PROBABILITY *)
```

```
Print["Number of parasites alive at end of simulation: ",
extinctionprob=Table[GsTable[{l,end}],{l,1,ender}]]
expb=0;
Do[If[extinctionprob[[h]]>0,expb=expb,expb=expb+1],{h,1,ender}];
Print["Number of zeros = ",expb]
Print["Extinction Probability = ",expb/ender//N]
```

## CHAPTER 5

```
(* Model B with immunity and trade-off *)
```

```
ans3=. ;
Manipulate[
With[{ans3=NDSolve[{
H'[t]==(a-b-s*H1[t])*H[t]-alpha*P[t],
P'[t]==beta*W[t]*H[t]+P[t]*(mu-(alpha+b+epsilon+I[t]+s*H[t]+lambda)-alpha*P[t]/H[t]),
W'[t]==(b+s*H[t]+alpha+((alpha*P[t])/H[t]+lambda)*P[t]-sigma*W[t]-beta*W[t]*H[t],
I'[t]==m-tilde*(P[t]/H[t])-zeta*I[t],
H[0]==Evaluate@h,P[0]==Evaluate@p,W[0]==Evaluate@w,I[0]==Evaluate@i,
{H,P,W,I},{t,0,1000}}]},
```

```
Show[
Plot[{H[t]/.ans3,P[t]/.ans3,W[t]/.ans3,I[t]/.ans3},{t,0,Evaluate@1000},
PlotRange→{{0,Evaluate@x},{0,Evaluate@y}},
PlotStyle→{{Thick,Blue},{Dashed,Thick,Blue},{Dotted,Thick,Darker[Green,0.6]},
{Thick,Dashed,Gray}},AxesOrigin→ {0,0},AxesLabel→ {time,Hosts & Parasites}},
ListPlot[{{0,150},{1000,150}},Joined→ True,PlotStyle→ {Black,Dotted}]]],
```

```

{{â,0.02-0.112*ñ},0,2},{b,0.005},0,2},{s,0.0001},0,2},{β,0.05},0,2},
{{ε,0.08},0,2},{μ,0.19},0,2},{α,0.02},0,2},{σ,0.24},0,2},{λ,0.1},0,2},
{{ñ,0},0,10},{ζ,0.005494505},0,1},
{{h,100},0,500},{p,50},0,500},{i,0},0,100},{x,500},0,1000},{y,200},0,5000}]

```

## CHAPTER 6

```

ans=. ;
ans2=. ;
Hplot=. ;
Pplot=. ;
Wplot=. ;
Iplot=. ;
Hplot2=. ;
Pplot2=. ;
Wplot2=. ;
Iplot2=. ;

max=25; (* NUMBER OF HOST STRAINS *)
years=1000; (* NUMBER OF SIMULATION YEARS *)
Gyears=25; (* YEARS AFTER WHICH Gs IS ADDED TO SIMULATION*)
StepsMax=years*365;
Gsadded=Gyears*365;
Ktab=Table[Kn=(an-b)/s,{n,1,max}]; (*CARRYING CAPACITIES FOR EACH HOST STRAIN*)

(* HOST EQUATIONS *)
Htab=Table[Hn'[t]==Piecewise[{{(1-φ)*an*Hn[t]+φ*an+1*Hn+1[t],n-1<1},
{φ*an-1*Hn-1[t]+(1-φ)*an*Hn[t],n+1>max}},φ*an-1*Hn-1[t]+(1-2*φ)*an*Hn[t]
+φ*an+1*Hn+1[t]]-(b+s*(Sum[Hj[t],{j,max}]))*Hn[t]-α*Pn[t],{n,1,max}]

(* ATTACHED PARASITE EQUATIONS *)
Ptab=Table[Pn'[t]==β *W[t]*Hn[t]+Pn[t]*(μn-(α +b+εn+I1[t]+s*(Sum[Hj[t],{j,max}]))+λ)
-α*Pn[t]/Hn[t]),{n,1,max}]

(* DETACHED PARASITE EQUATIONS *)
Wtab=Table[W'[t]==Sum[Pi[t]*(b+s*(Sum[Hj[t],{j,max}]))
+α +λ+((α*Pi[t])/Hi[t])),{i,max}]
-σ*W[t]-β*W[t]*(Sum[Hj[t],{j,max}]),{n,1}]

(* IMMUNITY EQUATIONS *)

```

```

Itab=Table[I1_n'[t]==m~n*(P_n[t]/H_n[t])-z*I1_n[t],{n,1,max}]

(* INITIAL CONDITIONS *)
H0=150;
H01=10;
H02=50;
P0=0;
W0=0;
I0=0;

(* CONDITIONS WHEN Gs ADDED*)
P02=0;
W02=0.1;
I02=0;

(* PARAMETERS *)
theta=-0.7;x1=0;y1=0.02;x2=0.017;y2=0.0181;
immpar1a=Sort[Flatten[{0,Table[(n-1)(0.0174776/(max-1)),{n,2,max-1}],0.0174776}]];
immpar=Table[m~n=immpar1a[[n]],{n,1,max}];
Print[m~n=,immpar, for n=1,...,max]
phi=0.0001;
atab=Table[a_n=y1-((y1-y2)*(1-((m~n-x2)/(x1-x2))))/(1+theta*((m~n-x2)/(x1-x2))),{n,1,max}];
b=0.005;s=0.0001;
alpha=0.02;beta=0.05;lambda=0.1;sigma=0.24;zeta=0.005;
gsbirth=Table[mu_n=0.19,{n,1,max}];
gsdeath=Table[epsilon_n=0.08,{n,1,max}];

(* COMPONENTS FOR USE WITH NDSOLVE *)
Htabsol=Table[H_n,{n,1,max}];
Ptabsol=Table[P_n,{n,1,max}];
Itabsol=Table[I1_n,{n,1,max}];
tabsol=Flatten[{Htabsol,Ptabsol,W,Itabsol}];

Htab01=Table[H1[0]==H0,{n,1,1}];
Htab02=Table[H2[0]==H01,{n,1,1}];
Htab03=Table[Hn[0]==H02,{n,3,max}];
Htab0=Flatten[{Htab01,Htab02,Htab03}]

```

```

Ptab0=Table[Pn[0]==P0,{n,1,max}]
Wtab0=Table[W[0]==W0,{n,1}]
Itab0=Table[I1n[0]==I0,{n,1,max}]

(* COMPONENTS FOR PLOTS *)
Hplot=Table[Hn[t]/.ans,{n,1,max}];
Pplot=Table[Pn[t]/.ans,{n,1,max}];
Wplot=W[t]/.ans;
Iplot=Table[I1n[t]/.ans,{n,1,max}];
HPWIPlot=Flatten[{Hplot,Pplot,Wplot,Iplot}];

Hstyle=Table[{Thick,CLn},{n,1,max}];
(*Hstyle2=Table[{Thick,Black},{n,max,max}];*)
Pstyle=Table[{{Thick,Dashed,CLn},{n,1,max}];
Wstyle={{Thick,Dotted,Black}};
Istyle=Table[{{Thin}},{n,1,max}];
(*Hstyle=Table[Thick,{n,1,max}];
Pstyle=Table[{{Thick,Dashed}},{n,1,max}];
Wstyle={{Thick,Dotted,Black}};
Istyle=Table[{{Thin}},{n,1,max}];*)
HPWISstyle=Flatten[{Hstyle(*,Hstyle2*),Pstyle,Wstyle,Istyle},1];

Hlabels=Table[Row[{Subscript["H",b]}],{b,1,max}];
Plabels=Table[Row[{Subscript["P",b]}],{b,1,max}];
Ilabels=Table[Row[{Subscript["I",b]}],{b,1,max}];
labels=Flatten[{Hlabels,Plabels,"W",Ilabels}];

CL1=Blue;CL2=Purple;CL3=Brown;CL4=Red;CL5=Green;CL6=Darker[Yellow,.2];
CL7=Darker[Blue,.5];CL8=Darker[Purple,.5];CL9=Darker[Brown,.5];CL10=Darker[Red,.5];
(* CL11...CLn=etc *)

(* NDSOLVE FOR SIMULATION WITH NO INFECTION*)
ans=NDSolve[{
Htab,Ptab,Wtab,Itab,Htab0,Ptab0,Wtab0,Itab0},tabsol,{t,0,StepsMax},
Method->{StiffnessSwitching,Method->{ExplicitRungeKutta,Automatic}},MaxSteps->∞];

(* CONDITIONS FOR ADDING Gs*)
HGsadded=Table[Hn[Gsadded]/.ans,{n,1,max}];

```

```

Htab02=Table[Hn[Gsadded]==HGsadded[[n,1]],{n,1,max}]
Ptab02=Table[Pn[Gsadded]==P02,{n,1,max}]
Wtab02=Table[W[Gsadded]==W02,{n,1}]
Itab02=Table[I1n[Gsadded]==I02,{n,1,max}]

(* COMPONENTS FOR PLOTS *)
Hplot2=Table[Hn[t]/.ans2,{n,1,max}];
Pplot2=Table[Pn[t]/.ans2,{n,1,max}];
Wplot2=W[t]/.ans2;
Iplot2=Table[I1n[t]/.ans2,{n,1,max}];
HPWIplot2=Flatten[{Hplot2,Pplot2,Wplot2,Iplot2}];

(* NDSOLVE FOR SIMULATION WITH INFECTION ADDED *)
ans2=NDSolve[{
Htab,Ptab,Wtab,Itab,Htab02,Ptab02,Wtab02,Itab02},t,absol,{t,Gsadded,StepsMax},
Method→{StiffnessSwitching,Method→{ExplicitRungeKutta,Automatic}},MaxSteps→∞];

(* PLOTTING RESULTS *)
(* NO INFECTION *)
plot1=Show[Plot[HPWIplot,{t,0,Gsadded},AxesOrigin→{0,0},
PlotRange→{{0,Gsadded},{0,All}},
PlotStyle→HPWIStyle,AxesLabel→{"Time (days)","Density"}]]

(* INFECTION ADDED *)
plot2=Show[Plot[HPWIplot2,{t,Gsadded,StepsMax},AxesOrigin→{0,0},
PlotRange→{{0,StepsMax},{0,All}},
PlotStyle→HPWIStyle,AxesLabel→{"Time (days)","Density"}]]

(* TOTAL NUMBER OF HOSTS *)
Hplottotal=Sum[Hn[t]/.ans,{n,1,max}];
Hplottotal2=Sum[Hn[t]/.ans2,{n,1,max}];
plot3=Show[
Plot[Hplottotal,{t,0,Gsadded},AxesOrigin→{0,0},
PlotStyle→{Thick,Darker[Red,.5]},PlotRange→{{0,StepsMax},
{0,All}},AxesLabel→{"Time (days)","Density"}],
Plot[Hplottotal2,{t,Gsadded,StepsMax},AxesOrigin→{0,0},
PlotStyle→{Thick,Darker[Red,.5]},PlotRange→{{0,StepsMax},
{0,All}},AxesLabel→{"Time (days)","Density"}]]

```

```
(* COMPLETE PLOT OF SIMULATION *)
```

```
Show[plot1,plot2,PlotRange→ {{0,All},{0,200}}]
```

```
(* PRINT OUT NUMBER OF SIMULATION YEARS, TOTAL HOSTS REMAINING
```

```
AND TOTAL PARASITES REMAINING *)
```

```
totalss=Sum[Hn[StepsMax]/.ans2,{n,1,max}];
```

```
totalohgs=Sum[Pn[StepsMax]/.ans2,{n,1,max}];
```

```
totalgs=totalohgs[[1]]+W[StepsMax]/.ans2[[1]];
```

```
Print["Simulating G. salaris - S. salar interactions over ",StepsMax/365//N," years"]
```

```
Print["Total number of salmon (all strains) at end of simulation = ",totalss[[1]]]
```

```
Print["Total number of G. salaris (on & off hosts) at end of simulation = ",totalgs]
```